NOTICE

The quality of this microform is heavily dependent upon the quality of the original thesis submitted for microfilming. Every effort has been made to ensure the highest quality of reproduction possible.

If pages are missing, contact the university which granted the degree.

Some pages may have indistinct print especially if the original pages were typed with a poor typewriter ribbon or if the university sent us an inferior photocopy.

Reproduction in full or in part of this microform is governed by the Canadian Copyright Act, R.S.C. 1970, c. C-30, and subsequent amendments.

AVIS

La qualité de cette microforme dépend grandement de la qualité de la thèse soumise au microfilmage. Nous avons tout fait pour assurer une qualité supérieure de reproduction.

S'il manque des pages, veuillez communiquer avec l'université qui a conféré le grade.

La qualité d'impression de certaines pages peut laisser à désirer, surtout si les pages originales ont été dactylographiées à l'aide d'un ruban usé ou si l'université nous a fait parvenir une photocopie de qualité inférieure.

La reproduction, même partielle, de cette microforme est soumise à la Loi canadienne sur le droit d'auteur, SRC 1970, c. C-30, et ses amendements subséquents.

STOICHIOMETRIC INTERACTIONS OF ATRAZINE AND HYDROXYATRAZINE WITH CHEMICALLY-CHARACTERIZED LAURENTIAN SOIL AND ITS KEY COMPONENTS

Zhendi Wang

A Thesis

in

The Department

of

Chemistry and Biochemistry

Presented in Partial Fulfillment of the Requirements
for the Degree of Doctor of Philosophy at
Concordia University
Montreal, Quebec, Canada

September, 1989

ISBN 0-315-51337-3

ABSTRACT

STOICHIOMETRIC INTERACTIONS OF ATRAZINE AND HYDROXYATRAZINE WITH CHEMICALLY-CHARACTERIZED LAURENTIAN SOIL AND ITS KEY COMPONENTS

Zhendi Wang

Concordia University, 1989

This work has systematically and stoichiometrically studied the interaction of the polar herbicide atrazine (AT) and its hydrolysis product, hydroxyatrazine (ATOH), first with the soluble fraction of soil organic matter known as fulvic acid (FA), second with the insoluble fraction known as humic acid (HA), and finally with their parent whole soil under various experimental conditions such as different pH values, low and high ionic strengths, a wide range of humics concentration, various equilibrium times, and in the presence of cations such as Cu(II). The soil and its key components, FA and HA, under investigation were derived from a sample of a podzol collected in the Laurentian Forest Preserve, and were well chemically-characterized.

The binding of AT requires extensive carboxylate site protonation but the binding sites only represent a very small fraction of total carboxylate. Binding of AT is not competitive with binding of ATOH. Binding is preferentially associated with larger molecular weight (MW) fraction of humic substances, and smaller MW fragments of humic mixtures compete with AT for sites on the larger MW fractions. Equilibration of binding is not rapid.

Two approaches have been applied to calculate the average weighted functions and the differential equilibrium functions of AT-FA and AT-HA. The second treatment based on the well-defined binding capacity, however, is preferably recommended. A model of binding involving H-bonding to specific sites created dynamically by the conformational equilibria of the polymer is proposed as the best accommodation of the variety of facts. Also, the fractions of FA were structurally characterized by UV/VIS spectrophotometry, fluorescence, FTIR and NMR.

The method used for binding and catalysis studies mainly is the ultrafiltration-HPLC method newly-developed in our laboratory. This method has been demonstrated to be sufficiently powerful, rapid, accurate and conservative of materials.

ACKOWLEDGEMENTS

My sincerest thanks to my supervisor, Dr. C. H. Langford, for both his continued guidance and the generous contribution of his time throughout this entire research project.

I would also like to extend my heartfelt thanks to Dr. D. S. Gamble for the valuable discussion with him and for his kind help in the interpretation of the results of this work; and to Dr. R. H. Zienius for his enthusiastic care and encouragement.

My thanks also to Dr. David J. Azrieli for the D. J. Azrieli Graduate Fellowship and to Graduate Studies of Concordia University for the Concordia University Graduate Fellowships.

TO MY MOTHER, MY WIFE AND MY CHILDREN

AND THE MEMORY OF MY FATHER

TABLE OF CONTENTS

CHAPTER 1

INTRODUCTION

CHAPTER 2

INTERACTION OF AT WITH LAURENTIAN FA: BINDING AND HYDROLYSIS

CHAPTER 4

INTERACTION OF ATRAZINE WITH LAURENTIAN HA

CHAPTER 5

INTERACTION OF ATRAZINE WITH LAURENTIAN SOIL

LIST OF TABLES

CHAPTER 1

INTRODUCTION

CHAPTER 2

INTERACTION OF AT WITH LAURENTIAN FA. BINDING AND HYDROLYSIS

CHAPTER 4

INTERACTION OF ATRAZINE WITH LAURENTIAN HA

CHAPTER 5

INTERACTION OF ATRAZINE WITH LAURENTIAN SOIL

LIST OF FIGURES

CHAPTER 1

INTRODUCTION

CHAPTER 2

INTERACTION OF AT WITH LAURENTIAN FA: BINDING AND HYDROLYSIS

CHAPTER 4

INTERACTION OF ATRAZINE WITH LAURENTIAN HA

CHAPTER 1
INTRODUCTION

1.1 HUMIC SUBSTANCES

Organic matter in soils is derived from decayed plants, animals, and microorganisms and their respective wastes [1]. The decayed products can be subdivided into two categories: (a) nonhumic substances and (b) humic substances. The definition of "humic substances" in the literature of natural system is variable. Recently three authoritative reference works gave definitions of humic substances:

Humic substances are structurally complex, polyelectrolytic, dark-colored organic acids that are found in soils, sediments and natural wastes [2].

Humic substances arise from the chemical and biological degradation of plant and animal residues and from synthetic activities of microorganisms. The products so formed tend to associate into complex chemical structures that are more stable than the starting materials. Important characteristics of humic substances are their ability to form water-soluble and water-insoluble complexes with metal ions and hydrous oxides and to interact with clay minerals and organic compounds.... [3]

Humic substances -- a series of relatively high molecular weight, brown to black substances formed by secondary synthesis reactions. The term is used as a generic name to describe the colored materials or its fractions obtained on the basis of solubility characteristics. These materials are distinctive to the

soil (or sediment) environment in that they are dissimilar to the biopolymers of microorganisms and higher plants (including lignin) [4].

These 3 descriptions show differences in scope and orientation, but they do tend to bring out the colour, polymeric character, and biological mediation connected intrinsically with the formation of humic substances.

Figure 1.1 represents a classification of organic matter. The molecular weight of humic substances range from as low as several hundred to perhaps over 300,000 [4]. The two main components of soil which are responsible for binding, degradation and hydrolysis of organic pollutants such as pesticides are clay and humic substances. Among humic substances, fulvic acid (FA) is the most hydrophilic polymers. As molecular weight (MW) increases from FA to humic acid (HA), HA becomes less hydrophilic.

The investigation of the molecular structure of humic substances remains a most difficult area of current research because of their extreme complexity. Several experimental approaches have been used to study the structure and aqueous comformations of humic substances, each technique having its potential to partially characterize the structural features of humic substances. The structure analysis techniques include functional group analysis [3-5], solution and solid-state ^{13}C-NMR spectroscopy [6-11], GC/MS [12,13], and time-resolved pyrolysis field ionization mass spectroscopy [14]. The aqueous conformation of fulvic acid has been studied by surface tension and viscometry, visible light scattering, small-angle X-ray scattering, steady-state fluorescence depolarization, and time-dependent

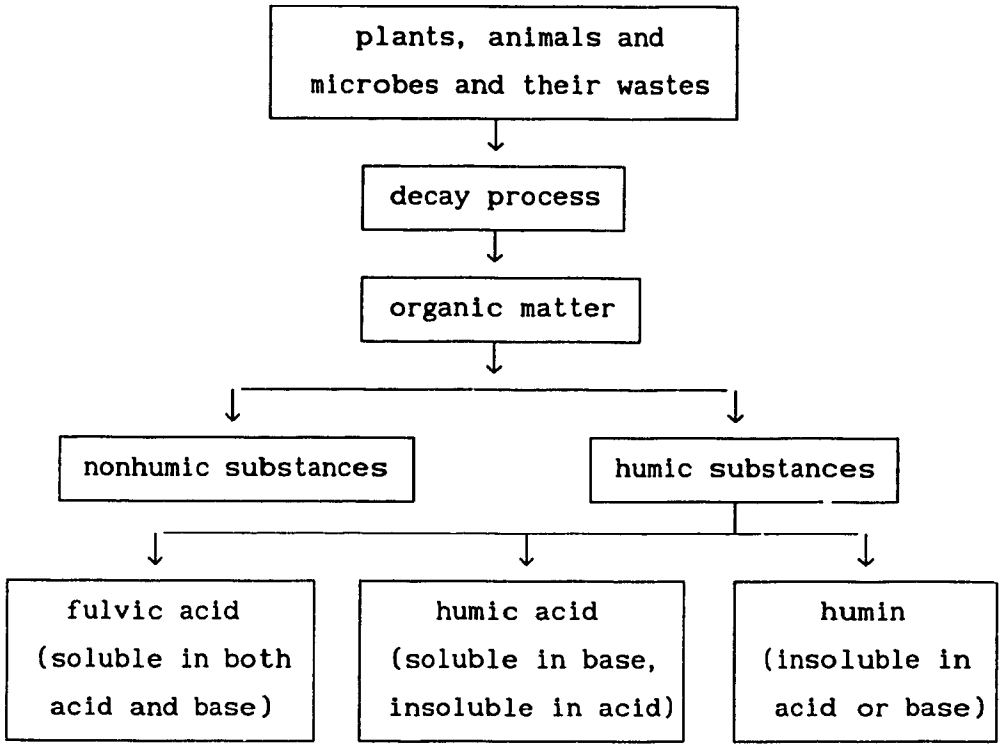

FIG.1.1 CLASSIFICATION OF SOIL ORGANIC MATTER

fluorescence depolarization spectroscopy [15-20].

More recently Schnitzer, Hindle and Meglic [11,13] used supercritical n-pentane to extract alkanes and alkanoic acids from Armadale humic materials, then to identify the components in the extracts by capillary GC/MS. The components identified included n-alkanes ranging from n-C_{12} to n-C_{32}, n-fatty acids (n-C_7 to n-C_{29}), unsaturated fatty acids and hydroxy-fatty acids (C_{12} to C_{16}). The total alkanes and alkanoic acids extracted from humic substances were only about one percent of the weight of humic materials.

Even though much work has been done, it is still not possible to describe the molecular configuration of even fractionated humic substances. On the other hand, this does not prevent substantial progress in understanding the properties of the materials. It has been shown that the functional groups, especially those most important for reaction with protons, organic pollutants, and trace metals, are carboxyl, phenolic and alcoholic hydroxyl, quinone and ketonic carbonyl, and amino groups. The prominence of carboxyl and phenolic hydroxyl groups contribute to the acidic nature of humic substances. Because of their importance, the characterization and binding behavior studies connected to these reactive functional groups have been focused upon by many researchers.

Buffle [21] recently has summarized the principal structural characteristics of humic substances that influence their chemical reactivity: (1) polyfunctionality, (2) macromolecular charge, (3) hydrophilicity, the tendency to form strong hydrogen bonds with water molecules solvating polar functional groups, and (4) structural lability, the capacity to associate intermolecularly

and to change molecular conformation in response to changes in pH values, ionic strength and functional group binding. These four properties reflect the behavior of a heterogeneous mixture of polymeric molecules in humic substances.

1.2 ATRAZINE AND HYDROXYATRAZINE CHEMISTRY

(1) Structure

Atrazine (AT) is the most widely used triazine herbicide in North America. Currently there are about 25 triazine derivatives that have been developed as commercial herbicides [22]. The triazine herbicides are based on a s-triazine structure containing two substituted amino groups, while the third ring carbon atom possesses a chloro, methoxy, or hydroxy grouping.

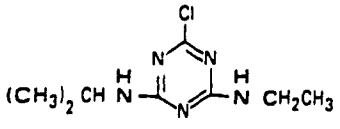

(1)

2-chloro-4-(ethylamino)-6-(isopropylamino)-1,3,5-triazine (AT)

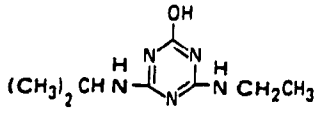

(2)

2-hydroxy-4-(ethylamino)-6-(isopropylamino)-1,3,5-triazine (ATOH)

The Geigy Laboratories in Basel, Switzerland first synthesized triazine compounds in 1952, and Gast, Knuesli and Gysin first described the selective herbicidal properties [22]. Soon thereafter, worldwide field trial established the commercial importance of atrazine and simazine.

It can be seen that the structures of AT and ATOH contains nitrogens with lone pairs of electrons so that both of them can act as electron donors, and that either -Cl or -O in the 2-position is a strong electronegative atom so that both AT and ATOH are polar molecules, and ATOH is more polar than AT because of the higher electronegativity of oxygen atom.

(2) Physical Properties of Atrazine

Physical description: white, crystalline, noncombustible, noncorrosive.

Melting point: 173-175 ^{o}C.

Solubility in water at 25 ^{o}C: 33 ppm.

Vapor pressure at 20 ^{o}C: 3.0×10^{-7} torr.

LD_{50} (acute oral for rats) value: 3800mg/Kg

pK_a value at 20 ^{o}C: 1.64

Recently, Plust et al [23] suggested that the protonation of AT in an acidic medium takes place on the aromatic nitrogens rather than on the nitrogen of the amino groups in the 4- and 6-positions. Since the equivalent of three nitrogens in the triazine ring, Plust et al concluded that the pK_a value should be a weighted average of the three nitrogens which were protonated.

(3) Chemical Properties

AT can undergo several reactions, especially those involving the substituents in the 2, 4 and 6 carbon positions.

$$AT \xrightarrow{H^+ \text{ or } OH^-} ATOH$$

The AT hydrolysis rate can be increased by heating or by the presence of soil organic matters such as fulvic acid and humic acid. It was concluded that hydrogen ion and undissociated carboxyl groups were the only catalytic agents in the soils, and that the mechanism of humic material catalysis is similar to that for hydrogen ion catalyzed hydrolysis of atrazine [24-26].

N-dealkylation of atrazine, an important degradation mechanism in biological systems, has been demonstrated to occur chemically, using Fenton's reagent (hydrogen peroxide and ferrous sulfate) [27]:

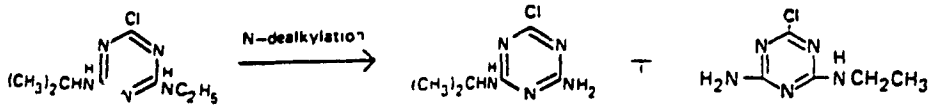

Direct chemical cleavage of the triazine ring of AT occurs only under drastic conditions, such as heating in concentrated sulfuric acid, melting with alkali.[22]

Atrazine is susceptible to photolysis under irradiation at UV wavelength [28]. The 2- position is the main reaction site and ATOH is the major photoproduct. However, the alkyl side chains can also removed by photolysis in the presence of fulvic acid [29].

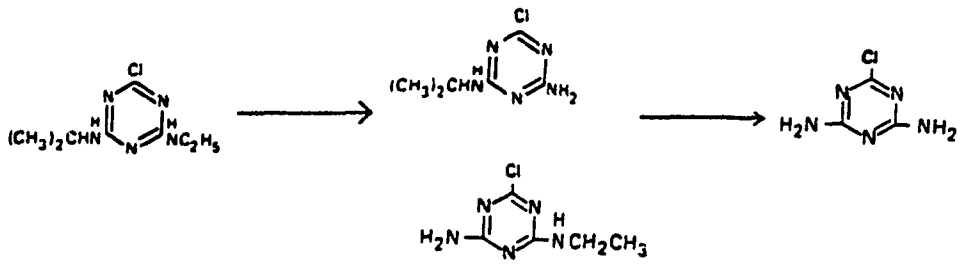

(4) Spectrophotometric Properties

The stable UV spectra of AT can be only obtained at pH 3.5 or higher in room temperature. When pH is lower than 3.5, proton catalyzed hydrolysis reaction will take place, thus its spectrum will change as pH changes and time goes on. The absorption maximum wavelength and absoptivity of AT determined in our experiments are 220 nm and 3.85×10^4, respectively (see details in Chapter 2).

For ATOH, the values of the absorption maximum and absorptivity of its protonated form we obtained are 238 nm and 2.53×10^4, respectively. If the pH is higher than 4.0, the hydroxyatrazine will exist in the reversible keto and enol form. Its spectra will consequently change as the pH changes (see details in chapter 2).

(5) FTIR Spectrum

The FTIR spectrum of atrazine recently measured in our laboratory is shown in Figure 1.2. The main vibration bands are assigned as follows: (A) N-H stretching, 3268 cm^{-1}. (B) Aliphatic CH stretching (CH_3 and CH_2): 2974, 2939 and 2874 cm^{-1}. (C) Asymmetric and symmetric N-H bending: 1654, 1623 1580 and 1559 cm^{-1}. (D) C-N (including chain C-N, ring C=N and C-N) stretching: variable, from 1400 to 1000 cm^{-1}. (E) C-H wagging: 805 cm^{-1}.

1.3 ENVIRONMENT ASPECTS

Triazine herbicides are among the most widely used herbicides in agriculture today and are applied both to growing crops and directly to soils. Thus, the fate of these herbicides in soil environment is of important since such factors as soil persistence, leaching and movement of residues by run-off can be

FIG. 1.2 FTIR SPECTRUM OF ATRAZINE

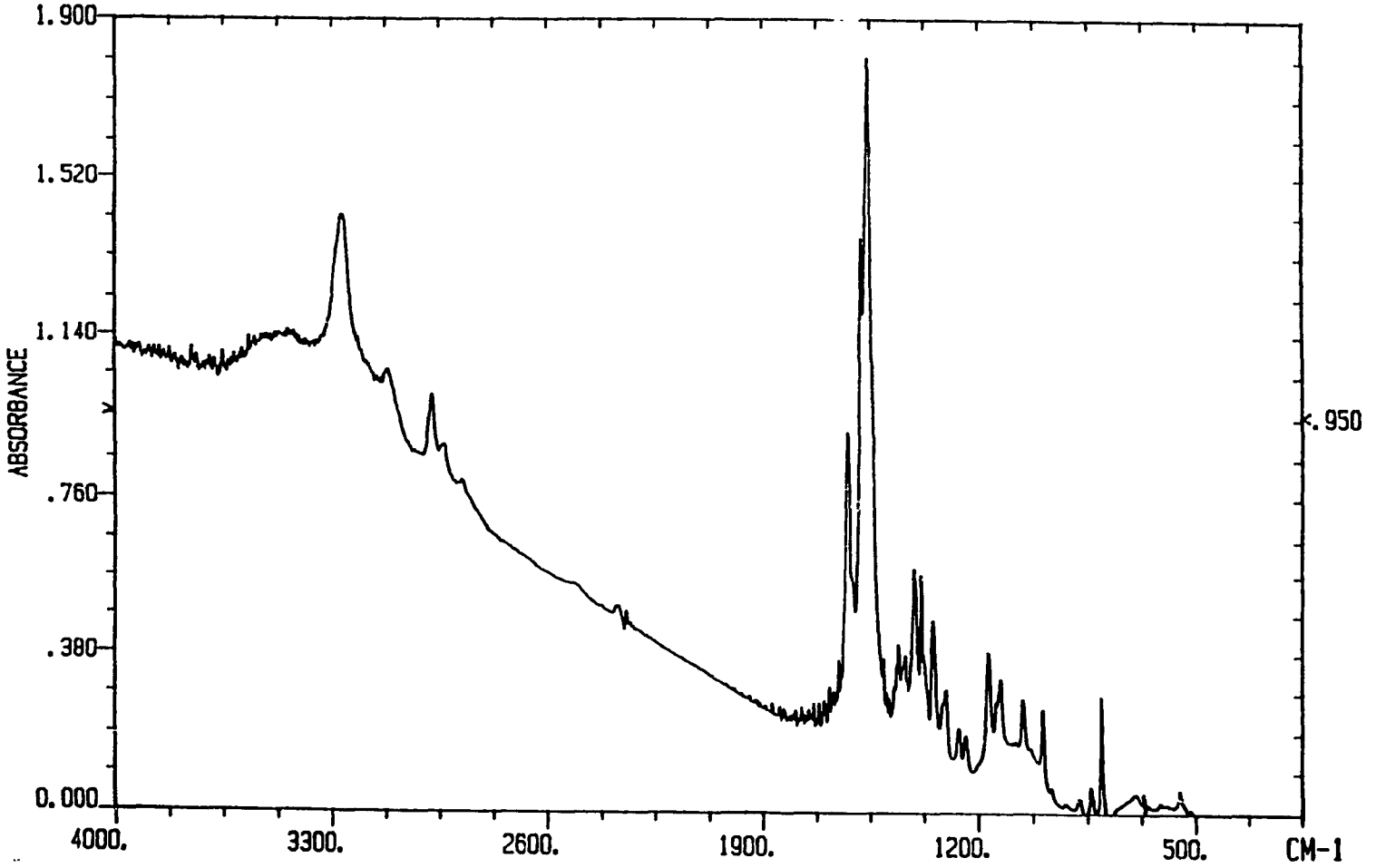

major influences governing contamination of ground water, streams, rivers, ponds and lakes. Such contamination has been observed in Ontario and other places of Canada.

The residue of atrazine can remain in soil at phytotoxic level for up to 18 months after application [30,31]. Atrazine residue has been reported in river water in corn-growing areas of the U.S and Canada [32-34].

Khan [35-39] and other authors [40,41] found that the major breakdown product of atrazine is hydroxyatrazine which was formed primarily by chemically induced hydrolytic reaction, and that the other major degradation pathway involves biological cleavage of the alkyl groups on the amino side chains. They concluded that the hydrolysis appears to be the principal mode of AT detoxification in soil, water and plants. The possible breakdown products of AT in soil are shown in Fig.1.3.

It has been shown that s-triazine can cause mutagenic and sometimes pathogenic effect on living organism [42]. As a result, environmental impact is a major factor in determining the desirability of these materials. Many governments including the Canadian government have enacted legislation which has rigidly controlled the introduction of herbicides and pesticides into the environment.

1.4. BINDING OF ATRAZINE

The adsorption, transfer, movement, degradation and hydrolysis of triazines are so important to the environment that many chemists and soil scientists have devoted themselves to the study of mechanism of binding of triazines with soil organic

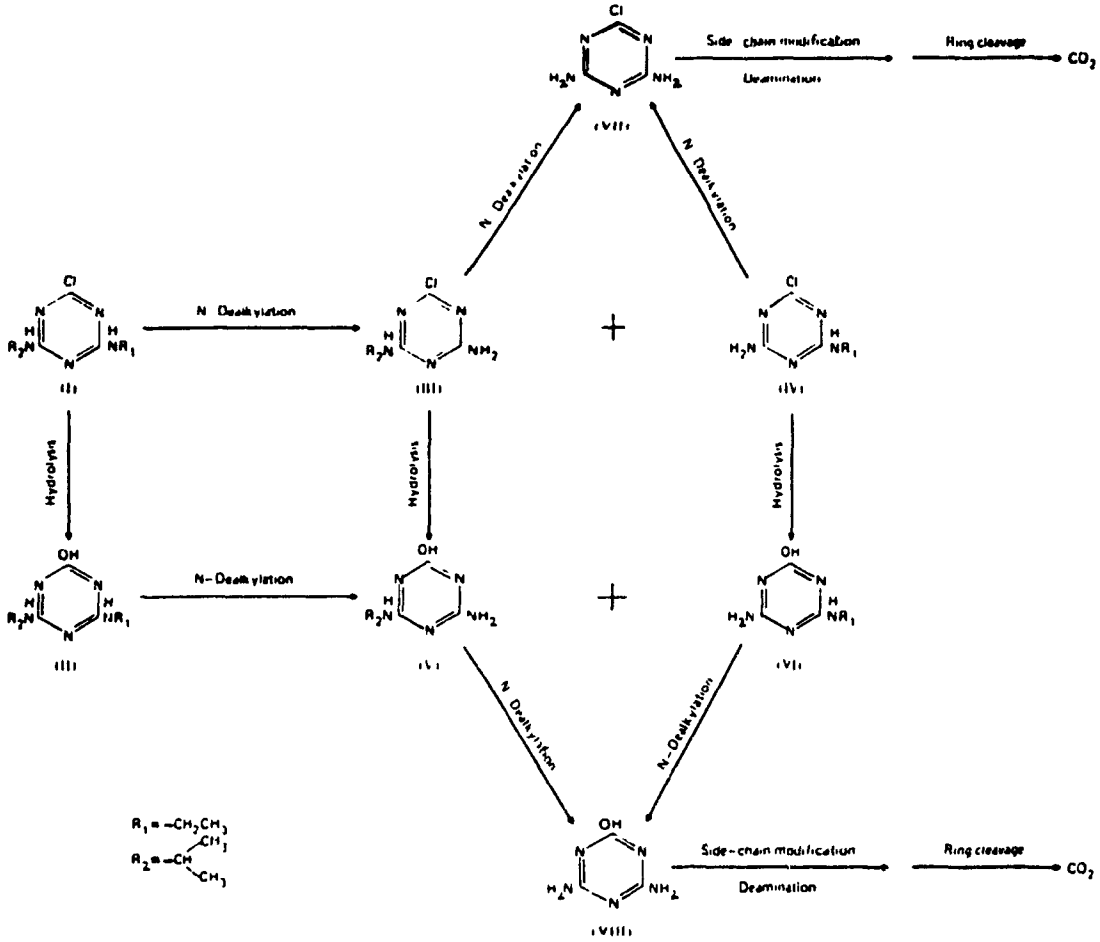

FIG.1.3 THE POSSIBLE BREAKDOWN PRODUCT OF ATRAZINE IN SOIL

matters. There have been books and reviews, and many articles concerned with the interaction between pesticides and soil constituents [29,43]. The phenomena of adsorption-desorption directly or indirectly influences the other factors which determine the fate and behavior of triazines. Several mechanisms have been proposed for adsorption of triazines by soil constituents, which are outlined as follows:

(1) Physical Adsorption

Physical adsorption can involve Van der Waals forces which result from short range dipole-dipole interactions of several kinds. A summation of dipole-dipole, dipole-induced dipole, induced dipole-induced dipole, and ion-dipole interactions. The role of Van der Waals forces in the adsorption of neutral polar and non-polar organic molecules by montmorillonite was demonstrated by the research of Bailey et al [44]. Bailey et al [44] argued that due to the rather large size of many pesticide molecules, the interlayer adsorption energy for the neutral molecules may be so high that adsorption will occur only on the external surfaces of expanding clay minerals.

(2) Hydrogen Bonding

It is difficult to classify hydrogen bonding as physical or chemical adsorption. Hydrogen bonding is a special kind of dipole-dipole interaction in which the hydrogen atom serves as a bridge between two electronegative atoms,. Hadzi [45] suggested there is a parallel between hydrogen bonding and protonation. Protonation may be considered as a full charge transfer from the

base (electron donor) to the acid (electron acceptor). Hydrogen bonding is a partial charge transfer.

For triazines possessing a basic chemical character and containing N-H groups, adsorption could occur by formation of a hydrogen bond between the amino group and the oxygen-containing group of humic substances. Hayes [46] stressed the participation of a hydrogen bonding mechanism in triazines and organic matter interactions. Evidence for this type of binding was obtained from IR studies by Sullivan and Felbeck [47]. They observed that hydrogen bonding may take place between C=O groups of the humic compounds and the secondary amino groups of triazines. The heat of atrazine-humic acid complex formation was estimated to be 8-13 kcal/mole, which most likely is the heat of formation of one or two hydrogen bonds. Recently, Haniff et al [48] studied AT binding by Armadale Fulvic Acid at various experimental conditions. What they concluded was that the hydrogen bonding seems to be the main mechanism of AT binding with FA.

In an aqueous medium, all H-bonding interaction are competitive since water is both an H-bond donor and acceptor.

(3) Chemical Adsorption

Chemical adsorption of triazines by soils and soil constituents can occur by at least 3 different mechanisms: a) protonation at the surface of gel phase of humic acid or soil by the reaction of the base with the hydronium ion on the exchange site, b) ion exchange of positively charged triazines with inorganic cations adsorbed on soil constituents, c) protonation in the solution phase with subsequent adsorption of the organic

pesticide via ion exchange.

a) Ion Exchange

The fact that ion-exchange occurs with organic cations has been documented. Gilmour and Coleman [49] found that protonated triazines competed with initially adsorbed cation Ca^{2+} for binding humic acid sites, which could be expressed by the following equation:

$$2\ TA\ H^{+} + MR \rightleftharpoons M^{+2} + (TAH)_2R$$

where R is the soil cation exchanges, TA is triazines, M is adsorbed cation. Protonated hydroxyatrazine also has been shown to be adsorbed as an organic cation at the surface of the Al^{3+}-montmorillonite [50].

b) Protonation

That adsorption may occur due to protonation at the gel surface and in the interiors of water-swollen gel solution, or in solution is an important adsorption mechanism, especially in regard to the adsorption of pesticides basic in chemical character such as triazines. Triazines can become cationic in solution through protonation:

$$TA + H^{+} \rightleftharpoons TA\ H^{+}$$

Protonation may also occur by transfer of H^{+} from the surface to AT and the protonated triazine remains on the surface as counter ion:

$$TA + HR \rightleftharpoons TAH^{+}R^{-}$$

Thus the acidity of the soil colloid surface will influence the protonation of the adsorbed basic triazines. The pH in the gel solution of soil colloids may be as much as 3-4 pH units lower than that of the solution [44]. The protonation of triazine may therefore occur even though the measured pH of the water-adsorbent system is much greater than the pKa value of the compound.

Gamble et al have characterized and standardized the weak acid properties of Armadale FA [51,52] and Chernozemic humic acid [53] using potentiometric titration and conductivity titration method. They stoichiometrically characterized the solution phase and colloidal dispersion solution binding of AT to this FA and HA, demonstrating the direct correlations with acidic functional groups. The AT-FA solution phase work has indicated that unionized carboxyl groups are hydrogen binding sites, and the only two catalysts for AT hydrolysis identified were hydrogen ion and unionized carboxyl groups [54].

1.5 REVIEW OF ANALYTICAL PROCEDURES FOR AT AND ATOH

There are three main procedures for the analysis of AT in waters, soils, and plant and animal tissues. These methods are based on spectrophotometry, GC and HPLC.

(1) Spectrophotometry

AT reacts with pyridine to give quaternary pyridinium halides, which can undergo the addition of hydroxyl group to form a carbinol base [55]. In the presence of alkali the heterocyclic ring of this system is cleaved to yield an anil of glutaconic dialdehyde, which exist in equilibrium with the enol form. This

mixture absorbs at about 440 nm, so that the spectrophotometric determination at this wavelength may be used to calculate the amount of AT. The overall reaction can be expressed as follows:

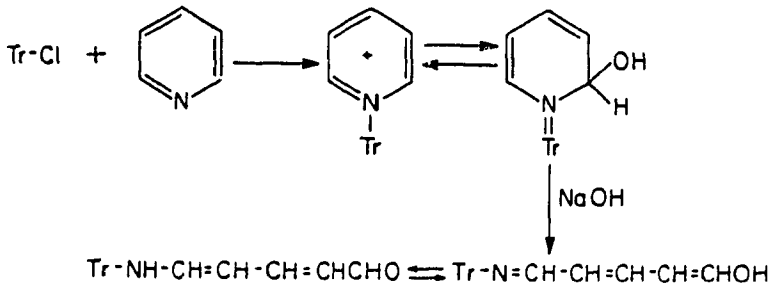

This procedure, however, suffers serious disadvantages The color generated is not stable and fades rapidly. The extracts derived from untreated soil can give rise to highly colored blanks, especially for those AT samples containing water-soluble fulvic acid which gives a strong interfering absorption band in the UV region. Thus this method is of very limited use.

A more useful spectrophotometric procedure is based on the principle that AT is converted to its respective hydroxyatrazine in 50% aqueous sulfuric acid. The cations of ATOH show absorption maximum at 240 nm. This procedure is quite sensive and rapid. However, it is non-specific because the hydroxytriazines all absorb at 240nm, so it can only be applied to samples containing single and known triazine residues.

(2) Gas chromatography

GC is a widely used procedure for the analysis of AT and other triazines in water, soil, and environmental and tissue samples. The detectors that have been used included flame ionization [56-58], electron capture [59,60], microcolormetric

[59-61], alkali flame ionization [62,63], flame photometric [64], electrolytic conductivity devices [65,66], and nitrogen-selective detector [67]. Recently, Haniff et al. [68-70] described the determination of AT using the batch-ultrafiltration and GC equipped with electron-capture detector. However, an important limitation of this procedure is that the hydrolyzed product of AT cannot be detected directly by GC. AT must be converted to its methoxy or silyl derivatives prior to analysis [35-39,71,72].

(3) HPLC

Theoretically, triazines can all be analyzed using HPLC equipped with UV detector, since the triazines have absorption maxima in the region of 220 nm. Up to now, however, only a few papers dealing with HPLC analysis of AT and ATOH have been published. Ramsteiner[73] reported HPLC determination of hydroxy s-triazine residue in plant materials. Solinas [74] determined AT and ATOH in the presence of one another by HPLC on μ-Bonapak column. Byast[75] found the HPLC analytical procedures have proved most successful for the determination of triazine residues in water. Recently, Xu et al. [76] determined triazines using microbore HPLC with UV detector at 222 nm. Average recovery obtained was 20 ppb. Obviously, the applicability of LC to multi-residue samples is still waiting to be developed. Currently, HPLC is successfully in use for the separation and simultaneous determination of AT and ATOH in humic and soil samples in our laboratory.

1.6 INTERACTION OF Cu^{2+} ION WITH HUMICS

Adsorption of trace metals such as Cu and Cd onto natural particulate matter can play an important role in determining trace metal speciation in biological uptake, and toxicity and mobility in environmental cycles. The "adsorption reaction" between a trace metal and humic substances is defined as follows [77]: If the humic substance is in colloidal form, the adsorption reaction is any process through which a net positive accumulation of the trace metal occurs at the common boundary of the humic colloid and the aqueous solution phase with which it is in contact. However, if the humic substance is dissolved in water, the reaction is the formation of a complex or chelate with one or more organic functional groups. In recognition of its potentially important role, there have been numerous studies of trace metal interaction with humic substances.

(1) Factors influencing Cu^{2+} complexation

In the previous works, studies were mainly concerned with the interaction between fulvic acid and metal ions. More fundamentally, the factors that influence metal ion complexing or chelation by fulvic acid include:

--the nature of the metal ion;

--the relative numbers and arrangement of carboxyl and phenolic -OH groups;

--the extent of protonation of the carboxyl groups;

--the concentration of the fulvic acid;

--competition from other metal ions for complexing sites;

--the screening out of polyelectrolyte charge by the background electrolyte.

The numerical values of equilibrium functions will depend on their definitions, but should not depend on the fashion in which data are manipulated.

The degree of ionization of the carboxyl groups is actually a key variable among all factors. At the same constant H^+ concentration or the same pH, two different ionic strength will give two different degrees of ionization. If therefore one specifies pH, then one must also specify ionic strength. This is a total of two variables. If however one specifies the degree of ionization, only one variable is required. Ions such as potassium might not only compete with divalent cations for binding sites on fulvic acid [78], but also promote the aggregation of fulvic acid [79]. Recently Cabannis and Shuman [80,81] studied copper binding properties of several fulvic acids and indicate that variations in Cu binding among different sources of dissolved organic matter appear to be much smaller than those due to chemical factors such as pH and ionic strength.

(2) Techniques for investigating complexing of metal ions by FA

Separation and non-separation techniques are the two major types of analysis applied to speciation problem. Table 1.1 listed commonly used techniques [82].

The main disadvantages of nonseparation methods are that they cover relatively few metal ions, and most of them need a supporting electrolyte. Another problem is that fulvic acid can be adsorbed onto the mercury electrode.

The chief advantage of separation techniques is that the wide range of metal ions can be measured, generally by means of atomic

TABLE 1-1

Techniques for investigating complexes of fulvic acid and metal ions

Technique	Applicability (which metal)	What measured	Adsorption problems	Shift equilibrium	Ionic strength	Advantages	Disadvantages
Separation							
Liquid chromatography (including reversed phase and gel filtration)/ atomic absorption spectrometry (AAS)	Any AAS metal	Total metal-ion and free metal-ion concentrations in various eluted fractions	Possibly	Possibly	No restrictions	Can use unmodified natural water samples	Not particularly applicable for stability constant calculations
Ultrafiltration (UF)/AAS	Any AAS metal	Total metal-ion and free metal-ion concentrations	Yes—on membrane and ultrafiltration cell; varies depending on metal	Possibly	No restrictions	Faster than equilibrium dialysis; no ionic strength or metal-ion restrictions	Adsorption; possible incomplete separation; special UF cell needed
Equilibrium dialysis/AAS	Any AAS metal	Total metal-ion and free metal-ion concentrations	Possibly (on membrane)	Possibly	~0.001 *M* or greater	No metal-ion restrictions; can use unmodified natural water samples	Possible adsorption and contamination by membrane; possible incomplete separation
Nonseparation							
Electron paramagnetic resonance spectroscopy (EPR)	EPR-active metals (e.g., V, Cu, Mn, Fe)	Various forms of metal ion	No	No	No restrictions	Provides information on types of complexes	Only EPR-active metals; high detection limit
Ion-selective electrode potentiometry	Cd, Cu, Pb, Ca	Hydrated metal-ion concentration	Possibly	No	~0.01 *M* or greater	Rapid titration	Few metal ions; possible adsorption on electrode; high detection limit
Hydrogen-ion potentiometry	Any	Increase in hydrogen ion concentration from which complexation is inferred	No	No	No restrictions	No ionic strength or metal-ion restrictions	Extreme care needed during titration
Anodic stripping voltammetry	Cu, Cd, Pb, Zn	Hydrated and ASV-labile metal ions	Yes	Possibly	~0.01 *M* or greater	Very low metal-ion concentration can be measured	Few metal ions; adsorption; possible equilibrium shift
Fluorescence	Paramagnetic metal ions like Cu	Uncomplexed fulvic acid	No	No	No restrictions	An alternative view of complexation; very sensitive; can use unmodified natural waters	Applicable to few metal ions

absorption spectrophotometry. Buffle [83,84] studied the influence of various factors on the retention of metal ions and ligands by some neutral and negatively charged membranes used in ultrafiltration techniques, and measured equilibrium constants for complexation of zinc by synthetic and natural ligands.

(3) Modeling

Various models have been developed and used to explain complexation of metal ions by fulvic acid. Recently, Sposito [77] gave an excellent review. It uses underlying concepts with which to give a unified discussion of the various theoretical mathematical models. Generally speaking, there are discrete and continuous multiligand models for metal-humate binding. Some experimental results have been modeled with sets of discrete ligands [85-88]. Discrete multiligand model assumes the fulvic acid molecules are macromolecules bearing one class of functional group that forms a 1:1 complex with a trace metal cation.

Models based on continuous ligand frequency distributions have been used increasingly. The complexity of the mixture of organic ligands in humic substances is significantly greater than the complexity of ligand sites on pure solids. The inherent complexity of the humic substances will become more complex when it is combined with the tendency of humic substances to undergo aggregation reactions, configurational and conformational changes, and with the electrostatic problems that arise from interactions two or more ligand sites on the same molecules. Considering that the structure of humic substances is so irregular that no two of its carboxyl groups can be assumed to be chemically identical, the

distribution of ligands of humic substances should be expressed as continuous functions. So far, three major continuous distribution models that have been applied to humates are the affinity spectrum model [89-91], the normal distribution model [92-94], and the continuous stability function model [17,51, 52,68, 94-97].

Among these continuous ligand distribution models, the rigorous method for describing proton and metal binding by humic substances which makes the fewest initial assumptions is the continuous function model developed by Gamble, Langford and coworkers [17,51,52, 68,94-97]. They suggested that humic substances contain a continuous distribution of non-identical functional groups that can bind proton or metal ions. Even they have subdivided proton binding sites into Type A and Type B (it should be noted that this distinction between A and B types of acidic functional groups was imposed by experimental results in the form of a discontinuity that caused a titration end point. The distinction was made by the experiment, and not by an arbitrary decision), the K values have been consistently treated as functions rather than constants. Also, they have applied polynomial equations to empirically describe the variation of weighted average $\bar{K}$ values with solution composition in some instances, and they have demonstrated that the differential K value can be estimated mathematically by partial differentiation of appropriate polynomial equations. This model has been successfully applied to proton-trace metal exchange reactions on both dissolved humic substances and humic colloids. Very recently, the stoichiometric sorption and kinetics chemistry has been done for the interaction of atrazine with Chernozem humic acid by

Gamble and Khan [53, 131].

1.7 RESEARCH OBJECTIVE

In order to be able to predict the fate of herbicides in the soils, detailed knowledge of the interaction between herbicide in question and organic soil components, and the effect of various factors such as pH, ionic strength, metal ion binding, interaction time and catalyzed hydrolysis must be acquired. As described above, a large number of studies have been done on the interaction of pesticides and soil components. However, most of these studies were focused on the interaction of pesticides with water-soluble fulvic acid, and were qualitative, rather than quantitative. Not much has been done on the interaction between pesticides with water-insoluble humic acid and whole soil, and little information has been given on the nature of the FA and HA involved, on the effect of metal ions on the pesticides-humic substances interaction. Also most studies did not take into account the hydrolysis of AT when they dealt with AT binding. Especially, the use of stoichiometrically defined humic substances has been rare. The design of systematic studies of the binding of polar herbicide AT first by the soluble fraction of soil organic matter, fulvic acid; second by the insoluble organic matter, humic acid; and finally by the whole soil are necessary. These can lead to deeper understanding of the interaction mechanisms. Stoichiometry and interpretation of experimental data and exact testing of the generality of the physical-chemical model which has been developed in our laboratory. can lead to results useful for predictive environmental studies. This sequences of studies is motivated by

the widely held view that organics play a major role in pesticide binding in soils.

The hope of this research is that mechanisms can be elucidated by proceeding from the case of dissolved polyelectrolyte binding (Laurentian FA) through the case of three dimensional colloidal gel particles (Laurentian HA) where Donnan equilibrium are present, to the case of the whole Laurentian soil. Stoichiometrically characterized samples of all these three components are available to us [98-100]. The soil is documented in the compilation of data for CSSC (Canada Soil Survey Committee) reference soil sample [100]. The FA and HA have recently been characterized with respect to ion exchange capacity and proton binding function [98,99] so that the stoichiometry of carboxylate protonation is defined. Elemental analysis is also available.

A standardized HA will constitute a two phase system when it is suspended in an aqueous solution. The HA becomes a carboxylic type cation exchanger having pH-dependent solubility. This requires the development of theoretical description for this heterogeneous system, and of experimental techniques which can be used to simultaneously determine sorption equilibrium constants for atrazine and the amount of hydroxyatrazine hydrolyzed, as well metal ions.

Binding studies will be carried out under conditions of (1) varying pH of the reaction solution, (2) varying ionic strength, (3) varying FA and HA concentration, and varying ratio of soil weight to solution volume, (4) varying atrazine concentrations, (5) different binding time, (6) different FA fractions having different molecular weight cut-off, and (7) varying or constant Cu

concentration. Some supplementary studies on the structural characterization of FA and HA will also be reported.

In the earlier work, the GC analysis method was used for investigations of the binding of AT to Armadale Fulvic Acid. Experiments have indicated that the GC method did not facilitate the simultaneous evaluation of hydrolysis kinetics or the binding of the product hydroxyatrazine. In this study we will develop an ultrafiltration-HPLC method for simultaneous determination of AT and ATOH, and even Cu^{2+} as well. The experimental errors will be minimized by using the advanced hydrophilic membranes with minimal adsorption and by using the point to point batch dilution curve method [69,70]. It is expected that the application of the newly-developed Ultrafiltration-HPLC method will allow small filtrate volumes to be taken from ultrafiltration cell solutions without the equilibria being disturbed.

CHAPTER 2

INTERACTION OF AT WITH LAURENTIAN FA: BINDING AND HYDROLYSIS

2.1 THEORY

2.1.1 Homogeneous AT-FA Binding

In a series of papers [26,68,101], it has been pointed out that the complex mixture of products obtained from mild degradation of FA's coupled with the polyelectrolyte character which complicates activity corrections as cation loading varies suggests the treatment of FA as a continuous distribution of binding sites. Thus, we do not begin by presuming one or a small number of "binding constants" for complexation by FA but exploit a continuum treatment which can reveal simplicity at the end. It is close in spirit to the theory of adsorption.

The complexing equilibrium of AT by FA as previously described [68] is given by equation (1):

$$[\text{AT-FA}] \overset{\bar{K}_{AT}}{\rightleftharpoons} \text{AT} + \text{FA} \qquad (1)$$

An average dissociation constant, $\bar{K}$, may be defined for any extent of binding as:

$$\bar{K}_{AT} = M_{AT}\, C_f / M^b_{AT} \qquad (2)$$

Where M_{AT} is the molarity of free AT, M^b_{AT} is the molarity of bound AT and C_f is the total carboxyl groups of FA in mmoles/g. (As long as M^b_{AT} is small, C_f approximates free carboxyl groups of FA.) In general, $\bar{K}$ is not a constant but a function ; $\bar{K}_{AT} = f(M_{AT}, M^b_{AT}, H^+)$.

A mole fraction variable, X_{AT} is defined by:

$$X_{AT} = M^{b}_{AT} / C_{f} \qquad (3)$$

As the reference [51], [52] and [102] demonstrated, a differential equilibrium function for the FA mixture called K_{AT} is defined by the expression:

$$\bar{K}_{AT} = 1/X_{AT} \int_{0}^{X_{AT}} K_{AT}\, dX_{AT} \qquad (4)$$

The importance of equation (4) lies in the fact that by determining the average equilibrium function one can get an insight into the "intrinsic" or differential equilibrium function K_{AT}. Differentiating equation (4) gives an equation for K_{AT} in terms of the experimental quantity $\bar{K}_{AT}$

$$K_{AT} = \frac{\partial (\bar{K}_{AT}\, X_{AT})}{\partial X_{AT}} \qquad (5)$$

K_{AT} represents an average over the contributions of microsite dissociation constants which contribute to the change of X_{AT} at the point in question. It is a mediating parameter whose significance with respect to the structure of binding sites awaits interpretation. Equation (5) is an important result which supplies an experimental way to calculate the equilibrium function KAT without any assumptions.

There are two approaches open for the treatment of the binding equilibria. They differ by the way the FA concentration defined. In the first approach, as described above, the total Type A carboxyl groups of FA, C, is used to define the mole fraction x. In the second approach, however, the empirical binding capacity of AT, C_{cap}, is used to define C for FA, and the x is obtained by the mole number of AT bound over the binding capacity of AT at the

tested pH, and it has the values runing from 0 to 1.0. In this case, the concentration of free AT, C_0, does not approximate C_{cap}, the observed binding capacity of AT. Equations (2) and (3), therefore, should become $\bar{K}_{AT} = M_{AT}C_0/M^b_{AT} = M_{AT}(C_{cap}-M^b_{AT})/M^b_{AT}$, and $x_{AT} = M^b_{AT}/C_{cap}$, respectively.

In the adsorption theory, the more conventional parameter is the differential free energy calculable as:

$$\Delta G^0 = RT \ln [K_{AT}/\Gamma] \qquad (6)$$

where Γ is the ratio of activity coefficients of AT bound over activity coefficient of AT free times the activity of the empty FA binding sites. Equation (6) may be rewritten to give only experimental quantities on the right:

$$\Delta G^0 + RT \ln \Gamma = RT \ln K_{AT} \qquad (7)$$

Since K_{AT} represents the dissociation equilibrium function, $1/K_{AT}$ is the formation equilibrium function for AT-FA complex, and equation (8) can be obtained:

$$-(\Delta G^0 + RT \ln \Gamma) = RT \ln 1/K_{AT} \qquad (8)$$

Empirically, the form of K_{AT} and the differential free energy can be extracted by plotting $\bar{K}_{AT}\ X_{AT}$ vs X_{AT} according to equation (5). The slope has the significance of K_{AT} at any point. In our work, the plots are commonly straight lines indicating that free energy does not vary with coverage at the level of coverage seen.

Notice that all equations written for AT could be paralleled for ATOH. Plots were also prepared using $K_{ATOH}\ X_{ATOH}$ vs X_{ATOH} to extract free energy of binding of ATOH.

In what follows since our focus is on binding, and not dissociation, we shall more commonly quote value of $1/K_{AT}$ or

$1/K_{ATOH}$ and the corresponding free energies of binding.

2.1.2 Atrazine Hydrolysis by Proton Catalysis

From the scheme of the catalysis reaction of atrazine:

$$AT + H^+ \overset{K_1}{\rightleftharpoons} ATH^+ \xrightarrow[+H_2O]{k} ATOH + 2H^+ \qquad (9)$$

one immediately has:

$$K_1 = \frac{M_{AT}\, a_H}{M_{ATH^+}} \qquad (10)$$

$$-\frac{d\, M_{ATH^+}}{dt} = k\, M_{ATH^+} \qquad (11)$$

where k is the apparent reaction rate constant for singly-protonated AT and K_1 is dissociation constant for singly protonated AT, and M_{AT} and M_{ATH^+} are the molarity of unprotonated and protonated AT, respectively.

Substituting (10) into equation (11):

$$-\frac{d\frac{M_{AT}\, a_H}{K_1}}{dt} = k\, \frac{M_{AT}\, a_H}{K_1} \qquad (12)$$

a_H and K_1 are constant under experimental conditions, so equation (13) can be obtained:

$$-\frac{d\, M_{AT}}{dt} = k\, M_{AT} \qquad (13)$$

The k is the pseudo-first order constant with the unit $(time)^{-1}$. α is used to represent the mole fraction of unprotonated AT, and M_T is the total molarity of atrazine including AT and ATH^+ species.

$$M_T = M_{AT} + M_{ATH^+} \tag{14}$$

$$\alpha = \frac{M_{AT}}{M_T} = \frac{M_{AT}}{M_{AT} + M_{ATH^+}} = \frac{1}{1 + M_{ATH^+}/M_{AT}} \tag{15}$$

substituting (10) to (15),

$$\alpha = \frac{1}{1 + a_H/K_1} = \frac{1}{K_1 + a_H} \tag{16}$$

Then,

$$\frac{M_{AT}}{M_T} = \frac{1}{K_1 + a_H} \tag{17}$$

$$M_{AT} = \frac{1}{K_1 + a_H} M_T \tag{18}$$

Combining (13) and (18), yields equation (19).

$$-\frac{K_1}{K_1 + a_H} \frac{dM_{AT}}{dt} = k\, M_{AT} \frac{1}{K_1 + a_H} \tag{19}$$

$$-\frac{dM_T}{dt} = k\, M_T \tag{20}$$

There are three species in the solution in the studied pH range, AT, ATH^+ and ATOH. By using the material balance relationship for the analytical concentration of atrazine, one has:

$$C = M_{AT} + M_{ATH^+} + M_{ATOH} \tag{21}$$

$$C = M_T + M_{ATOH} \tag{22}$$

$$M_{ATOH} = C - M_T \tag{23}$$

where C is the analytical concentration of atrazine. Substituting (22) into (20):

$$\frac{dM_{ATOH}}{dt} = k\,(C - M_{ATOH}) \tag{24}$$

It is very important to notice the chemical meaning of equations (20) and (24). They are the basis of the calculation and explanation of the experimental results, which tell that the apparent rate constant can be obtained if the total concentration of AT including the unprotonated and protonated forms of atrazine, or the concentration of ATOH can be monitored.

If the experimentally measurable parameters, absorbances are spectrophotometrically monitored, the equation (20) and (23) can be expressed by absorbances:

$$t = \frac{1}{k} \ln \frac{A_0 - A_\infty}{A_t - A_\infty} \qquad (25)$$

$$\ln(A_t - A_\infty) = -kt + \ln(A_0 - A_\infty) \qquad (26)$$

where A_t is the absorbance of AT solution at time t at any analytical wavelength chosen. A_0 and A_∞ are the absorbances at zero and infinite time (that means all AT species exist as AT or ATOH forms) at the chosen wavelength, respectively. The apparent rate constant can be obtained just by plotting $\ln(A_t - A_\infty)$ versus time t. Usually 220 nm or 238 nm (the maximum absorption wavelength of AT and ATOH, respectively) are chosen as analytical wavelengths.

If the HPLC method is used, equation (25) which is directly derived from (20) and (24) can be used to obtain k:

$$t = \frac{1}{k} \ln \frac{C}{M_T} = \frac{1}{k} \ln \frac{C}{C - M_{ATOH}} \qquad (27)$$

In consideration of the effect of catalyst, H^+, one has

$$k = k_0 + k_H a_H^n \qquad (28)$$

where k_0 is the reaction rate constant as a_H approaches zero, k_H is the acid catalysis rate constant, and n is the reaction order of hydrogen ion. Based on equation (28), a plot of k versus the concentration of H^+ can be made. The curve is extrapolated to the concentration of H^+ equal to zero allowing k_0 to be obtained.

$$k - k_0 = k_H a_H^n \tag{29}$$

$$\log(k - k_0) = n \log a_H + \log k_H \tag{30}$$

$$\log(k-k_0) = -n(pH) + \log k_H \tag{31}$$

According to equation (31), the plotting of $\log(k-k_0)$ vs. pH gives the reaction order of H^+, n, as the slope.

2.1.3 Atrazine Hydrolysis by Fulvic Acid

According to Gamble and Khan [26], in all forms of FA functional groups, only the protonated type A carboxyl groups, R-COOH, act as catalyst, so the kinetic equation for AT hydrolysis in the presence of FA can be written in the following form:

$$-\frac{dC}{dt} = k_{ATH^+} M_{ATH^+} + k_{FA} M_{FA} C \tag{32}$$

where C and M_{ATH^+} as described in 2.1.2, is the molarity of initial total atrazine and the molarity of singly protonated AT, respectively. M_{FA} is the molarity of protonated type A carboxyl groups of Laurentian Fulvic Acid, and the k terms are the corresponding kinetic rate constant of proton and type A carboxyl groups. The experimentally observed form of the reaction rate law can be expressed by equation (33):

$$-\frac{dC}{dt} = k_{obs} C \tag{33}$$

where k_{obs} is the experimentally observed overall first order rate constant. A general equation for k_{obs} is obtained directly from equation (32) and (33):

$$k_{obs} = k_{ATH^+} \frac{M_{ATH^+}}{C} + k_{FA} M_{FA} \qquad (34)$$

The mole fraction of protonated atrazine is given by

$$x = \frac{M_{ATH^+}}{C} \qquad (35)$$

By definition the rate constant that accounts for the effect of AT protonation on hydrolysis of AT is

$$k = k_{ATH^+} x \qquad (36)$$

After subtraction of the proton catalysis term, equation (34) becomes:

$$(k_{obs} - k) = k_{FA} M_{FA} \qquad (37)$$

From the basic kinetic equation (33), equations (38) and (39) which contain the terms of AT and ATOH concentrations at time t can be finally obtained,

$$t = \frac{1}{k_{obs}} \ln \frac{C}{M_T} \qquad (38)$$

$$t = \frac{1}{k_{obs}} \ln \frac{C}{C - M_{ATOH}} \qquad (39)$$

where M_T is the molarity of total atrazine including protonated and unprotonated atrazine at time t. Equations (38) and (39) are reduced to equation (26) when they are applied to the situation where no FA exists.

Gamble et al have recently established the equation, which describes the dependence of k on pH,

$$k = \frac{0.14 \times 10^{-pH}}{2.45 \times 10^{-2} + 10^{-pH}} \text{ days}^{-1} \qquad (40)$$

Hence, the k_{FA} can be experimentally obtained by combining equation (37) and (40):

$$k_{FA}M_{FA} = \left(k_{obs} - \frac{0.14\times10^{-pH}}{2.45\times10^{-2} + 10^{-pH}} \right) \qquad (41)$$

$$t_{1/2} = \frac{\ln 2}{k_{obs}} \qquad (42)$$

Equation (41) can be used to calculate k_{FA} values and to describe AT persistence in FA solutions if the acid-base titration curve can been determined and the FA has been well characterized.

2.2 EXPERIMENTAL

2.2.1 Materials

(1) Atrazine stock solution

Exactly 0.04314 gram of atrazine (99.99% pure, Polyscience Corp.) was weighed (±0.00001g), and transferred to a 200 mL Erlenmeyer flask, and about 1500 ml deionized water was added. The mixture was stirred with a magnetic bar and heating until all atrazine was dissolved. The heat was then removed and the AT solution was stirred overnight at room temperature. The solution was transferred to a 2000 ml volumetric flask and diluted with water to the mark. The concentration of AT stock solution was 1.000×10^{-4} M.

(2) Hydroxyatrazine stock solution

Exactly 0.01972 gram of hydroxyatrazine (supplied by Dr. D.S. Gamble) was weighed and transferred to a 2000 ml Erlenmeyer flask, and the same procedure as described above was used to obtain ATOH stock solution. The concentration of ATOH stock solution was

0.5000×10^{-4} M (at about pH 4.5). The purity of ATOH was verified by the absence of the 220 nm absorbance maximum of AT and the peak for ATOH at 238 nm which agreed with the literature [103], and was further confirmed by the appearance of one-peak in HPLC with a retention time 6.2 minutes which is the characteristic peak of ATOH.

(3) FA stock solution

The fulvic acid used was Laurentian Fulvic Acid prepared and purified according to the procedure described in references [104, 105].

(4) Other chemicals were reagent grade and used as received.

2.2.2 Equipment

(1) pH meter

The pH meter used for pH measurement and pH adjustment was Metrohm Herisau pH meter, Model E 300B equipped with a Fisher EA 120-UX glass combination electrode. It was calibrated with pH 4.00, 7.00 and 9.00 standard buffer solutions, depending on the measurement requirements.

(2) Atomic absorption spectrophotometer

A Perkin-Elmer Flame Absorption Spectrophotometer (model 503) equipped with a copper hollow cathode lamp was used to analyze total copper concentrations in some filtrates and some cell solutions, so as to compare the results with the obtained from the HPLC method. The wavelength and current used for analysis was 324.8 nm and 5 mA, respectively.

(3) UV-VIS spectrophotometer

A Perkin-Elmer UV/VIS spectrophotometer, Model 502, equipped

with a deuterium and a Tungsten lamp was used to measure the absorption spectra of samples. Silica cells of 10 mm light path length and slit 1nm were used. The recorder coupled with spectrophotometer was Servocorder type SR 6254 (Watanabe Corp, Japan).

(4) Ultrafiltration stirred cell

An Amicon Ultrafiltration Stirred Cell, Model 8050, having a maximum volume 50 ml was used for binding studies in the batch ultrafiltration technique, in which the advanced hydrophilic YM-2 membranes with molecular weight cut-off 1000 were used. Before use, the membrane was rinsed by floating it skin (glossy) side down in a beaker of deionized water for six hours, changing water three times. Then the membrane was mounted in its respective cell for filtration. The filtration technique will be described later. When the membrane was temporarily not in use, it was stored in deionized water.

During filtration, a Fisher magnetic stirrer (Cat. No. 14-511-2) was used to rotate the magnetic bar in the Amicon stirred cell.

(5) HPLC

The high performance liquid chromatography system used for most of this study was the Waters Associates Liquid Chromatography system which consisted of Model U6K injector, Model M-6000A pump and Model 440 UV absorption detector. The wavelength used was 254 nm at 0.02 and 0.05 a.u.f.s. The flow rate for C_{18} column is 1.0ml/min. The eluent throughout this work was mixture of 50% acetonitrile and 50% deionized water, for which the pH value was adjusted to 2.50 by adding the hydrochloric acid. The column used

was a C_{18} (LC-7, silica, 10 μm, 250 x 4.6 mm) reverse phase packed column. A 25 μL syringe was used for injecting samples. The detailed HPLC experimental conditions for analysis of atrazine, hydroxyatrazine and copper ion are shown in Table 2.1

Table 2.1 Conditions used for HPLC analysis

PARAMETERS	CONDITIONS
column	C18, LC7, silica, 10μm, 250×4.6 mm
column temperature	room temperature (about 22°C)
eluent	CH_3CN : H_2O = 50:50 (V/V) pH = 2.50 (HCl = 3.18×10^{-3}M)
flow rate	1.0 ml/min
pressure	around 150 psi.for new column
UV detector wavelength	254 nm
a.u.f.s	0.02 or 0.05
injection volume	20 or 50 μl
recorder	Servocorder, type SR 6254 (Watanabe Corp, Japan), 10mV range
chart speed	0.5 cm/min

Aliquots of FA stock solutions (1.000g/100ml or 2.500g/100ml) and AT (1.000×10^{-4}M) or ATOH stock solutions (0.5000×10^{-4}M) were used for sample preparation. Standard HCl or NaOH solution was added to adjust pH to the desired pH values then each sample solution was diluted to a final volume of 25.00 ml and sealed securely with Parafilm. Paired controls (no FA) and samples were shaken together for three days at room temperature (21±2°C). After three days, a solution was transferred to the ultrafiltration cell for filtering at 50 psi. The first ten drops of filtrate were discarded then an aliquot of about 1 ml was collected for free equilibrium atrazine and hydroxyatrazine analysis. The analysis for AT and ATOH was carried out by injection of 20.0 or 50.0 μl

filtrate to the HPLC instrument using 50% CH_3CN/50% water (V/V) with 3.18×10^{-3} M HCl as eluent. Total handling time was about 12 minutes.

2.2.4 Measurement Procedures

2.2.4.1 Determination of total acidity of Laurentian FA

The determination of the operationally defined total acidity was carried out using the method employed by Schnitzer and described by Stevenson [106]. 0.1000 gram of FA was accurately weighed and transferred to a 125 ml Erlenmeyer flask. 20 ml of saturated $Ba(OH)_2$ solution (about 0.095 M) were added followed by deareation by gently bubbling 99.99% pure nitrogen into solutions for five minutes. The flasks were tightly sealed with parafilm. Simultaneously, the blank $Ba(OH)_2$ solutions without FA were prepared by same procedure. Both sample and blank solutions were shaken for 24 hours at room temperature. Following this, the sample solutions were filtered, the residue was washed thoroughly with CO_2-free distilled water, then titrate the blank and sample were titrated potentiometrically (Fisher EA-1210-UX glass combination electrode) with standardized 0.06048 M HCl solution to pH 8.0. Triplicate titrations were done to give an average result.

2.2.4.2 Atrazine hydrolysis by proton catalysis

Table 2.2 gives the experimental condition for the hydrolysis of a constant AT concentration at different pH. The UV/VIS spectrometer was used for the measurement of absorbance as a function of time at 3 days intervals. The samples were thermostatted at 24 ± 1^{0}C. The results of this experiment are

described in section 2.3.

Table 2.2 The experimental conditions for hydrolysis of AT at different pH values

(AT=3.00×10^{-5}M, Final volume = 50.00 ml)

No	1.0N HCl (ml)	0.01N NaOH (ml)	H_2O (ml)	pH (±0.03)
1	6.00		29.00	1.07
2	4.00		31.00	1.20
3	2.00		33.00	1.40
4	1.00		34.00	1.66
5	0.50		34.50	1.90
6	0.20		34.80	2.20
7	0.10		34.90	2.45
	0.1N HCl			
8	0.50		34.50	2.80
9	0.20		34.80	3.18
10	0.05		34.95	3.40
11	0.01		34.99	4.09
12	0.00		35.00	5.22
13		0.10	34.90	7.01
14		0.20	34.80	7.94
15		0.50	34.50	9.50

2.2.4.3 Atrazine binding

(1) Atrazine variation at constant pH and low ionic strength

The design of a typical batch experiment on AT variation at constant pH and low ionic strength is given in Table 2.3.

It should be emphasized here that the exact amount of acid or base for a particular pH was determined by preliminary tests. Different amount of acid or base were needed to keep AT control and AT-FA samples at the same pH level because FA, as a weak organic acid, is a very effective buffer.

Table 2.3 Atrazine variation experiment at pH 2.20

(Total volume = 25.00 ml, pH = 2.20)

AT-FA samples (1.00ml FA + 1.00ml 0.25N HCl +AT)				AT control (1.00 ml 0.25N HCL + AT)		
No	1.00×10^{-4}M AT (ml)	[AT] ($\times10^{-5}$M)	H_2O (ml)	1.00×10^{-4}M AT (ml)	[AT] ($\times10^{-5}$M)	H_2O (ml)
1	2.00	0.80	21.00	2.00	0.80	22.00
2	3.00	1.20	20.00	3.75	1.50	20.25
3	4.00	1.60	19.00	5.00	2.00	19.00
4	5.00	2.00	18.00	6.25	2.50	17.75
5	7.00	2.80	16.00	7.50	3.00	16.50
6	10.00	4.00	13.00	10.00	4.00	14.00
7	12.00	4.80	11.00	12.50	5.00	11.50
8	14.00	5.60	9.00	15.00	6.00	9.00
9	17.00	6.80	6.00	20.00	8.00	4.00
10	20.00	8.00	3.00			

* the concentration of FA stock solution was 2.500g/100ml, each AT-FA solution had 1.00ml of such FA stock solution, so the final concentration of FA was 1.000g/L.

AT and ATOH calibration curves were fitted by the linear regression to straight lines respectively. The equilibrium concentration for free AT and free ATOH hydrolyzed from AT in AT-FA samples was obtained by interpolating on regression lines.

Similar experiments were carried out at pH 1.24, 1.66, 1.90, 2.20, 2.40, 2.80, 3.10, 3.65, 4.40, 5.00, 5.50, 6.60, 7.80 and 9.50 as to find the effect of pH on the atrazine binding to fulvic acid. The details of these experiments are given in section 2.3.

(2) Atrazine variation at constant pH in the presence of 0.1M KCl

These experiments were designed and carried out in the same fashion as those in the above section. The only exception was the addition of KCl electrolyte to all solutions so as to do binding studies in the high ionic strength medium.

1.00 ml of 2.5 M KCl was added to each AT control and AT-FA solution. The final concentration of KCl in solutions was 0.1 M. It was observed that AT-FA samples became somewhat turbid after 3 days shaking when pH was lower than 2. At pH 1.40, a little yellow-brown precipitate could be seen.

(3) Effect of FA concentration on AT binding

The FA effect was investigated at a pH 1.40 in the absence of KCl and pH 2.20 in the presence of 0.1 M KCl. These pH's were chosen to be near the maximum binding capacity. Fulvic acid concentrations were varied from 0.1000 to 1.000 g/L.

(4) Time effect on AT binding

The time effect was studied at pH 2.10 and pH 3.30 with varying shaking time from a few hours to 3 days. When the designed shaking time was reached, control and sample solutions were filtrated for HPLC measurement.

2.2.4.4 Hydroxyatrazine Binding

All experiments described below were carried on in the same way as AT binding experiments, which included:

(1) ATOH variation at constant pH and low ionic strength.

The pH values tested were 2.00, 2.50, 2.85, 3.00, 3.85, 4.70, 6.80 and 8.50. For each pH, ATOH variation range was from 4.0×10^{-6} to 4.0×10^{-5}M, and the final FA concentration was 0.500g/L.

(2) ATOH variation at constant pH in the presence of 0.1M KCl.

The pH tested were 3.10, 4.40 and 5.30. These experiments were designed and carried out in the same fashion as that described in the above section. The only difference is the addition of KCl electrolyte to all solutions.

(3) Effect of FA concentration on ATOH-FA binding at pH 3.00.

The FA concentration chosen for studying the effect of FA on ATOH binding were 0.1000, 0.5000 and 0.7500g/L.

(4) Competition for binding sites between AT and ATOH

This experiment was designed to study the AT and ATOH binding behavior when they coexist in a same solution. The pH chosen was 3.05. FA concentration was 0.5000g/L, and AT and ATOH concentration was 0.40 to 4.00 $\times 10^{-5}$M and 0.20 to 2.00$\times 10^{-5}$M, respectively.

2.3 RESULTS

2.3.1 Characterization of Laurentian Fulvic Acid

The total acidity was found according to the calculation equation given by Schnitzer [106] to be 11.63±0.10 mmoles per gram FA.

The acidic carboxyl functional group data obtained by potentiometric titration [98] are the following: 5.11±0.25 mmoles/g FA of total Type A carboxyl groups (which include highly acidic carboxylic groups on the aromatic rings, ortho to phenolic OH groups, referred to as Type I carboxyl groups, and moderately acidic carboxylic groups, referred to as Type II carboxyl groups), 3.49±0.30 mmoles/g FA of total Type B acidic carboxyl functional groups which are very weak acidic groups. For comparison, the Armadale Bh FA has been found to have corresponding values of 4.99

and 2.72 mmole/g FA. The acidic ionization equilibrium of Type I and Type II carboxyl groups has been calculated as a function of its degree of ionization in 0.1 M KCl at 25^{0}C, which are listed in Table 2.4 and 2.5, respectively.

The phenolic content of Laurentian FA was simply determined by subtracting the total carboxyl contents from the total acidity, which is 3.03±0.10 mmole per gram FA.

2.3.2. Evaluation of Ultrafiltration-HPLC Method

A representative HPLC chromatogram of AT-Cu-FA solution at pH 2.20 is shown in Figure 2.1.

The coupling of ultrafiltration with HPLC (UF-HPLC) has a number of advantages: (1) The retention times (t_r) and basal peak widths (W) for AT and ATOH are: t_r= 8.7 and 6.2 min., W = 0.4 and 0.3 min., respectively.(The retention time of Cu(II) is 4.2 min.,) According to HPLC theory [107], an R_s=1 value (R_s is the resolution of the column) would give complete separation at the base line. The resolution of AT and ATOH, R_s=7.7, can be obtained from the equation $R_s = 2\left(\frac{t_{R2} - t_{R1}}{W1 + W2}\right)$, which indicates very satisfactory separation at the base line between AT and ATOH. (2) Precision of the estimation is better than 1.5% (95% confidence) at 1.000×10^{-5}M atrazine (see the Table 2.6). (3) Analytical curves are linear (R >0.999) over a wide concentration range. (4) The detection limit is as small as 0.9 ng atrazine.

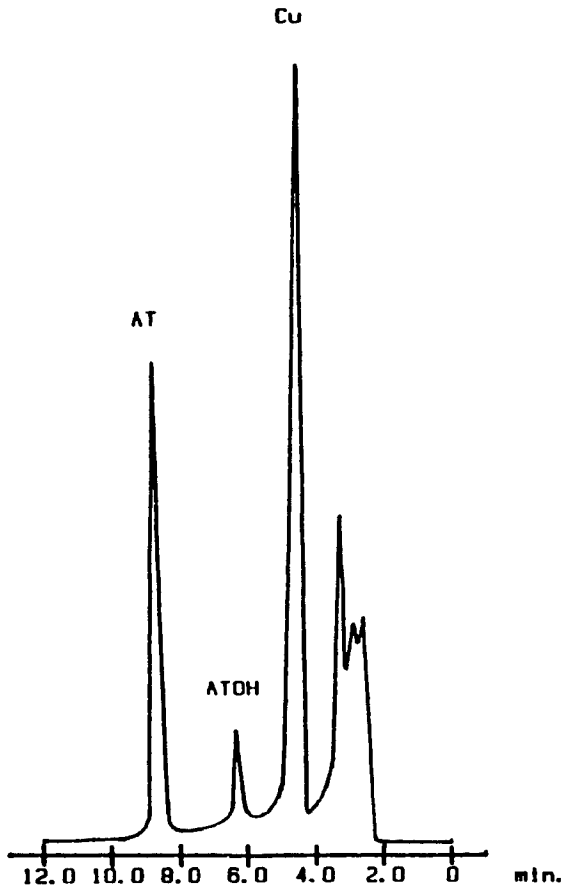

FIG. 2.1 HPLC CHROMATOGRAM OF AT-Cu-FA AT pH 2.20

Table 2.4 Ionization of Type I carboxyl groups in 0.1 M KCl at 25°C

H^+molarity ($x10^{-3}M$)	$\bar{K}_1(x10^{-3})$	α_1
1.423	1.918	0.5741
1.339	1.829	0.5773
1.221	1.714	0.5839
1.175	1.653	0.5845
1.082	1.530	0.5858
1.013	1.471	0.5921
0.9331	1.376	0.5959
0.8673	1.314	0.6024
0.7950	1.232	0.6078
0.7384	1.186	0.6163
0.6742	1.115	0.6232
0.6083	1.034	0.6296
0.5387	0.9392	0.6355
0.4816	0.8701	0.6437
0.4305	0.8108	0.6531
0.3867	0.7641	0.6640
0.3473	0.7237	0.6757
0.3066	0.6736	0.6872
0.2720	0.6341	0.6998
0.2413	0.6001	0.7132
0.2168	0.5800	0.7279
0.1875	0.5381	0.7416
0.1622	0.5028	0.7561
0.1415	0.4779	0.7715
0.1189	0.4380	0.7865
0.1047	0.4273	0.8032
0.08986	0.4088	0.8198
0.07590	0.3883	0.8365
0.06354	0.3705	0.8536

Compared to the use of GC in these studies, the main advantage of HPLC is simultaneous determination of AT and ATOH without involvement with extraction and methylation. Previous work has demonstrated that the 2-hydroxy analogs of s-triazines cannot be readily gas chromatographed and it is necessary to derivatize them into methylated, alkylated or silylated derivatives before GC analysis [106,108]. As well, the HPLC

method is rapid, conservative of material and more precise and reproducible.

A theoretical analysis with supporting experimental results has been done previousely for the particular case of AT, FA, and YM2 membranes [69].

Table 2.5 Ionization of Type II carboxyl groups in 0.1 M KCl at 25°C

H^+ molarity ($\times 10^{-6}$M)	$K\bar{2}(\times 10^{-6})$	$\alpha 2$
5.285	1.139	0.1773
4.098	1.008	0.1974
2.880	0.7992	0.2172
2.023	0.6320	0.2380
1.398	0.4898	0.2594
0.8114	0.3361	0.2929
0.7367	0.3221	0.3042
0.5314	0.2582	0.3270
0.3608	0.1941	0.3498
0.2480	0.1474	0.3728
0.1650	0.1082	0.3960
0.1179	0.08513	0.4193
0.07515	0.05965	0.4425
0.04701	0.04049	0.4625
0.02686	0.02573	0.4893
0.01584	0.01668	0.5127
0.009471	0.01095	0.5362
0.005452	0.006930	0.5597
0.003018	0.004225	0.5833

Various factors influencing the binding equilibrium and retention of AT and ATOH such as filtrate volume, pH values, concentration of AT and ATOH, ionic strength have been thoroughly studied. (1) Filtrate volume. With a sample of 25.00 ml, filtrate of up to 3.0 ml produces no noticeable perturbation in the AT and ATOH values and therefore, collection of 1.0 ml was adopted

(Table 2.7) (2) Solute concentration. The concentration change of AT and ATOH had no effect on the retention of AT and ATOH molecules. Both AT and ATOH exhibit very good linear relationships of HPLC peak heights vs. concentrations in a wide range of concentration of AT and ATOH. (3) pH. The excellent agreement of the UV and HPLC measurements demonstrated the pH change in wide range had no effect on the passage of AT and ATOH through YM2 membrane. (4) Electrolyte. UV and HPLC measurements clearly showed that the presence of 0.1 M KCl had no effect on the passage of AT and ATOH through the membrane.

Saar and Weber [82] pointed out in an excellent review that the chief advantage of ultrafiltration separation technique is that it is fast, and free from ionic strength, metal ion or species restrictions. It has, however, two major pitfalls: adsorption of species on membranes and the possibility of shifting equilibria. These two pitfalls have been overcome in our newly developed UF-HPLC method. First, YM-2 membrane exhibits minimal adsorption, furthermore, we always simultaneously run the control and sample solutions and used the point to point dilution curve method, so that the interference of membranes can be minimized if interferences exist. Second, the very small filtrate volume taken from the cell solution, less than 1.0 ml which is only 4% of bulk solution volume, had no observable perturbation effect on the equilibria of bulk solution.

The combination of these distinct advantages makes UF-HPLC method much more powerful and useful for the study and routine monitoring of binding and hydrolysis of pesticides by humic substances than other methods. We anticipate that its

elaborations will find many uses.

Table 2.6 Precision of UF-HPLC method

(a.u.f.s = 0.02, injection volume = 20 μl)

AT = 1.00×10^{-5}M		AT = 2.50×10^{-5}M, ATOH = 1.25×10^{-5}M		
No	H_{AT} (cm)	No	H_{AT} (cm)	H_{ATOH} (cm)
1	2.30	1	5.70	4.55
2	2.35	2	5.75	4.55
3	2.28	3	5.80	4.60
4	2.28	4	5.80	4.60
5	2.32	5	5.70	4.55
average	2.31		5.75	4.57
S	0.0265		0.0447	0.0245
$\mu=\bar{x} \pm t\frac{s}{\sqrt{n}}$	2.31±0.037		5.75±0.062	4.57±0.034

Table 2.7 Effect of filtrate volume

AT = 4.00×10^{-5}M			ATOH = 4.00×10^{-5}M		
No	Filtrate V (ml)	H_{AT} (cm)	No	filtrate V (ml)	H_{ATOH} (cm)
1	0 - 0.5	discarded	1	0 - 0.5	discarded
2	0.5 - 1.0	6.30	2	0.5 - 1.0	10.00
3	1.0 - 1.5	6.50	3	1.0 - 1.5	9.80
4	1.5 - 2.0	6.40	4	1.5 - 2.0	10.05
5	2.0 - 2.5	6.40	5	2.0 - 2.5	9.95
6	2.5 - 3.0	6.60	6	2.5 - 3.0	10.15
average		6.44			9.99
S		0.102			0.116
		6.44±0.139			9.99±0.147

2.3.3 pK_a Determination and The Extraction Properties of ATOH

(1) pK_a determination

Infrared spectral data and NMR double resonance experiments suggests the presence of keto form of ATOH [110,111]. Two tautometric forms of ATOH are possible in which the keto form predominates in the protonated ATOH. Figure 2.2 shows unprotonated (1), (2) and some possible tautometric (3) and resonance structure of protonated ATOH [111, 112]. Structure (4) was suggested to be the most likely form of the adsorbed, protonated hydroxyatrazine.

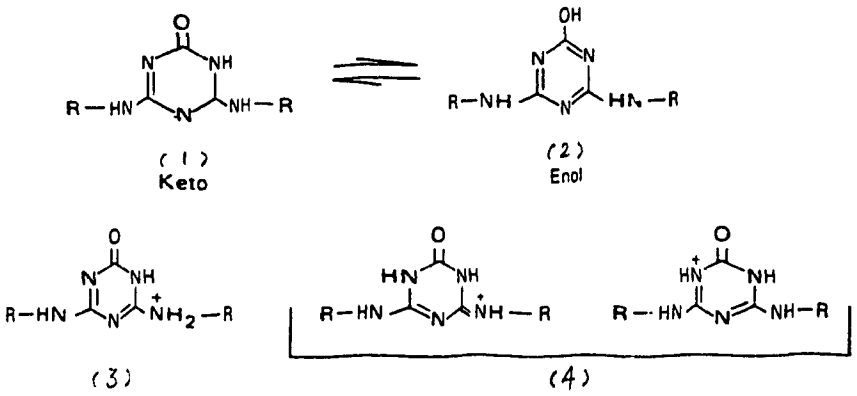

Figure 2.2 Structures of ATOH

The calculation of the pK_a value of ATOH was performed according to the following equation [113]:

$$pK_a = pH - \log\frac{A - A_I}{A_M - A}$$

Where A is the absorbance of all species of ATOH at each pH, A_I is the absorbance of pure ionic species, and A_M is the absorbance of pure molecular species.

The analytical wavelength used for ATOH was 220 nm. Figure

2.3 contains a set of absorption curves obtained from a series of ATOH solution with different pH values and resulting plot of absorbance versus pH.

The pK_a value of ATOH was determined from the plot in Figure 2.4 to be 5.05 ± 0.05. Table 2.8 summarized some properties of atrazine and its methoxy- and hydroxy- derivatives.

It can be seen clearly from Figure 2.3 that the great changes took place as pH values of ATOH solution changed. The interpretation of spectra may account for both acid-base and tautometric equilibria.

It was observed that even at pH 2.05, 5.30 and 9.30 ATOH shows different UV spectra, although it gives the same chromatograms with same peak height and same retention time in HPLC. This is because the protonation of ATOH is a fully reversible reaction.

Table 2.8 Chemical properties of AT and its derivatives

No	Common name	Group in 2-pos	pK_a	pH	λ_{max} (nm)	ε
1	atrazine	-Cl	1.68[43] 1.62[23]	3.50-9.50	220	*3.85x10^4
2	ametryne	-SH3	3.12[43]			
3	atratone	-OCH3	4.20[43]	10.0	217	3.64x10^4
4	hydroxy-atrazine	-OH	5.05	1.20-3.00	238	*2.53x10^4

a. The values with "*" were determined in this paper.
b. If the pH is lower than 2.50, the hydrolysis reaction of AT will take place, thus its spectrum will change as pH changes and time goes on.
c. For ATOH, the values 238 nm and 2.53 x 10^4 are the absorption maximum and absorptivity of its protonated form, respectively. If pH is higher than 4.0, the ATOH will exist in the keto and enol forms, its spectra will change as pH changes.

FIG. 2.3 ABSORPTION SPECTRA OF ATOH AT DIFFERENT pH

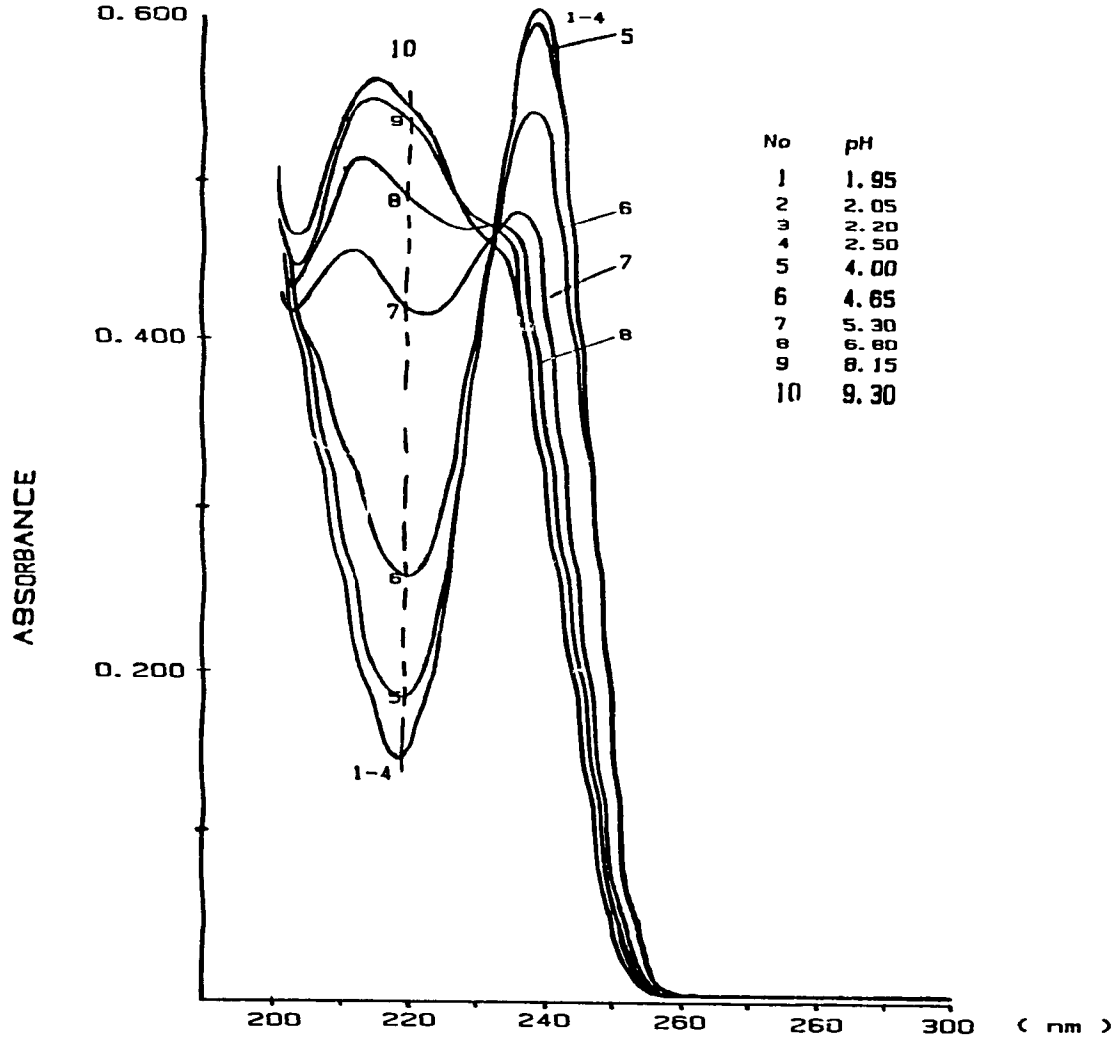

FIG. 2.4 DETERMINATION OF pK VALUE OF ATOH

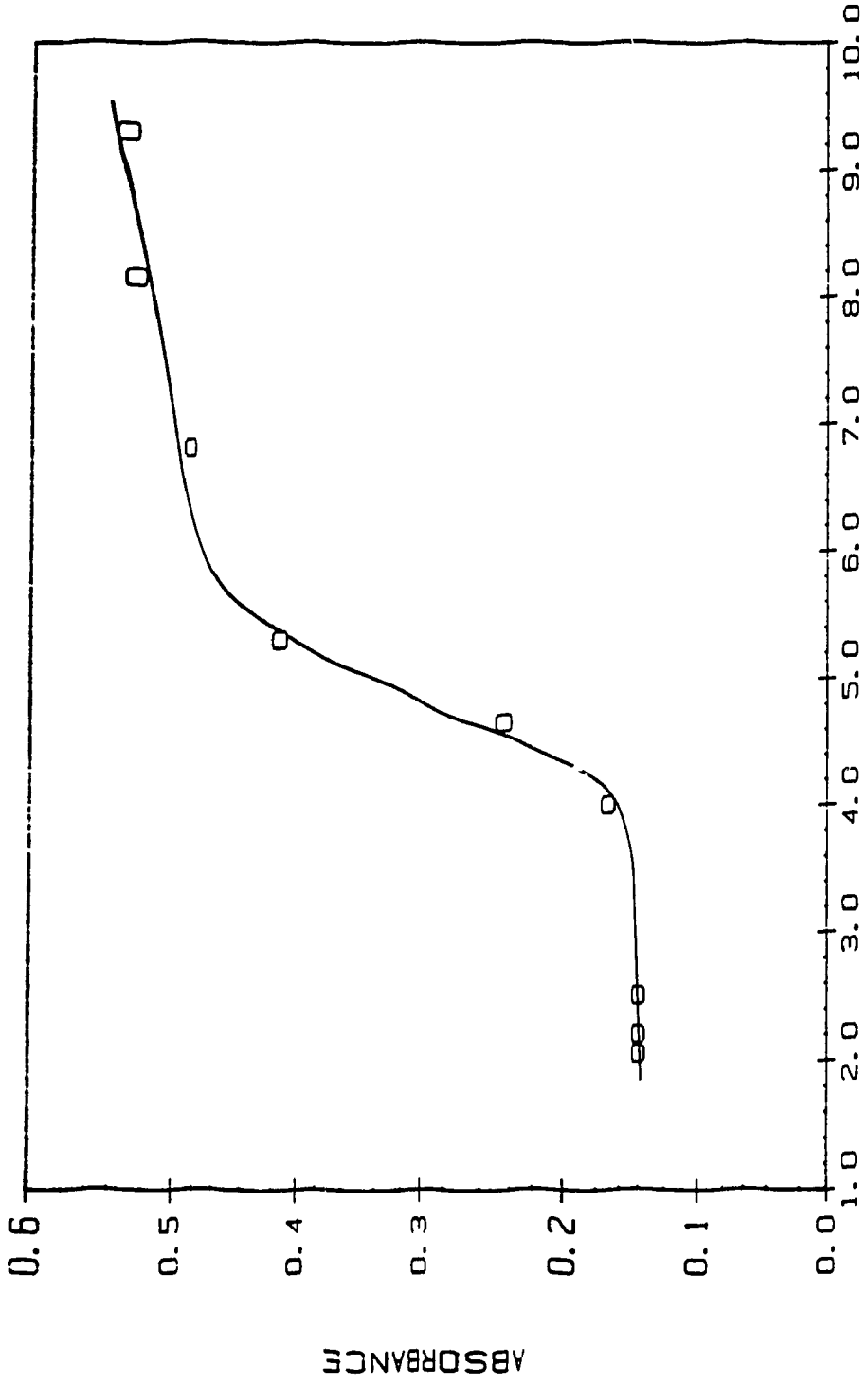

(2) The extraction properties of ATOH

It is found from experiments that, unlike atrazine, ATOH at any pH value cannot be extracted with benzene. The experimental procedure used is as follows: 5.00 ml ATOH solutions at different pH were transferred to 60 ml glass stoppered separatory funnels, and 20 ml pesticide grade benzene was added. The funnels were securely stoppered and placed on a shaker, shaking vigorously for 1 hour. The water was then removed to small beakers, and the benzene phase was discarded. The amount of ATOH in aqueous samples before and after extraction were determined through injecting 20 μl to HPLC and by taking the height of ATOH peaks. The results are shown in Table 2.9.

Table 2.9 Determination of ATOH before and after extraction

No	pH	Samples	Retention time (min.)		H_{ATOH}	$\Delta H/H_{ATOH}$
			ATOH	BENZENE	(cm)	(%)
1	2.05	before ext.	6.2		8.85	
		after ext.	6.2	9.5	8.80	0.7
2	5.30	before ext.	6.2		9.00	
		after ext.	6.2	9.5	8.80	2.2
3	8.15	before ext.	6.2		9.00	
		after ext.	6.2	9.5	8.90	1.1
4	9.50	before ext.	6.2		8.80	
		after ext.	6.2	9.5	8.65	2.8

Table 2.9 shows that in the pH range studied there are no significant differences of ATOH contents between the original ATOH solution and its corresponding solution after extraction. That means the hydroxyatrazine, whether it exist as the neutral form,

the protonated form, or tautometric forms, was unextractable by nonpolar organic solvent benzene.

Atrazine can be readily extracted by benzene, but ATOH cannot. This fact suggests the importance of the substituent in 2-position of triazine ring. A comparison of atrazine, ametryne, atratone and hydroxyatrazine yields the following ranking of compounds with their pK_a values in a decreasing order of basicity:

compounds:	ATOH	Atratone	Ametryne	Atrazine
pK_a :	5.05 >	4.20 >	3.12 >	1.62
2-substituent:	-OH	$-OCH_3$	$-SCH_3$	-Cl

It is apparent that the substituents in the 2-position have a great effect on the electron density of triazine ring and hence a great effect on the pK_a values and the extraction properties. The combination of resonance and the strong induction effect of oxygen atom makes ATOH have the highest basicity among these four compounds, and also makes ATOH molecule very polar, consequently, ATOH cannot be extracted by nonpolar benzene.

2.3.4 The Hydrolysis of Atrazine by Proton Catalysis

A number of publications have dealt with the problem of atrazine hydrolysis in various conditions[23,25,28,44,54,103,115].

It has been shown that the chemical reaction of AT in soil involves hydroxylation, which results in the loss of the herbicide phytotoxicity. Among soil components, fulvic acid is known as an important factor of catalysis of AT hydrolysis. However, before the interaction of AT with such a complex system can be properly interpreted, the proton catalysis of AT must be first well

understood. If the contribution of the proton to the total catalysis could be quantitatively predicted, then the investigation of the fulvic acid, humic acid and even whole soil would be more feasible.

All of the hydrolysis experiments were run for 40 days, and about 250 spectrophotometric measurements and about 50 HPLC measurements as a function of time were conducted, and 600 data points were taken from UV spectra and HPLC chromatograms. The samples with the initial AT concentration 3.00×10^{-5}M, having a wide pH range from 1 to 10, were thermostatted at 24 ± 2^{o}C.

Two typical series of UV spectra are shown in Figure 2.5 and 2.6. One series has the spectra of AT at different pH values and the another has the spectra of an AT solution at a certain pH value (pH 1.67) at different time periods.

It can be seen clearly from Fig. 2.5 and 2.6 that the spectra of AT greatly depend on the pH and time. The existence of the isochromatic point explicitly indicates the existence of two species, atrazine and its hydrolyzed product, hydroxyatrazine, and their closed relation to the concentration of hydrogen ion. The lower the pH, the faster the conversion of AT to ATOH.

The curves of the absorbance of AT at the measurement wavelength, 220 nm and 238 nm, versus the time during 40 days of the period are shown in Figure 2.7A and 2.7B.

Both Fig.2.7A and Fig.2.7B show that when pH values are higher than 3.40, there is no significant change of absorbance at either 220 nm or 238 nm during the whole period. This conclusion is strongly supported by the HPLC measurements. Table 2.10 lists the results of HPLC measurements.

FIG. 2.5 ABSORPTION SPECTRA OF ATRAZINE AT 17 DAYS

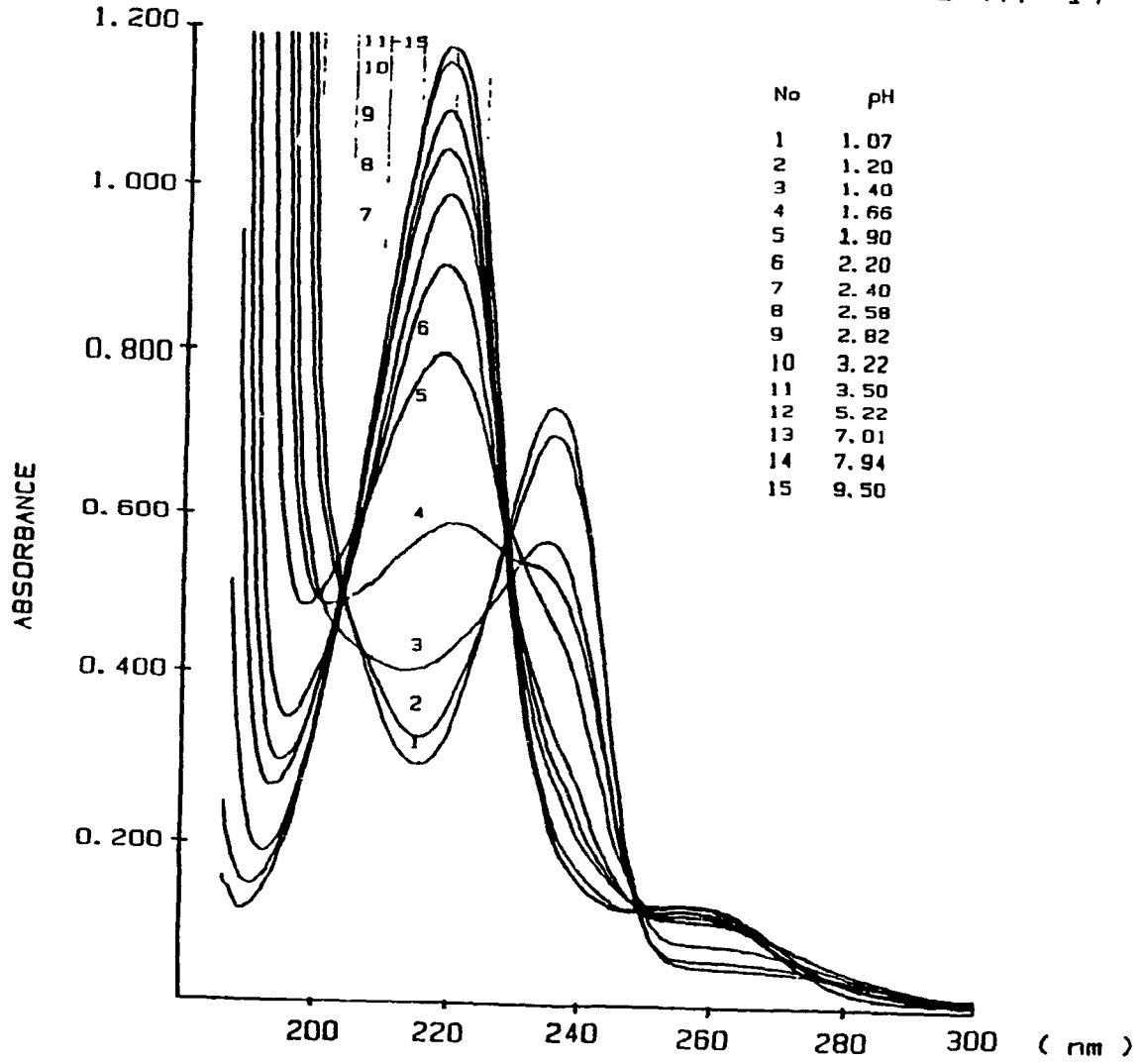

FIG. 2.6 ABSORPTION SPECTRA OF ATRAZINE AT VARIOUS TIMES

(pH=1.66, AT=3.00X10^{-5} M)

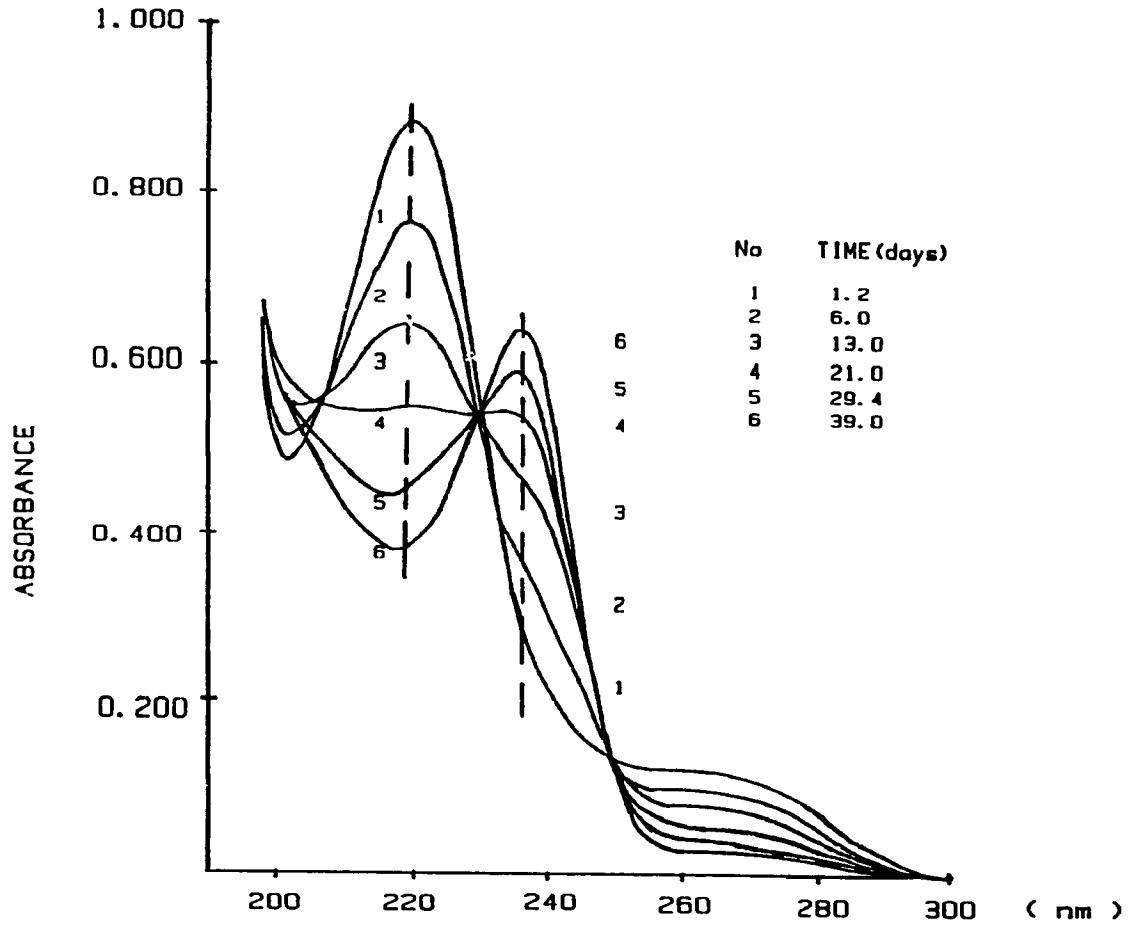

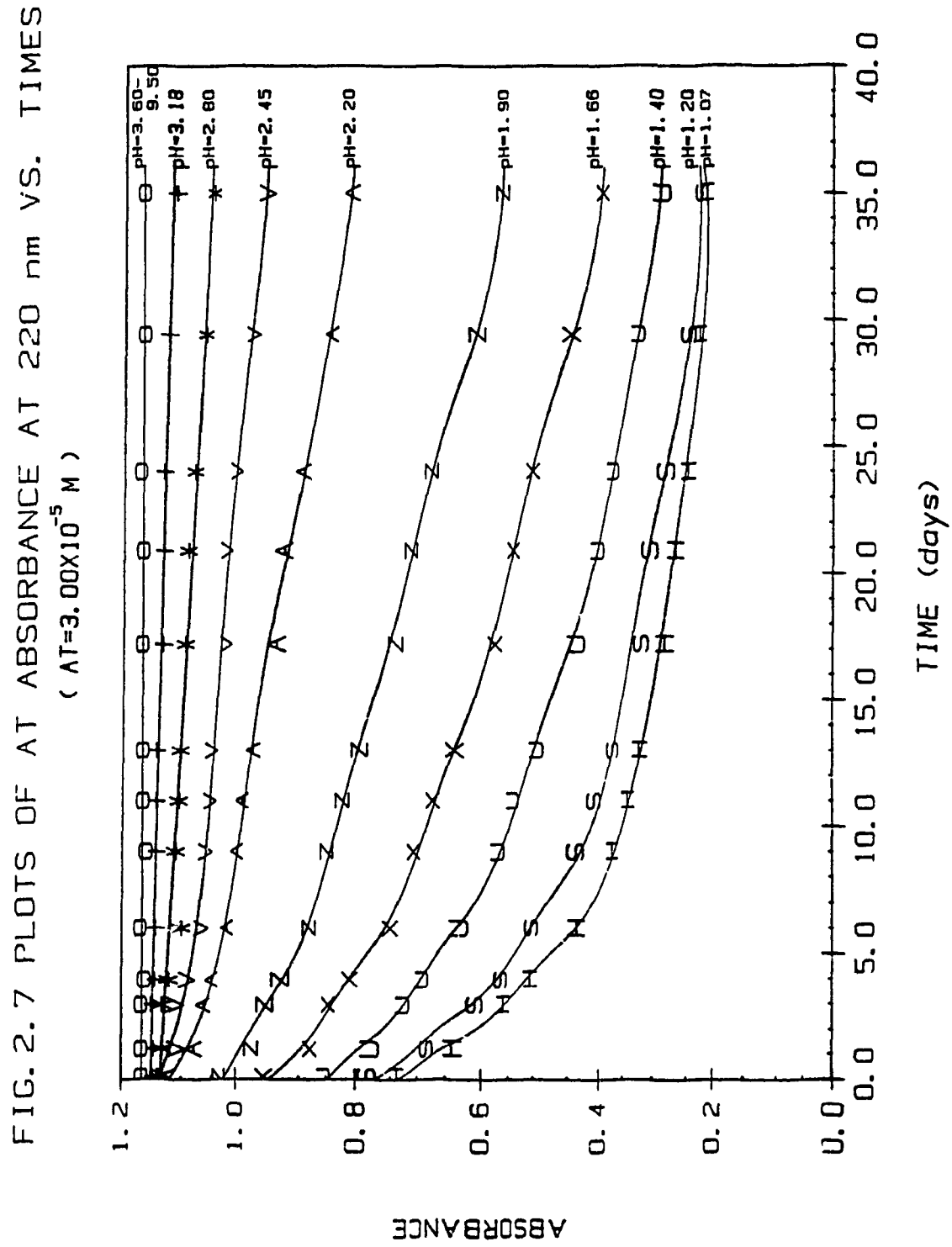
FIG. 2.7 PLOTS OF AT ABSORBANCE AT 220 nm VS. TIMES
(AT=3.00X10^{-5} M)
pH=3.60-9.50
pH=3.18
pH=2.80
pH=2.45
pH=2.20
pH=1.90
pH=1.66
pH=1.40
pH=1.20
pH=1.07
ABSORBANCE
TIME (days)
0.0
0.2
0.4
0.6
0.8
1.0
1.2
0.0
5.0
10.0
15.0
20.0
25.0
30.0
35.0
40.0

FIG. 2.7 PLOTS OF AT ABSORBANCE AT 238 nm VS. TIMES

(AT=3.00X10^{-5} M)

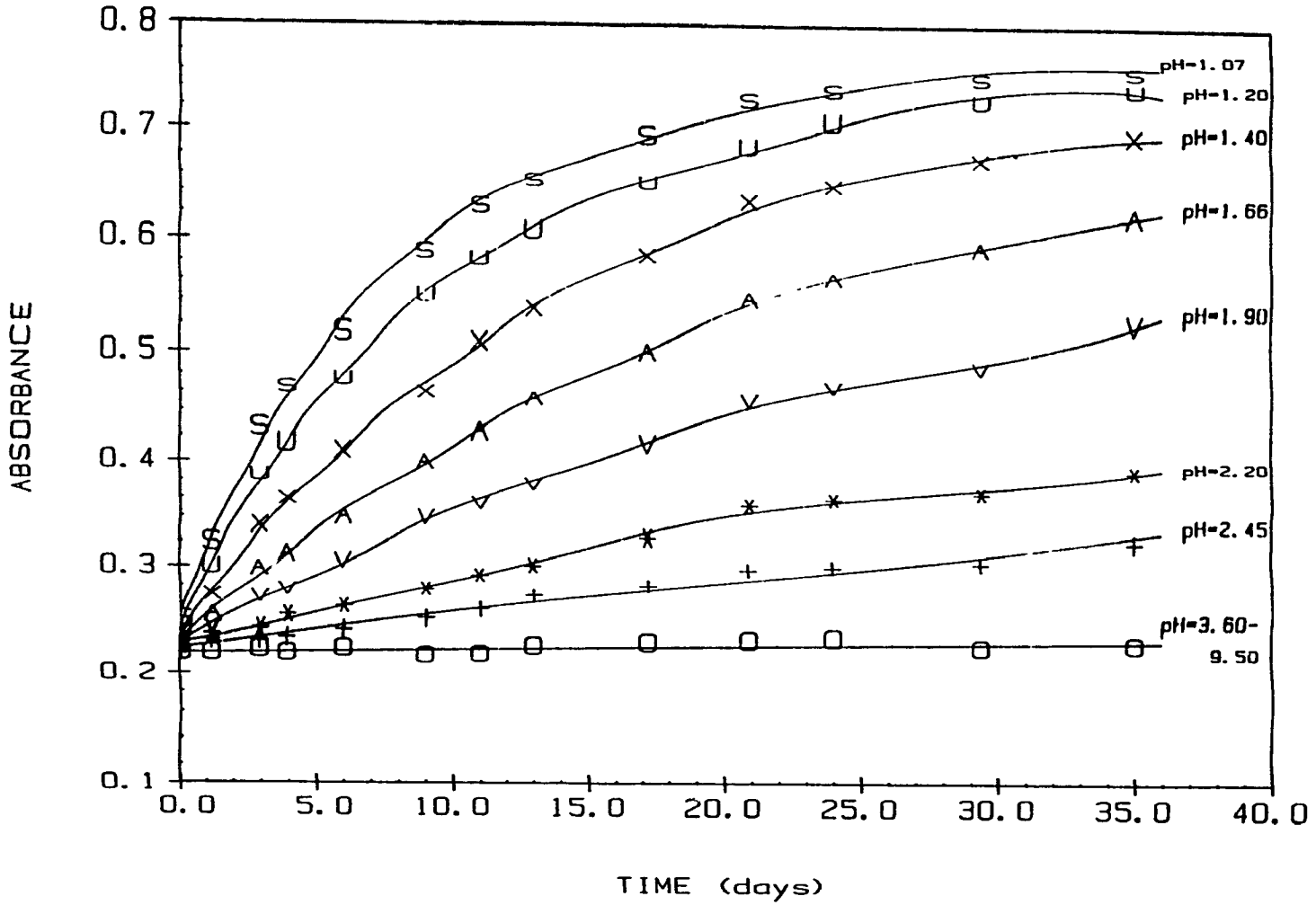

Using the data shown in Fig. 2.7A and 2.7B, the apparent reaction rate constant k can be obtained by plotting the $\ln(A_{220nm}-A_{\infty})$ versus reaction time t (see Figure 2.8).

Table 2.10 Percentages of conversion of AT to ATOH after 29.4 days and 35.5 days by HPLC

(AT = 3.00×10^{-5}M)

No	pH	29.4 day		35.5 days	
		C_{ATOH}/C (%)	C_{AT}/C (%)	C_{ATOH}/C (%)	C_{AT}/C (%)
1	1.07	94	6	100	0
2	1.20	89	11	~100	~0
3	1.40	83	17	93	7
4	1.66	66	34	77	23
5	1.90	50	50	58	42
6	2.20	29	71	32	68
7	2.45	17	83	19	81
8	2.80	11	89	12	88
9	3.18	6	94	6	94
10	3.40		~100		~100
11	4.09		100		100
12	5.22		100		100
13	7.01		100		100
14	7.94		100		100
15	9.50		100		100

Table 2.11 lists the k values and the half time calculated from UV spectrophotometric and HPLC measurements.

The numerical values taken from the work of Plust et al [23] for the apparent rate constant of total atrazine in 0.1 M HCl, and calculated from the equation established by Gamble et al [123] for

FIG. 2.8 DETERMINATION OF APPARENT RATE CONSTANT

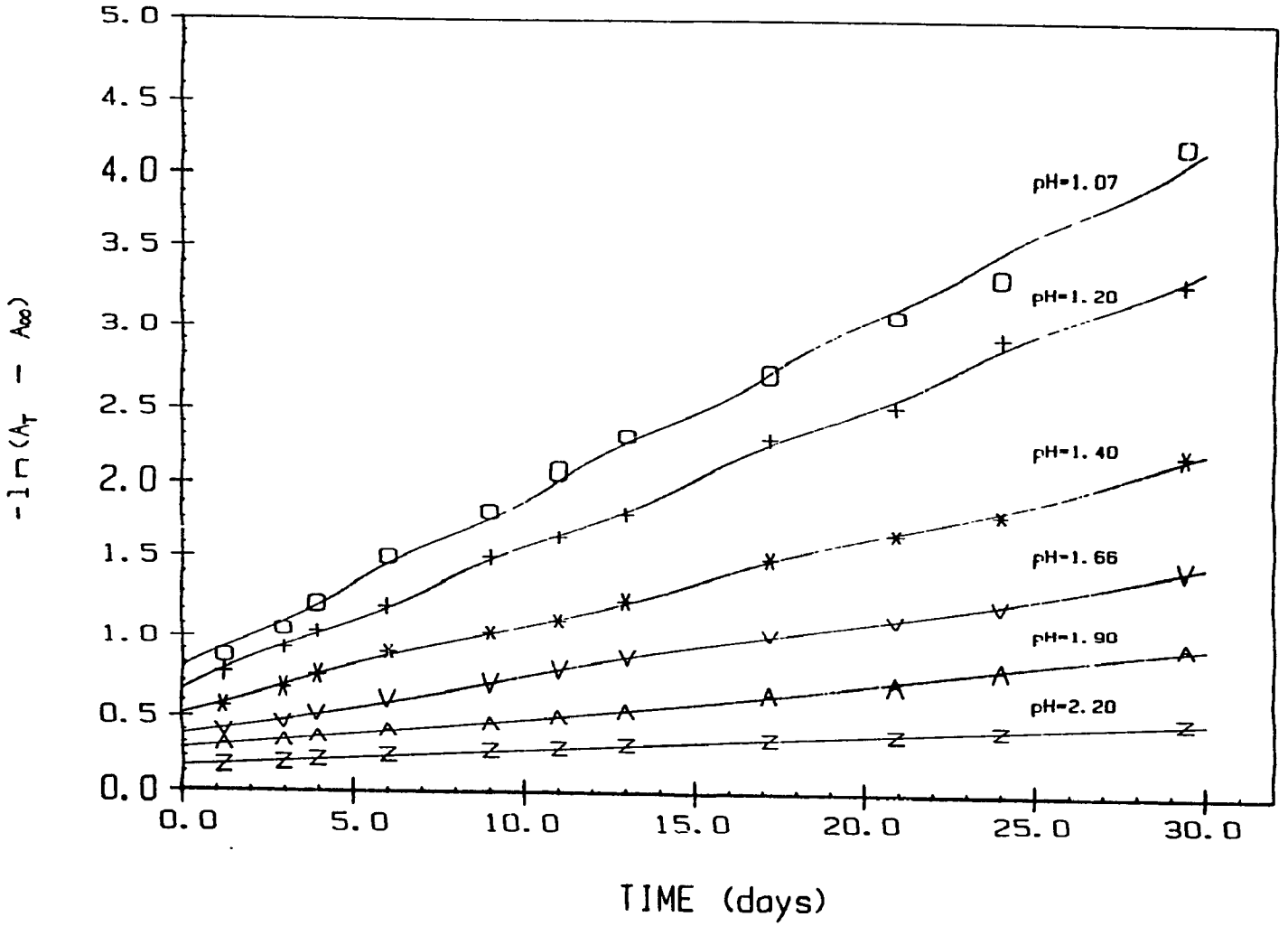

the apparent hydrolysis rate constant of AT at pH 1.00 were k = 0.0946 $days^{-1}$ and 0.135 $days^{-1}$, respectively. The value of sample $1^{\#}$ obtained here is 0.1132 and 0.1164 $days^{-1}$. Considering the differences of the concentration of hydrochloric acid, these four values are in very good agreement.

Table 2.11 Apparent first-order reaction rate constant for the H^+ catalyzed hydrolysis of total atrazine at 22±2°C and the half time by UV and HPLC measurements

sample	pH	k ($days^{-1}$)		$t_{1/2}$ (days)	
		by UV	by HPLC	by UV	by HPLC
1	1.07	0.1132	0.1164	6.12	5.96
2	1.20	0.08664	0.08502	8.00	8.15
3	1.40	0.05587	0.06138	12.4	11.3
4	1.66	0.03634	0.03709	19.1	18.7
5	1.90	0.02219	0.02396	31.0	28.9
6	2.20	0.01054	0.01096	65.8	63.2
7	2.45		0.006146		113
8	2.80		0.003412		203
9	3.18		0.001934		358

According to equation (31), the catalysis reaction order of hydrogen ion can be obtained from the plot of log k against pH (Figure 2.9).

Both UV and HPLC measurement results give the n value equal to 1. Now the values of n = 1 and k_0 = 0 are substituted back into equation (28), one can obtain the equation (43).

$$k = k_H a_H \qquad (43)$$

FIG. 2.9 DETERMINATION OF CATALYSIS REACTION ORDER OF H^+
BY UV/VIS AND HPLC METHODS

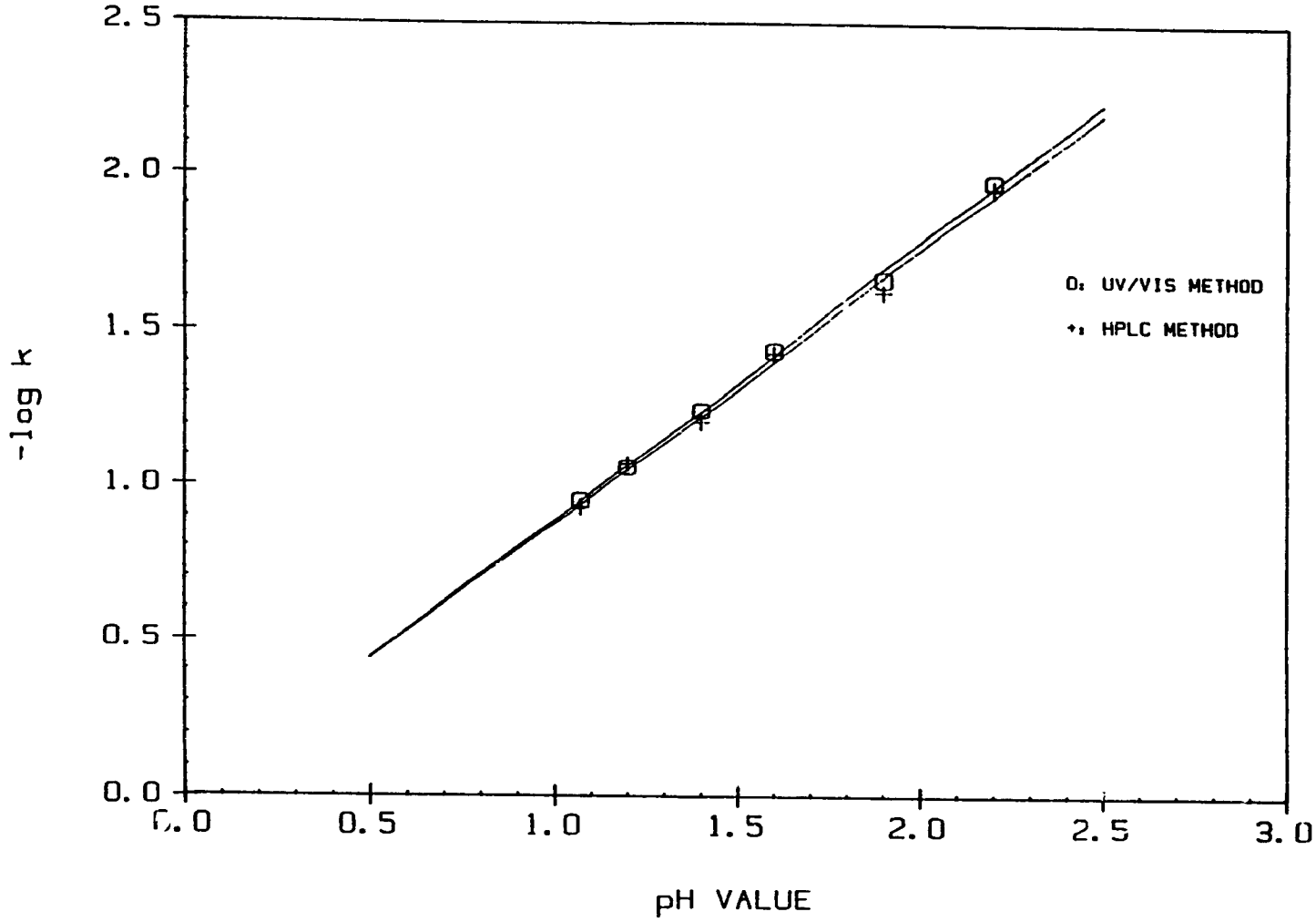

Equation (43) clearly shows the dependence of k value on the concentration of H^+. The calculated k_H values are given in Table 2.12.

Table 2.12 The calculated k_H values from UV and HPLC measurements

No	pH	a_H ($\times 10^{-3}$ M)	UV method		HPLC method	
			k (day^{-1})	k_H (day M)$^{-1}$	k(day^{-1})	k_H (day M)$^{-1}$
1	1.07	85.10	0.113	1.33	0.116	1.37
2	1.20	63.10	0.0866	1.37	0.0850	1.35
3	1.40	39.81	0.0559	1.40	0.0614	1.54
4	1.66	21.90	0.0363	1.65	0.0371	1.69
5	1.90	12.60	0.0222	1.7	0.0224	1.78
6	2.20	6.310	0.0105	1.66	0.0110	1.73
7	2.45	3.550			0.00615	1.72
8	2.85	1.995			0.00341	1.71
	average k_H			1.53		1.61
	S			0.17		0.16
				1.53±0.17		1.61±0.1

It should be pointed out that the apparent first-order reaction rate constant k and the acid catalysis constant have different chemical meaning. At a fixed pH, k keeps constant at varying reaction time. But, it has different values at different pH. However, the acid catalysis rate constant k_H should theoretically be constant at different pH values for those reaction which are catalyzed by H^+.

2.3.5 Atrazine Binding

(1) pH effect

The experiments examining the pH effect on AT binding with FA were designed in such a way that AT concentration were varied from 4.00×10^{-6} to 8.00×10^{-5}M with FA concentration at 1.000g/L at each pH so that the binding behavior of AT to FA could be thoroughly investigated and more quantitative data could be obtained. The tested pH range was from 1.25 to 10.0. The conclusion drawn from over 1000 data point is that: (a) at pH above 5.50, no measurable binding of AT occurs; (b) in the pH range of 3.65 - 5.50, no ATOH is catalytically hydrolyzed within three days, and only significant AT bound by FA is observed; (c) at pH below 3.65, not only significant AT bound by FA, but also a noticeable amount of ATOH is detected. The evidence that more ATOH is produced in AT-FA solutions than in AT controls with the same pH clearly demonstrated that FA catalyzes the hydrolysis of AT. Another interesting phenomenon in this pH range is that even though quite a large amount of ATOH is produced, no binding of hydrolyzed ATOH by FA occurs.

Representative binding curves for these three cases are shown in Figure 2.10A, 2.10B and 2.10C.

Figure 2.10A showed that approximately 20% of atrazine was hydrolyzed to hydroxyatrazine at pH 1.90 after three days. The control could be fitted to two straight lines; one was for the remaining AT in the solution and another for ATOH hydrolyzed from AT; whereas the free AT and ATOH in AT-FA sample could be fitted to two and one straight lines, respectively. The linear regression equation for AT and ATOH in control were $y = 1.3348\times10^{-7} + 0.80895\ x$ ($r = 0.9999$) and $y = 3.4822\times10^{-7} + 0.18358x$

FIG. 2. 10A AT BINDING CURVES BY LAURENTIAN FA

(FA=1.000g/L, pH=1.90)

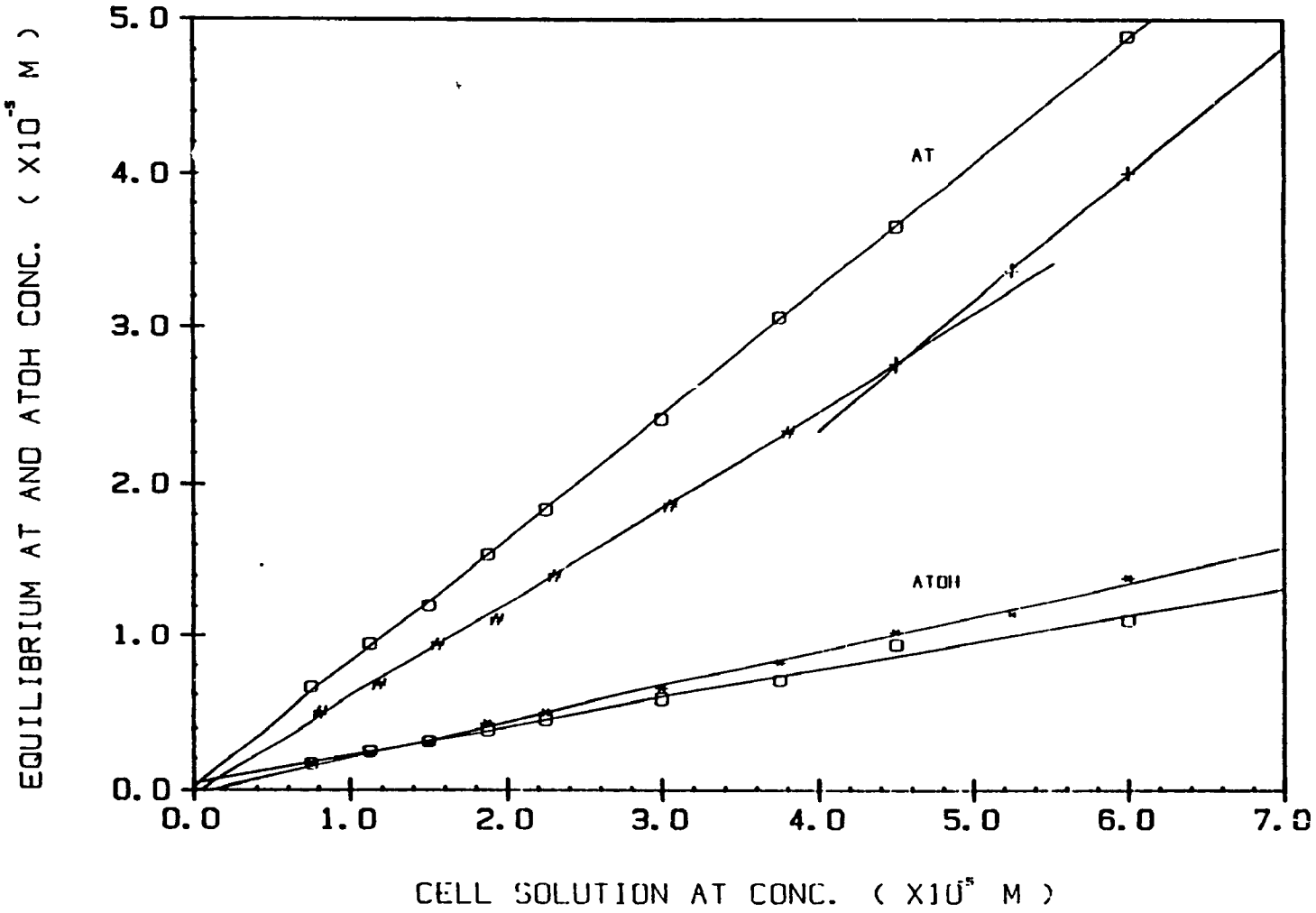

FIG. 2.10B AT BINDING CURVES BY LAURENTIAN FA

(FA=1.000g/L, pH=5.00)

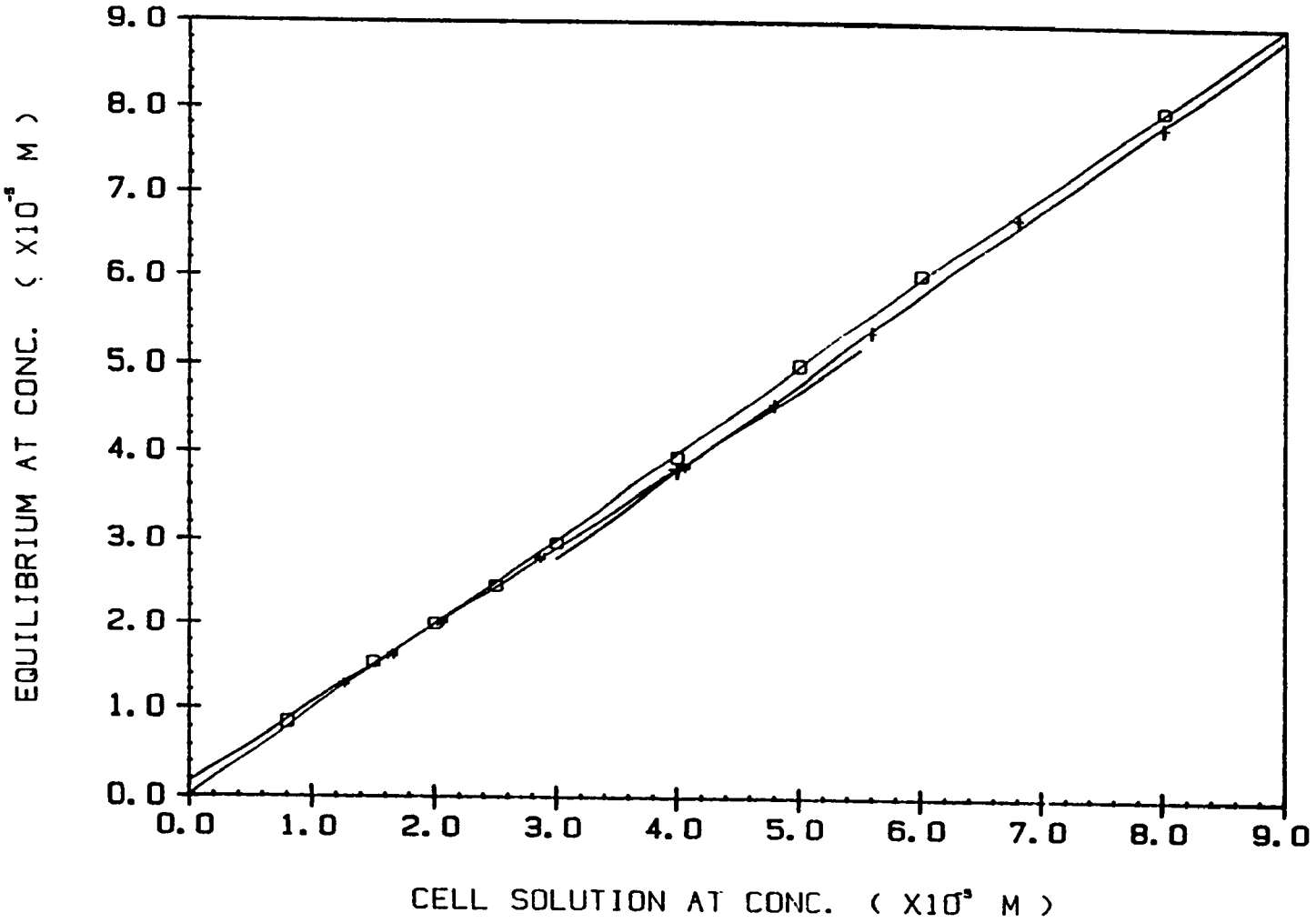

FIG. 2. 10C AT BINDING CURVES BY LAURENTIAN FA

(FA=1.000g/L. pH=6.60)

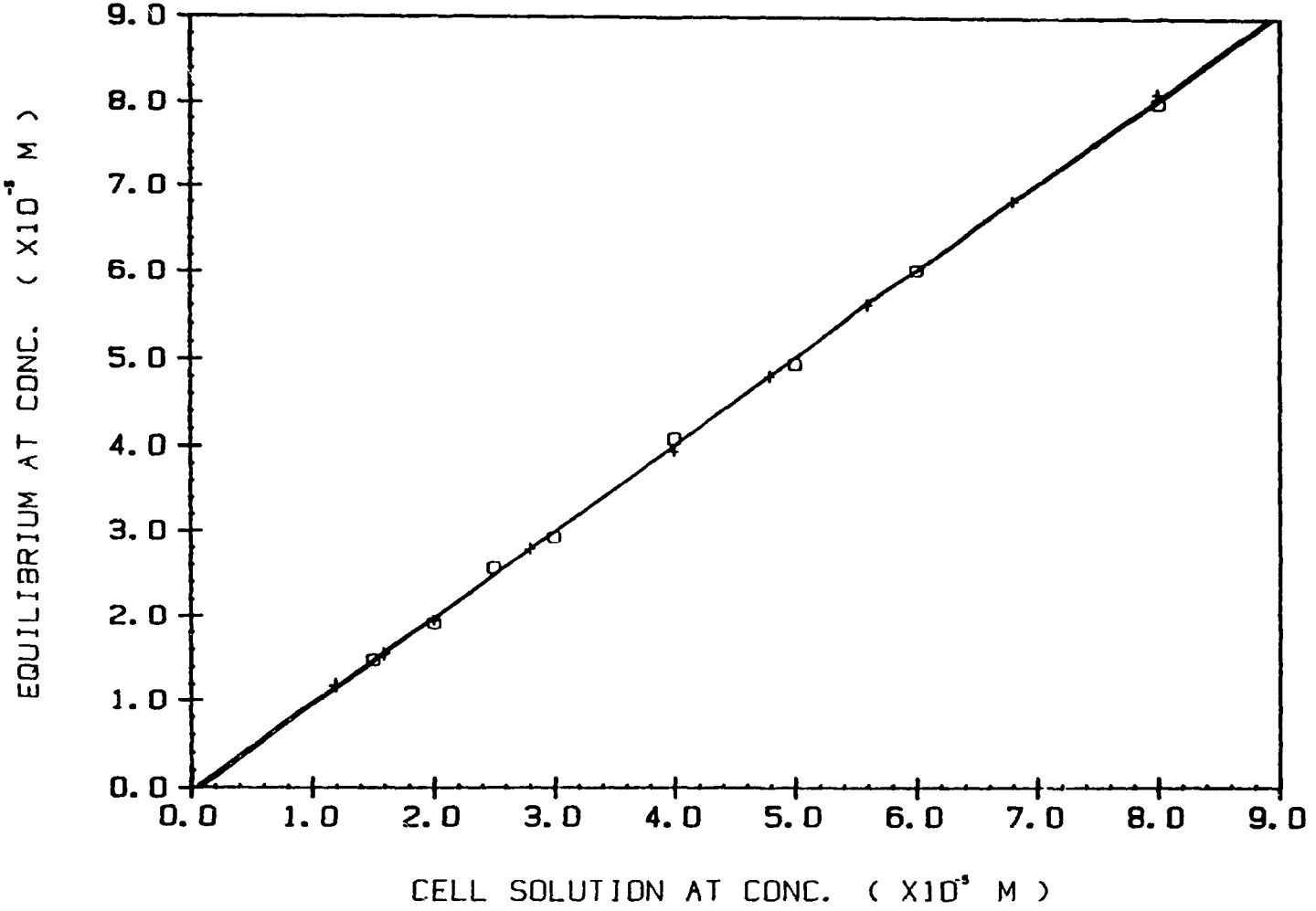

(r = 0.9948). The first 7 and last 3 data points for AT in AT-FA solution were fitted to equations $y = 0.18748 \times 10^{-5} + 0.53784\ x$ (r = 0.9935) and $y = -0.95127 \times 10^{-5} + 0.82360\ x$ (r = 0.9996), respectively. The same procedure for ATOH data points in AT-FA samples gives $y = -2.9962 \times 10^{-7} + 0.23012\ x$ (r = 0.9984).

Fig. 2.10B shows that at pH 4.40 no ATOH was produced; only AT bound can be observed. Fig. 2.10C demonstrates that no observable binding occurs at pH 6.60.

Table 2.13 summarized the a (intercept) and b (slope) values of the linear regression lines of the equilibrated AT against the total AT added for AT controls and AT-FA samples at various pH.

It can be found from Table 2.13 that (1) the slopes of the fitted equations for AT controls are functions of pH, They increase with increase in pH, smaller b means more ATOH formed. When the pH reaches 3.60, the b value equals approximately 1, which means no observable ATOH is hydrolyzed at pH 3.60 and higher. (2) b values before equivalence point are always smaller than the corresponding b values of controls. (3) the slopes after equivalence point are almost same as b values of controls, which means the bound AT does not change as the added AT concentration increases after equivalence point. That is, the binding sites available for AT are saturated.

Table 2.13 a and b values of linear regression equations

pH	AT control		AT-FA before equivalence point		AT-FA after equivalence point	
	a($x10^{-5}$M)	b	a($x10^{-5}$M)	b	a($x10^{-5}$M)	b
1.24	0.1494	0.5234	0.2293	0.3070	-0.3417	0.5303
1.40	0.3156	0.5954	0.2370	0.3802	-0.5335	0.5922
1.66	0.7024	0.7024	0.1331	0.4804	-0.7845	0.7059
1.90	0.01335	0.8090	0.1875	0.5378	-0.9513	0.8236
2.20	0.1118	0.8782	0.3390	0.6187	-0.6982	0.8873
2.40	0.03999	0.9105	0.3175	0.6466	-0.5634	0.8914
2.80	0.03632	0.9660	0.1751	0.7594	-0.3686	0.9612
3.10	0.02588	0.9846	0.1900	0.8045	-0.3448	0.9935
3.60	0.00883	0.9997	0.08065	0.8158	-0.3982	1.005
4.40	0.000863	0.9997	0.1451	0.8352	-0.2248	0.9954
5.00	0.02394	0.9995	0.1107	0.9417	-0.2642	1.014
5.50	0.00293	0.9992	-0.0005156	1.005		
6.60	0.002911	0.9992	0.03802	1.010	after pH 5.50, no	
7.80	0.003120	0.9991	0.06676	0.9774	binding was observed)	
9.50	0.003355	0.9991	-0.02701	1.011		

Using the linear analytical curves established in the FA free controls in conjunction with signals obtained for AT and ATOH in the filtrate of AT-FA solution, bound AT and hydrolyzed ATOH by FA were evaluated. Figure 2.11 shows plots of AT bound versus AT total at various pH values. It is evident that a limit is reached at each pH value and that an empirical binding capacity can be defined at each pH.

The respective binding capacities of AT are 5.0 (pH 1.24), 8.7 (pH 1.40), 8.6 (pH 1.66), 8.8 (pH 1.90), 8.1 (pH 2.20), 6.5

FIG. 2.11 TOTAL AT BOUND VS. CELL CONC. OF AT

AT VARIOUS pH VALUES

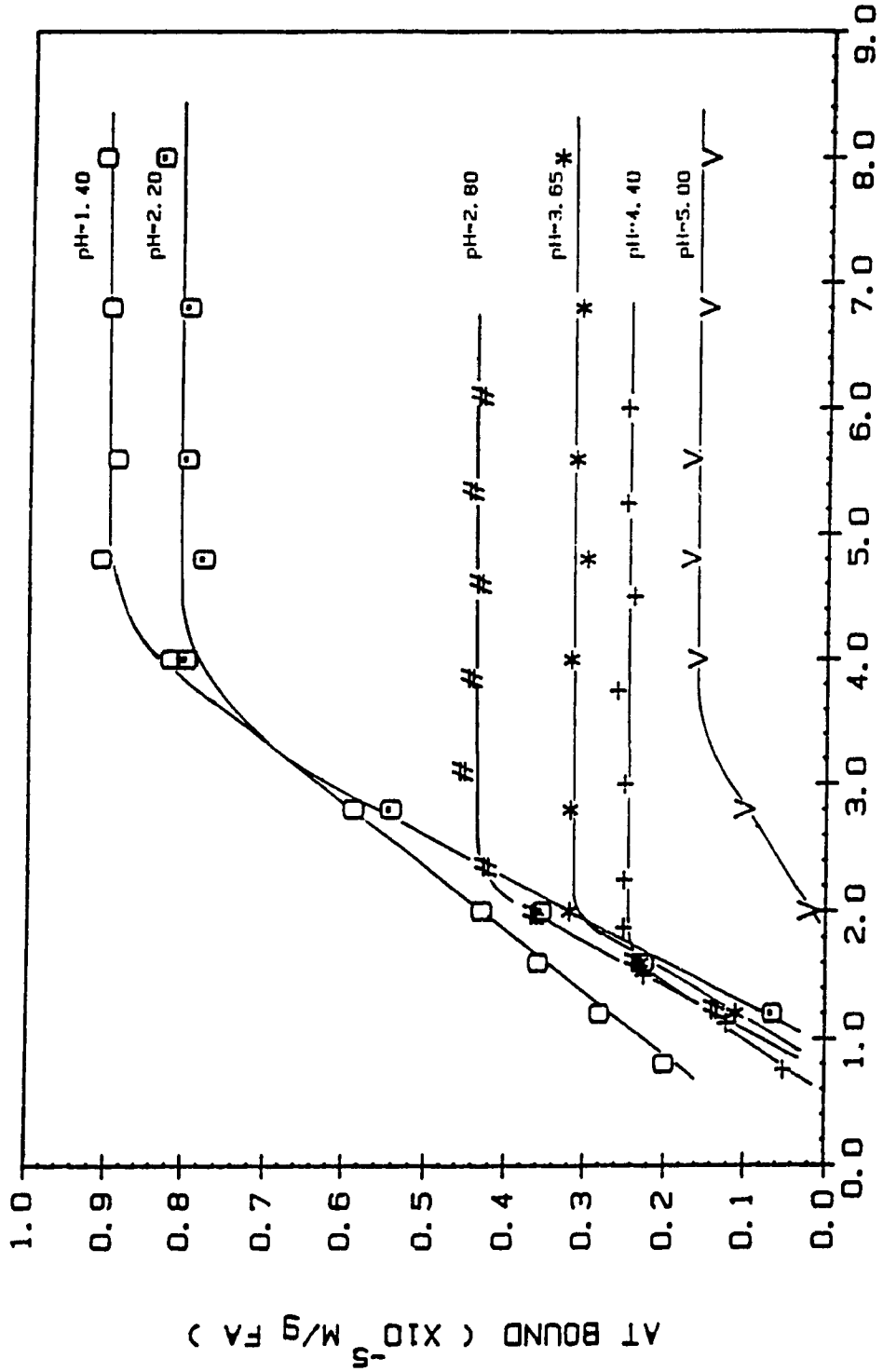

(pH 2.40), 4.4 (pH 2.80), 3.8 (pH 3.10), 3.3 (pH3.65), 2.5 (pH 4.40) and 1.5(pH 5.00) μ moles per gram FA. Figure 2.12 shows a plot of binding capacity of AT versus pH for the data in figure 2.11 and for solutions with an ionic strength of 0.1 M KCl. The shape of the curves is qualitatively quite similar to those reported for prometryne, prometone, propazine and hydroxypropazine on Na-montmorillonite by Weber [116]. (see details in Table 2.14)

Table 2.14 The pKa, pH at which maximum binding is observed, and the amount of herbicide bound

sample	pKa	pH	amount bound (μmol/g FA)
propazine	1.85	1.9	3.5
premetryne	4.05	4.3	8.3
prometone	4.28	4.4	7.0
hydroxypropazine	5.20	5.5	7.8
AT by Laurentian FA	1.68	1.40-1.90	8.8 (this work)

(2) AT binding equilibrium functions

As we described in section 2.1, there are two approaches open for the treatment of the equilibria. They differ by the way the FA concentration, C, is defined. In one approach, the total Type A carboxyl groups (5.11 mmoles/g FA) of FA may be used to define x (which will then be limited to a very small range, mole% < 1%) on the notion that the pH dependent limit on binding capacity is determined by the number of sites protonated in a competition which the low AT concentration cannot influence. The second

FIG. 2. 12 AT AND ATOH BINDING CAPACITY VS. pH

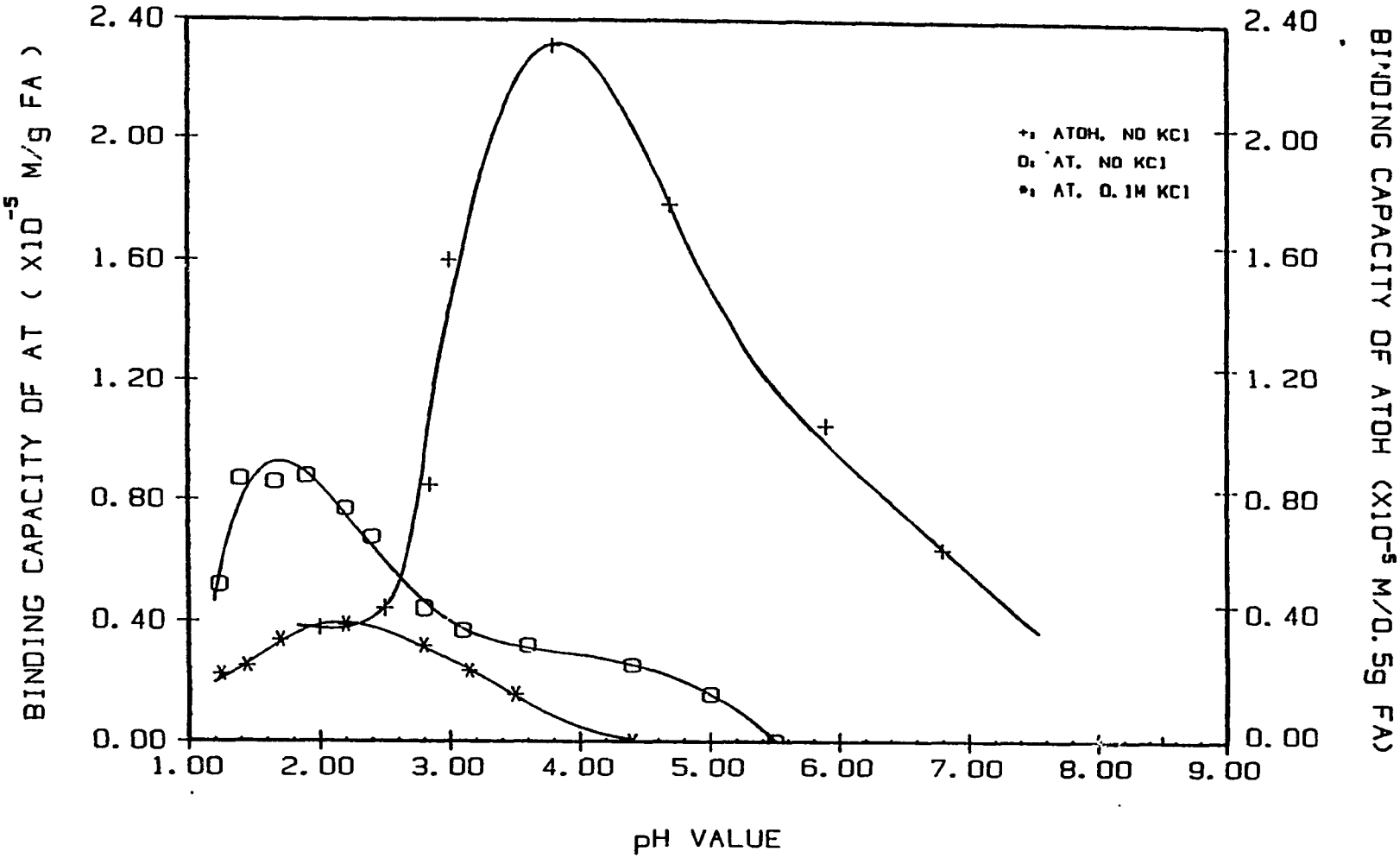

approach uses the empirical binding capacity to define C for the FA and has values of x running from near 0 to 1.0. As an example, the relevant values needed to calculate K_{AT} at pH 1.90 according to equation (5) by using the first approach is given in Table 2.15. The Table 2.16 gives the values needed to calculate the K_{AT} at pH 1.66 by using the second approach.

Table 2.15 Determination of bound AT, fractions bound and K value at pH 1.90 by the first approach

(pH = 1.90, FA = 1.000 g/L, stock AT = 0.7500×10^{-4}M)

Added AT (ml)	Free species in controls		Free species in AT-FA		Bound AT	x
	M_{AT} ($\times 10^{-5}$M)	M_{ATOH} ($\times 10^{-5}$M)	M_{AT} ($\times 10^{-5}$M)	M_{ATOH} ($\times 10^{-5}$M)	($\frac{\times 10^{-5}\text{mol}}{\text{g FA}}$)	($\times 10^{-5}$)
2.50	0.6103	0.1632	0.5908	0.1632	0.0195	3.820
3.75	0.9143	0.2381	0.7926	0.2382	0.1217	23.82
5.00	1.2182	0.3078	0.9942	0.3141	0.2240	43.84
6.25	1.5222	0.3773	1.1959	0.4007	0.3263	63.86
7.50	1.8262	0.4469	1.3976	0.4872	0.4286	83.87
10.00	2.4340	0.5860	1.8010	0.6604	0.6330	123.9
12.50	3.0420	0.7251	2.2044	0.8335	0.8376	163.9
K_{AT} (mole/L)					0.101	
$1/K_{AT}$ (L/mole)					99.2	
$-(\Delta G^0+RT\ln\Gamma)$ (KJ/mole)					11.4	

* The total volume of solutions is 25.00 ml.
* The binding sites will be saturated when the added AT reaches to 15.00 ml or higher.
* The amount of free ATOH hydrolyzed from AT in AT-FA is greater than that in the corresponding AT controls. The hydrolyzed ATOH by the Type A carboxyl groups can be easily obtained from subtracting the amount of ATOH in AT-FA from that in AT controls.

Using the first approach, a single value of the binding constant 82 ± 16 and a single value of the binding free energy (minus activity coefficient term), -10.9 ± 0.5 kJ/mole provides an adequate fit to data at all pH values. There is some indication of a possible trend to greater binding constants with decrease of pH. (see Table 2.17).

Table 2.16 Determination of bound AT, fractions bound and K value at pH 1.66 by the second approach (pH=1.66, FA=1.000g/L, binding capacity of AT=0.86×10^{-5}mole/g FA)

M_{AT}	M^b_{AT}	$C_0=C_{cap}-M^b_{AT}$	$x=\frac{M^b_{AT}}{C_{cap}}$	$\bar{K}_{AT}$	$\bar{K}_{AT}\,x$
($\times10^{-5}$M)	($\times10^{-5}$mol/g FA			($\times10^{-5}$M)	($\times10^{-5}$M)
0.4934	0.064	0.8000	0.07023	6.535	0.4594
0.6471	0.1618	0.6835	0.1881	2.734	0.5144
0.8118	0.2353	0 6274	0.2736	2.155	0.5896
1.000	0.3235	0.5365	0.3761	1.658	0.6238
1.214	0.3894	0.4706	0.4528	1.467	0.6643
1.647	0.5000	0.3600	0.5814	1.186	0.6895
K_{AT} (mole/L)				0.47×10^{-5}	
$1/K_{AT}$ (L/mole)				2.1×10^{5}	
$-(\Delta G^0+RT\ln\Gamma)$ (KJ/mole)				30.4	

Using the second approach, the average value of 1/K and free energy for the AT-FA reaction product were found to be (2.1±0.17) x 10^5 and -30.2 KJ/mole respectively, which provides an adequate fit to data at all pH values (also see Table 2.17). There is a reason to prefer this treatment for it is strictly based on the

stoichiometrically measured quantities which are chemically meaningful. The first approach , however, was often accounted most probably for the reason that the binding capacity was not well defined and stoichiometrically known. The data in Figure 2.11 strongly support the notion of a well defined binding capacity much less than the carboxylate stoichiometry of the sample.

Table 2.17 The formation functions and free energy for AT-FA at various pH and α values by the first and second approaches

pH	α_{FA}	$1-\alpha_{FA}$	$\frac{\partial \bar{K} x}{\partial x}$ (mole/L)	1/K (L/mole)	$-(\Delta G^{o}+RT\ln\Gamma)$ (KJ/mole)
			by the first approach		
1.40	0.28	0.72	0.009016	111	11.7
1.66	0.32	0.68	0.01171	90.4	11.2
1.90	0.38	0.62	0.01008	99.2	11.4
2.20	0.44	0.56	0.01218	82.1	10.9
2.40	0.485	0.515	0.01428	70.0	10.5
2.80	0.567	0.433	0.01365	73.3	10.7
3.10	0.608	0.392	0.01453	68.8	10.5
3.60	0.700	0.300	0.01546	64.7	10.4
average				82.4±16	10.9±0.5
			by the second approach		
1.40	0.28	0.72	0.41×10^{-5}	2.4×10^{5}	30.7
1.66	0.32	0.68	0.47×10^{-5}	2.1×10^{5}	30.4
1.90	0.38	0.62	0.52×10^{-5}	1.9×10^{5}	30.1
2.20	0.44	0.56	0.50×10^{-5}	2.0×10^{5}	30.2
2.40	0.485	0.515	0.50×10^{-5}	2.0×10^{5}	30.2
2.80	0.567	0.433	0.49×10^{-5}	2.0×10^{5}	30.2
3.10	0.608	0.392	0.53×10^{-5}	1.9×10^{5}	30.1
average				$(2.1\pm0.17)\times10^{5}$	30.2±0.21

FIG. 2.13 BINDING CONSTANT AS A FUNCTION
OF THE FRACTION OF DEPROTONATED TYPE A CARBOXYL GROUPS OF FA

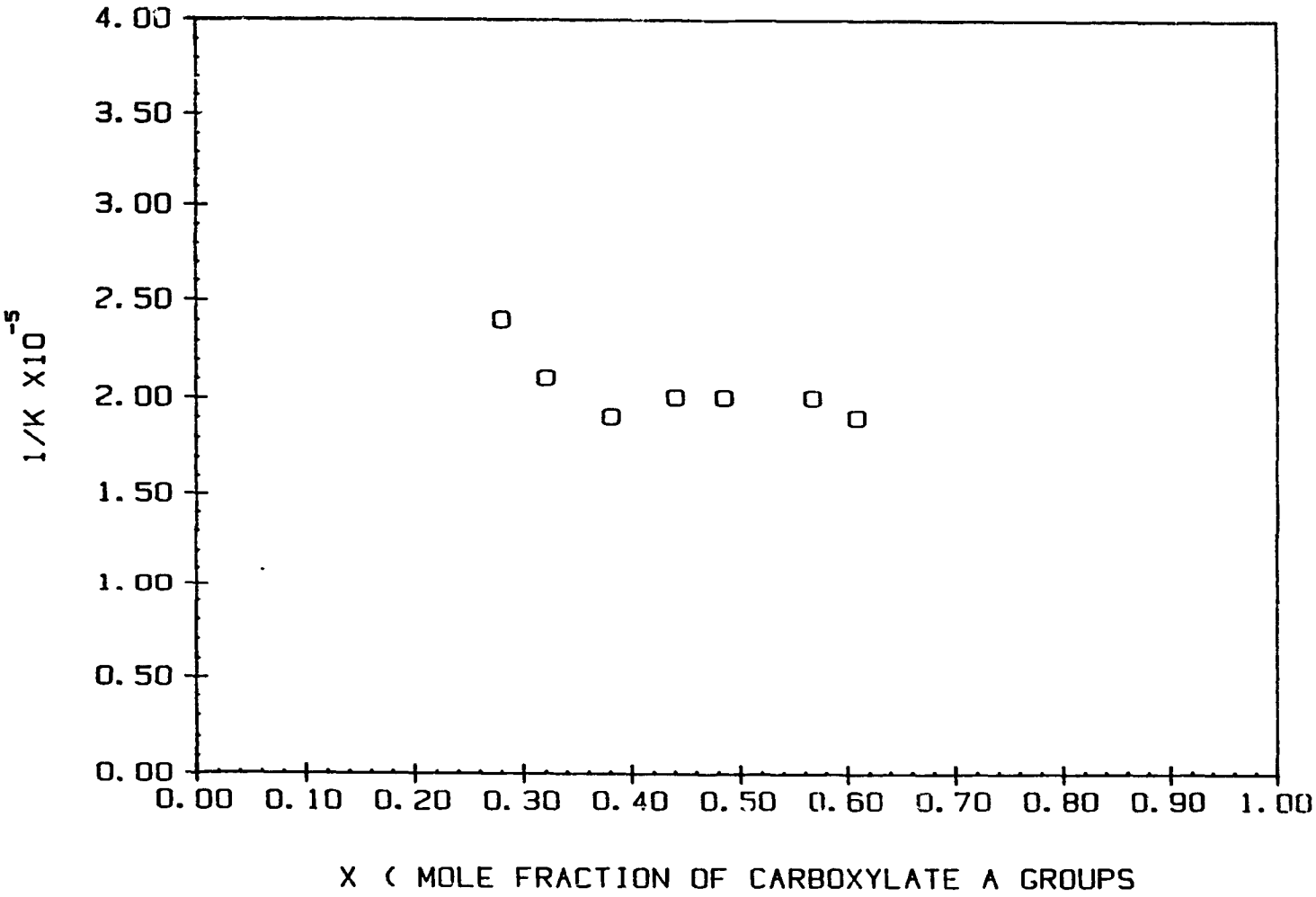

It can be seen from the Table 2.17 that (1) single values of the differential binding constant and free energy provides an adequate fit to data at the tested pH values. It might indicate that these special sites which prefer H-bonding AT over water have approximately the same chemical environment and capability of binding AT. (2) the binding constant obtained by the second approach is much greater than that by the first approach, because the mole fraction of bound AT calculated on the basis of the AT binding capacity has a much larger value than the mole fraction of bound AT over the total Type A carboxyl groups.

(2) Effect of ionic strength

The experiments designed for the examination of effect of ionic strength are similar to those described above. The only exception is the addition of electrolyte KCl to the solutions so as to make binding studies at a high ionic strength (the final concentration of KCl is 0.1 M). The pH values ranged from 1.25 to 7.10, including pH 1.25, 1.45, 1.70, 2.20, 2.80, 3.10, 3.50, 4.40, 4.75, 5.70 and 7.10. The plots of equilibrated AT and hydrolyzed ATOH versus the total AT added at each pH clearly show that (a) there was ATOH catalytically produced at pH 3.50 and lower in both AT-KCl and AT-KCl-FA solutions; (b) the amounts of AT bound were much less than the corresponding solutions at same pH value but without KCl; (c)the amount of free ATOH measured in AT-KCl-FA solutions was a little greater than that in their respective AT-KCl controls, which demonstrated the catalytic function of protonated carboxylic groups; (d) at pH 4.40 and higher, no AT binding was observed, while for AT-FA solutions at low ionic

strength, the AT binding at pH 5.50 can still be observed; (e) at pH 1.40 and 1.25, the solutions became turbid.

From the titration curves, bound AT and hydrolyzed ATOH by FA were evaluated. Figure 2.14 shows plots of AT bound versus AT total at various pH, and Figure 2.15 shows plots of ATOH hydrolyzed by FA carboxyl groups as a function of the total AT added at various pH values.

The plot of binding capacity in the presence of 0.1M KCl versus pH for the data in Fig. 2.14 is also presented in Fig. 2.12.

There are several significant features for AT binding in the presence of 0.1 M KCl worth pointing out: (a) 0.1 M KCl greatly depress AT binding in the whole pH range studied. (2) the maximum binding of AT occurs at pH 2.20, shifting about 0.5 pH unit from the maximum in the low ionic strength.

Using the first approach, a single value of binding constant 18.5±5.2 and a single value of binding free energy -7.2±0.6 kJ/mole are obtained. If using the second approach, the average binding constant $(1.28\pm0.098)X10^5$ and binding free energy 29.1±0.18 KJ/mole are obtained. Table 2.18 presents the formation functions and free energy for AT-FA complexes at various pH in the presence of 0.1 M KCl.

FIG. 2. 14 TOTAL AT BOUND AS A FUNCTION OF AT ADDED

(KCl=0. 1M, FA=1. 0000g/L)

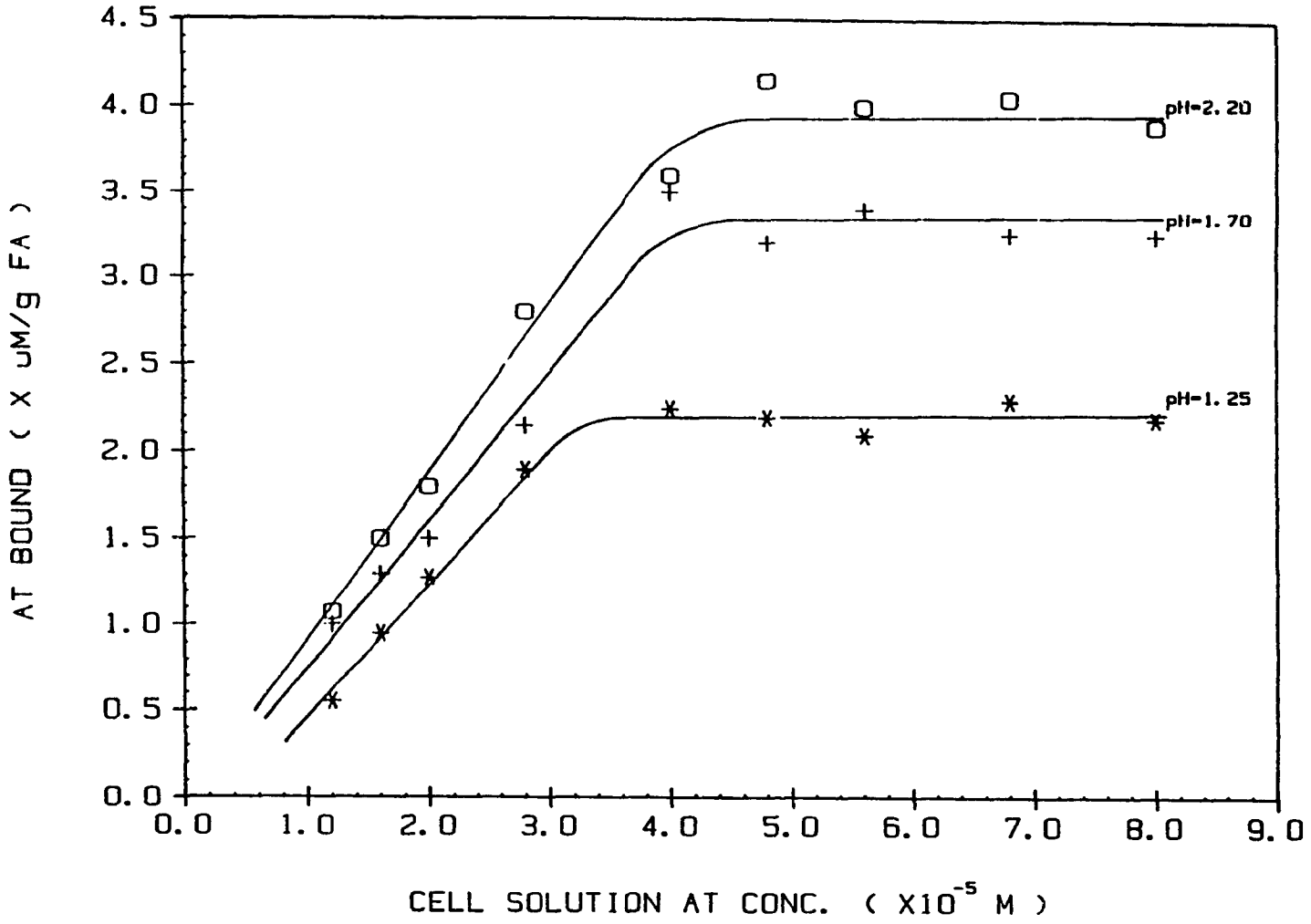

FIG. 2. 15 HYDROLYZED ATOH AS A FUNCTION OF AT ADDED

(KCL=0. 1M, FA=1. 0000g/L)

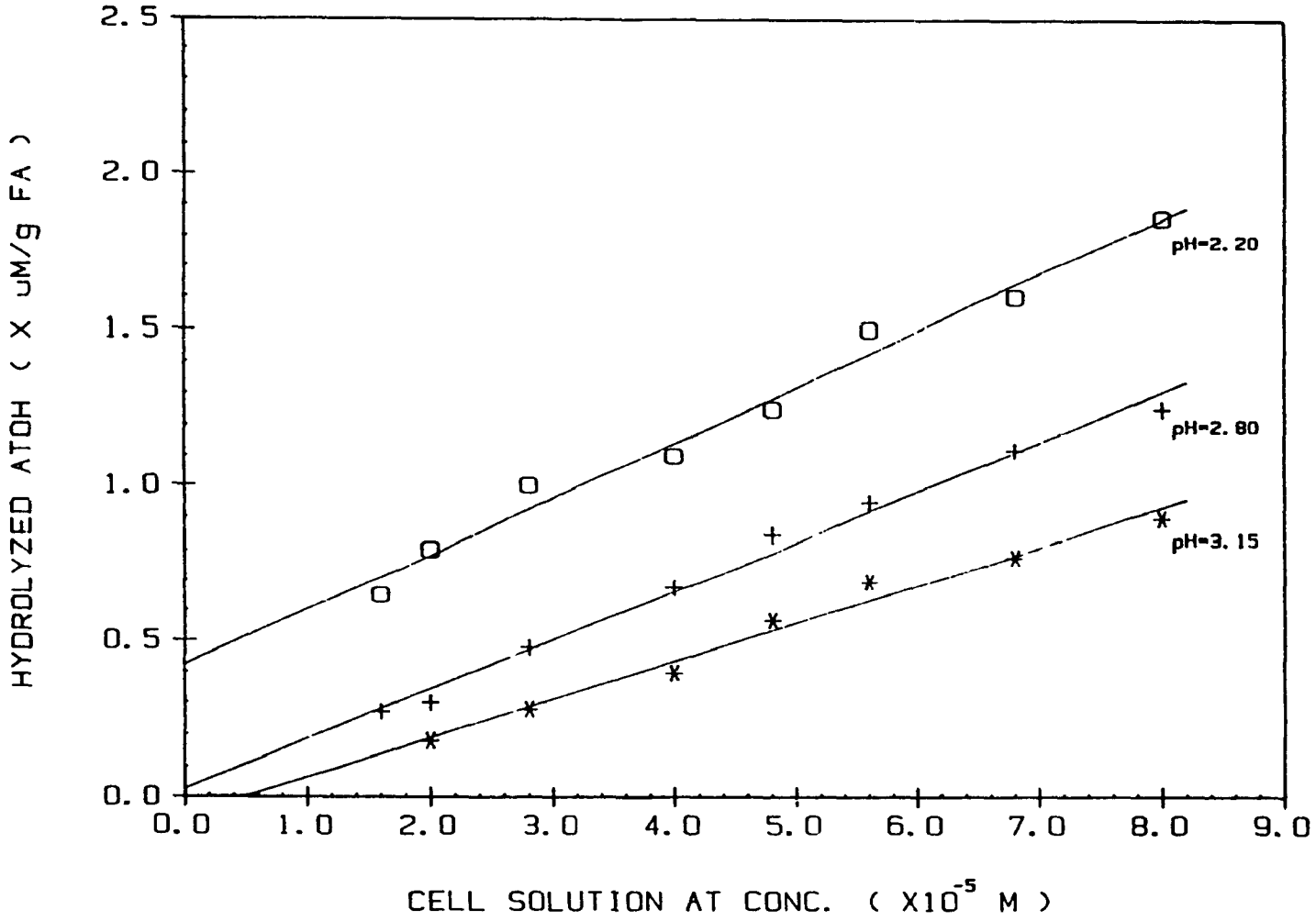

Table 2.18 The formation function and energy for AT-FA complexes at various pH in the presence of 0.1 M KCl

(FA = 1.0000g/L, AT = 8.00×10^{-6} - 8.00×10^{-5}M)

pH	α_{FA}	$1-\alpha_{FA}$	$\frac{\partial \bar{K} x}{\partial x}$ (mole/L)	1/K (L/mole)	$-(\Delta G^0+RT\ln \Gamma)$ (kJ/mole)
			by the first approach		
1.25	0.24	0.76	0.0737	13.6	6.46
1.45	0.28	0.72	0.0666	15.0	6.71
1.70	0.35	0.65	0.0460	21.8	7.63
2.20	0.45	0.55	0.0366	27.3	8.19
2.80	0.56	0.433	0.0383	18.8	7.26
3.15	0.61	0.382	0.0677	14.8	6.67
				18.5±5.2	7.2±0.6
			by the second approach		
1.25	0.24	0.76	0.75×10^{-5}	1.33×10^{5}	29.2
1.45	0.28	0.72	0.79×10^{-5}	1.27×10^{5}	29.1
1.70	0.35	0.65	0.72×10^{-5}	1.43×10^{5}	29.4
2.20	0.45	0.55	0.86×10^{-5}	1.16×10^{5}	28.9
2.80	0.56	0.433	0.87×10^{-5}	1.15×10^{5}	28.9
3.15	0.61	0.382	0.76×10^{-5}	1.32×10^{5}	29.2
average				$(1.28\pm0.098)\times10^{5}$	29.1±0.18

(3) Effect of FA concentration

AT binding also varies with the total FA concentration. This effect was investigated quantitatively at a pH of 1.40 in the absence of KCl and pH 2.20 in the presence of 0.1 M KCl. These were chosen to be near the maximum binding capacity. FA concentrations were varied from 0.1000 to 1.000 g/L.

For FA concentrations of 0.100, 0.300, 0.800 and 1.000 gram per liter in the presence of 0.1M KCl, the binding capacity obtained from the titration curves is 1.1, 3.0, 7.5 and 9.2 μmoles per gram FA, respectively.

For FA concentrations of 0.100, 0.300, 0.500 and 1.000 gram per liter in the presence of 0.1 M KCl, the respective binding capacity evaluated from the titration curves is 0.9, 1.9, 2.8 and 4.0 μmoles per gram FA.

If all the tested concentrations are converted to 1.000g/L, and then plotted against the binding capacity, Figure 2.16 is obtained. Fig. 2.16 shows the decline in the binding capacity of AT (μM/g FA) as the concentration of FA increases (ATOH data also appear in the Figure). The results can be related to slight upward curvature in a plot of 90^{0} light scanning versus concentration of FA in this range [79] suggesting a relationship to FA aggregation.

(4) Effect of equilibration time ----kinetic factors in AT binding

The period of equilibration of three days was chosen because of the binding of AT is not an instantaneous process. Experiments have demonstrated that the binding equilibrium significantly depends on the binding time. The time dependent binding results

FIG. 2. 16 DEPENDENCE OF AT AND ATOH BINDING CAPACITY ON FULVIC ACID CONCENTRATION

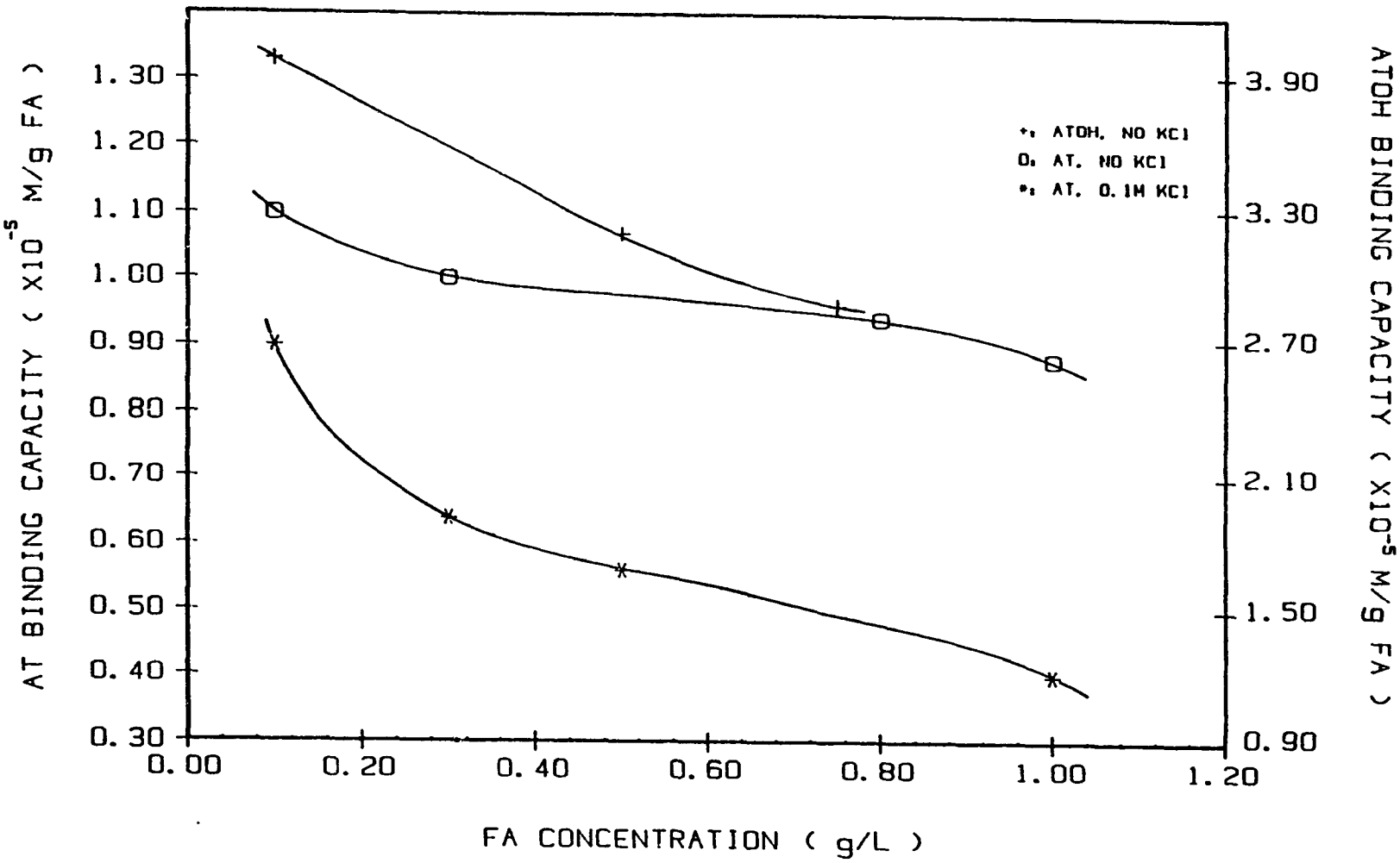

recorded at two pH values, pH 2.10 and 3.30, are shown in Table 2.19. It can be seen from Table 2.19 that at least 2 days are needed to establish the binding equilibria, and that the time required to establish binding equilibria does not appear to be sensive to pH: at pH 2.20, two days are required; at pH 3.30, two days are required too.

Table 2.19 AT binding as a function of time

(FA = 1.0000g/L, AT = 0.800 to 8.000×10^{-5}M)

No	pH	Shaking time (hour)	Reach to equilibrium (μmol/g FA)	AT bound at 8.00×10^{-5}M (μmol/g FA)	Binding capacity (μmol/g FA)
1		3.5	no	2.2	/
2		9.0	no	3.0	/
3	2.10	27	no	3.7	/
4		48	yes	5.9	6.0
5		72	yes	6.0	6.0
1		28	no	3.1	/
2	3.30	54	yes	4.4	4.4
3		77	yes	4.5	4.5

2.3.6 ATOH Binding

The ATOH formed by hydrolysis of AT in three days permits the evaluation of ATOH binding from the experiments used to study AT binding. A typical binding curve of ATOH at pH 2.00 is shown in Figure 2.17. The binding capacity of ATOH as a function of pH is shown in Figure 2.12 as curve C.

Using the first approach and the second approach described in section 2.3.5 for AT binding, the formation function of ATOH-FA complex and free energy were calculated and shown in Table 2.20 and Table 2.21, respectively

FIG. 2.17 ATOH BINDING CURVE BY LAURENTIAN FA

(FA=0.5000g/L. pH=2.00)

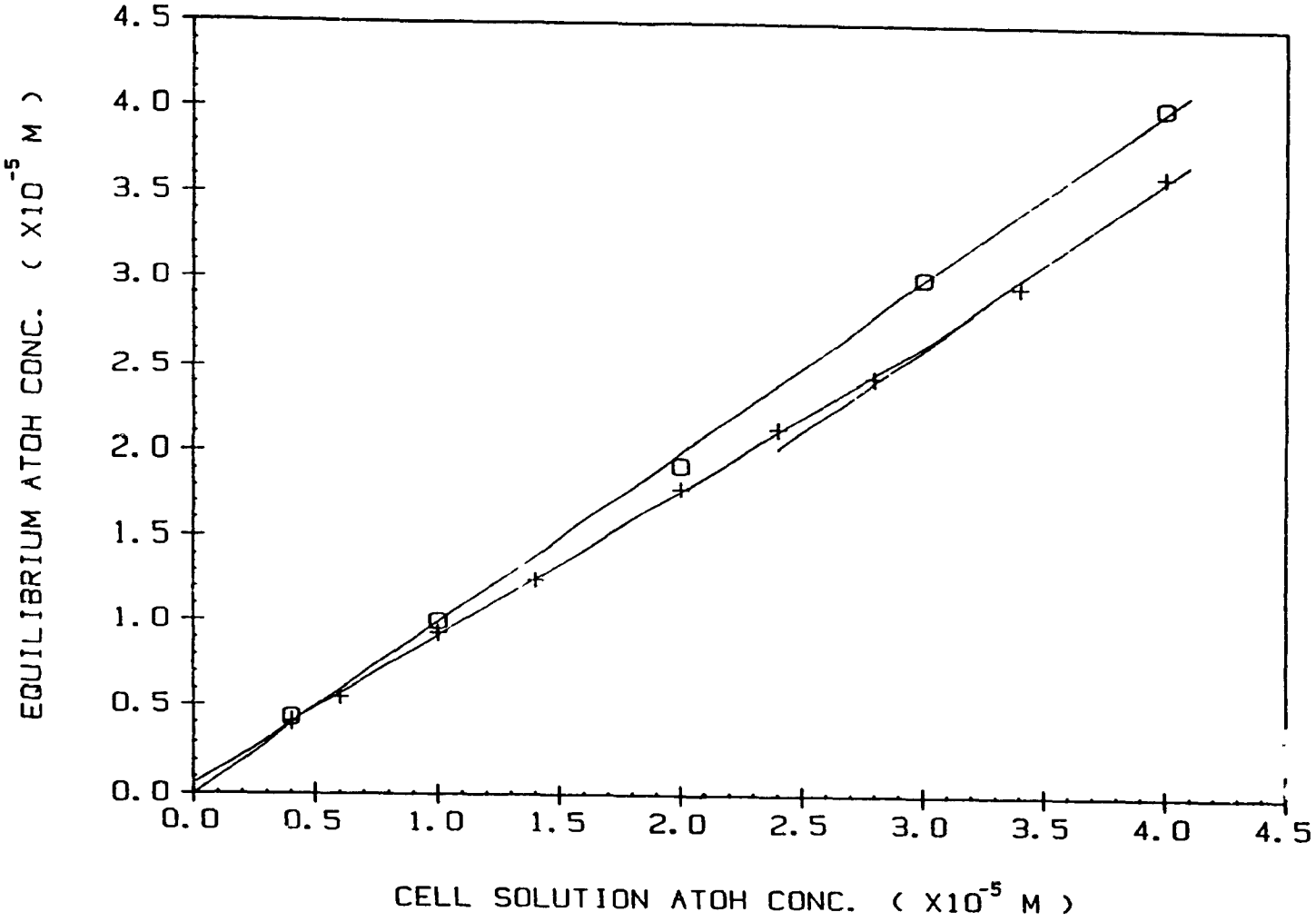

Table 2.20 The formation function and free energies for ATOH-FA complexes at various pH and α values

(FA = 0.5000g/L, ATOH = 4.00×10^{-6}M — 4.00×10^{-5}M)

No	pH	α of FA	(1-α)	$\frac{\partial \bar{K} x}{\partial x}$ (mole/L)	1/K (L/mole)	$-(\Delta G^{o}+RT\ln\Gamma)$ (kJ/mole)
1	2.00	0.40	0.60	0.0163	61.3	10.2
2	2.50	0.50	0.50	0.0179	61.2	10.2
3	2.85	0.575	0.425	0.00846	118	11.8
4	3.00	0.595	0.405	0.00283	354	14.5
5	3.80	0.755	0.245	0.00120	831	16.7
6	4.70	~0.975	~0.025	0.00204	490	15.4
7	5.90	~1.000	~0.000	0.00592	169	12.7
8	6.80	1.000	0.000	0.0108	92.7	11.2

Table 2.21 The formation constant based on observed binding capacity For ATOH-FA at various pH and α values

(FA = 0.5000 g/L, AT = 4.00×10^{-6}— 4.00×10^{-5}M)

No	pH	α of FA	(1-α)	K ($\times10^{-5}$mole/L)	1/K ($\times10^{5}$L/mole)	$-(\Delta G^{o}+RT\ln\Gamma)$ (kJ/mole)
1	2.00	0.40	0.60	0.83	1.20	29.0
2	2.50	0.50	0.50	0.84	1.19	29.0
3	2.85	0.575	0.425	0.84	1.19	29.0
4	3.00	0.595	0.405	0.75	1.33	29.2
5	3.80	0.755	0.245	0.60	1.67	29.8
6	4.70	~0.975	~0.025	0.72	1.39	29.3
7	5.90	~1.000	~0.000	0.89	1.12	28.8
8	6.80	1.000	0.000	0.92	1.09	28.7

Comparing the three binding curves in Figure 2.12, one can immediately find that (a) the binding curve for ATOH is much higher than that for AT at same pH. For example, at pH 3.00, the binding capacity of ATOH is 32.00 μM ATOH per gram FA, but it is only 3.8 μM for AT (we will discuss it later). (b) the maximum binding capacity of ATOH is at pH 3.80 with the value of 46.6 μM ATOH per gram FA, shifted to higher pH about two pH units if compared with the maximum of AT binding curve. (c) even at pH 7.00, the binding of ATOH with FA still occurs.

KCl is very effective in suppression of binding of ATOH. Experimental results showed that at pH 3.10 and 4.40, the binding capacity is only 3.0 and 5.2 μM per gram FA, respectively. (In contrast, the corresponding binding capacity is 40 and 34 μmols ATOH per gram FA in the absence of KCl.) This interesting phenomenon reveals a important fact that the electrolyte has much greater effect on the complex of more polar molecule ATOH with FA than on the complex of less polar molecule AT with FA.

The variation of FA concentration leads to the results similar to AT binding case. The binding capacities of ATOH by 0.1000, 0.5000 and 0.7500 gram FA per liter were found to be 4.0, 16.0 and 21.5 μM ATOH, respectively. Converting all FA concentration to 1 00 gram per liter, the corresponding values are 40.0, 32.0 and 28.7 μM ATOH per gram FA, which was also presented in Figure 2.16 as a plot of binding capacity defined as micromoles per gram of FA against the concentration of FA used.

2.3.7 Competition between AT and ATOH

Since ATOH binds significantly more strongly than AT, it is

important to determine whether ATOH can block AT binding. Figure 2.18 shows the results of a series of experiments in which a constant ratio of 2:1 AT to ATOH was used with variation of the sum. Since both AT and ATOH curves are linear, and the binding capacity of AT, 4.2 μM/g FA is obtained in very good agreement with the value obtained from AT-FA binding alone without adding ATOH, direct competition appears to be undetectable.

2.3.8 Kinetics of AT Hydrolysis

The kinetics of AT hydrolysis can be calculated for every run for which ATOH was measurable. Table 2.22 collects the kinetics data and presents the extraction of the experimentally observed overall rate constant (k_{Obs}), and the corresponding rate constants by proton and protonated Type A carboxyl groups (k and k_{FA}), according to the general catalytic equation given by Gamble and Khan [54]. The average rate constant of AT hydrolysis by the protonated Type A carboxyl groups of Laurentian FA was found to be 6.88±2.94 $days^{-1}$ M^{-1} in the absence of KCl. As a comparison, the k_{FA} for Armadale FA determined by spectrophotometric method was 7.88 $days^{-1}$ M^{-1} [54].

Figure 2.19 shows the catalytic rate constant obtained at various pH values in the absence and presence of 0.1 M KCl plotted as a function of binding capacity. The trends of the curves reveals some correlation between catalytic rate constant and binding capacity. That is, higher binding capacity would lead to higher catalytic rate constant of Type A carboxyl groups of FA.

It can be seen from Table 2.22 that the $\bar{k}_{FA}$ value in the presence of 0.1 M KCl is smaller than the corresponding $\bar{k}_{FA}$ value

FIG. 2. 18A COMPETITION FOR BINDING SITES BETWEEN AT AND ATOH

(FA=0. 500g/L, pH=3. 05, ATOH=0. 200-2. 00X10^{-5} M)

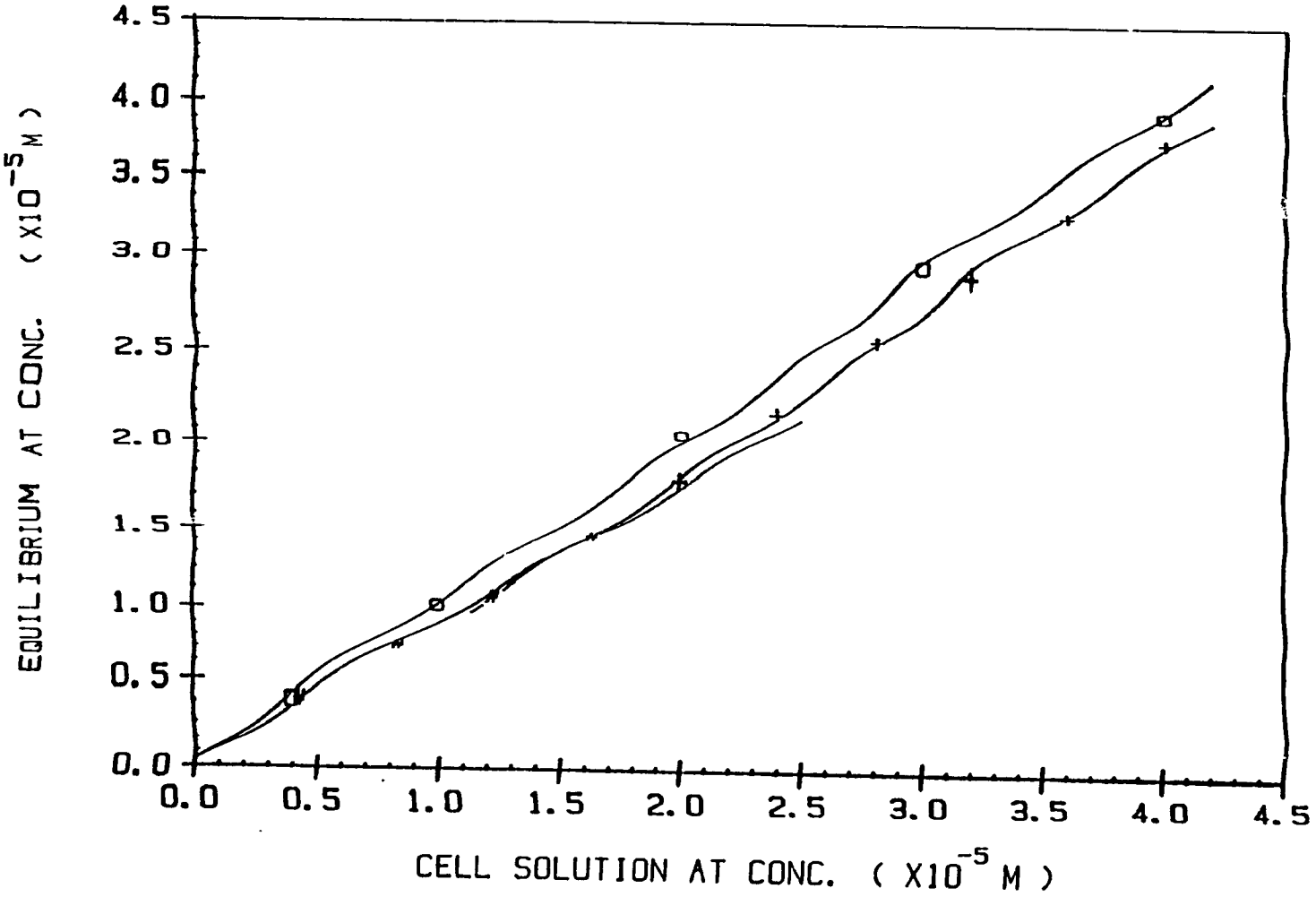

FIG. 2. 18B COMPETITION FOR BINDING SITES BETWEEN AT AND ATOH

(FA=0. 500g/L, pH=3. 05, AT=0. 400-4. 00X10^{-5} M)

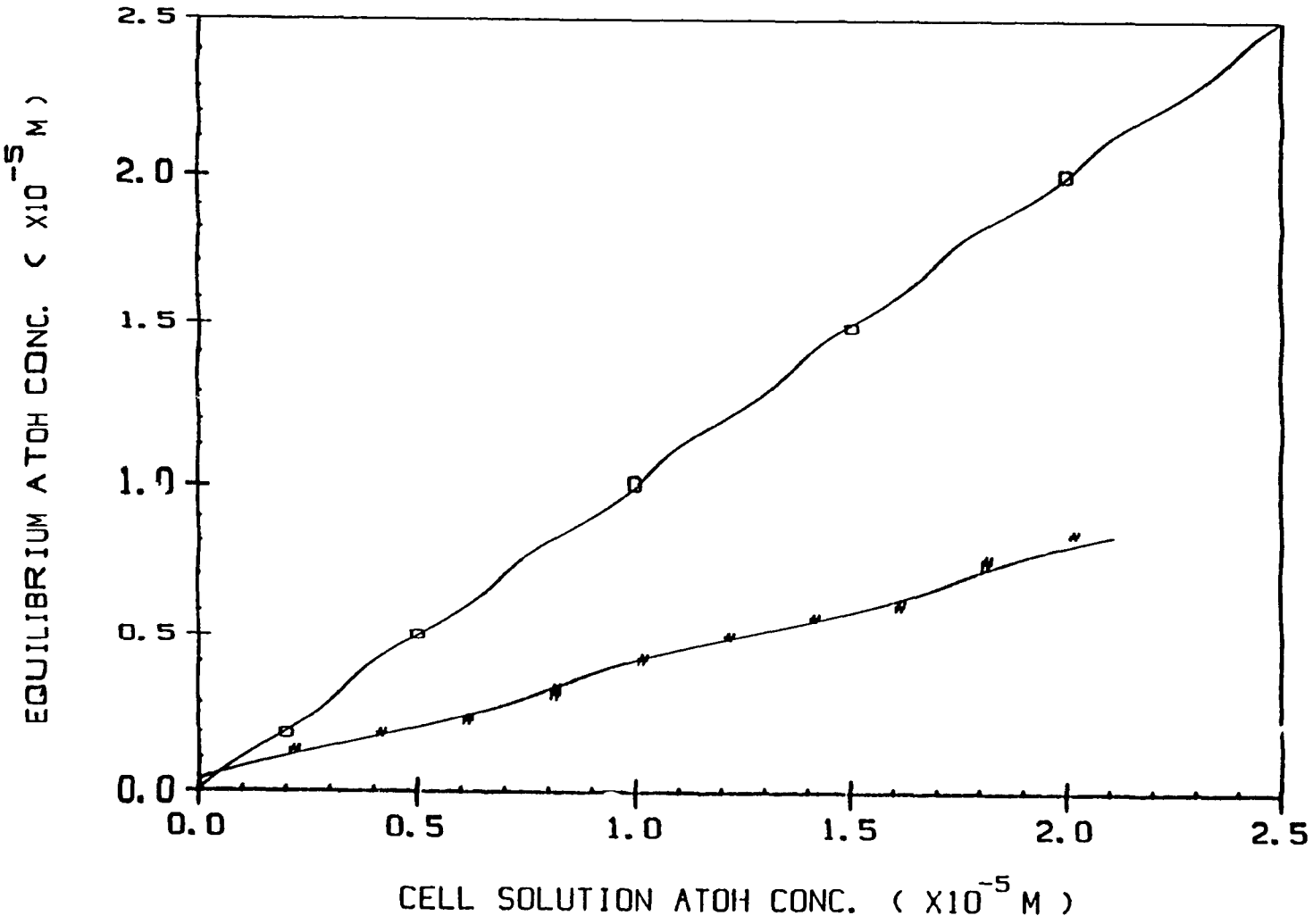

FIG. 2.19 CATALYTIC RATE CONSTANT AT VARIOUS pH VALUES

AS A FUNCTION OF APPARENT BINDING CAPACITY

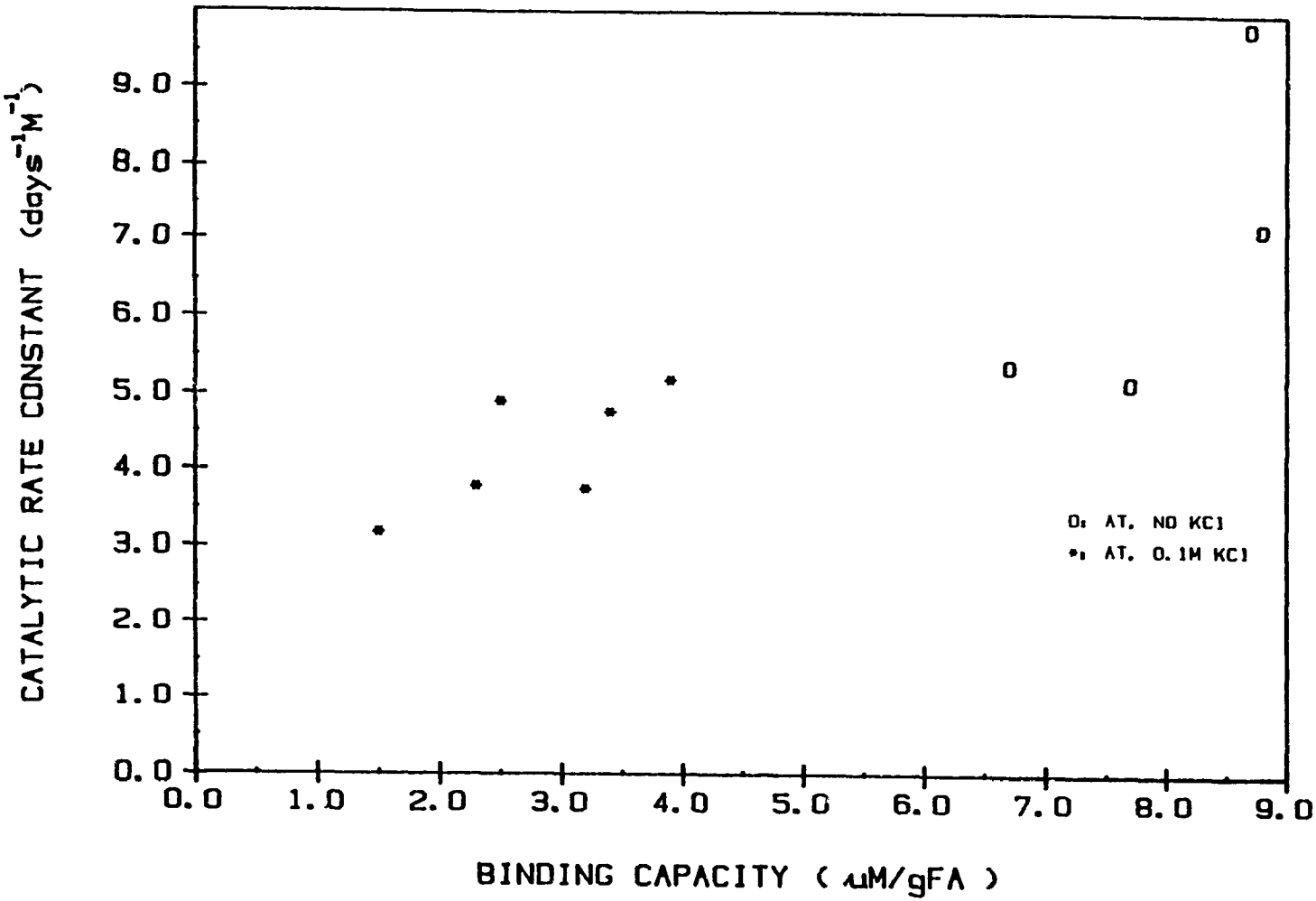

without KCl. This obviously is the effect of the electrolyte KCl. The addition of KCl makes the carboxyl groups more acidic, that means less protonated Type A sites available for AT binding in the presence of KCl, compared with the one at same pH but without KCl. As a result, less AT was catalytically hydrolyzed to ATOH, and smaller k_{FA} values were measured.

Table 2.22 AT hydrolysis: Catalysis by The Undissociated Type A Functional Groups of Laurentian FA at (25±1)^{0}C

(FA=1.0000g/L, AT=0.8000—8.0000x10^{-5}M, Type A=5.11 mmole/g FA)

pH	KCl (M)	Shaking Time (days)	k ($x10^{-3}day^{-1}$)	k_{obs}	k_{cor} [a]	$(1-\alpha)$ [b]	M_{FA} ($x10^{-3}$M/L)	k_{FA} [c] (1/day M)
2.40	/	3.00	19.55	33.55	14.00	0.51	2.606	5.37
2.20	/	3.17	28.67	43.41	14.74	0.56	2.861	5.16
1.90	/	3.25	47.52	70.23	22.71	0.62	3.168	7.16
1.63	/	3.42	68.37	102.5	34.13	0.68	34.75	9.82
$\bar{k}_{FA}$, Average of k_{FA} (1/day M)							6.88±2.94	(S=1.85)
3.52	0.1	3.00	1.705	6.734	5.029	0.31	1.584	3.18
3.15	0.1	3.00	3.932	11.38	7.452	0.385	1.967	3.79
2.80	0.1	3.00	8.506	16.84	8.330	0.435	2.223	3.75
2.20	0.1	3.20	28.67	43.28	14.61	0.56	2.811	5.19
1.70	0.1	3.20	62.84	78.69	15.85	0.65	3.322	4.77
1.45	0.1	3.20	82.82	100.9	18.08	0.72	3.676	4.91
$\bar{k}_{FA}$, Average of k_{FA} (1/day M)							4.27±0.76	(S=0.73)

a. k_{cor} is k_{obs} - k where k is the calculated H^{+} catalysis rate constant so that the differences represents catalysis by undissociated carboxyl groups.
b. $1-\alpha$ represents the fraction of Type A carboxyl groups on the fulvic acid which are protonated.
c. The second order rate constant for fulvic acid catalyzed pathway. $\bar{k}_{FA}$ represents the average values for the catalysis constants in the presence or absence of KCl.

2.4 DISCUSSION

2.4.1 Definition of K

The present sample is one of the few stoichiometrically defined soil fragments available. Thus, it is common to express binding function in terms of an operationally accessible FA concentration such as mg/L or g/L. This corresponds in the present case to our use of the total carboxyl concentration to define FA concentration for calculation of K. The binding site concentration obtained from the limiting bound AT concentration gives better representation (that is, the second approach to calculate K values). The results presented in Figure 2.13 underline the improvement in data resolution which follows from proper scaling.

2.4.2 AT and ATOH binding mechanisms

The study of AT and ATOH binding and AT hydrolysis brings out eight factors which are important to the binding of AT and ATOH to fulvic acids. In consequence, very strong constrains are imposed on the choice of models of the interaction between the herbicides and the fulvic acid. The factors will be enumerated to clarify the logic of the interpretation.

(1) There is a close connection between binding and protonation of the FA carboxylates. Generally, the lower the pH, the higher the binding should be. But the maximal binding does not correspond to complete protonation of either FA or AT because of the FA aggregation caused by high hydrogen ion concentration.

(2) The factors which are connected to increased FA aggregation,

increase of FA concentration and increase of ionic strength [79] tend to suppress binding.

(3) The binding capacity for AT or ATOH is well defined at each pH and is a small fraction of the total of the important carboxylate groups.

(4) The binding of AT is not competitive with ATOH binding.

(5) All runs are well fit by a single value of free energy of binding, consistent with homogeneity of the relatively scarce binding sites.

(6) The time to reach binding equilibrium is measured in days not seconds.

(7) The free energies of binding are of the order of H-bonding energies.

(8) Binding is preferentially associated with the larger fraction of the sample. (see details in Chapter 3)

Factors 1 and 7 are those which have directed attention of previous workers to hydrogen bonding as the interaction responsible for AT and ATOH binding. The binding process may be proposed by the following equations in which ROOH represents FA:

$$AT + H^+ \rightleftharpoons ATH^+ \quad (43)$$

$$RCOO^- + H^+ \rightleftharpoons RCOOH \quad (44)$$

$$AT + RCOOH \rightleftharpoons RCOOH \ AT \quad (45)$$

$$ATH^+ + RCOOH \rightleftharpoons RCOOH \cdot ATH^+ \quad (46)$$

$$ATH^+ + RCOOH \rightleftharpoons RCOOATH + H^+ \quad (47)$$

$$ATH^+ + RCOO^- \rightleftharpoons RCOO^-H^+AT \rightleftharpoons RCOOH - AT \quad (48)$$

$$n\ RCOOH \rightleftharpoons (RCOOH)_n \quad (49)$$

From the above proposed reaction equations, there obviously are three competitive factors affecting AT binding: protonation,

formation of hydrogen bonds, and aggregation. All are pH and electrolyte dependent. pH (in the pH range of 1.9-5.5) decrease shifts reactions (43-48) to right side, in favor of AT-FA binding. If pH further decreases (lower than 1.4) especially for the case that the protonated sample is exposed to high electrolyte concentration, reaction (49) occurs and the aggregation sharply increases with pH decrease, the aggregation becomes the dominant factor, resulting in the loss of binding sites, and hence in the reduction of the AT-FA binding. Experimentally, it was evident to the eye that AT-FA sample solutions became more or less turbid when pH decreased to that lower than pH 1.9. The competition of these two factors leads to the appearance of the maximum of binding capacity. The position of the maximum depends on the nature of pesticides and the composition of the solution.

If a hydrogen bonding mechanism is correct, what must be explained is why such a small fraction (factor 3) of the total carboxylates participate in binding sites. In an aqueous medium, hydrogen bonding is highly competitive process because water molecules can function as both donors and acceptors in H-bonds.

For AT to be bound to the highly oxidized and significantly hydrophilic FA, AT must "find" a site where it can compete with water. It is reasonable that such sites are rare. Moreover, it is reasonable that such AT specific sites are not the same as the ATOH specific sites (factor 4.). These rare sites may well be fairly homogeneous (factor 5.).

To understand the role of FA aggregation (factor 2.), it is important to remember that the FA's are polydisperse mixtures which show higher weight average MW than number average MW (79).

This means that an FA mixture is composed of a relatively large number of lower MW particles mixed with a smaller number of high MW particles. All FA particles are sufficiently oxidized to participate in H-bonding. As FA concentration rises, mass action principles lead us to expect aggregation of FA particles by interactions including H-bonding. The smaller FA particles block sites which are involved in AT or ATOH binding.

A model of the special sites which bind AT or ATOH is strongly limited by the time required for equilibration (factor 6.). H-bonds are very labile. For a very labile interaction to result in long equilibration times requires a complex mechanism. The source of the complex mechanism is the FA itself. The special sites are created by dynamic rearrangements in the FA itself. Among these is a conformational H-bonding equilibration analogous to the interactions which control tertiary structure of proteins. A site which prefers H-bonding AT or ATOH over water may not exist in the unperturbed conformation of the FA polymers. It may arise as the product of a quasi-random walk through the variety of conformations accessible at comparable energies. Each step is rapid, but the critical combination of polymer reconfiguration and solute diffusion required leads to long equilibration times.

The model proposed here bears a strong resemblance to the binding processes of enzyme-substrate complexes where the tertiary structure of the enzyme is critical. The difference is that the enzyme have genetically programmed well defined sites. In the present case, binding site generation is an inefficient, quasi-random process.

The idea of conformation controlling pesticide binding is

probably more general than the case of atrazine. In a series of recent studies in these laboratories [48,98,99] the interaction of the non-polar species, lindane, the polar species atrazine, and the cationic species, paraquat with FA's has revealed a common dependence on carboxylate protonation and a capacity which is low compared to carboxylate stoichiometry. The one factor which is common to the three electrostatically different substrates is the dependence on FA conformation. It is probably also worth pointing out that the way aggregation disfavors binding underlines a need for caution about binding originating from generalized hydrophobic interactions, even for non-polar molecules.

2.4.3 Catalysis of hydrolysis

The k_{FA} value of Type A carboxyl groups of Armadale Bh horizon FA was determined by the spectrophotometric method to be 7.88 $days^{-1}M^{-1}$ [54]. Considering the differences between thetwo FA and between the HPLC and spectrophotometric techniques, the results of the present study by UF-HPLC method on the kinetics of conversion of AT to ATOH are entirely consistent with the results obtained by Gamble and Khan [54]. The FA sites appear to function as general acid catalysts for the hydrolysis reaction. The demonstrated absence of competition between AT and ATOH binding allows simple kinetics to be maintained.

2.4.4 ATOH binding, H-bonding and ion-exchange

It has been pointed out that ATOH is the most polar with the highest pKa value and highest basicity among all AT derivatives. Unlike AT, in the case of ATOH, not only amino groups, but also

oxygen groups from ATOH resonance structures can form hydrogen bonds with protonated carboxyl groups of FA. The complexing sites of ATOH-FA could be:

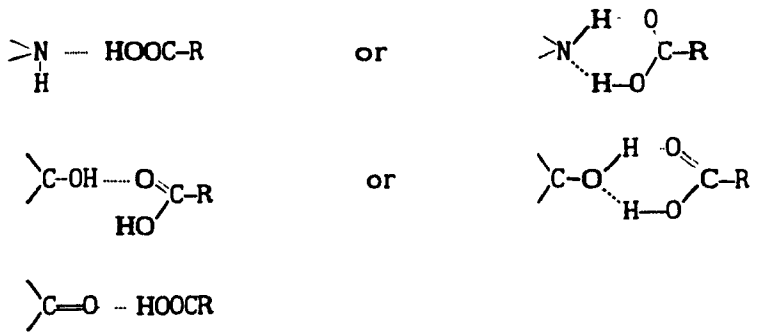

All these factors result in the much higher binding capacity of ATOH than AT.

It should be emphasized that when pH of the ATOH solution decreases to 4.0 and lower, the ion exchange mechanism for ATOH binding becomes significantly important. The importance of ion exchange to the ATOH binding is reflected by much greater binding capacity of ATOH by FA at higher pH compared with the AT binding case. The maximum binding capacity of ATOH, which has been shown, is at pH 3.80 with the value as high as 46.6 μM ATOH per gram FA. At this pH, almost all of ATOH exist in the protonated form (pK_a of ATOH is 5.05!). ATOH H^+ behaves as organic cation to react with COOH groups of FA via cation exchange and the release of hydrogen ion. It can be expected that if KCl is added to ATOH-FA samples, K^+ with much greater concentration (0.1M) will effectively suppress the binding of ATOH, for K^+ can effectively compete with ATOH H^+ for ion-exchange sites subsequently resulting in the drastic reduction of binding capacity of ATOH. Experiments have clearly confirmed this explanation. As a result, the calculated free energies of ATOH-FA complexes were higher than

that of the corresponding AT-FA complexes, which implies more and stronger binding formed between ATOH and carboxyl groups of FA. However, it must be realized that even so, the site bound by ATOH is still a very small fraction of the total of the carboxylate groups.

The related complexing reactions proposed as follows:

$$ATOH + H^+ \rightleftharpoons ATOH_2 \quad (50)$$

$$RCOO^- + H^+ \rightleftharpoons RCOOH \quad (51)$$

$$ATOH + R\text{-}COOH \rightleftharpoons RCOOH\text{—}ATOH \quad (52)$$

$$ATOH\ H^+ + R\text{-}COOH \rightleftharpoons RCOOH\ \ ATOH\ H^+ \quad (53)$$

$$ATOH\ H^+ + RCOO^- \rightleftharpoons RCOO^-H^+ATOH \rightleftharpoons RCOOH\ \ ATOH \quad (54)$$

$$ATOH\ H^+ + RCOOH \rightleftharpoons ATOH\ H^+RCOO^- + H^+ \quad (55)$$

$$n\ RCOOH \rightleftharpoons (RCOOH)_n \quad (56)$$

An explanation similar to AT-FA case as to why there is a maximum in the curve of binding capacity against pH can be applied to ATOH-FA case. The only difference is that ATOH is more polar than AT and has higher pK value, resulting in the shift of maximum to pH 3.80. At this pH, ATOH exists as nearly 100% of the protonated species, and also no significant aggregation of Type A carboxyl groups of FA molecules occurs at this pH; hence, the maximum binding capacity of ATOH is observed. At pH 8.0 and higher, no binding was observed because at these pH values ATOH and FA exist only as unprotonated forms.

CHAPTER 3

STRUCTURAL CHARACTERIZATION OF LAURENTIAN FULVIC ACID AND ITS FRACTIONS

3.1 THE PRESENT STATUS OF THE STRUCTURAL STUDIES OF HUMICS

It is understood that humic substances are very complex mixtures with organic polyelectrolyte properties. Their molecular weight could be as low as several hundred to perhaps over 300,000 [4]. Humic substances play an important role in natural systems, and they can complex metal ions, and react with and bind organic pollutants. It has been demonstrated in Chapter 2 that the interaction between Laurentian Fulvic Acid and the pesticide atrazine is strongly influenced by pH, ionic strength, FA concentration, and a kinetic factor. All of these factors are related to the conformation, that is macromolecular size and shape, of fulvic acid in solution, which in turn is a function of solution pH, ionic strength and the concentration of itself.

Several experimental approaches have been used to study the structure and aqueous conformation of humic substances, each technique having its potential to contribute to the characterization of structural features of humic substances. The structure analysis techniques include functional group analysis which can supply probable range for the distribution of oxygen-containing functional groups in humic substances [3-5]; solution and solid-state ^{13}C-NMR spectroscopy which has been commonly used to estimate the fraction of aromatic carbons and other different types of carbons [6-11]; GC/MS [12,13] which has

been used to separate and identify some amino compounds, alkanes, fatty acids and hydroxy-fatty acids from the extracts of humic substances; and Time-Resolved Pyrolysis Field Ionization Mass Spectrometry which has been used to get structural information on the behaviour of humic substances and their degradation products [14].

The aqueous conformation of fulvic acid has been studied by surface tension and viscometry, and steady-state fluorescence depolarization [15-19]. Recently Lochmuler and Saavedra [20] applied time-dependent fluorescence depolarization spectroscopy to study the dependence of fulvic acid on the independent parameters specifying the solution composition.

Even though considerable, if not incomplete, information about structural features of humic substances has been obtained, little is known about the relation between pesticide binding and molecular size and shape of water-soluble FA in solution. We report here the results of a study in which the ultrafiltration technique in combination with UV/VIS absorption and Fluorescence, FTIR and NMR is used to characterize size fractions of the Laurentian Fulvic Acid, and to investigate the binding behaviour of AT with different fractions and the interaction among fractions themselves.

Compared with other techniques, the method described below is quite attractive because (1) it is sensitive to changes in FA particle size and shape; (2) it can supply us direct evidence of the effect of FA fractions having different molecular weight (MW) range on AT binding; (3) it can reveal some relationships between

MW and structural features of FA fractions; (4) experimental results support the proposed model in chapter 2, which assigns binding of herbicides to specific sites determined by the dynamic conformational equalibria of the polymer mixture; (5) it is inexpensive, time-saving and rich in H-bond information.

3.2 EXPERIMENTAL

3.2.1 Materials:

The fulvic acid and atrazine used has been described in Chapter 2. Other chemicals were reagent grade and used as received.

3.2.2 Apparatus:

The pH values were obtained with a Metrohm Model E 300 B equipped with a Fisher EA-1210-UX glass combination electrode, which was calibrated with pH 4.00 ± 0.01, pH 7.00 ± 0.01, and pH 9.00 ± 0.01 standard buffer solutions. UV/VIS spectra were recorded on a HP 8452 Diode-Array UV/VIS spectrophotometer equipped with a deuteriom lamp and interfaced to an IBM PC/XT computer. HPLC was performed on a Waters Associates System (Model U6K injector, Model 6000A pump and Model 440 UV absorption detector) with UV detection at 254 nm. The column used was CSC-Chromosorb LC-7 reverse phase (C_{18}, Silica, 10 um, 25 x 0.46 cm).

Ultrafiltration was conducted using an Amicon stirred ultrafiltration cell, Model 8050, having a maximum volume of 50 ml. The filters were Amicon YM-2 membranes with MW cut-off 1000

dalton.

FTIR spectra ranging from 4000-500 cm-1 were recorded on a Michelson 102 FTIR spectrophotometer (Bomem) equipped with a Globar source, a CsI beamsplitter and a wide range and high speed deuterated triglycine sulfate (DTGS) detector sperating at a nominal resolution of 4 cm^{-1}.

FA fractionation was conducted in the same way as the filtration according to nominal MW by ultrafiltration.

Proton NMR specrum of the lowest MW FA fraction in D_2O solution was recorded on Bruker 400 MHz NMR spectrometer, at 299.5 MHz frequency using gated-decoupling technique. The following conditions were chosen to obtain reasonable intensity distribution while maintaining usable signal-to-noise ratio, acquisition time 1.997 seconds, relaxation delay 2.0 sec, pulse width 75 degrees, ambient temperature, spin rate 25 Hz and spectral width 5000 Hz. The total acquisition time is 11.7 minutes.

The fluorescence measurements were made on a Perkin-Elmer MPF-44B Fluorescence Spectrometer. The slit of the instrument was set at 5 nm, and the signal gain was set at 1 or 3 according to the recorded spectrum intensity.

3.2.3 Procedure

(1) FA Fractionation

The membranes chosen for FA fractionation were Amicon hydrophilic YM series, which have the lowest adsorption of any Amicon membrane. The 250.0 ml FA solution containing 2.5000 g FA were sequentially passed through YM30 (nominal MW cut-off 30,000

dalton). Five fractions were collected, and were then freeze-dried to yield sub-fraction FA solid samples.

AT binding by different MW fractions of FA were carried in the same way as described in Chapter 2.

(2) FTIR Spectra Measurements

The interaction product between FA and Cu^{+2} ion was obtained according to the following procedure: 5.00 ml of 1.00 x 10^{-2}M Cu^{+2} solution is added to 0.25 ml 2.5000 g/100 ml FA solution, it is diluted to about 24.0 ml with deionized water, and the pH value of the solution is then adjusted to about 5.0 by adding 0.05 and 0.01 M NaOH. The final volume of Cu-FA solution is 25.00 ml. The solution is sealed securely with parafilm and then shaken for 3 days at room temperature (21±2^{0}C). After three days the solution is centrifuged for 15 minutes at a speed 5000 rpm in IEC B-20 Centrifuge. The precipitate obtained is succesively washed with deionized water to remove non-precipitated FA and Cu^{+2} ion. Finally the interaction product is vaccum desiccator dried for use.

The KBr pellet for FTIR measurement had a weight ratio of 1:200 (sample/KBr). The original unratioed spectra of the sample and of the empty beam were computed from 500 signal-averaged scans (about 60 minutes total measurement for each spectrum). Difference spectra between FA and Cu-FA complex were obtained by subtraction of the spectrum of the Cu-FA complex from that of the original FA, or in reverse way.

(3) Fluorescence Spectra Measurements

The concentrations of the lowest and highest fractions of FA used were 0.1000 g/L. Sample solutions were prepared by dissolving the precisely weighed FA in deionized water, then diluted to the desired concentration followd by overnight equilibration. The pH of each sample was adjusted with 0.01 and 0.1 N HCl or NaOH solution. The cuvette used was a standard 10 mm silica fluorescence cuvette. The excitation wavelength was set at 355 nm, and the recorded emission wavelength was in the range of 365 to 610 nm.

3.3. RESULTS

3.3.1 Physical Properties of Fractions

The main criteria of FA fractionation method should be that it allows the separation of various fractions having different molecular weight (MW) ranges, as well as simple, sufficient rapid and nondestructive. These requirements greatly limit the possibilities of using methods such as precipitation, extraction, ion exchange or common filtration. The better choice for meeting the requirements is an ultrafiltration method because it permits the concentration of large molecules by passing the solvent and other small molecules through the membrane with a certain pore sizes.

Ultrafiltration of the FA into 5 fractions yielded material with the physical properties summarized in Table 3.1.

Table 3.1 Characteristics of Five Fractions Fractionated by UF Method

MW range*	Solid colour	% Total mass	pH (0.5g/L)	pH (1.0g/L)	Solution colour (0.5g/L)
>30,000	Deep brown (floc powder	37.0	3.00	2.80	Orange-yellow
10,000-30,000	Brown	2.8	2.95		Yellow
5,000-10,000	Brown	7.2	2.92		Yellow
1,000-5,000	Yellow-brown	15.5	2.87		Pale-yellow
<1,000	Yellow	37.5	2.84	2.50	Pale-yellow

* The MW range are Amicon "nominal" cut-off and are not calibrated for humic substances. Our experience is that humics retained are smaller than the values suggested.

One can immediately see from Table 3.1 that (1) the distribution of mass percentage of Laurentian FA fractions is a dish-like shape, that is, the two ends (the smallest and the highest) fractions have nearly equal high mass percentage, 37% and 37.5 % respectively, and the second highest MW fraction (MW 10,000 - 30,000) has the lowest mass percentage, 2.8%. (2)The highest MW fraction has the deepest colour. This fact suggests

that the higher MW fractions contain more and bigger conjugated chromophores than lower fractions. (3). The pH value of fraction solutions having the same concentration (0.5000 g/L or 1.000 g/L) changes with nominal MW of fractions, which indicates the lowest MW fraction has the highest contents of acidic functional groups per unit weight.

3.3.2 UV-Vis Spectrophotometric Behaviour of Fractions

All five fractions have strong absorption in UV regions. Basically, the higher the MW, the higher the absorbance. In order to see whether there is any interaction between different FA fractions an experiment was designed as follows: to mix the highest fraction solution with the lowest fraction solution having same concentration (g/L) in the ratio 1:1, then to measure its UV/Vis spectra at different intervals, and to compare it with the spectra of its parent solutions. The absorbance values at various wavelengths are listed in Table 3.2.

Fig 3.1 shows the spectra of the lowest and highest fractions, and their mixture having the same concentration 0.01% in the range of 600-250 nm at 2 hour intervals. From Table 3.2 and Fig 3.1 it can be seen that absorbance of the mixture significantly changes after mixing. This fact implies some interaction must occur between the molecules of larger and smaller fraction. No noticeable absorbance change can be observed after equilibrium is established in solution approximately 24 hours later.

FIG. 3.1 UV/VIS SPECTRA OF FA FRACTIONS

(TOTAL FA CONCENTRATION=0.01%)

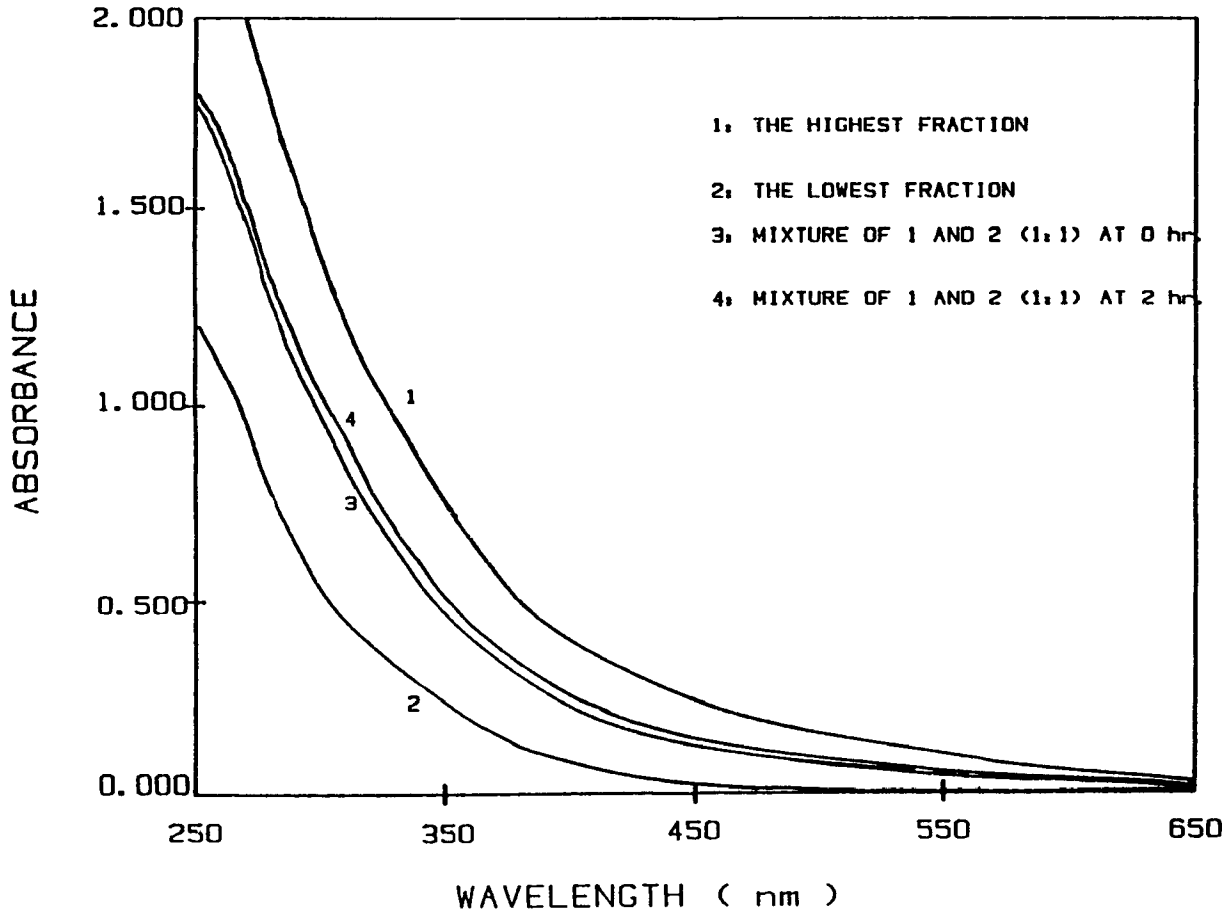

Table 3.2 UV/VIS Absorbance of Mixture at Various Intervals

($FA_{MW<1000}$:$FA_{MW>30,000}$ = 1:1, Total conc. of FA = 0.005%)

λ(nm)	absorbance at various intervals (hours)				
	0 hr.	1.7 hr.	2.3 hr.	4.7 hr.	$A_4 - A_1$
200	1.478	1.498	1.498	1.510	0.0320
210	1.462	1.474	1.476	1.487	0.0250
220	1.361	1.370	1.371	1.379	0.0180
230	1.226	1.235	1.236	1.242	0.0160
240	1.083	1.092	1.092	1.098	0.0150
250	0.9746	0.9825	0.9833	0.9876	0.0130
260	0.9005	0.9076	0.9086	0.9125	0.0120
270	0.8084	0.8157	0.8169	0.8205	0.0121
280	0.7002	0.7084	0.7096	0.7124	0.0122
290	0.6044	0.6130	0.6140	0.6163	0.0119
300	0.5241	0.5335	0.5345	0.5361	0.0120
310	0.4531	0.4629	0.4641	0.4653	0.0122
320	0.3932	0.4035	0.4047	0.4054	0.0122
330	0.3432	0.3543	0.3554	0.3557	0.0125
340	0.2983	0.3100	0.3110	0.3111	0.0128
350	0.2558	0.2682	0.2690	0.2689	0.0131
360	0.2162	0.2292	0.2298	0.2295	0.0133
370	0.1820	0.1953	0.1959	0.1954	0.0134
380	0.1525	0.1662	0.1668	0.1660	0.0135
390	0.1281	0.1425	0.1429	0.1420	0.0139
400	0.1086	0.1233	0.1236	0.1228	0.0142
410	0.0932	0.1082	0.1085	0.1075	0.0143
420	0.0807	0.0963	0.0966	0.0966	0.0159
430	0.0708	0.0868	0.0871	0.0861	0.0153
440	0.0627	0.0792	0.0794	0.0783	0.0156
450	0.0559	0.0724	0.0724	0.0713	0.0154
460	0.0494	0.0662	0.0662	0.0650	0.0156
470	0.0438	0.0605	0.0605	0.0593	0.0155
480	0.0372	0.0547	0.0548	0.0535	0.0163
490	0.0317	0.0495	0.0494	0.0480	0.0163
500	0.0273	0.0447	0.0446	0.0434	0.0161

3.3.3 Fluorescence Spectrophotometric Behaviour of Fractions

The Laurentian FA fractions and the mixture of the lowest and highest fractions exhibit broad emission spectra, three of which are shown in Figure 3.2, in which the curve A is the fluorescence spectrum of the lowest fraction, and the curve B is of the highest fraction and the curve C is of their mixture. All of these three samples have the same concentration, 0.100g/L. The fluorescence intensity and emission maxima for those solutions having different pH values are listed in Table 3.3.

Table 3.3 Fluorescence intensity and emission maxima as a function of fractions and pH

(signal gain = 1)

the lowest fraction (0.1000g/L)		the highest fraction (0.1000g/L)		the mixture (0.1000g/L)	
pH	intensity at λ_{max}	pH	intensity at λ_{max}	pH	intensity at λ_{max}
2.58	71	2.60	8.2	3.80	30
3.75	84	3.90	10.3		
6.50	87	6.80	10.0		
8.10	81	8.60	8.7		
10.8	69	10.1	8.0		
maximum	463nm		475nm		465nm

It has been concluded from the previous study by mild chemical degradation of FA followed by separation and analysis of the products that FA is a polydisperse mixture of structurally heterageneous polymers [17]. The polymers are composed of single

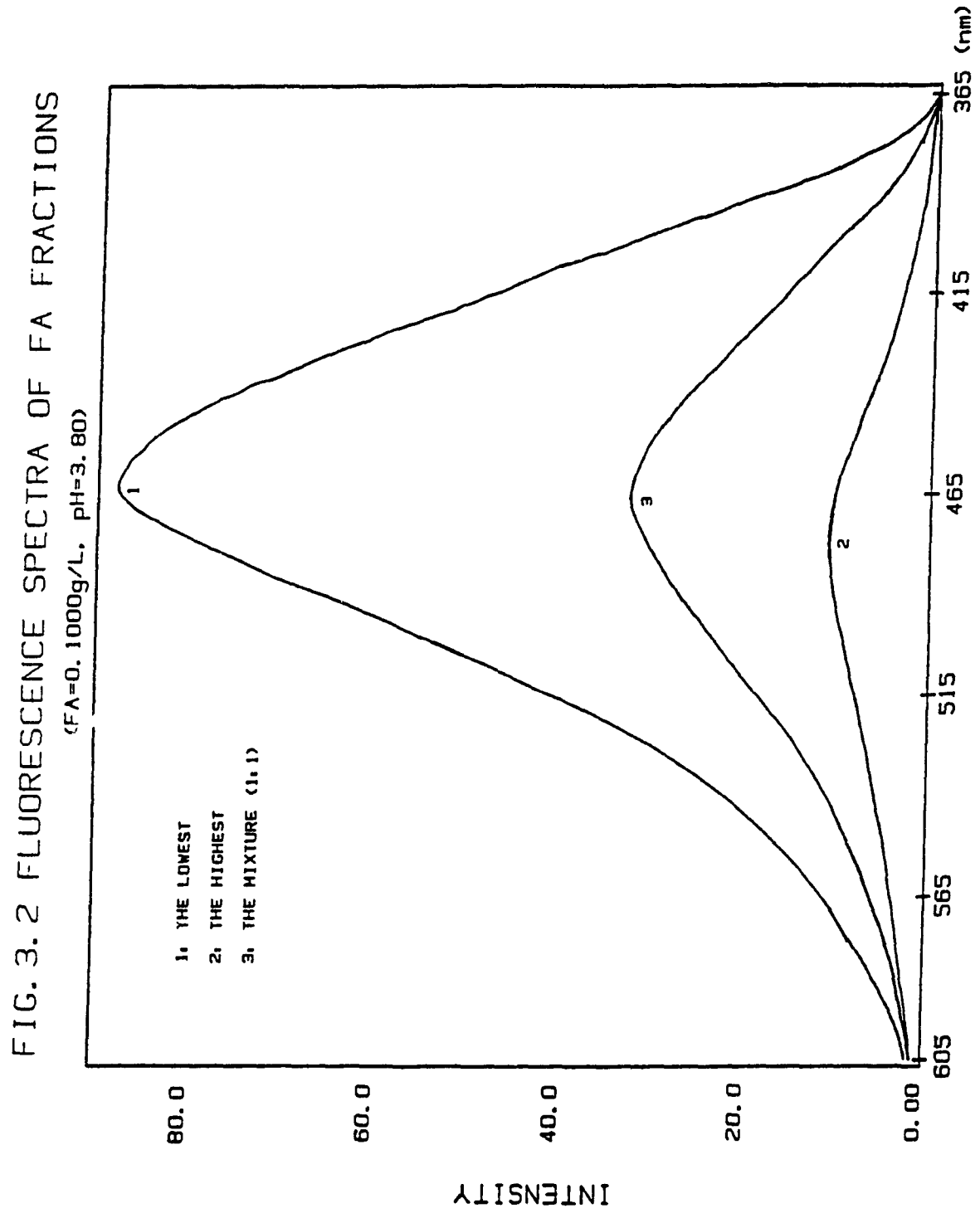
FIG. 3.2 FLUORESCENCE SPECTRA OF FA FRACTIONS
(FA=0.1000g/L, pH=3.80)
1: THE LOWEST
2: THE HIGHEST
3: THE MIXTURE (1:1)
INTENSITY
80.0
60.0
40.0
20.0
0.00
605
565
515
465
415
365 (nm)
1
2
3

and polycyclic aromatic rings bearing oxygen-containing substituents that are randomly linked together by short aliphatic chains. This variety of substituted aromatic system is presumed to be the source of the fluorescence emission. Because the mixtures of these fluorophores are surrounded by a continuous distribution of molecular environment, fulvic acid exhibits a broad emission spectra.

After absorption of a photon, a molecule of FA exists in an excited state, it will, in general, have only a short lifetime since a number of processes can contribute to the deactivation of exited FA molecule to the lower state. These include both chemical and physical process. The physical process for dissipation of exitation energy could include conversion to thermal energy, conversion between states, energy transfer and radiative dissipation; the chemical process could be free radical formation and intramolecular rearrangement.

At low pH, the protonated FA forms more hydrogen bond, inducing some aggregation of FA components. This allows closer contact between the donor and acceptor, and more collisions between molecules. This conformational change will cause energy transfer to vibrational modes in the other molecules from the electronic exited state. Also at low pH higher quantum yield to the triplet state from exited state can be obtained (which has been demonstrated in Power's work [122]), leading to lower fluorescence intensity. In one word, more self-quenching occurs at lower pH. As the pH of the FA solution increase, the molecules of FA uncoil, becoming more elongated and rigid due to accumulation

of negative charge from carboxylate ionization. Therefore, the fluorescence intensity increases as a result of fewer collisions and less energy transfer between FA molecules. When a neutral solution of FA turns to basic, OH^- ions probably act as energy acceptors and also a quenching reagent. This results in a reduction of fluorescence intensity from its maximum.

Figure 3.2 and Table 3.3 shows that the fluorescence emission is associated with the lower molecular weight fraction. It is most probably because the lower MW fraction has more oxygen-containing substituents, especially has more acidic functional groups (see 3.3.1); and also possibly because the smaller molecules of the lower MW fraction are less coiled, and less self H-bonding intramolecular interactions. In contrast, the higher MW fraction of FA having the same concentration gives much lower fluorescence intensity, due to much more intramolecular (energy transfer from one group to another in the same molecule) and intermolecular interactions, and more frequent and much easier energy transfer processes. Another distinguishing feature is the shift in emission maximum 12 nm to the red, which can be attributed to a larger amount of lower energy vibrational states in higher MW fraction than the lower MW fractions.

Theoretically, the fluorescence intensity of the mixture should be half of the intensity sum of the lowest and highest MW fraction if there is no interaction between them. However, the experimental value (intensity:30) was much lower than the expected value (1/2(84+10.3) = 47.2), which clearly demonstrated there must be some interaction between molecules of the lowest and

highest fraction. Guillet [123] pointed out in his recently published book that one of the energy transfer processes of polymer molecules involves the transfer of excitation to a large molecule from a small molecule, or alternatively, which thus quench a photochemical or photophysical process. This appears true in the present case. The self-binding between smaller and larger fraction must result in more energy transfer, more overlap of electronic charge clouds occuring during collision than the lowest or highest fraction alone. Consequently, lower intensity than the expected value is observed.

3.3.4 AT Binding by Different Fractions

Fig 3.3A shows the binding curves of AT by the smallest and the highest fraction, and by their mixture (1:1). Fig. 3.3B shows the curves of the middle fragments of FA, and 3.3C shows the curves by the smallest and highest at 1.000 g FA/L concentration level. The data of AT binding capacity are collected in Table 3.4. Fig 3.4 shows the relation of AT bound to AT free for comparable concentrations of AT-humic substances for each of the five MW fractions.

It is immediately apparent that (1) most of the binding capacity is associated with the highest MW fraction, some binding is exhibited by the next fractions and the smallest fraction contributed a little to binding. (2) The theoretical binding capacity of AT by the mixture of the smallest (MW <1,000) and the highest (MW > 30,000) fraction with ratio 1:1 is obviously greater than the experimental value. The difference is about 20% of the

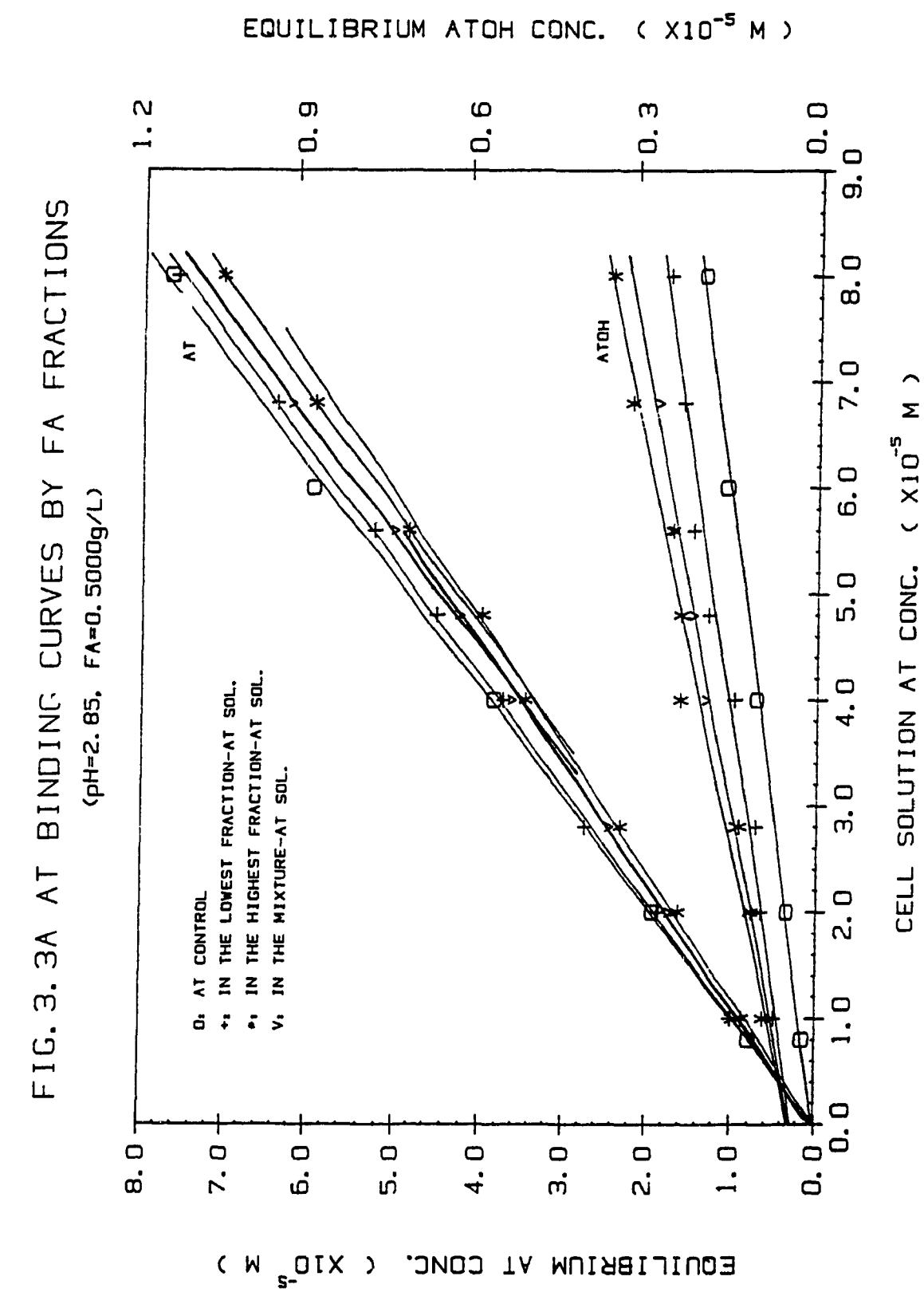
FIG. 3. 3A AT BINDING CURVES BY FA FRACTIONS
(pH=2.85, FA=0.5000g/L)
EQUILIBRIUM ATOH CONC. (X10⁻⁵ M)
EQUILIBRIUM AT CONC. (X10⁻⁵ M)
CELL SOLUTION AT CONC. (X10⁻⁵ M)
AT
ATOH
O: AT CONTROL
+: IN THE LOWEST FRACTION-AT SOL.
*: IN THE HIGHEST FRACTION-AT SOL.
V: IN THE MIXTURE-AT SOL.

FIG. 3.3B AT BINDING CURVES BY FA FRACTIONS

(pH=2.85, FA=0.5000g/L)

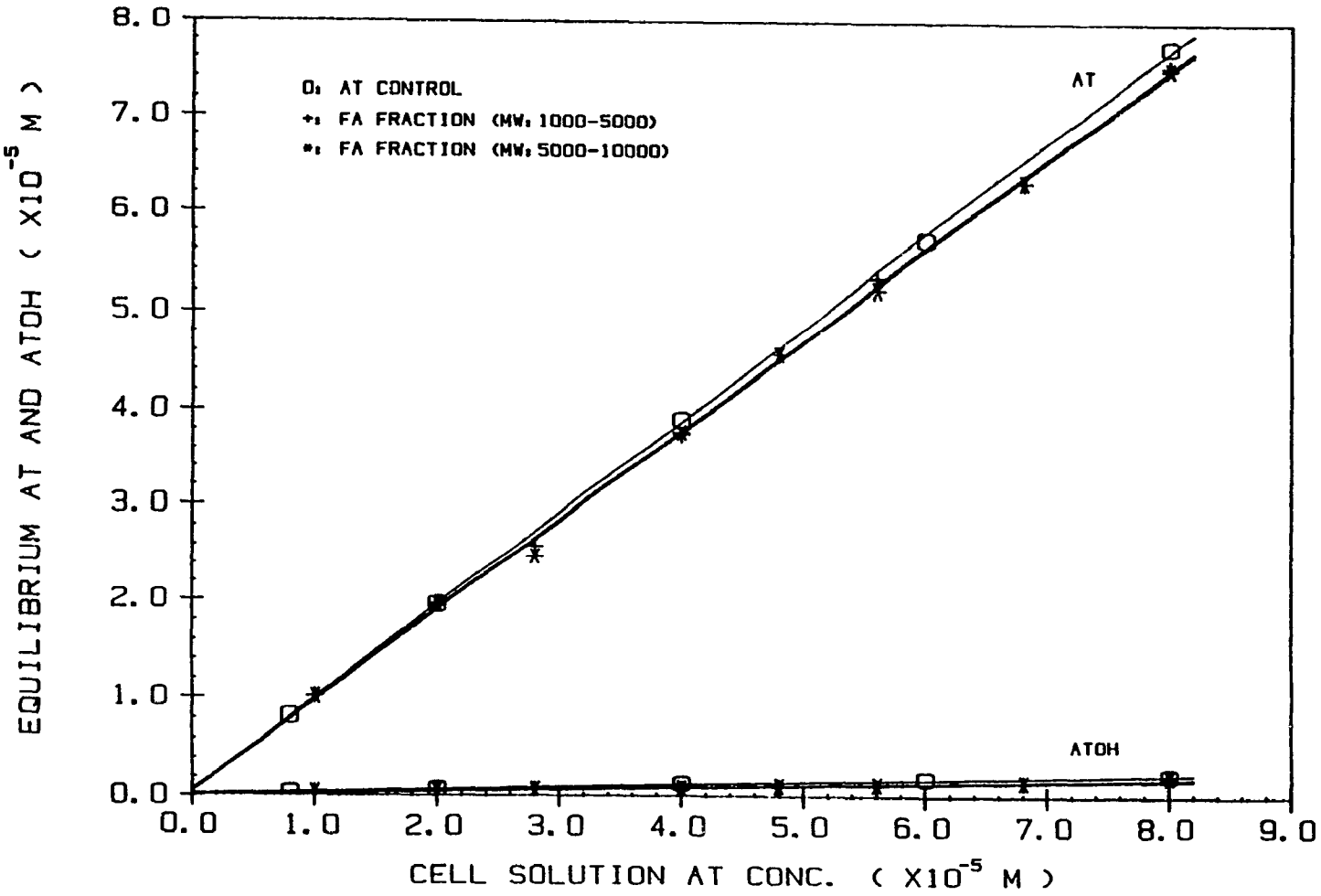

FIG. 3.3C AT BINDING CURVES BY FA FRACTIONS

(pH=2.60, FA=1.000g/L)

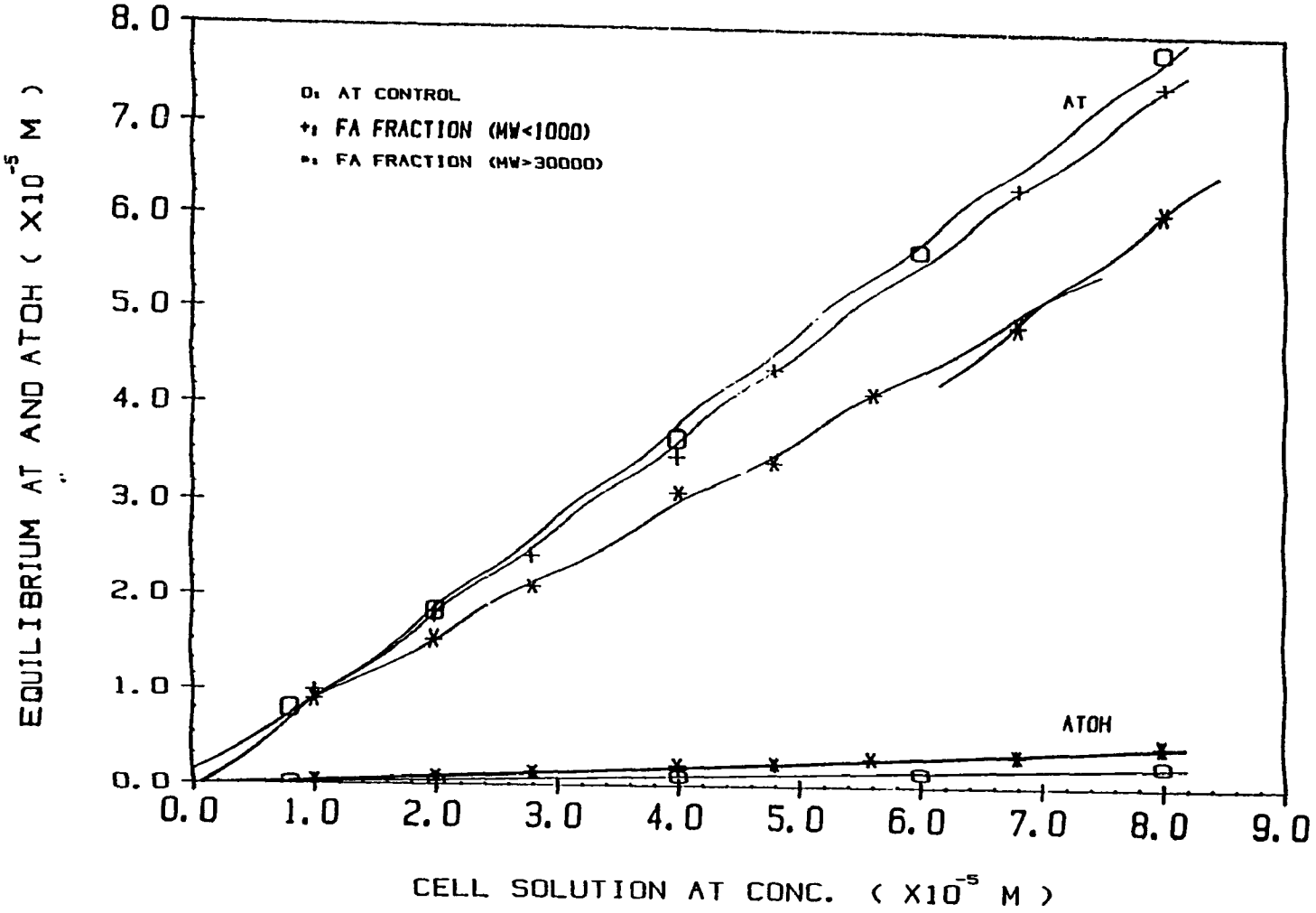

FIG. 3. 4 AT BOUND BY FA FRACTIONS

(AT ADDED=4.00X10^{-5} M, pH=2.92, FA=0.5000g/L)

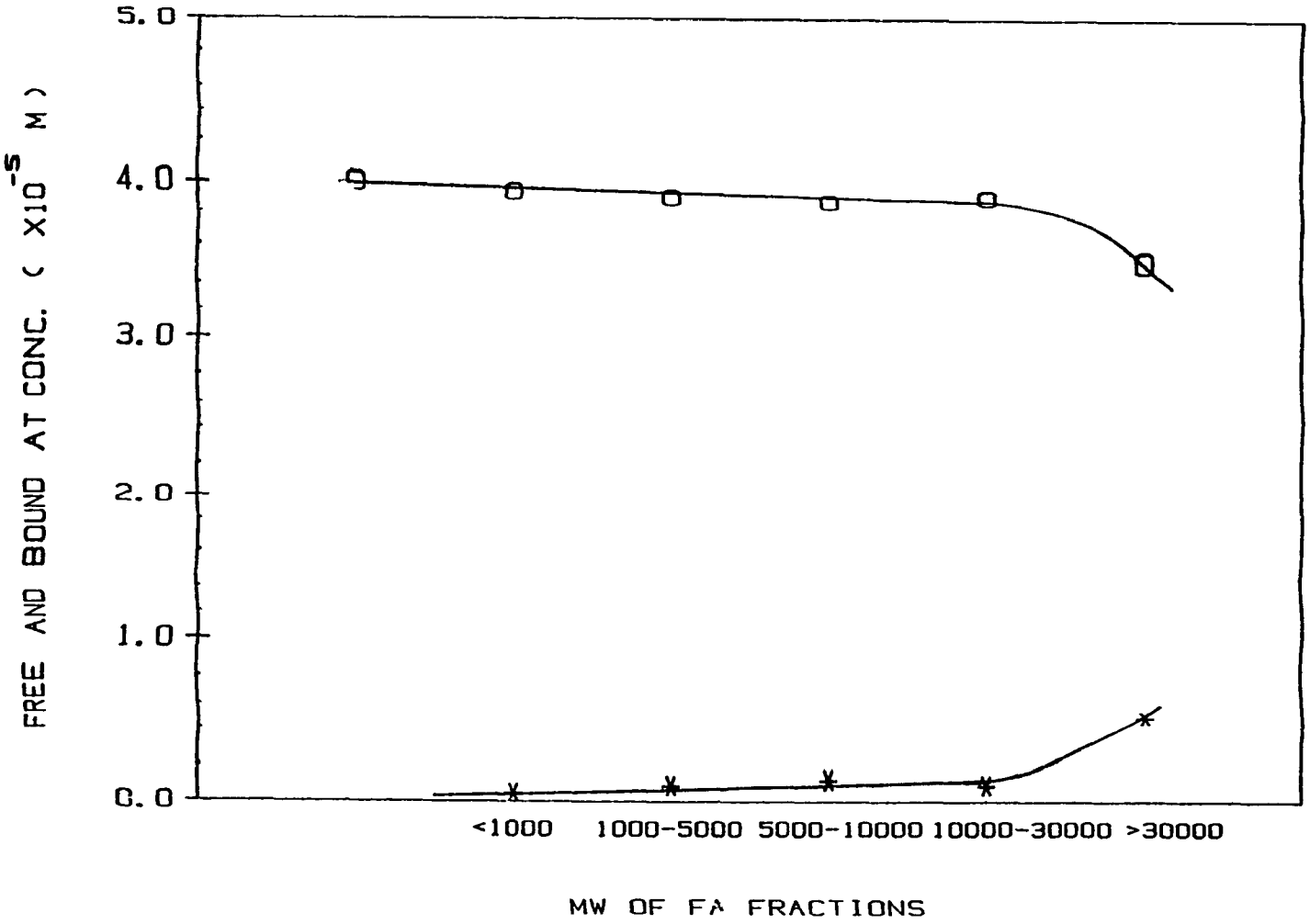

measured binding capacity. This important and meaningful result indicates that there must be some binding sites of higher MW fraction for AT binding to be competitively occupied by lower MW fraction, most probably through the same mechanism--hydrogen bonding. This fact is in good agreement with UV-Vis spectrophotometric evidence.

Table 3.4 Comparison of Binding Capasity of The Lowest and Highest Fractions and Their Mixture(1:1)

(pH = 2.85, total FA = 0.5000g/L)

MW range of FA Fraction	Binding capacity (μM AT/0.5000g FA)	Comment
<1,000	1.8	The expected binding capacity of the mixture should be 1/2(1.8+7.2) = 4.5 μM/0.5000g FA
>30,000	7.2	
FA(<1,000) + FA(>30,000) (1:1)	3.7	The difference between the expected and exper. value is 4.5 - 3.7 = 0.8 μM/0.5000g FA

3.3.5 FTIR Spectra of FA Fractions

Fig 3.5. shows the 5000-500 cm region of FTIR spectra of the lowest and highest MW fraction.

One can immediately see from Fig 3.5 that the major functional groups present in both fractions are: (1) broad OH stretching band (possibly N-H stretching from trace amine groups) around 3410 cm^{-1} region; (2) protonated carboxyl groups, -COOH, with characteristic frequencies around 1720 cm^{-1} (C=O stretching),

FIG. 3.5 FTIR SPECTRA OF FA FRACTIONS

(A: THE LOWEST FRACTION, B: THE HIGHEST FRACTION)

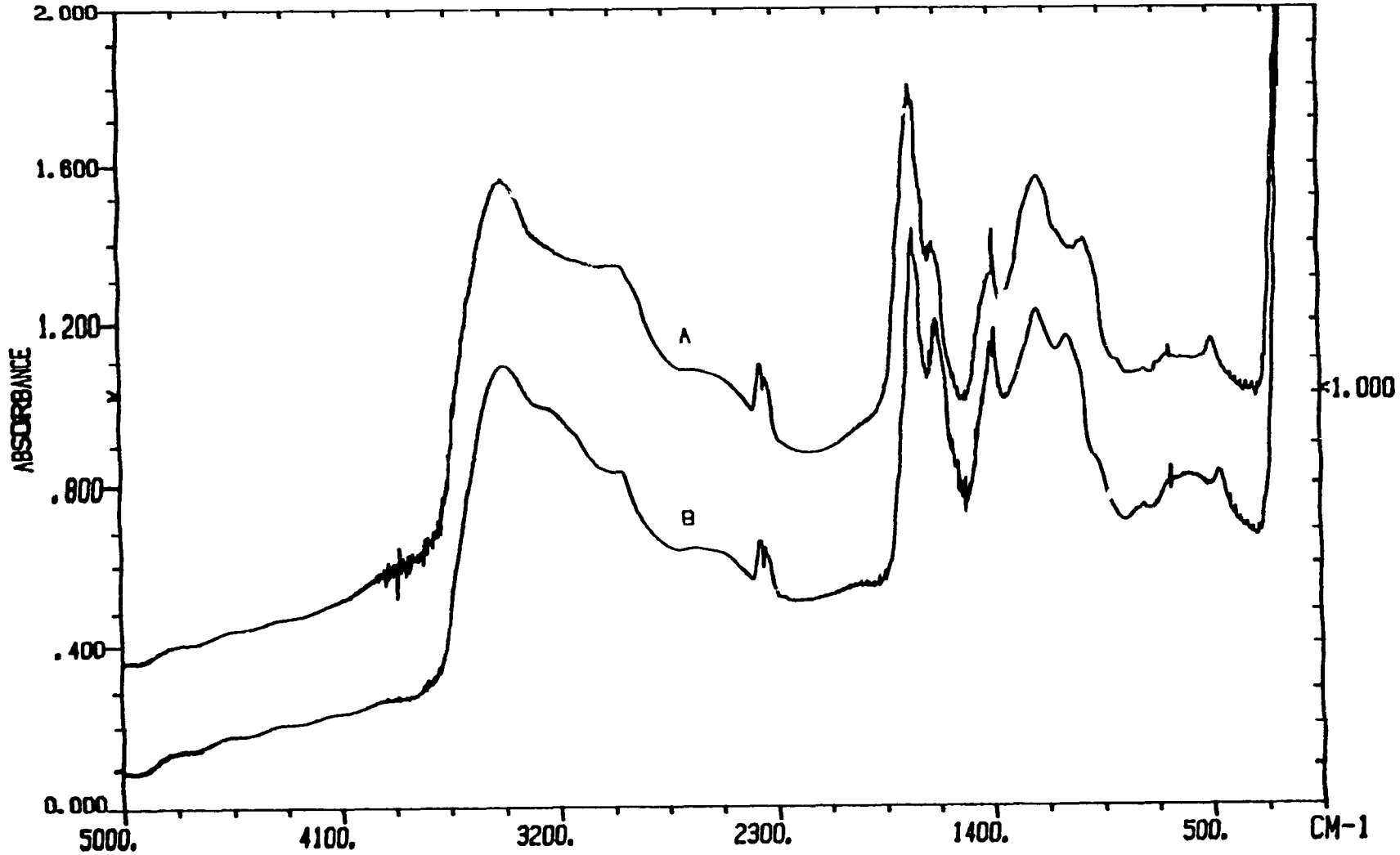

as well as around 1200 cm^{-1} (coupled C-OH deformation and C-O strethcing modes of COOH), (3) carboxylate groups, COO, with characteristic bands at 1630 and 1390 cm^{-1} regions; (4) aliphatic hydrocarbon groups exhibiting quite broad bands centered at 2940 cm^{-1}, which are characteristic $-CH_3$ and $-CH_2$ symmetric and asymmetric stretching [[4, 117-120].

Table 3.5 presents the details of the major observed absorption bands in their FTIR spectra.

Qualitatively, the FTIR spectra of the lowest and highest MW fractions are similar. Some interesting and significant differences are that (1) the intensity of the main FTIR peaks (1720 cm^{-1} and 1200^{-1} cm) as well as the ratio of intensity of 1720 cm^{-1} peaks to the intensity of the 1630 cm^{-1} peaks are greater for lower MW fractions. In contrast, the intensity of 1625 and 1384 cm^{-1} peaks are greater for higher MW fraction; (2) reduction in band intensity in 3410 cm^{-1} region for higher MW fraction; (3) explicit and broad band around 3070 cm^{-1} in the spectrum of the highest MW fraction, which is characteristic frequency of aromatic or substituted aromatic groups.

These facts clearly demonstrate that low MW fractions have a higher contents of carboxyl groups per unit weight, which explains why the lower MW fraction solutions have lower pH values (see Table3.1), and that high MW fractions have more aromatic structure than lower MW fractions. Another important piece of structural information worth noting is that higher contents of deionized carboyxlate groups in higher MW fractions indicates greater and stronger interaction between protonated carboxyl groups, or

between protonated carboxyl groups and other functional groups, leading to dissociation of the proton of the carboyxl groups.

Table 3.5 Comparison of FTIR Spectra of The Lowest and Highest FA Fraction

assignment	FA(MW<1000) (cm^{-1})	FA(MW>30000) (cm^{-1})	remark
OH stretching and NH stretching	3410 region	3411 region	
H-bonded OH stretching Of COOH	2600 region	2600 region	
aromatic C-H stret.	/	3070 region	it implies higher fraction has more aromatic structure
aliphatic stret. (symmetric and asy. stret. of CH_3, CH_2)	2934	2950	
aliphatic CH_3 and CH_2 bending	~1450(w)	~1450(w)	
C=O stret. of COOH	1728	1721	the lower frac. has stronger peaks in this region
C-Ostret. and COH deformation of COOH and phenolic groups	1204	1220	
COO^- asymmetric stret. (and stretching of aromatic C=C)	1630	1625	the higher frac. has stronger and and more complex peaks. it may suggest more different COO^- groups.
COO^- symmetric stret. (and CH deformation, CO stretching of phenolic OH)	1384	1397 1384	
aromatic ring stret. (and N-H bending and C-N stretching)	1580 — 1480	1580 — 1480	more and more complex peaks can be observed in this region for higher fraction.
C-OH bending, C-O stret. of alcohol and ethers	1011	1093	
C-H out-of plane deformation of hydrocarbons	~880		

3.3.6 NMR Spectrum of The Lowest MW Fraction

Figure 3.6 shows the -0.2--9.0ppm region of the FT-NMR proton spectrum of the lowest MW fraction of FA.

UP to seven distinct broad resonances in the range between -0.2 to 9.0 ppm are observed. These bands arise fron the presence of methyl and methylene proton of hydrocarbons and alicyclics (centered at 0.9 and 1.2 ppm), β-substituted aliphatic proton (centered at ~1.5ppm), α-monosubstituted aliphatic proton (centered at 2.7 and 3.7 ppm), α-disubstituted aliphatic proton (centered at 4.8 ppm), aromatic and heteroaromatic proton (centered at 7.5 ppm). Table 3.6 summarized the possible assignment for the NMR bands.

The very broad, weaker resonance of aromatic and heteroaromatic protons suggests the lowest MW fraction contains less aromatic groups (possibly less than 5%). This fact is in good agreement with FTIR measurement where noticeable aromatic C-H stretching vibration band (>3000 cm^{-1}) is not observed.

3.3.7 Comparison between FTIR spectra of FA and Cu-FA complex

Figure 3.7 shows the 4000--500 cm^{-1} region of the FTIR spectra of FA (curve A) and Cu-FA complex (curve B). Major absorption bands for fully protonated FA occurs at 3420 cm^{-1} primarily O-H stretching); 2680-2500 cm^{-1} broad band (H-bonded OH stretching); 2940 cm^{-1} (aliphatic C-H stretching); 1724 cm^{-1} (C=O stretching of COOH and ketons) and 1205 cm^{-1} (C-O stretching and OH deformation of COOH); 1635 cm^{-1} (COO^- asymmetric stretching and aromatic C=C stretching) and 1384 cm^{-1} (COO^- symmetric stretching,

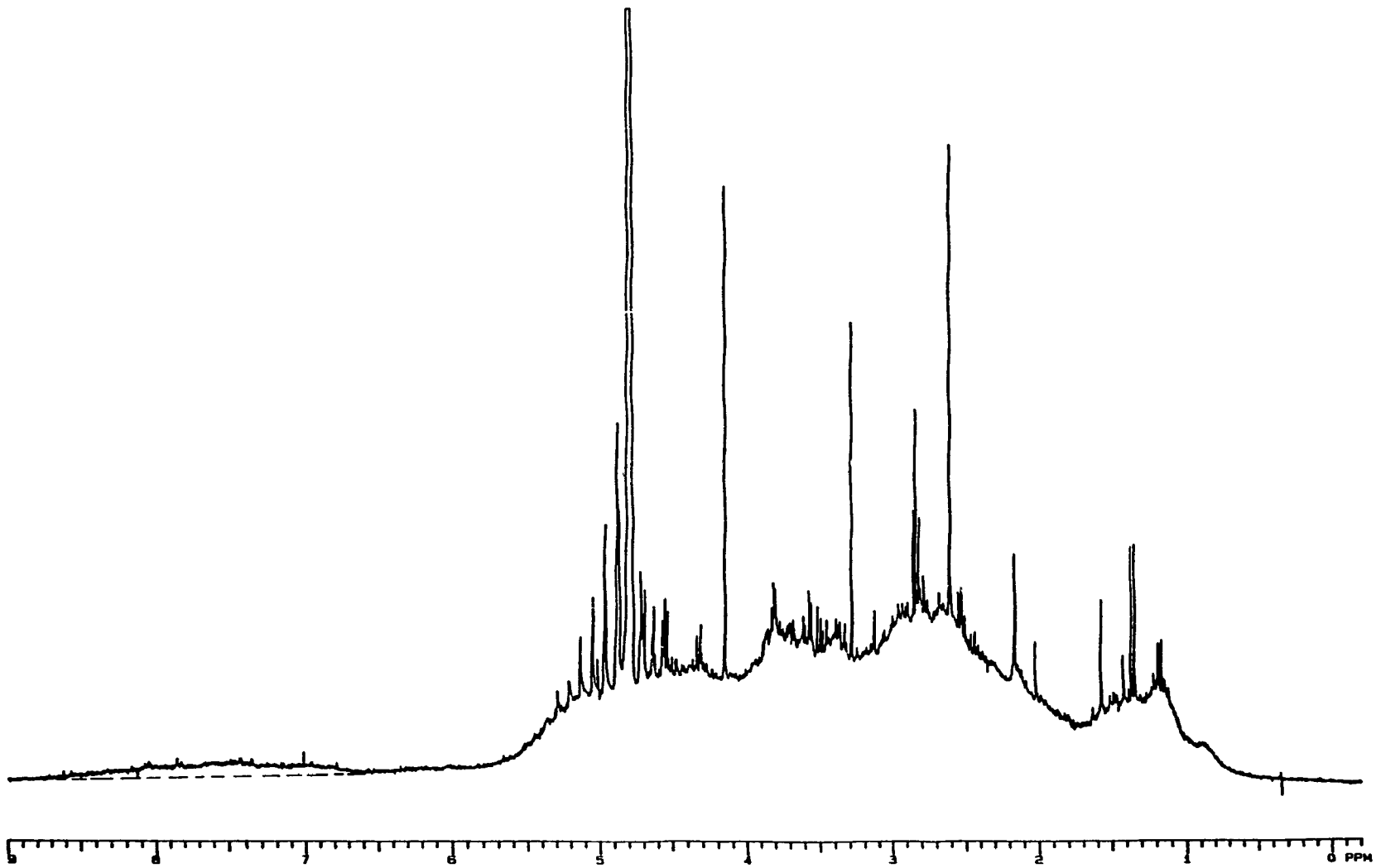

FIG. 3.6 PROTON NMR SPECTRUM OF THE LOWEST FA FRACTION

FIG. 3.7 FTIR SPECTRA OF FA (A) AND FA-Cu (B)

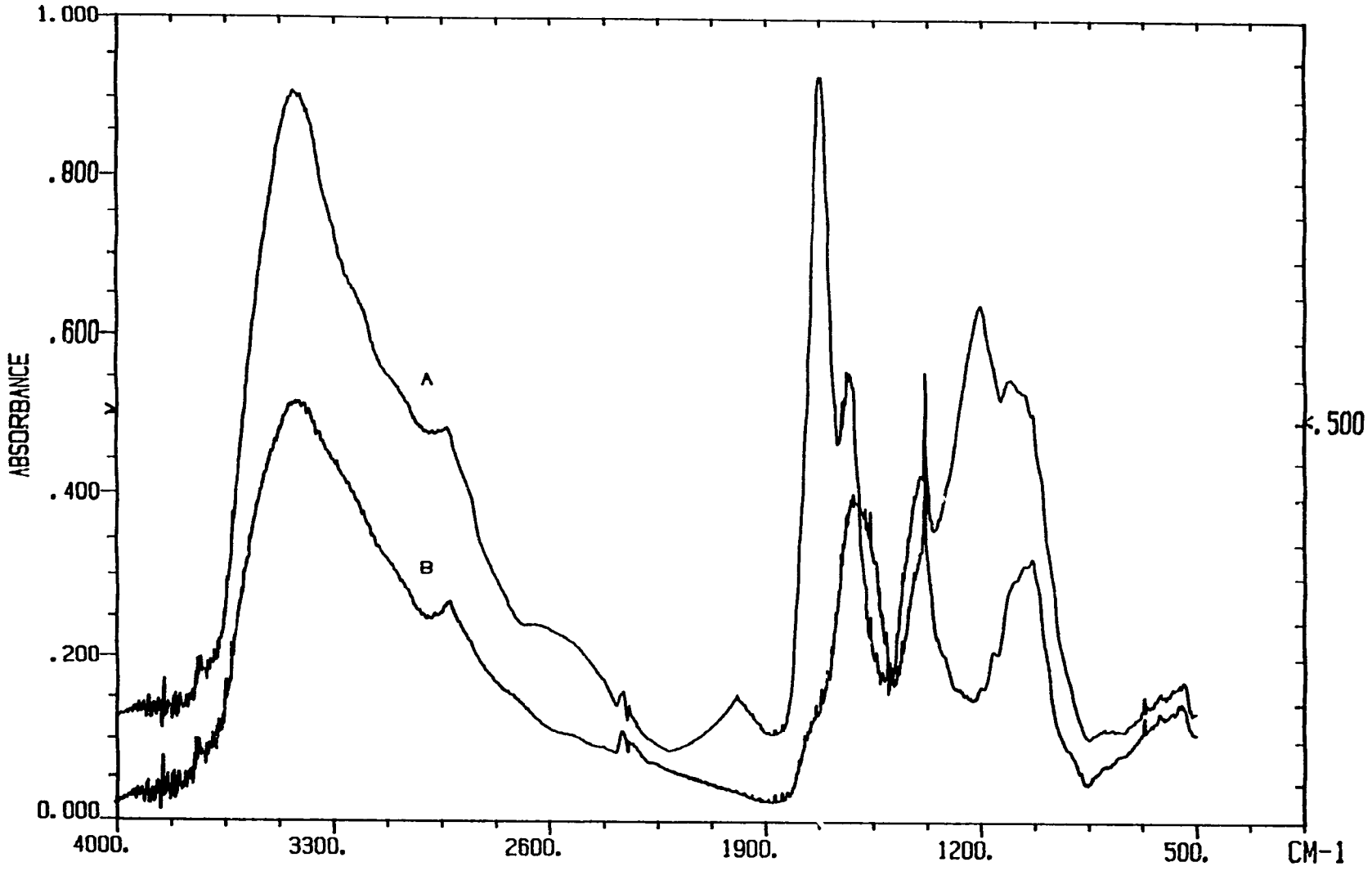

CH deformation of aliphatic groups or C-O stretching of phenolic OH).

Table 3.6 Possible Assignment for Proton NMR Spectrum of The Lowest MW Fraction

possible assignment	δ (ppm)
methyl proton of hydrocarbon	~ 0.9
methylene proton of hydrocarbon and alicyclics	~ 1.2
aliphatic proton, β-substituted (such as $CH_3-C-N<$, $CH_3-C-C=O$, and $CH_3-C-\phi$)	~ 1.5
α-monosubstituted aliphatic proton, possibly some aliphatic and cyclic amine NH proton (such as $CH_3-C(=O)O^-$, $CH_3-C(=O)\phi$, CH_3-O-R, $R-CH_2-C(=O)O^-$, and $R-CH_2-C(=O)NH$)	~ 2.7 region ~ 3.7 region
α-disubstituted aliphatic proton	~ 4.8 region
proton of HOD (proton exchange product of D_2O with -OH or -COOH)	4.8 (very sharp)
aromatic and heteroaromatic protons	~ 7.5 region (very broad and weak)
carboxylic and phenolic proton	beyond the observed scale

The conversion of COOH to COO^- by the formation of Cu-FA complex led to the significant loss of absorption at 1724 cm^{-1} and 1205 cm^{-1}, which are due to COOH vibrations. Neutralization of COOH is accompanied by a significant increase of characteristic

bands due to asymmetric and symmetric stretching of COO^- near 1615 and 1388 cm^{-1}, respectively.

The assignment of main FTIR bands is presented in Table 3.7, together with the assignment of difference spectra between FA and Cu-FA.

For the 3410 cm^{-1} region, the strong band intensity reduction for Cu-FA complex results in the decreased OH absorption due to the interaction of COOH and phenolic OH groups with Cu^{+2} ion (it leads to less protonated COOH and phenolic OH groups, subsequently less OH stretching). Simultaneously, the absorption reduction in 2680-2500 cm^{-1} region due to H-bonded OH stretching is also expected for the same reason.

Absorption bands due to C-H stretching of aliphatic CH_2 and CH_3 groups centered at 2940 cm^{-1} became more pronounced for the Cu-FA complex. This may be attributed to the reduction of OH absorption in the 3400 cm^{-1} region resulting in unmasking of C-H absorption bands.

In the very important 1900-1200 cm^{-1} region, as described above, the extreme decrease of C=O absorption of COOH at 1724 cm^{-1} and 1205 cm^{-1}, and simultaneously increase of COO^- absorption at 1600 and 1384 cm^{-1} in Cu-FA spectrum confirm that almost all COOH groups had reacted with Cu^{+2} ions.

It is well known that there is competition between proton and Cu^{+2} ion for FA binding sites. The amount of Cu bound is strongly dependent on the pH value of the FA solution. It can be expected that the decrease of absorption bands at 1720 cm^{-1} will be less pronounced if the pH value of the solution is lower.

Table 3.7 Observed FTIR Bands of Laurentian FA and FA-Cu Complex, and of Substraction Spectra

assignment	FA (cm^{-1})	FA-Cu (cm^{-1})	FA-(FA-Cu) (cm^{-1})	(FA-Cu)-FA (cm^{-1})
OH stretching and NH stretching (trace)	3420* (broad)	3410	3426	3420 (negative)
H-bonded OH stret.	2680-2500	2560* (w. shoulder)	2560	2560 (negative)
aliphatic CH stret. (symmetric and asym. stret. of CH_3 and CH_2)	2940	2930	2950	2950 (negative)
aliphatic CH_2 and $C-CH_3$ bending	1456, 1435 1417, 1400			
weak stret. of amines	~ 2000	/		
C=O stretching of COOH and ketones	1724	/	1724 (very st.)	1724 (negative)
C-O stretching and O-H deformation of COOH and phenolic groups	1205	/	1210 (very st.)	1210 (negative)
COO^- asymmetric stret. (and stretching of aromatic C=C)	1629 (1652 cm^{-1} shoulder)	1600	1560 (negative)	1560 (very st.)
COO^- symmetric stret. (and CH deformation, CO stret. of phenolic OH)	1388	1384	1384 (negative)	1384 (very st.)
aromatic ring stret. (NH bending and CN stretching)	1560—1480 (small peaks)	1560—1480 (small peaks)		
C-OH bending, C-O stret. of alcohols and ethers	1110	1045		

* Aromatic C-H IR absorption generally occurs at frequencies slightlyhigher than 3000 cm^{-1}, the absence of a pronounced band may be caused by extensive substitution of the aromatic ring or masking from the broad OH stretching band.

* W means "weak", and st. means "strong".

A very interesting phenomenum in this region is that the band of the Cu-FA complex at 1600 cm^{-1} shows a shift to lower frequency compared with the 1629 cm^{-1}(1652 cm^{-1} shoulder) band of FA. This may be attributed to the resonance of the weakened C=O of COO^- group by the formation of complex [117].

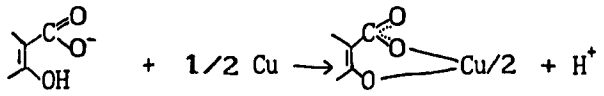

The band in the 1205 cm^{-1} region is assigned to C-O stretching and OH deformation of COOH and phenolic groups (possibly alcoholic OH groups). Because of the formation of the Cu^{+2}-salicylic complex, this band nearly disappears. Figure 3.8A and 3.8B present the difference spectra of [FA - (Cu-FA) complex] and [(Cu-FA) complex - FA], respectively. Figure 3.8A shows the pronounced band characteristics of protonated COOH groups at 1724 cm^{-1} and 1210 cm^{-1}. In contrast, Figure 3.8B presents the strong absorption difference in the 1560 and 1384cm^{-1} regions. Also, one can see that pure FA shows a stroger OH stretching band (3426 cm^{-1} region) and H-bonded OH stretching (2560 cm^{-1}) which indicates that some self binding can occur among different COOH groups through hydrogen bonding. The benzoic acid exhibits broad IR band from 2500 to 3500cm^{-1} [121]. It is attributed to the hydrogen-bonded OH stretching by the formation of dimer in which the hydrogen bands are particularly strong [121]:

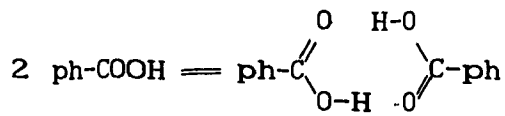

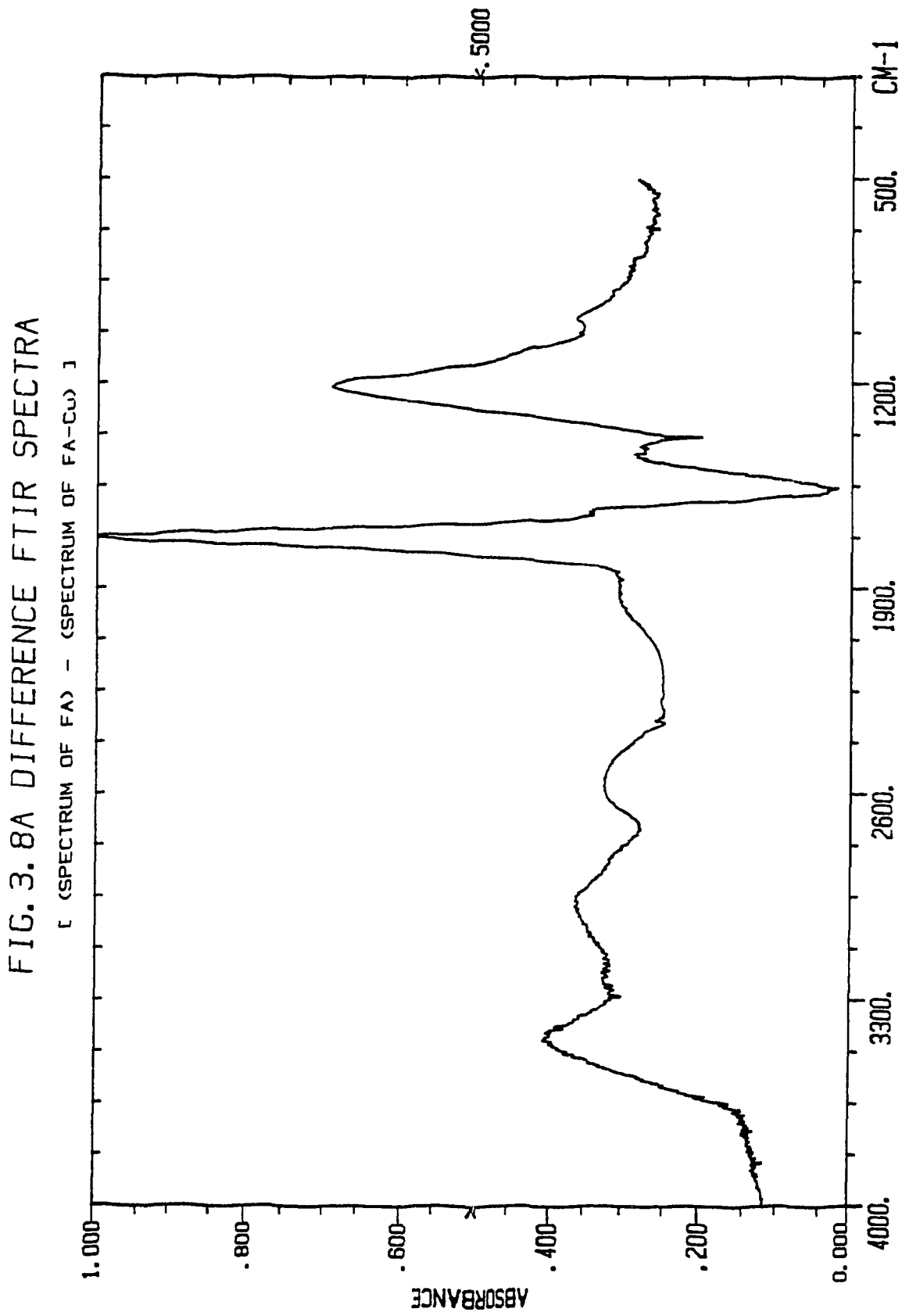
FIG. 3.8A DIFFERENCE FTIR SPECTRA
[(SPECTRUM OF FA) - (SPECTRUM OF FA-Cu)]
ABSORBANCE
1.000
.800
.600
.400
.200
0.000
4000.
3300.
2600.
1900.
1200.
500.
CM-1
.5000

FIG. 3.8B DIFFERENCE FTIR SPECTRA

[(SPECTRUM OF FA-Cu) - (SPECTRUM OF FA)]

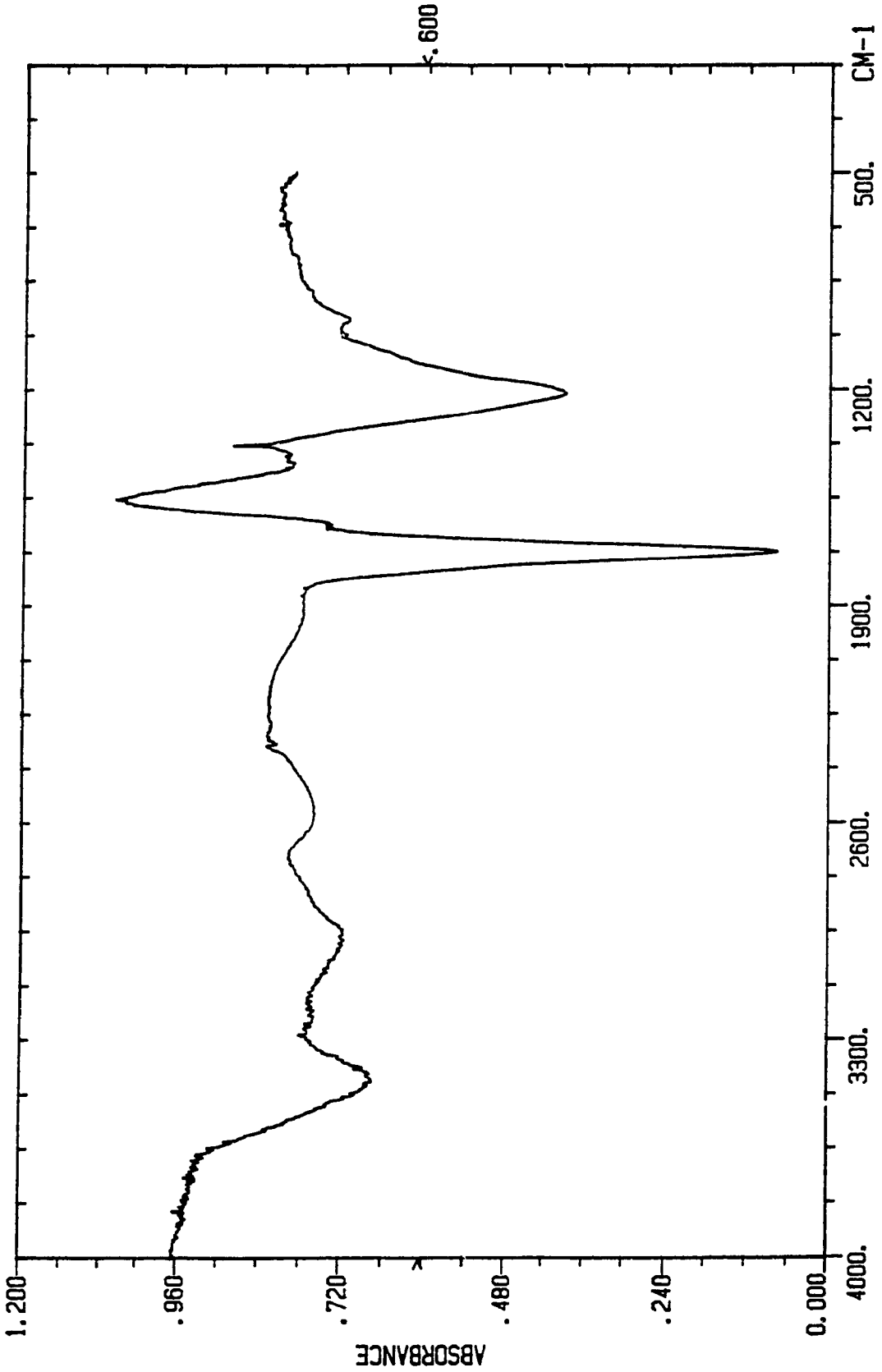

The formation of H-bonds is quite general in samples containing COOH and OH groups. For FA, th H-bond may take place not only in the solid state of FA, but also in FA solution where the smaller MW fraction can be bound to higher MW fractions, consequently the mixture of the lowest and highest MW fraction exhibits smaller binding capacity for AT than expected.

Even though the results are not very quantitative, they clearly demonstrated that (1) Cu-FA complex forms through metal-carboxylate linkage; (2) the Cu^{+2} ions are increasing the ionization of carboxyl groups; (3) binding sites of higher FA fraction can be blocked by smaller MW fraction mainly through hydrogen-bond.

3.4 Discussion

3.4.1 Interaction between fractions

Three points extracted from the structure characterization study are: (1) interaction can occur between different fractions of FA; (2) AT binding is preferentially associated with the large fraction of the sample; (3) smaller fraction blocks AT binding to larger fraction. These three points are important to the understanding of the mechanism of AT binding with FA, and of the relationship between FA structure and binding.

It should be remembered that the fulvic acids, even after purification, are still polydisperse mixtures. The continuous MW distribution creates different chemical environments for carboxyl groups, the most important fractional groups for AT binding among all functional groups of FA. Based on this structural feature,

the $\bar{K}$ (weighted average dissociation function) and K (differential equilibrium function) are used to describe the binding equilibrium of FA with pesticides.

It was shown in section 3.3 that the fractions of FA exhibit broad featureless spectra indicating that the FA contain a mixture of chromophores in an environment of a continuous distribution of molecular structures. All FA molecules have a sufficiently high content of oxygen bearing functional groups to participate in H-bonding. When the smaller fraction is mixed with larger fraction, interaction between them occurs through H-bonding. This interaction leads to the increase, to some extent, of the average size of the FA chromophore. Consequently, the absorbanc in a wide range increases after mixing. Of interest is another fact that the absorbance does not become constant until approximately two days later after mixing, which implies the interaction between fractions is a random and slow equilibration process. In Chapter 2 we have pointed out that the binding capacity for AT and ATOH is only a very small fraction of the total of the important carboxylate groups. These special sites of the larger fraction suitable for AT binding can be blocked by small fraction. Because of this reason, the experimental binding capacity of AT by the mixture of the lowest and highest MW fraction is smaller than the expected value.

3.4.2 Structure and binding

Binding experiments have shown the important fact that most of the binding is associated with the higher MW fraction, some

binding is exhibited by the next fractions and the smallest fraction contributed a little to binding. Another fact from FTIR and NMR is that the smallest fraction has higher contents of carboxyl groups per unit weight and less aromatic structure, and the highest fraction has lower contents of carboxyl groups per unit weight and more aromatic structure. The combination of these two facts suggest that not all carboxyl groups can act as AT binding sites. Only some special sites connected to certain structures will prefer H-bonding with AT and ATOH over water. Undoubtedly, the higher MW fraction can supply most of the special functional groups (possibly those directly connected with aromatic structure) as binding sites for AT.

CHAPTER 4

INTERACTION OF ATRAZINE WITH LAURENTIAN HA

4.1 AT SORPTION THEORY

It has been demonstrated in the work with AT in FA solutions that the interaction occurs between AT and unionized carboxyl groups and hydrogen ions. The AT-FA solution phase work has indicated that the unionized carboxyl groups are hydrogen bonding sites. In addition, the only two catalysts for AT hydrolysis identified were hydrogen ions and unionized carboxyl groups. Under field conditions, some AT could be sorbed from solution into water swollen particles, encountering an internal gel solution containing unionized carboxyl groups and free a hydrogen ions. Therefore, the next work following AT-FA study will logically be the stoichiometrically exact investigation of heterogeneous system, that is humic acid water-gel solution system.

By definition, a humic acid is a humic fraction that is insoluble in the free acid form but soluble in the Na^+ salt form. Undissolved humic acid in an aqueous system can therefore be expected to behave as a carboxylic type cation exchanger having pH dependent solubility. The important equilibria, such as cation exchange and solubility, are governed by the acidic functional groups. They especially include the carboxyl groups. The carboxyl groups are however, distributed over the polymer molecules of polydisperse polyelectrolyte. At a certain pH value, the polyelectrolyte molecule will have some of its carboxyl groups protonated and some of them unprotonated. When the mole fraction

of its unprotonated carboxyl groups becomes sufficiently great, the polyelectrolyte molecule will go into solution. The most general possible postulate is that each of two physical phase will have both unionized carboxyl groups and carboxylate anions. The sorption of water creates an internal gel solution in the particles of undissolved humic acid, just as it does with other cation exchangers [122,54,69].

Equation (1) describes the acid dissociation equilibrium for the mixture of chemically nonidentical carboxyl groups in the internal gel phase.

$$HA \overset{\bar{K}_{GA}}{\rightleftharpoons} H^+ + A^+$$

$$\bar{K}_{GA} = \frac{M_{GH}\, M_{GA}}{M_{GHA}} \qquad (1)$$

The subscript designate the molarities of the carboxyl groups HA, free protons H^+, and carboxylate anions A^- in the internal gel solution. Because it is defined for a mixture of carboxyl groups, $\bar{K}_{GA}$ is known to be a weighted average equilibrium function [123-125]. In terms of the effects of humic acid on atrazine, this equilibrium is important for at least two reasons. One is that unionized carboxyl groups are expected to provide hydrogen bonding sorption sites. The other is that unionized carboxyl groups and free protons both act as catalysts for the hydrolysis of atrazine.

The qualitatively observed solubilities of the free acid and sodium salt forms imply an interdependence between H^+ and Na^+ ion exchange and solubility. Upon addition of NaOH, more and more HA dissolves as pH of the external solution goes up. This solubility dependence of pH is linked to the solubility of the Na-humate

formed during the addition of base. The replacement of protons by Na^+ disrupts the forces holding together the three-dimensional configuration making up the humic gel. The nature of these force is likely to be hydrogen bonding between electron donor groups (oxygen-containing group) and protons. Equations (2) and (3) represent two solubility equilibria that are linked to each other and to the acid dissociation equilibrium of equation (1).

$$A_G^- + H_G^+ \overset{\bar{K}_{SH}}{\rightleftharpoons} A^- + H^+$$

$$\bar{K}_{SH} = \frac{M_A M_H}{M_{GA} M_{GH}} \qquad (2)$$

$$A_G^- + Na_G^+ \overset{K_{SNa}}{\rightleftharpoons} A^- + Na^+$$

$$\bar{K}_{SNa} = \frac{M_A M_{Na}}{M_{GA} M_{GNa}} \qquad (3)$$

Equation (2) and (3) again defined weighted average equilibrium functions for the reactions.

For the sorption of AT and ATOH from solution, reversible labile equilibria are assumed to exist. Equation (4) defines the equilibrium function $\bar{K}_1$ for the sorption of AT. In the most general case, as described in Chapter 2, $\bar{K}_1$ will be a weighted average equilibrium function

$$AT + HA \overset{\bar{K}_1}{\rightleftharpoons} AT\ HA$$

$$\bar{K}_1 = \frac{\theta_{AT}}{M_{AT}\,\theta_0} \qquad (4)$$

M_{AT} is the molarity of AT in the solution, θ_{AT} is the moles of AT sorbed per gram of HA, and θ_0 is the moles of carboxyl groups unoccupied by sorbed molecules, per gram of humic acid. In the

same way, equation (5) described the equilibrium sorption of ATOH.

$$ATOH + HA \overset{\bar{K}_2}{\rightleftharpoons} ATOH\ HA$$

$$\bar{K}_2 = \frac{\theta_{ATOH}}{M_{AT}\ \theta_0} \qquad (5)$$

Here M_{ATOH} is the molarity of ATOH in the solution, θ_{ATOH} is the moles of sorbed ATOH per gram of HA. Notice that our work has shown there is no competition between AT and ATOH for binding sites of HA (see details in experimental part), so all equations below written for AT could be paralled for ATOH.

The total of all carboxyl groups, both free and occupied, is obtained from equation (6):

$$\theta_T = \theta_0 + \theta_{AT} \qquad (6)$$

If ATOH is produced by hydrolysis during AT sorption process, the total number of moles of AT and ATOH, θ_t, must equal all of the AT and ATOH in solution, plus all AT that is sorbed. This material balance is expressed by equation (7):

$$\theta_t = V_S(M_{AT} + M_{ATOH}) + W_{HA}\ \theta_{AT} \qquad (7)$$

V_S and W_{HA} are liters of sample solution and gram of humic acid. The moles/g of total sorbed AT molecules, θ_{AT}, are calculated directly from experimental data using equation (8)

$$\theta_{AT} = \frac{\theta_t}{W_{HA}} - \frac{V_S}{W_{HA}}(M_{AT} + M_{ATOH}) \qquad (8)$$

The θ_{AT} values derived from the experiment may be related to the equilibrium function $\bar{K}_1$ (Rearange equation (4)):

$$\theta_{AT} = \bar{K}_1\ M_{AT}\theta_0 \qquad (9)$$

It is useful to introduce the experimental determined ratio Y_{AT} ($Y_{AT} = \frac{\theta_{AT}}{\theta_0}$), and obtain equation (10):

$$Y_{AT} = \bar{K}_1 M_{AT} = Y_{AT}(M_{AT}) \qquad (10)$$

As long as θ_{AT} is small if compared with θ_T, θ_T approximates θ_0, free carboxyl groups. Y_{AT} can be expressed by

$$Y_{AT} = \frac{\theta_{AT}}{\theta_T} \qquad (11)$$

The most general postulate is that $\bar{K}_1$ will depends on sorption site coverage and hence on solution composition. This most general possible case is described by equation (12):

$$\bar{K}_1 = \bar{f}_1(M_{AT}) \qquad (12)$$

It has been proposed by Gamble et al [126] that as binding sites covered by AT, each AT molecule entering into the gel solution will "see" a slightly chemically different environment. It is theoretically correct to write, therefore, that:

$$K_{1i} = \frac{\theta_{ATi}}{M_{AT}\,\theta_{0i}} \qquad (13)$$

$$\Delta Y_T = \frac{\theta_{ATi}}{\theta T} \qquad (14)$$

The material balance require the equation (15):

$$\theta_0 = \sum_{i=1}^{n} \theta_{0i} = \sum_{i=1}^{n} \frac{\theta_{ATi}}{M_{AT}\,K_{1i}} \qquad (15)$$

Substituting equation (15) to (4), one has

$$\bar{K}_1 = \frac{\theta_{AT}}{M_{AT} \sum_{i=1}^{n} \frac{\theta_{ATi}}{M_{AT}\,K_{1i}}} = \frac{\theta_{AT}}{\sum_{i=1}^{n} \frac{\theta_{ATi}}{K_{1i}}} = \frac{\theta_{AT}}{\theta_T} \frac{1}{\sum_{i=1}^{n} \frac{\theta_{ATi}}{K_{1i}\,\theta_T}} \qquad (16)$$

Introducing equation (11) and (14) to (16):

$$\bar{K}_1 = Y_{AT} \frac{1}{\sum_{i=1}^{n} \frac{\Delta Y_{AT}}{K_{1i}}} \qquad (17)$$

Because $\bar{K}_1$ approximates a continuous function, the summation of equation (17) may be replaced by an integration:

$$\bar{K}_1 = Y_{AT} \frac{1}{\int_0^{Y_{AT}} \frac{1}{K_1} d Y_{AT}} \qquad (18)$$

$$\frac{Y_{AT}}{\bar{K}_1} = \int_0^{Y_{AT}} \frac{1}{K_1} d Y_{AT} \qquad (19)$$

Differentiating equation (19) gives an equation for K_1 in terms of the experimental quantity $\bar{K}_1$

$$K_1 = \frac{\partial Y_{AT}}{\partial M_{AT}} = \frac{\partial \bar{K}_1 M_{AT}}{\partial M_{AT}} \qquad (20)$$

Equation (20) is practical to determine the differential equilibrium function K_1.

If the second approach, as described in chapter 2, is used, the $\bar{K}_1$ and Y_{AT} should be expressed by equation (21) and (22), respectively:

$$\bar{K}_1 = \frac{\theta_{AT}}{M_{AT}\theta_0} = \frac{\theta_{AT}}{M_{AT}(\theta_{cap} - \theta_{AT})} \qquad (21)$$

$$Y_{AT} = \frac{\theta_{AT}}{\theta_{cap}} \qquad (22)$$

where θ_{cap} is the observed binding capacity of AT at each pH. It should be noted that the θ_0 does not approximate θ_{cap} here because

it is a quite large value if compared with θ_{cap}.

K_1 may be related to thermodynamic equilibrium constant in the conventional way,

$$\kappa_1^0 = K_1 \Gamma \qquad (23)$$

where Γ is the ratio of activity coefficients of AT bound over activity coefficient of AT free times activity coefficient of HA. Then the Gibbs free energy value can be calculated according to the following equation:

$$\Delta G_0 = -RT \ln \kappa_1^0 = -RT \ln K_1 \Gamma \qquad (24)$$

Rearranging equation (24) gives equation (25) in which only experimental quantities are on the right:

$$-(\Delta G^0 + RT \ln \Gamma) = RT \ln K_1 \qquad (25)$$

4.2 EXPERIMENTAL

4.2.1 Materials and Apparatus

Most of the chemicals and apparatus used in this part are same as described in chapter 2 and chapter 3.

4.2.2 Extraction and Purification of Laurentian Humic Acid

The humic acid used was Laurentian HA obtained from the soil of Laurentian Forest Preserve of Laval University according to the following preparation procedure:

2 kg sample of air-dried soil was weighed into a polypropylene jug and extracted with 20 L of 0.5M NaOH solution under N_2 atmosphere to avoid any oxidation of humic materials. The extraction is allowed to take place for 24 hours. Any insoluble materials such as sand and clay can be removed from soil extract

by setting and centrifuging at 3500 rpm for 30 minutes.

One column (150x7.5 cm ID) filled with 4 kg new Dowex HCR cationic resin (reprocessed before use with 1N HCl and then washed completely with deionized water until the pH value of water was constant) was used to obtain HA. Care was taken not to allow air spaces between beads and tokeep the liquid level above the bed top. The eluate flow rate was maintained at about 3-5 ml per minute. When the pH value of the eluate became greater than 7.0, the collection was stopped. This eluate solution was used to obtain the brown powder of fulvic acid by lyophilization technique.

The HA precipitated in the column is then washed out with 0.1N NaOH. When the pH of the washed-out HA solution is greater than 6.0, the collection is stopped. Approximately 11 L of eluate can be collected. The eluate is then acidified with 6M HCl to pH 1.5, and allowed to stand overnight. The supernatant is decanted and the resulting HA slurry is further washed by 0.5M HCl and centrifuged at 3500 rpm for 30 minutes to remove the remaining FA having smaller molecular weight. Finally, it is suspended in deionized water and dialyzed using dialysis tubing of 1000 MW cut-off to remove the remaining HCl and excess salts. The external water is replaced every 3-5 hours for three times and then every 12 hours until pH does not change and no more chloride is detected. The disappearance of HCl can be determined by testing the external solution for Cl^- with $AgNO_3$.

The dialyzed HA sample is then freeze-dried. A dark-brown powder is obtained. This HA sample is stored in dark brown container to prevent undesired photochemical reactions.

The analytical properties of Laurentian HA are shown in Table 4.1.

In the case of humic acid, the number of carboxyl groups per gram is much less than that of fulvic acid, but for phenolic groups, the amount in HA is much higher than that in FA per gram. This should be kept in mind when correlating Cu(II) complexing capacities with bidentate sites.

Table 4.1 Analytical properties of Laurentian HA

Element	Content(%)	Element	Content(%)
C	51.9	Na	0.0006
O	39.9	K	$5x10^{-5}$
H	5.5	Ca	0.0004
N	2.3	Mg	not detected
S	0.26	Fe	0.0002
Total acidity		7.60 mmol/g (±10%)	
COOH		2.50 mmol/g (±5%)	
OH		5.10 mmol/g (±10%)	
Ash		<0.1%	

4.2.3. Procedure for The Determination of Sorption AT by HA

(1) Atrazine-Humic Acid Titration

A series of 8 to 10 humic acid samples weighing exactly 10.00 mg were equilibrated with 25.00 ml of AT solutions of increasing concentration. Initially, aliquots of AT ($1.00x10^{-4}$ M) stock solutions were added to 10.00 mg HA, then a varying volume of deionized water was added to each of the samples to about 20.00 mls. The pH of the resulting suspension was adjusted to the desired values by the addition of dilute HCl or NaOH, and each

sample was diluted to a final volume of 25.00 ml and sealed securely with parafilm. Controls were prepared in the same way but without HA. Paired controls and AT-HA samples were shaken together for three days at room temperature (21 ± 2 ^{o}C). After the equilibration period, the pH of suspensions was measured. It was followed by ultrafiltration on a YM2 1000 MW cut-off membrane. The first 10 drops of filtrate were discarded, and an aliquot of about 1.0 ml was collected for analysis of free AT and ATOH hydrolyzed from AT during 3 days.

The conditions of HPLC for determination of AT and ATOH are same as those used for the AT-FA samples.

(2) Atrazine-Humic Acid Titration in The Presence of Excess of Cu

The same procedure was used for the titrations of HA with AT in the presence of excess Cu(II). The only exception is that the certain volume of standard Cu(II) stock solution was added to each sample solution followed by filtration. Aliquots (20.0 or 50.0 μl) of the filtrates were injected into the HPLC for quantification of AT, ATOH and Cu(II).

(3) FTIR Spectral Measurements

The interaction product between Cu(II) ion and HA was obtained according to the following procedure: 2.50 ml of 1.0 x 10^{-2} M Cu(II) stock solution was added to 10.00 mg HA, and then diluted to a total volume of 25.00 ml. The pH of the Cu-HA solutions was approximately 3.5. The solutions were securely sealed with parafilm, and then were shaken for 3 days at room temperature (22 ± 2^{o}C). After 3 days, the solutions were

centrifuged for 15 minutes at a speed of 5000 rpm in IEC B-20 centrifuge with the temperature controlled at 10°C. The precipitates obtained were carefully rinsed with deionized water to remove unreacted Cu(II) ion. Finally, the interaction product was dried under vacuum.

The KBr pellet for FTIR measurement was made having a weight ratio of 1:200 (sample/KBr). The original unratioed spectra of the sample and of the empty beam were computed from 500 signal averaged scans (about 60 minutes total measurement time for each spectrum)

4.2.4. Experimental Design

The experiments designed for the investigation of interaction of AT with Laurentian humic acid include the following.

(1) AT variation at constant pH in low ionic strength. At each pH, AT concentration was varied from $4x10^{-6}$M to $8x10^{-5}$M and HA concentration was kept constant. The same experiments were conducted from pH 1.8 to pH 8.0 as to see the pH effect on AT sorption.

(2) AT variation at constant pH in high ionic strength. The chosen electrolyte was 0.1M KCl. The aim of this series of experiments was to see the effect of electrolyte on AT sorption.

(3) variation of HA concentration at constant pH and low ionic strengths.

(4) competition for binding sites between AT and ATOH.

(5) AT binding in the presence of excess of copper ions.

(6) FTIR spectra measurements of HA, and Cu(II)-HA interaction product. The aim of these experiments was to obtain some

structural information of HA and its interaction product with and Cu ion especially some information about the functional groups of HA. The FTIR spectrum of HA will be used to compare with the spectrum of FA so as to study the structural similarity and difference between FA and HA.

4.3. RESULTS

4.3.1. AT Variation at Constant pH in Low Ionic Strength

The experiments of this section were designed in such a way that AT concentrations were varied from 4.00×10^{-6} to 8.00×10^{-5} M with HA 10.00 mg at each added AT concentration, and then the binding behavior of AT to HA and hydrolysis of AT by HA in a wide range of pH could be thoroughly investigated. The tested pH include pH 1,85, 2.15, 2.70, 3.25, 4.68, 5.80, 7.15 and 7.70. The AT sorption behavior was very similar to AT-FA binding: (1) at pH 3.60 and lower, not only was AT sorbed by HA, but ATOH produced by hydrolysis of AT was also evident. At pH 2.15, approximately 19% AT was hydrolyzed to ATOH during 3 days. The ATOH in AT-HA samples at each pH of this pH range was larger than that in AT controls. (2) from pH 3.65 to 5.80, only AT bound to HA was observed. No ATOH was catalytically produced during 3 days. (3) at pH 7.70 and higher, no measureable AT binding was observed. Typical sorption curves for these 3 cases are shown in Fig 4.1 A, B and C.

Using the linear analytical curves established in the HA free controls in conjunction with signals obtained for AT and ATOH in the filtrate of AT-HA suspension solution, sorbed AT and ATOH hydrolyzed from AT by carboxyl groups of HA could be evaluated. The added AT, free and bound AT, and hydrolyzed ATOH at pH 2.15

FIG. 4. 1A AT BINDING CURVES BY LAURENTIAN HA

(HA=10.00 mg/25.00 ml, pH=2.15)

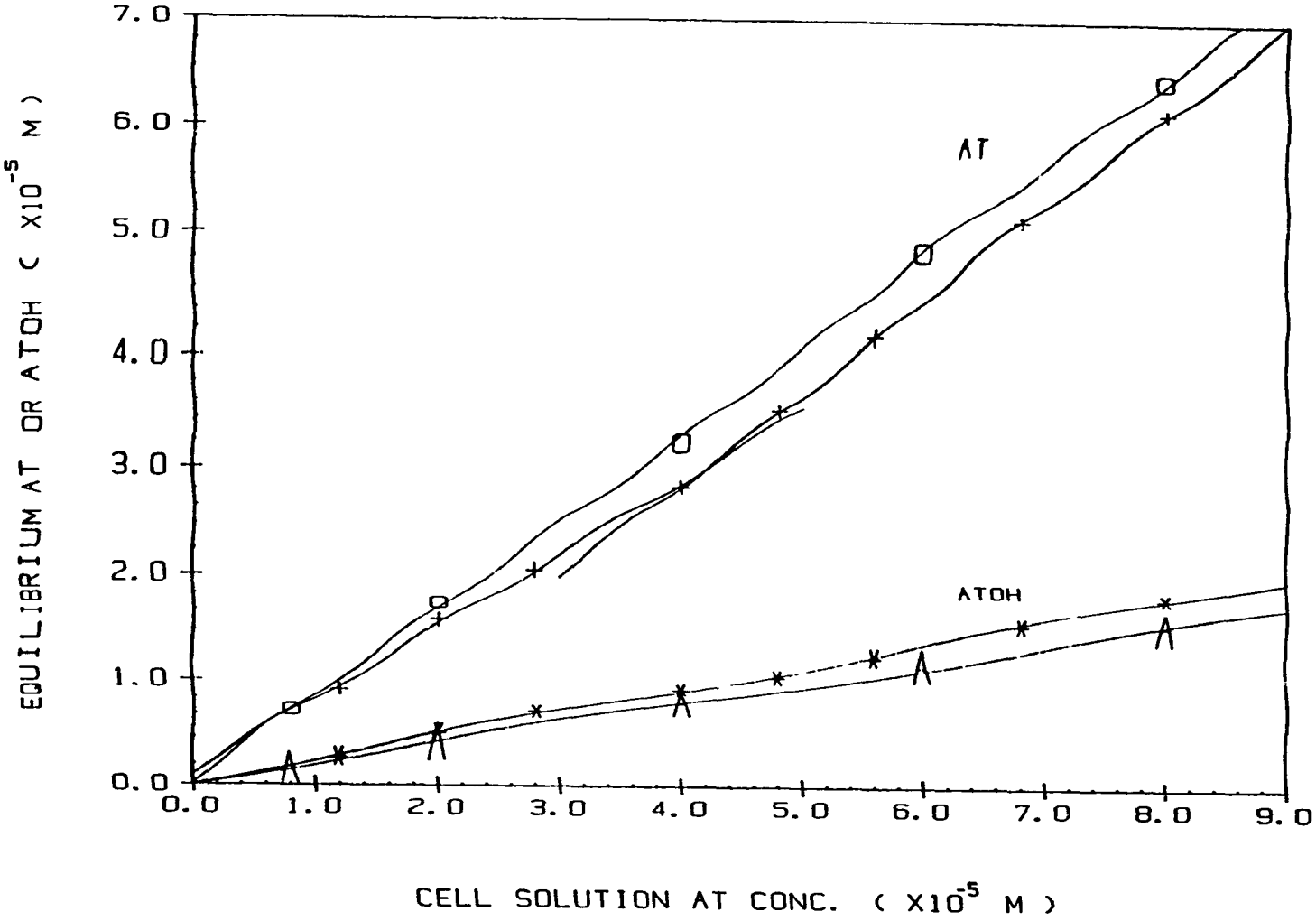

FIG. 4. 1B AT BINDING CURVES BY LAURENTIAN HA

(HA=10.00 mg/25.00 ml, pH=4.68)

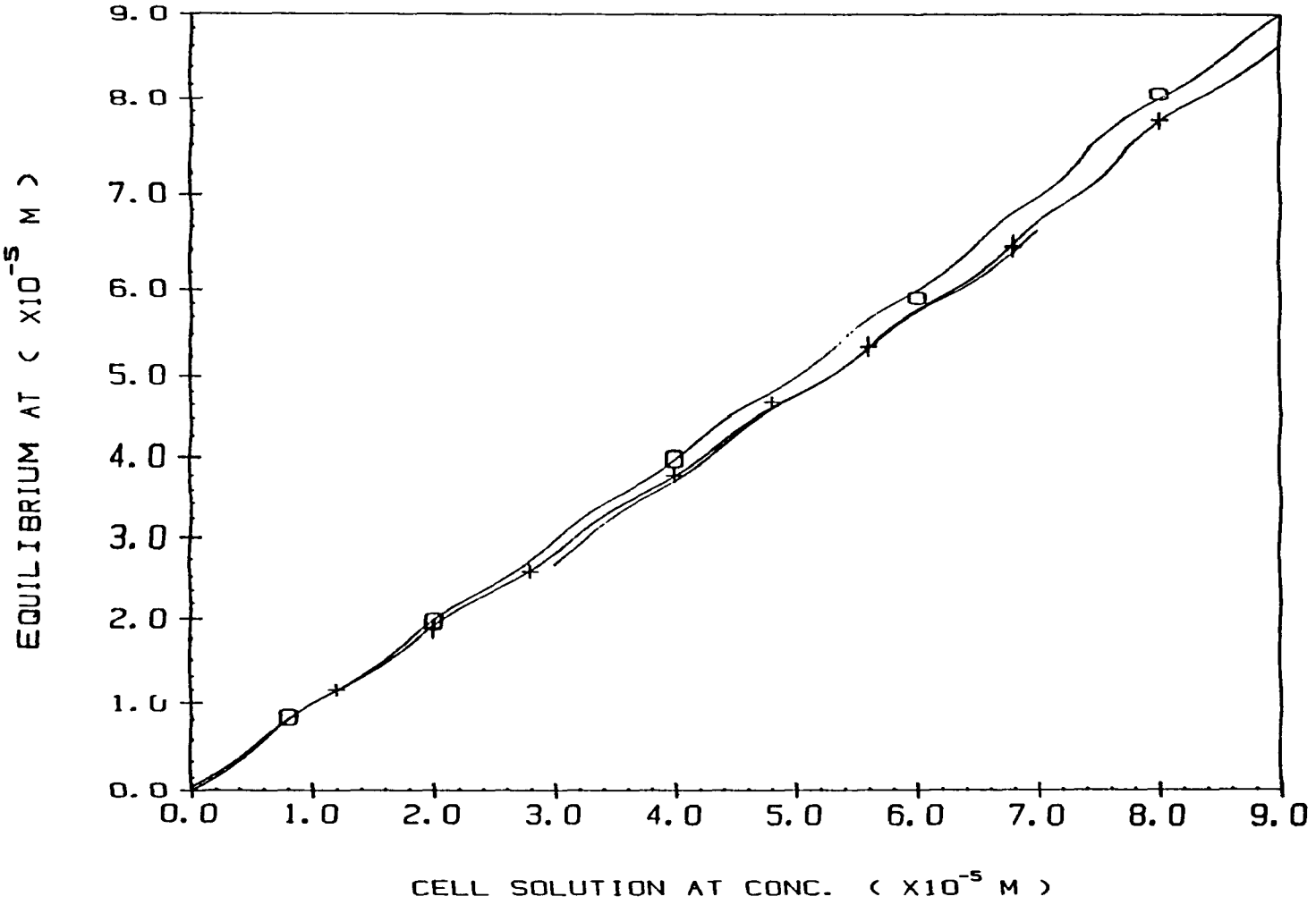

FIG. 4. 1C AT BINDING CURVES BY LAURENTIAN HA

(HA=10.00 mg/25.00 ml. pH=7.70)

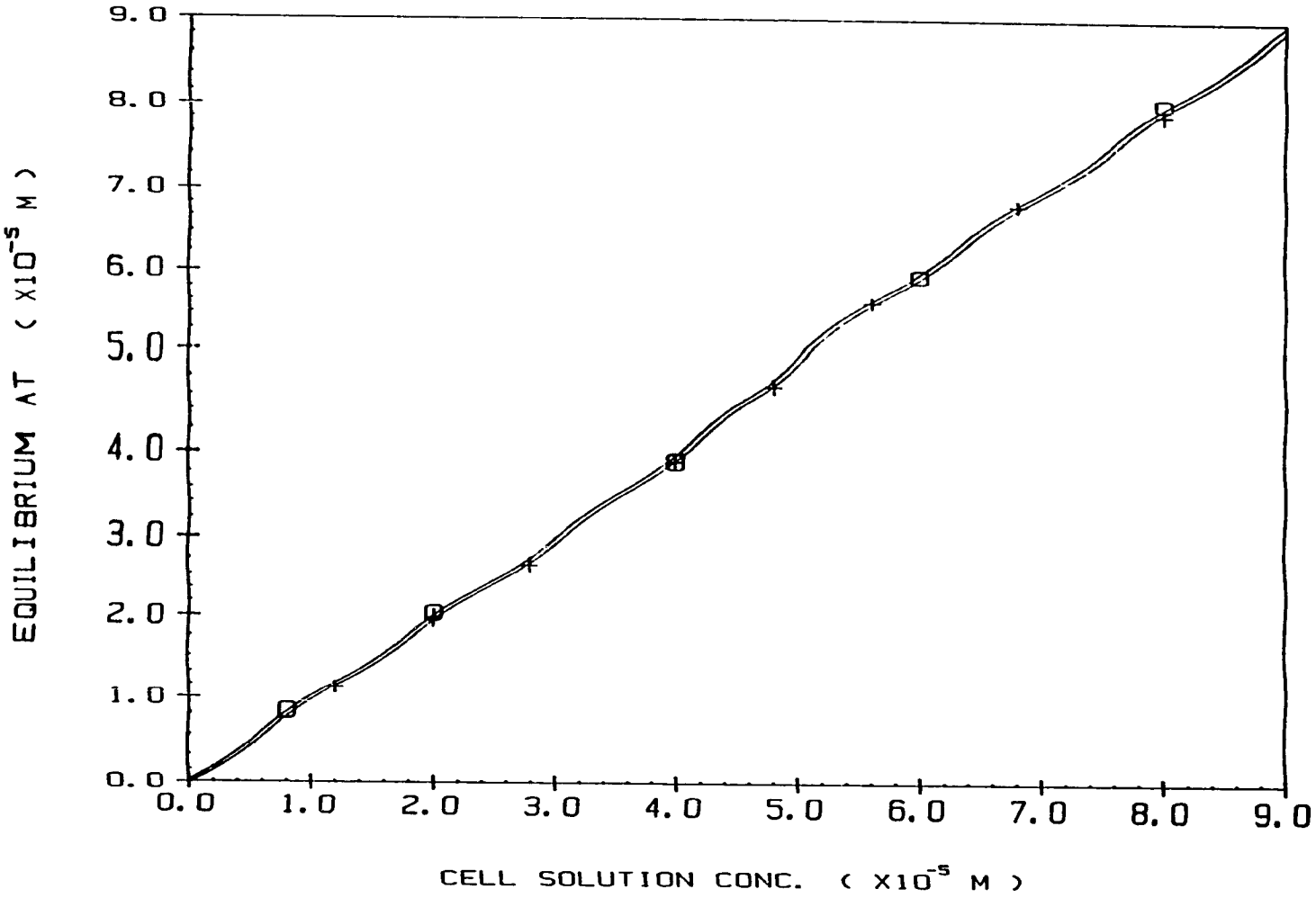

and pH 4.68 are presented in Table 4.2 and 4.3. Fig.4.2 shows plots of AT bound vs AT total at various pH values. It is immediately evident that a limit is reached at each pH value, and that an empirical binding capacity can be defined at each pH.

Table 4.2 determination of bound AT and hydrolyzed ATOH

(pH=2.15, HA=10.00 mg/25.00 ml, Stock AT=1.00×10^{-4}M)

Added AT (ml)	in control ($\times10^{-5}$M)		in AT-HA ($\times10^{-5}$M)		Bound AT ($\frac{\mu mol}{0.4g\ HA}$)	Hydrolyzed ATOH (μM)
	AT	ATOH	AT	ATOH		
3.00	0.9899	0.2284	0.9254	0.2580	0.645	0.296
5.00	1.639	0.3777	1.504	0.4480	1.35	0.703
7.00	2.288	0.5271	2.046	0.6460	2.42	1.19
10.00	3.262	0.7511	2.834	0.9120	4.28	1.61
12.00	3.911	0.9005	3.501	1.064	4.10	1.64
14.00	4.561	1.050	4.148	1.239	4.13	1.89
17.00	5.535	1.274	5.140	1.497	3.95	2.23
20.00	6.511	1.498	6.101	1.786	4.10	2.88

Table 4.3 Determination of bound AT by HA

(pH=4.68, HA=10.00 mg/25.00 ml, stock AT=1.00×10^{-4}M)

Added AT (ml)	Equilibrium AT in cont. ($\times10^{-5}$M)	Equilibrium AT in AT-HA ($\times10^{-5}$M)	Bound AT ($\frac{10^{-5}mol}{0.4g\ HA}$)
3.00	1.197	1.198	0.00
5.00	1.997	1.910	0.087
7.00	2.798	2.673	0.125
10.00	3.998	3.819	0.179
12.00	4.799	4.618	0.181
14.00	5.599	5.292	0.307
17.00	6.800	6.482	0.318
20.00	8.001	7.693	0.308

FIG 4.2 BOUND AT VS TOTAL AT ADDED

(HA=10.00 mg/25.00 ml, KCl=0)

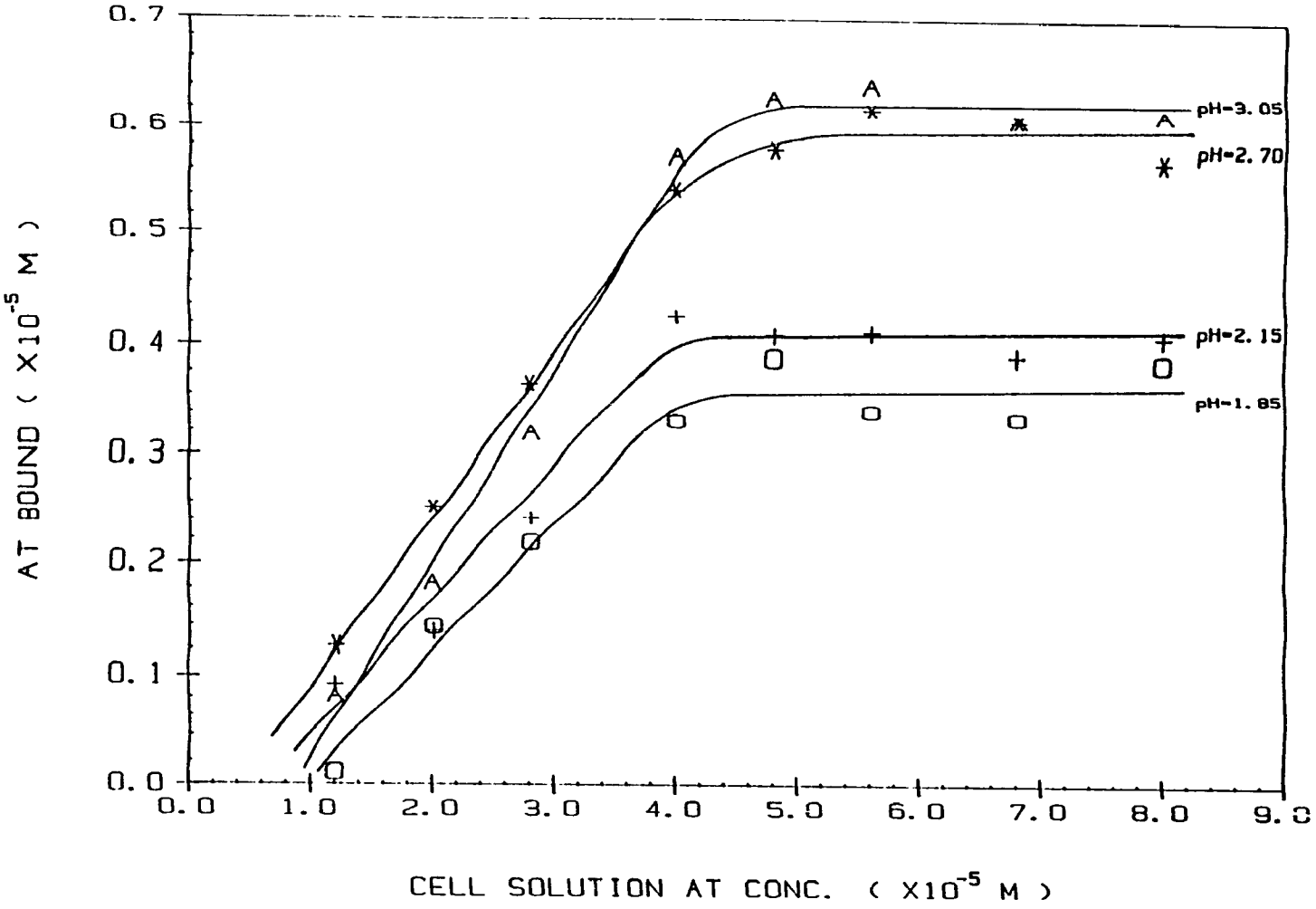

Fig 4.3 shows plots of hydrolyzed ATOH vs total added AT at pH 2.15 and pH 3.05. The ATOH, hydrolysis product of AT, consists of ATOH from two pathway, one from proton catalysis, and another part from carboxyl groups catalysis. Because controls and AT-HA sample solutions were kept at same pH value, the ATOH hydrolyzed by carboxyl groups could readily obtained by subtracting ATOH in controls from ATOH in AT-HA samples, as shown in Fig 4.3. The hydrolyzed ATOH by carboxyl groups can be directly related to the total AT. The higher the initial AT concentration is, the more the amount of ATOH.

The plot of binding capacity of AT vs pH for the data in Fig 4.2 is shown is Fig. 4.4. The shape of the curve is qualitatively quite similar to that of AT-FA. It is evident from Fig 4.4 that (1) the maximum of apparent AT binding capacity equals approximately 15.3 μM AT per gram of HA, a very small fraction of the total of the carboxyl groups (less than 1%). (2) the maximum of binding capacity occurs at pH 3.05. By contrast, the maximum by fulvic acid occurs at pH 1.40-1.90. The difference could probably be attributed to the nature of FA and HA. The pKa values of type A groups of FA (2.7-3.4) is much smaller than the value for acidic sites of HA; that is, at pH 3.0, almost 100% carboxylate ion exchange sites of HA is occupied by hydrogen ion, which is very favorable to the sorption of AT. (3) in the range of pH 7.7-3.0, it is evident that the colour of the solution becomes deeper and undissolved HA becomes less because more HA molecules enter the bulk solution as the pH increases. The increase of binding capacity with the decrease of pH can be mainly attributed to the decrease in the competition for ion exchange sites between

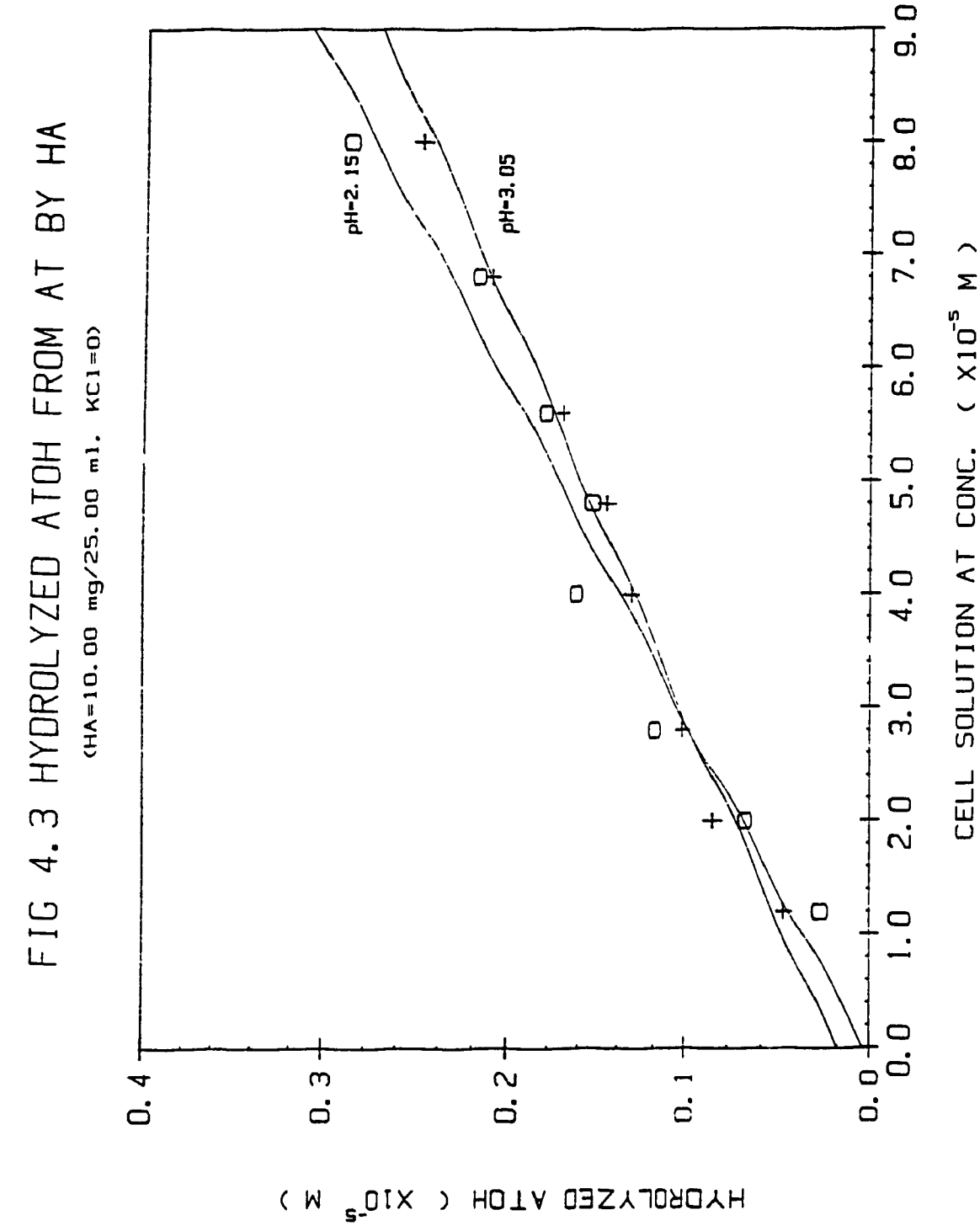
FIG 4.3 HYDROLYZED ATOH FROM AT BY HA
(HA=10.00 mg/25.00 ml. KCl=0)
pH=2.15
pH=3.05
HYDROLYZED ATOH (X10^{-5} M)
CELL SOLUTION AT CONC. (X10^{-5} M)
0.0
0.1
0.2
0.3
0.4
1.0
2.0
3.0
4.0
5.0
6.0
7.0
8.0
9.0

FIG 4.4 AT BINDING CAPACITY VS. pH

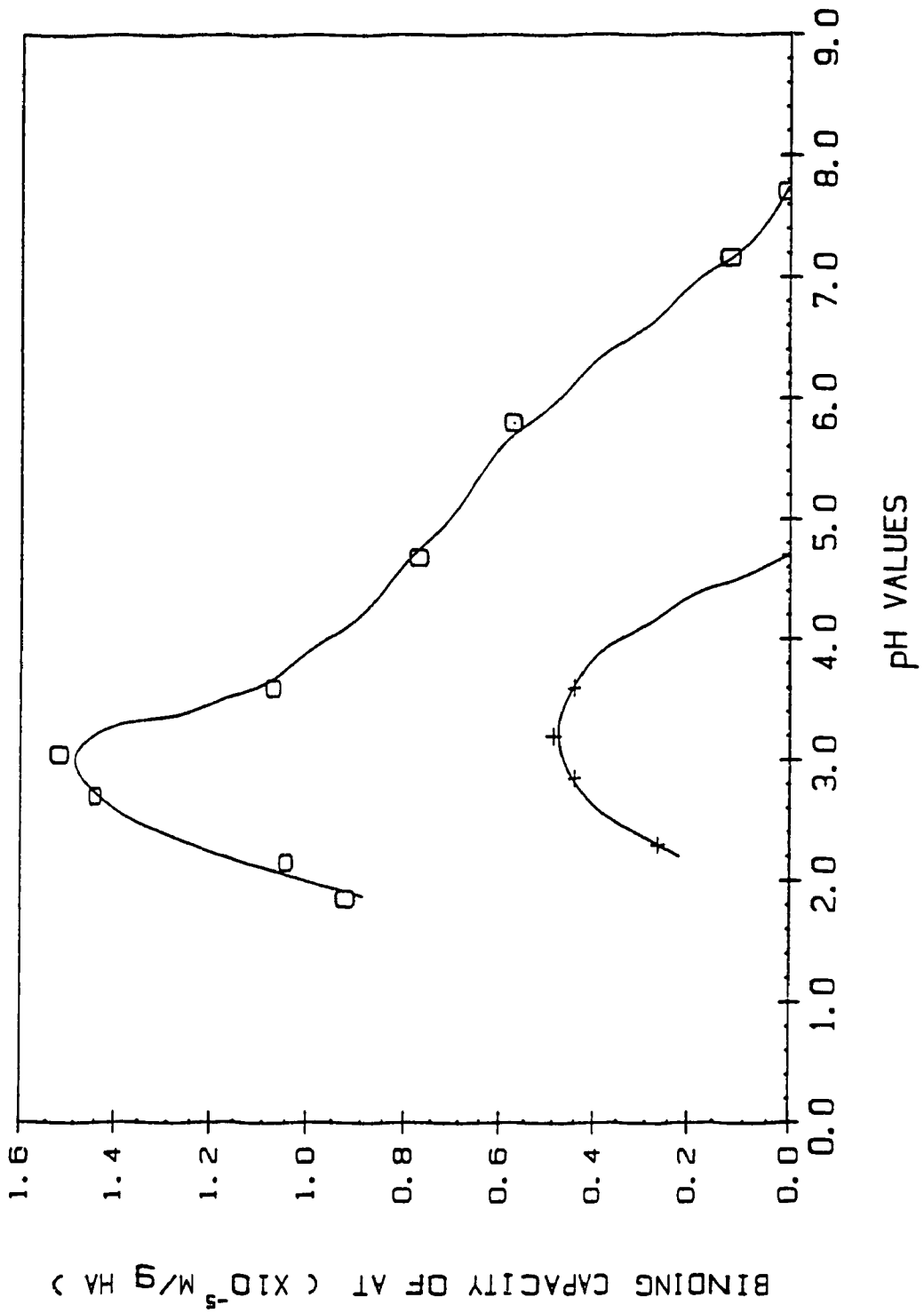

sodium and hydrogen ion. More sodium ions enter the gel solution as pH increases, and fewer protonated carboxyl group sites are available for AT sorption. (4) In the pH range of 3.0 - 1.8, the reduction of AT binding capacities is significant with pH decrease. This can be explained by the structural change in humic acid due to aggregation. This change could allow for the exposure of sites now not accessible to AT binding. Also in this situation, more AT would exist as protonated species (ATH^+) as pH decreases, which would not be entering the gel domain as easily as the neutral AT species because of the Donnan potential.

Table 4.4 summarized the values of the carboxyl groups and binding capacity of AT for both FA and HA.

Table 4.4 Comparison of Binding Capacities of AT by FA and HA

	Fulvic Acid	Humic Acid
Carboxyl groups	Type A: 5.11 mmol/g Type B: 3.49 mmol/g	2.50mmol/g
Maximal AT binding capacities	8.8 μmoles AT/g FA (at pH 1.4-1.9)	15.3 μmoles AT/g HA (at pH 3.05)

4.3.2. Sorption Equilibrium Functions

Using the first approaches for the treatment of the equilibria, described in Chapter 2, the weighted average binding constant can be calculated. Plots of Y_{AT} against M_{AT} were fitted by linear regression to obtain the differential equilibrium function. Table 4.5 shows the experimental data for the calculation of $\bar{K}$ and K at pH 2.15 and 3.05.

Table 4.5 Determination of Equilibrium Function For AT-HA

(HA=10.00 ml, Total volume=25.00 ml)

pH	Bound AT ($x10^{-5}$M/L)	Y_{AT} ($x10^{-4}$)	M_{AT} ($x10^{-5}$M/L)	$\bar{K}$ (L/M)	K (L/M)	$-(\Delta G^0+KT\ln \Gamma)$ (kJ/mol)
2.15	0.0645	6.45	0.9254	69.8	198	13.0
	0.135	13.5	1.504	89.8		
	0.242	24.2	2.046	118.3		
	0.428	42.8	2.834	151.0		
3.05	0.081	8.10	1.071	75.1	214	13.2
	0.185	18.5	1.734	106.7		
	0.319	31.9	2.397	133.1		
	0.573	57.3	3.315	172.8		

Table 4.6 Equilibrium Functions and Free Energies of AT-HA

pH	HA in gel phase	K (L/M)	$-(\Delta G^0+RT\ln \Gamma)$ (kJ/mol)
1.85	~100%	186	12.8
2.05	~100%	198	13.0
2.70	~100%	212	13.1
3.05	~100%	214	13.2
3.60	>90%	198	13.0
average		201±12	13.0±0.15

The calculated equilibrium functions, K, at various pH values and their corresponding free energy are presented in Table 4.6.

It can be seen from Table 4.5 that the differential equilibrium function is greater than the average equilibrium function. A single value of the sorption constant 201 ± 12 and a single value of the sorption free energy (minus activity coefficient term) - 13.0 ± 0.15 kJ/mol provides an adequate fit to the data at the five pH values tested. This single value leads to the idea that the K values do not show the variation with protonated sorption site loading, perhaps a reflection of the fact that the sorption sites are only a very small fraction of the total carboxylate sites.

Compared with the differential equilibrium function and free energy values, 82 ± 16 and -10.9 ± 0.5 kJ/mole for AT-FA complexes, one can immediately see that the interactions between AT and HA are somewhat stronger than that between AT and FA, which is quite consistent with the fact that the apparent binding capacity per gram of HA is higher than the binding capacity per gram of FA.

Using the second approach, the values of K and free energy were found to be $(2.30\pm0.20)\times10^{5}$ and -30.3 ± 0.24 KJ/mol, respectively. Table 4.7 shows the calculated values. Fig 4.5 shows the plot of differential functions for AT on HA at zero ionic strength vs the apparent sorption capacities.

FIG. 4.5 DIFFERENTIAL BINDING FUNCTIONS
OF AT-HA ON THE BASIS OF THE OBSERVED BINDING CAPACITY

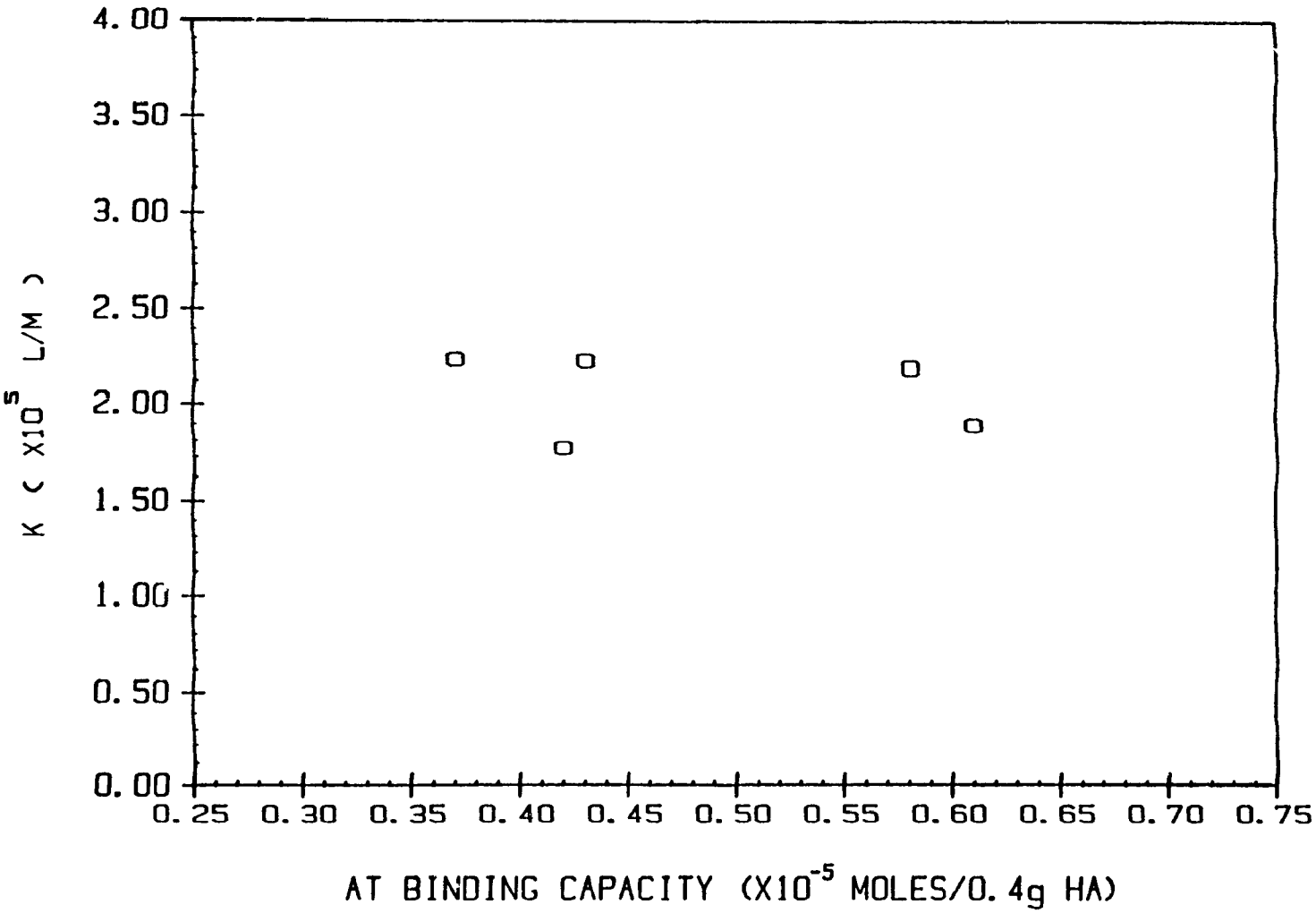

Table 4.7 Equilibrium Function and Free Energies on The Basis of The Observed Binding Capacity

pH	HA in gel phase	θ_{cap} (μmol/0.4gHA)	K (x10^5L/M)	$-(\Delta G^0+RT \ln \Gamma)$ (kJ/mol)
1.85	~100%	3.7	2.21	30.5
2.15	~100%	4.2	1.75	29.9
2.70	~100%	5.8	2.16	30.4
3.05	~100%	6.1	1.89	30.1
3.60	>90%	4.3	2.20	30.5
average			2.03±0.20	30.3±0.24

4.3.3. AT Variation at Constant pH in The Presence of 0.1 M KCl

The experimental methods were the same as for the sorption studies at low ionic strength. The final concentration of electrolyte was 0.1 M KCl. The tested pH values include pH 2.30, 2.85, 3.22, 3.60 and 4.70 and the AT variation is from 0.80 to 8.00 x 10^{-5} M at each pH. The plots of equilibrated AT and hydrolyzed ATOH versus the total AT added at each pH are very similar to that in the absence of KCl: (1) at pH 3.60 and lower, not only was AT sorbed by HA, it was also observed to be hydrolyzed by HA to form ATOH; (2) no AT hydrolysis was observed during 3 days if pH higher than 3.60. (3) no AT binding was observed if pH was higher than 4.70. (4) the increase of ionic strength of the external solution greatly decreases the amount of AT sorbed. As an example, Table 4.8 shows the bound AT and hydrolyzed ATOH at pH 3.22. Fig 4.6 shows the plots of AT bound vs AT total at pH 2.30, 2.85 and 3.22 in the presence of 0.1 M KCl.

FIG. 4.6 AT BOUND VS. CELL CONC. OF AT

(IN THE PRESENCE OF 0.1 M KCl)

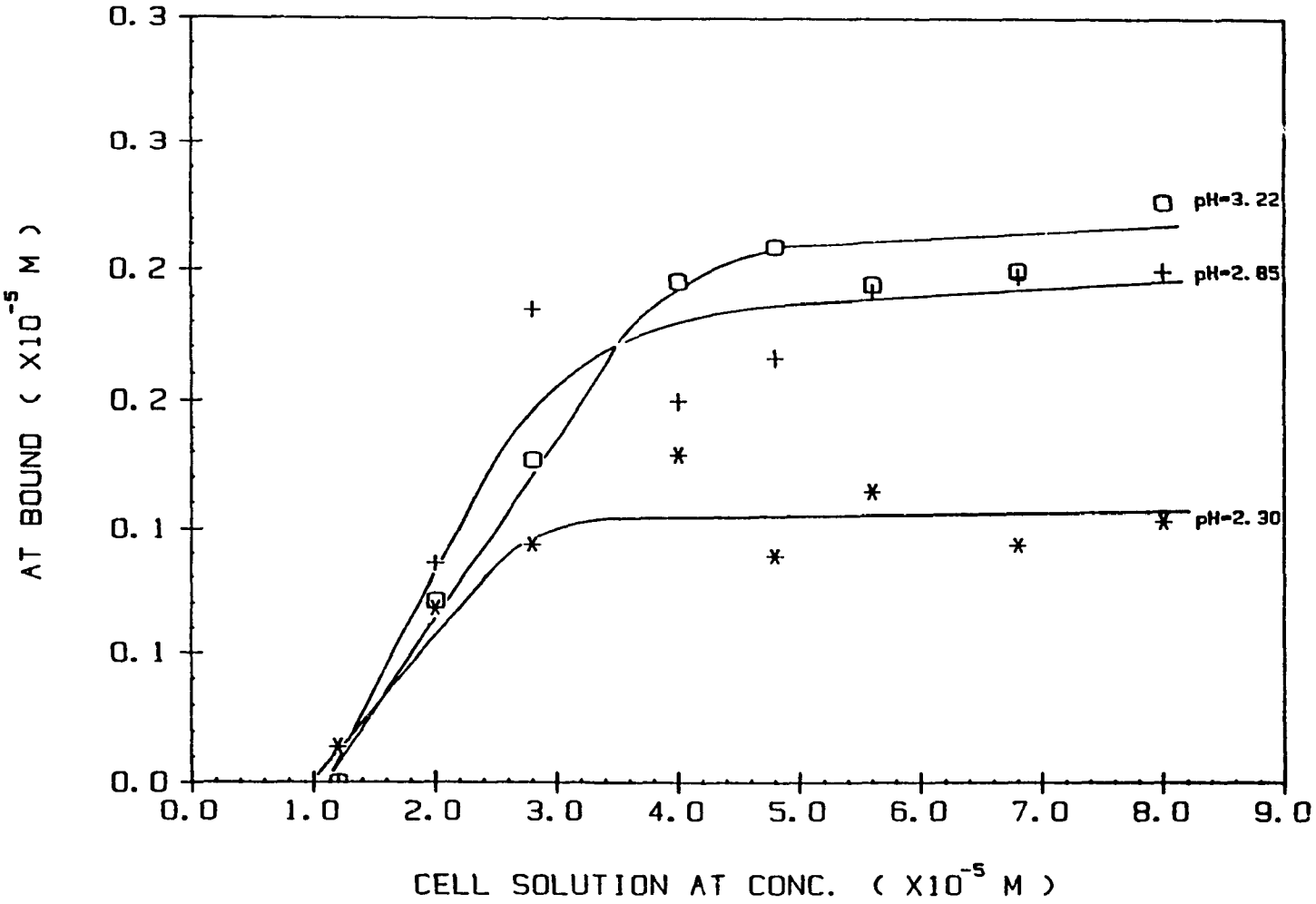

Table 4.8 Determination of Bound AT and Hydrolyzed ATOH

(KCl=0.1M, pH=3.22, HA=10.00 mg/25.00ml, Stock AT=1.00×10^{-4}M)

Added AT (ml)	in control($\times 10^{-5}$M)		in AT-HA($\times 10^{-5}$M)		Bound AT ($\frac{\mu mol}{0.4g\ HA}$)	Hydrolyzed ATOH(μM)
	AT	ATOH	AT	ATOH		
3.00	1.192	/	1.195	/	/	/
5.00	1.974	0.0399	1.903	0.0438	0.71	0.039
7.00	2.756	0.0543	2.629	0.0730	1.27	0.187
10.00	3.929	0.0759	3.733	0.1095	1.96	0.336
12.00	4.711	0.0903	4.502	0.1387	2.09	0.486
14.00	5.493	0.105	5.300	0.1642	1.93	0.592
17.00	6.666	0.126	6.466	0.2007	0.200	0.747
20.00	7.839	0.148	7.612	0.2263	0.227	0.783

The plot of binding capacity of AT vs pH is also presented in Fig 4.4. The pronounced features which can be seen from the comparison between two curves in the presence or absence of KCl are that (1) KCl greatly depresses AT binding at the whole pH range studied. (2) the maximum binding of AT occurs at pH 3.22, shifted about 0.2 pH unit from the maximum at low ionic strength. (3) at pH 4.7 and higher no noticeable AT sorption was observed. However, binding can still be observed at pH 7.2 in the absence of KCl.

This phenomenon could be explained by a reduction of the Donnan potential and the dependence of dissolution equilibrium of HA. At 0.1 M KCl, the Donnan potential must be much lower than in the absence of an electrolyte. The ion exchange of K^+ with

hydrogen ion in a gel domain makes the carboxylic acid groups more acidic, leading to the less protonated HA, and consequently, the smaller sorption capability of the HA. The pKa values of HA from the titration with standard base [99] clearly shows the electrolyte's effect on the dissolution of HA (See Table 4.9).

Table 4.9 Effect of KCl on The Apparent Ionization Constant of HA

pH	pK_a (with 0.1M KCl)	pK_a (without 0.1M KCl)
3.6	~3.65	~4.5
3.8	~3.63	4.6
4.0	~3.60	4.7
4.2	~3.60	4.8
4.4	~3.57	4.95
4.6	~3.54	5.1
4.8	~3.50	5.2

This phenominon, coupled with the effect of KCl on the dissolution-precipitation equilibrium, more effectively reduces the binding capacity of HA. As was explained before, the appearance of a maximum in the binding curve is the result of the competition of two factors, (one is protonation, favourable to AT sorption; another is aggregation due to the increase of H^+ concentration especially the increase of electrolyte, unfavourable to AT sorption). The high concentration of KCl makes the second factor more effective than the first one, which results in greater reduction of sorption capacity and the shift of maximum binding

capacity to higher pH, as shown in Fig 4.4.

4.3.4. Effect of HA Concentration on AT Sorption

The experimental results of this part show that unlike the case of AT-FA, the HA concentration has not so much effect on AT sorption by HA. This effect was investigated quantitatively at pH 3.60 and constant AT concentration (4.00×10^{-5} M) with HA concentration variation from 5.00 mg to 30.00 mg. Fig 4.7 shows the plot of bound AT against various HA weight used.

It can be seen from Fig 4.7 that in the range of HA concentration from 0 to 20.00 mg/25.00 ml, the plot of bound AT vs the weight of HA is almost a straight line. The curve shows a little downward trend only until HA concentration reaches 30.00 mg/25.00 ml.

This fact could be explained from the nature of gel the phase itself. In the pseudo-homogeneous FA solution, FA molecules have more degrees of freedom; hence, interactions occurs much easily than in gel domain. When the concentration increases, more interaction between FA molecules takes place and leads them to form much "bigger" molecules, mainly through H-bonding. As a result, some specific binding sites are lost due to aggregation. By contrast, the protonated HA stay in the gel phase; they enter into the external solution in the deionized form when the pH of the solution increases. Every gel particle is surrounded by water molecules and some counter ions, so the collision and interaction between HA molecules are more difficult than for FA molecules.

FIG. 4.7 DEPENDENCE OF AT BINDING ON HA CONC.

(AT=4.000X10^{-5} M, pH=3.60)

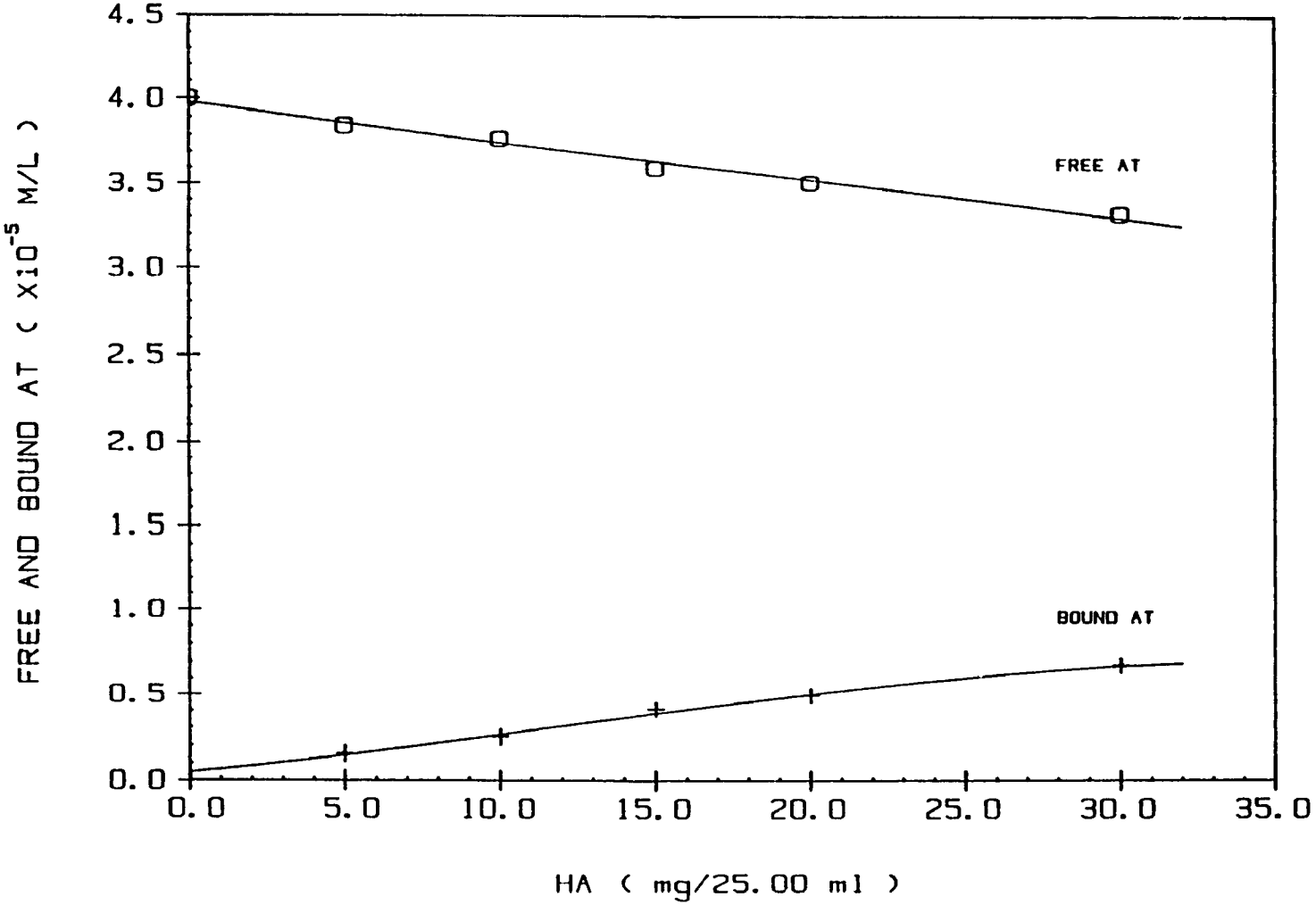

4.3.5. Competition between AT and ATOH

A series of experiments in which the ratio of AT to ATOH was kept constant (2:1) with a variation of sum at pH 3.10, 3.75 and 4.75 were conducted in order to determine whether ATOH can block AT binding to humic acid. Fig 4.8 shows the binding curve of AT at pH 3.10 in the low ionic strength. This pH was chosen to be near the maximum binding capacity.

Fig 4.9 A and B shows the plots of bound AT vs AT total or added, and bound ATOH vs the total ATOH added.

It can be seen from Fig 4.9 that (1) a binding limit for AT at each pH is still reached in the presence of stronger binding competitor ATOH, and the empirical binding capacity can be defined as 6.0 μM AT at pH 3.10. 4.1 μM at pH 3.75 and 3.0 μM at pH 4.75. (2) no binding limit for ATOH at each pH is reached in range of ATOH concentrations used. This is because ATOH binds more strongly than AT and has significantly higher binding capacity than AT does. (3) the highest ATOH binding occurs at pH 3.75 among the 3 tested pH values. This pH is quite near the pH (3,80) at which the maximal binding capacity of ATOH by FA was observed (see Chapter 2). This implies that the behavior of ATOH sorption by HA is quite similar with that of ATOH binding by FA.

A quite interesting comparison of AT binding capacity in the absence and presence of ATOH is presented in Table 4.10.

Table 4.10 clearly shows that the addition of ATOH does not effect AT sorption by HA, in another words, there was no noticeable competition between AT and ATOH for sorption sites. This is an important experimental result. It allows us to separately to treat AT and ATOH binding data in the coexistence of

FIG. 4.8A COMPETITION FOR BINDING SITES BETWEEN AT AND ATOH

(pH=3.10, HA=10.00 mg/25.00 ml, KCl=0)

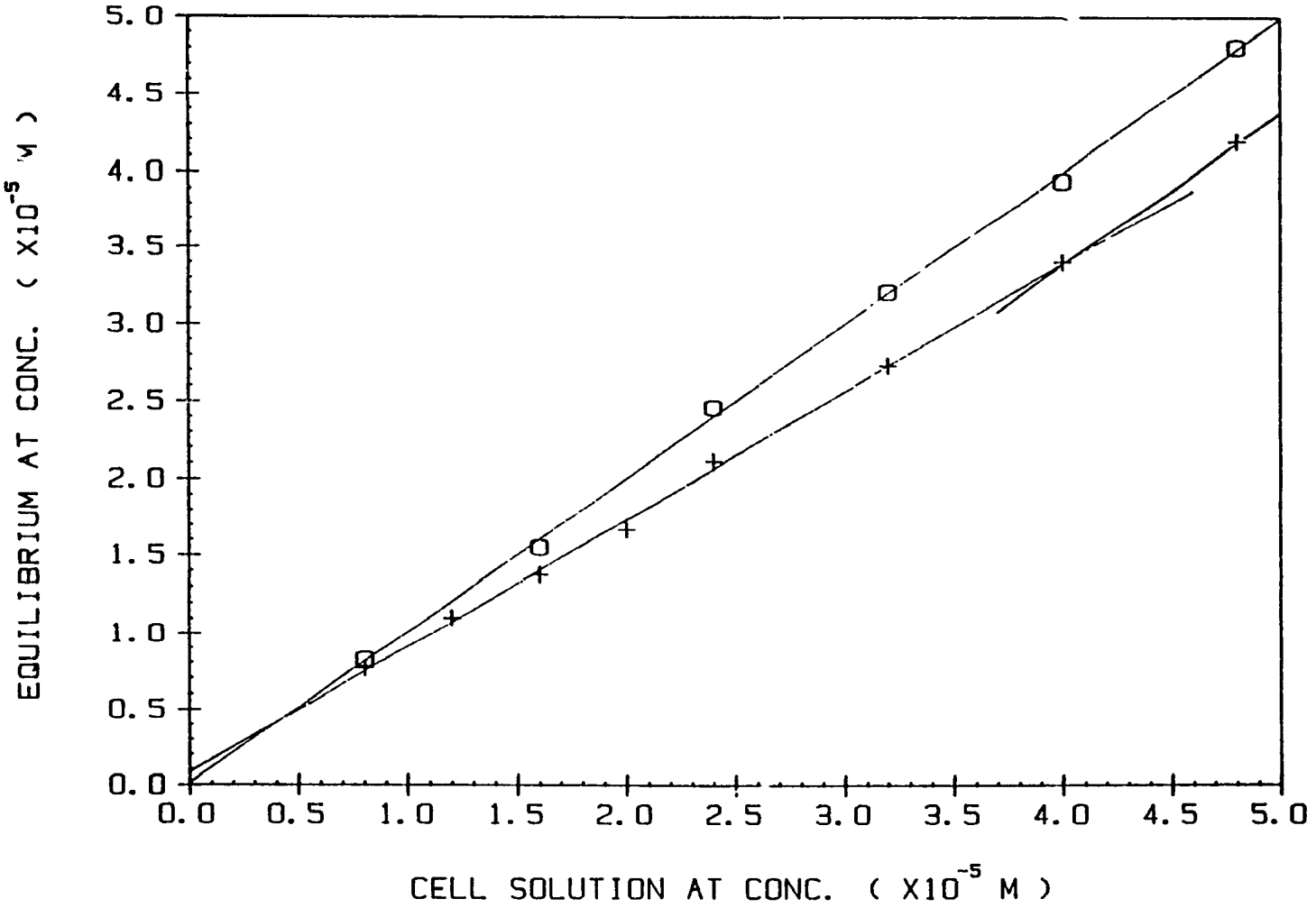

FIG. 4.8B COMPETITION FOR BINDING SITES BETWEEN AT AND ATOH

(pH=3.10, HA=10.00 mg/25.00 ml, KCl=0)

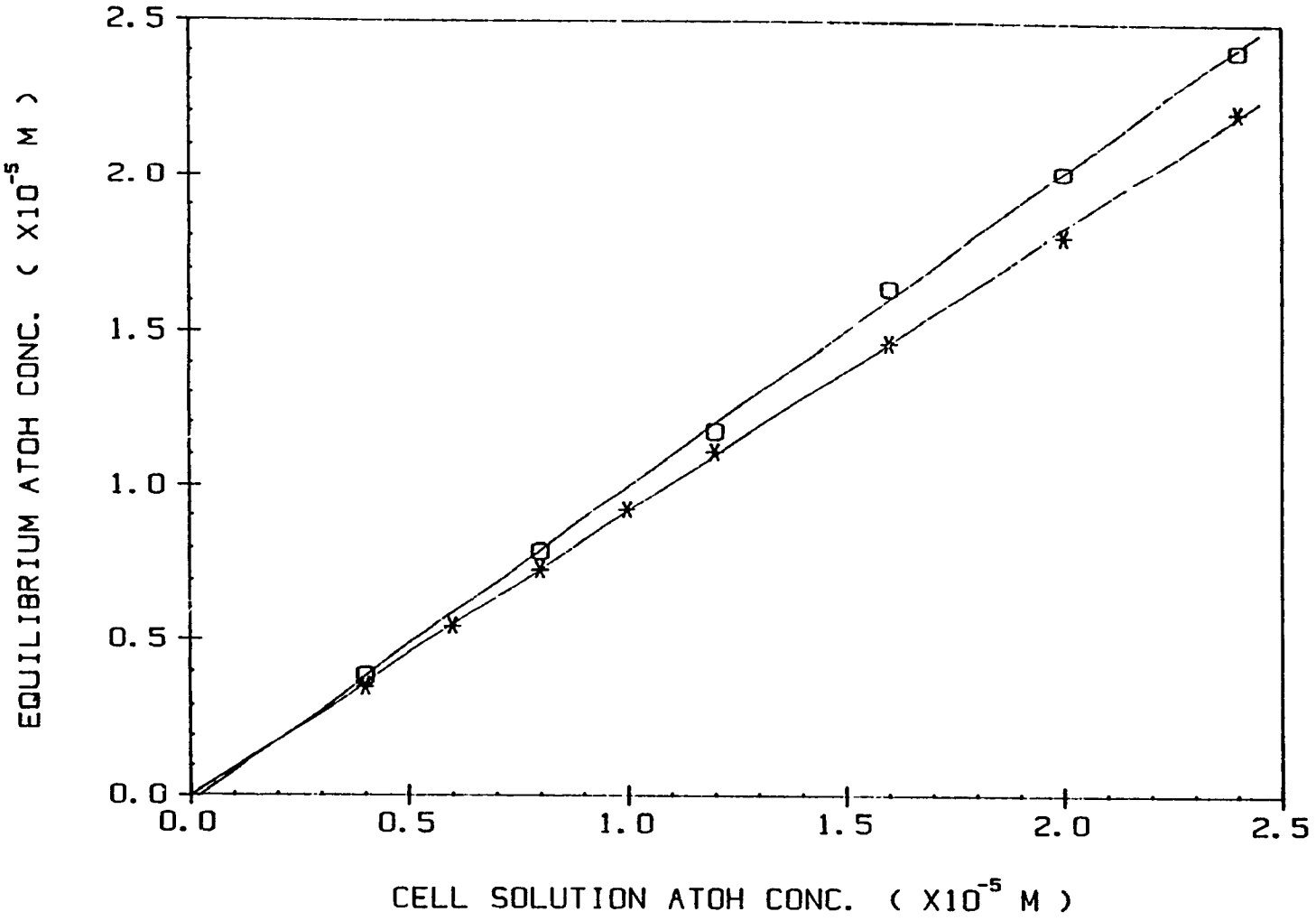

FIG. 4.9A AT BOUND VS. AT ADDED IN PRESENCE OF ATOH

(HA=10.00 mg/25.00 ml, KCl=0)

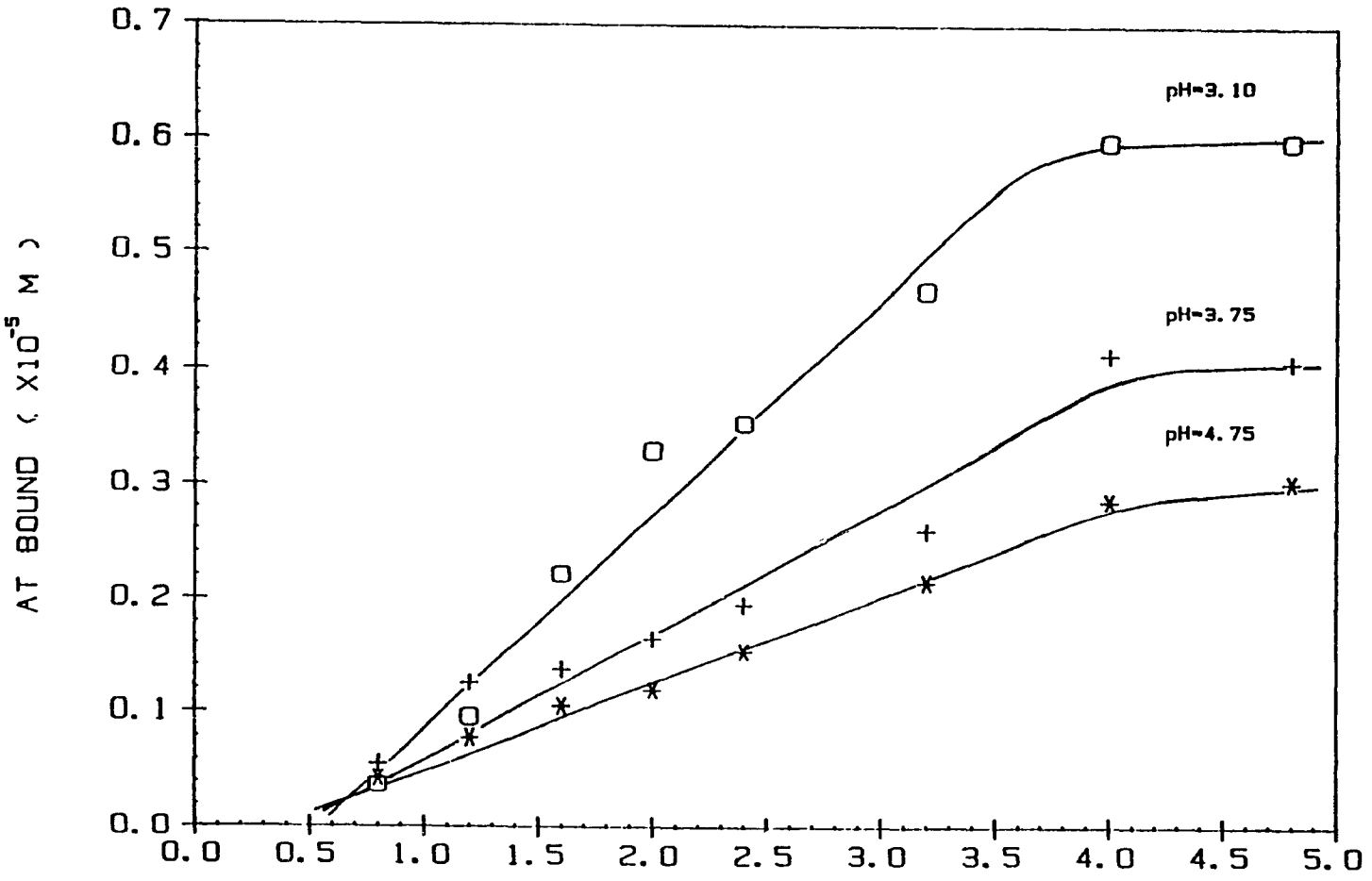

FIG. 4.9B ATOH BOUND VS. ATOH ADDED IN PRESENCE OF AT

(HA=10.00 mg/25.00 ml, KCl=0)

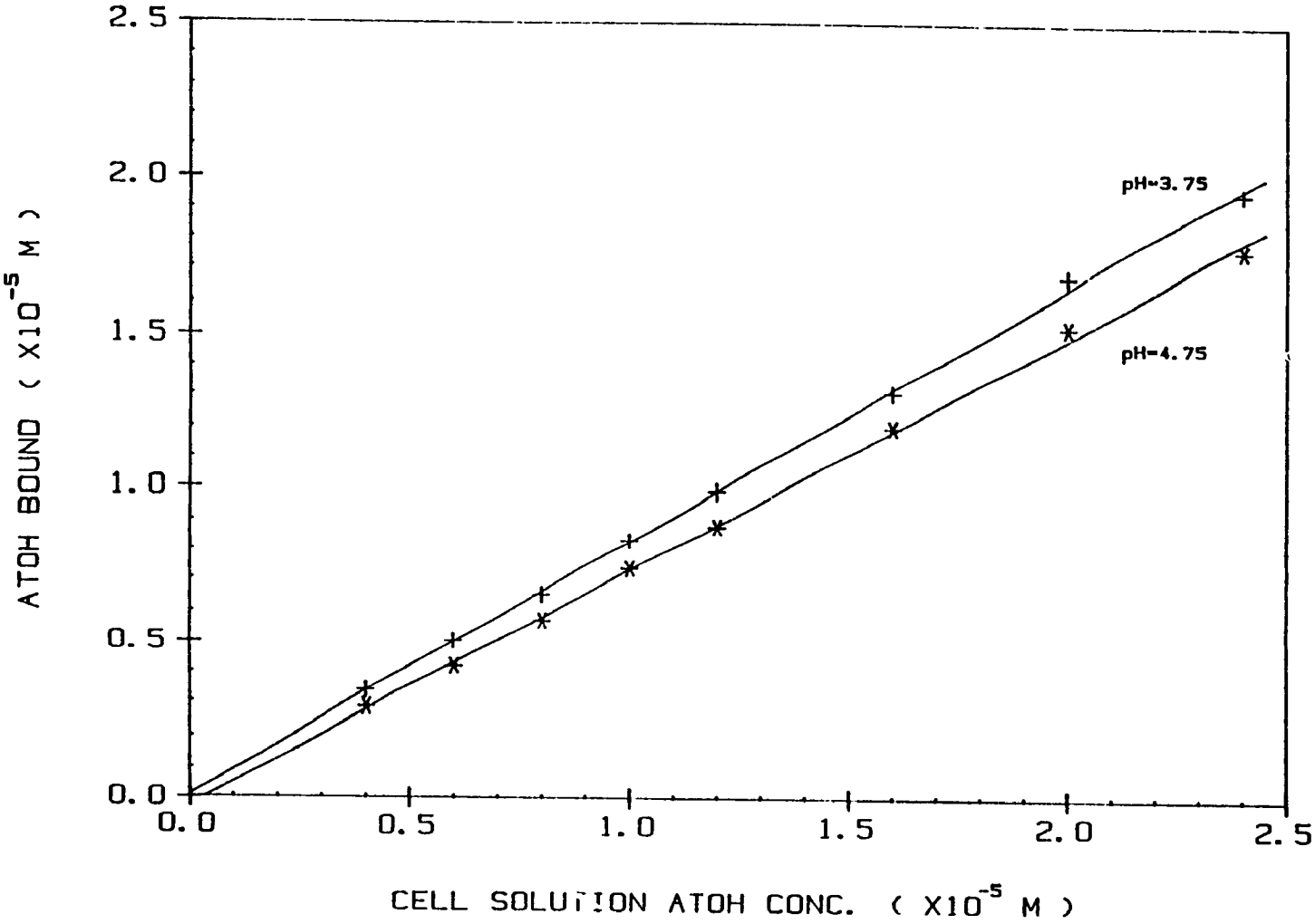

AT and ATOH. This fact has its theoretical importance: in some previously published papers, AT and ATOH were expected to compete for protonated carboxyl groups as sorption sites. The mathematical modeling must be quite complex in order to cover the competition between AT and ATOH. Now, the mathematical treatment can be much simplified according to this experimental evidence. This fact also implies that the hydroxyatrazine reaction product does not cause catalyst poisoning.

In the treatment of organic molecules having similar structure such as AT and ATOH, one aspect to be considered is that AT and ATOH have their own respective favorable "specific sorption sites" (a sum of such sites is still a very small fraction of total carboxylate sites of HA); another aspect to be considered is the amounts bound by HA at same pH and same ionic strength seem to be mainly dependent on the sorbents, that is, their chemical structure and polarity.

Table 4.10 Comparison of AT Binding Capacity

In The Absence and Presence of ATOH

pH	AT binding capacity (μmol/0.4g HA)	
	without ATOH	with ATOH
3.10	6.1	6.0
3.75	4.0	4.1
4.75	3.0	3.0

4.3.6. AT binding in The Presence of Copper Ions

The amount of AT per gram needed to saturate humic acid has been determined from AT titrations of HA at various pH. By equilibrating the appropriate amount of AT with a known amount of HA, the AT-HA complex was formed. The main aim of these experiments was to see whether the copper ions compete with AT for the same sorption sites in HA, and what kind of effect copper ions can have on AT-HA binding.

(1) Copper complexing with HA in the absence and presence of AT

Experiments in which humic acid was saturated by excess of Cu ions in the absence and presence of AT show that at low AT loading (compared with Cu concentration), Cu(II) binding is almost the same as that in the absence of AT. Fig 4.10 shows a typical titration curves of HA by AT at pH 2.90 in the presence of constant Cu (1.00×10^{-3} M). Fig 4.11 shows the titration curves of HA by Cu at pH 3.68 in the presence of constant AT.

For Fig 4.10, averaging the experimental data for Cu in both controls and AT-Cu-HA sample solutions, the Cu complexing capacity can be easily obtained simply by subtraction of Cu(II) amount in samples from Cu(II) amount in controls, which equals 0.15×10^{-3} mole/0.400 g HA (about 15% of the total carboxyl groups are bound by copper ions). The AT and hydrolyzed ATOH can be fitted to a straight line, respectively, and bound AT at each total AT added can be evaluated from the differences between the control AT and the sample AT. For Fig 4.11, averaging the AT data in both controls and samples, the bound AT at the level of total added AT (4.00×10^{-5} M) can be found to be 2.2 μM/0.400g HA. When added Cu concentration was larger than 4.00×10^{-4} M, the sorption sites of

FIG. 4.10 BINDING CURVE OF AT IN PRESENCE OF Cu

(pH=2.90, TOTAL Cu ADDED=1.00X10^{-3} M, HA=10.00 mg/25.00 ml)

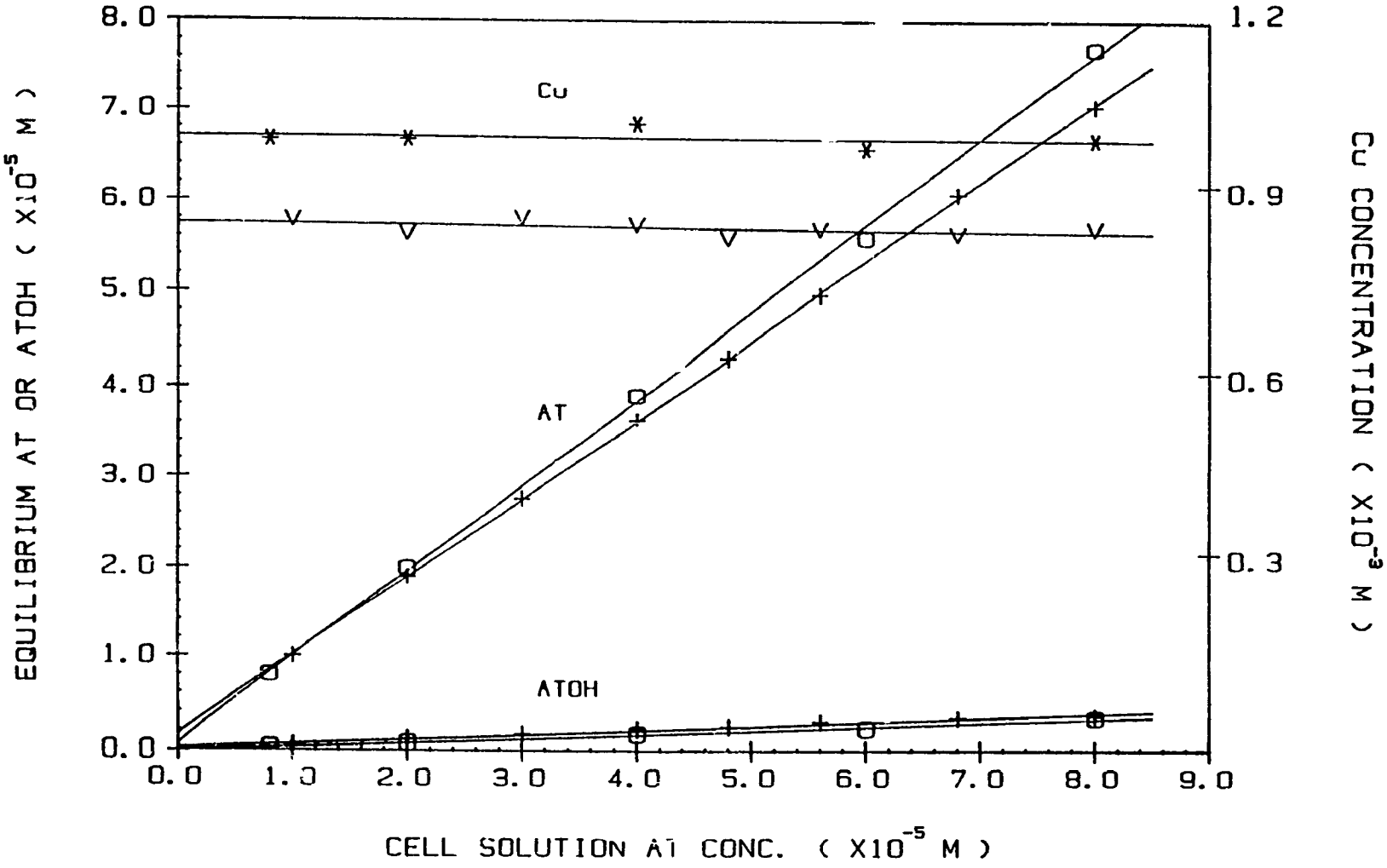

FIG. 4.11 Cu TITRATION CURVE IN PRESENCE OF AT

(pH=3.68, AT ADDED=4.00X10^{-5} M, HA=10.00 mg/25.00 ml)

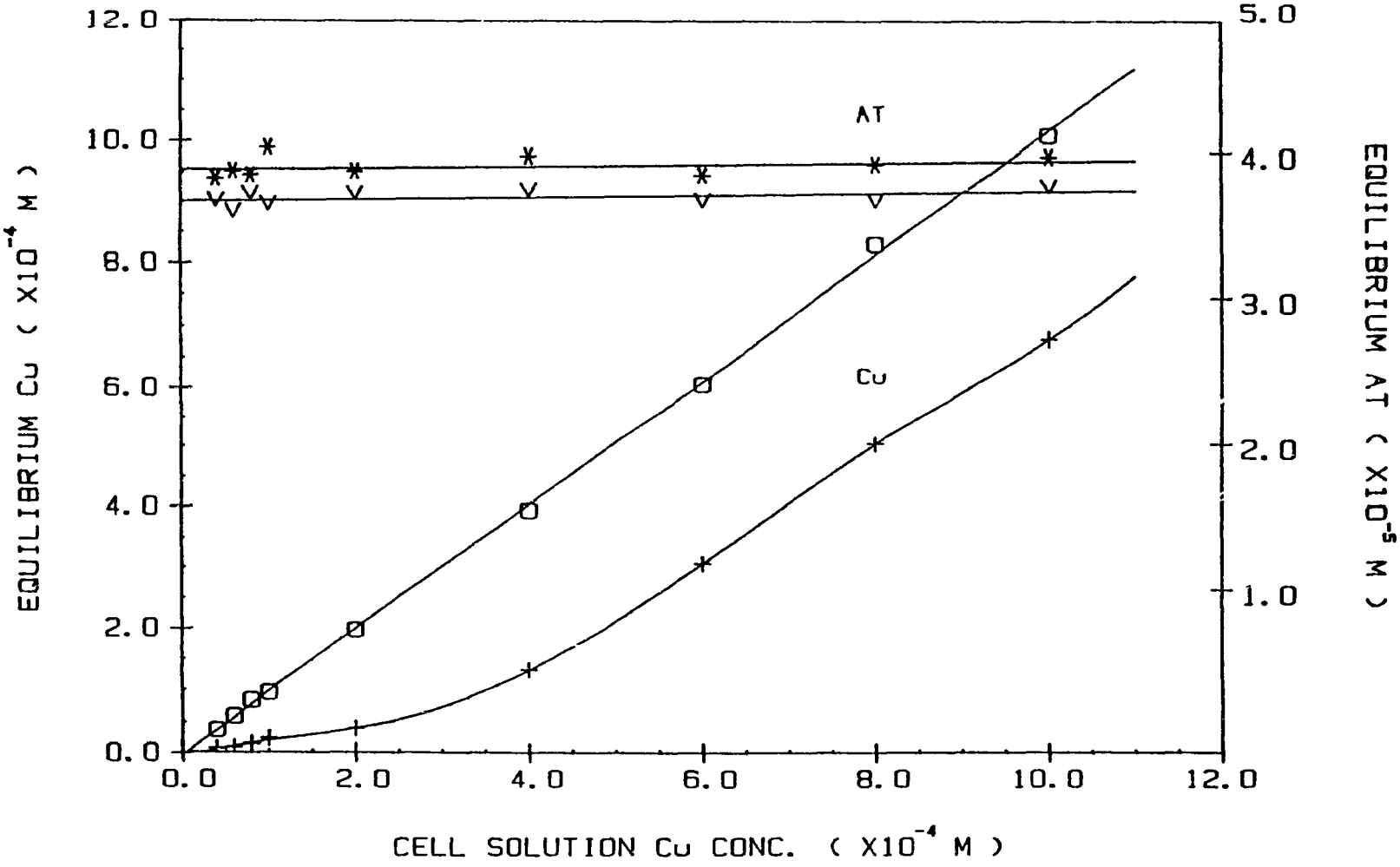

HA were saturated. Then the Cu(II) complexing capacity is determined to be 3.3. x 10^{-4} moles per 0.400 g HA, which is in good agreement with the value without AT.

Table 4.11 listed the copper complexing capacity at various pH values in the presence and absence of AT.

Table 4.11 Comparison of Copper Complexing Capacity in The Presence and Absence of AT

pH	Saturated Cu(II) without AT (mmol/g HA)	% Total Carboxylate	pH	Saturated Cu(II) with AT (mmol/g HA)	% Total Carboxylate
			2.64	0.275	11.0
2.90	0.383	15.3	2.90	0.375	15.0
3.40	0.695	27.8	3.30	0.683	27.3
3.60	0.815	32.6	3.80	0.908	36.3
4.40	1.388	58.3	4.40	1.438	57.5
			5.10	1.843	73.7
			5.38	2.063	82.5
5.65	2.325	93.0	5.55	2.300	92.0
			6.25	2.433	97.3
			6.80	2.475	99.0

Fig 4.12 shows the plots of Cu complexing capacity vs pH for the data in Table 4.11. One feature in Figure 4.10 and Fig 4.12 is that no significant change of Cu complexing capacity due to the added AT loading occurs, mainly because the concentration of AT-HA complex is much too small to affect Cu-HA complex.

FIG. 4.12 Cu COMPLEXING CAPACITY AS A FUNCTION OF pH

IN THE ABSENCE AND PRESENCE OF AT

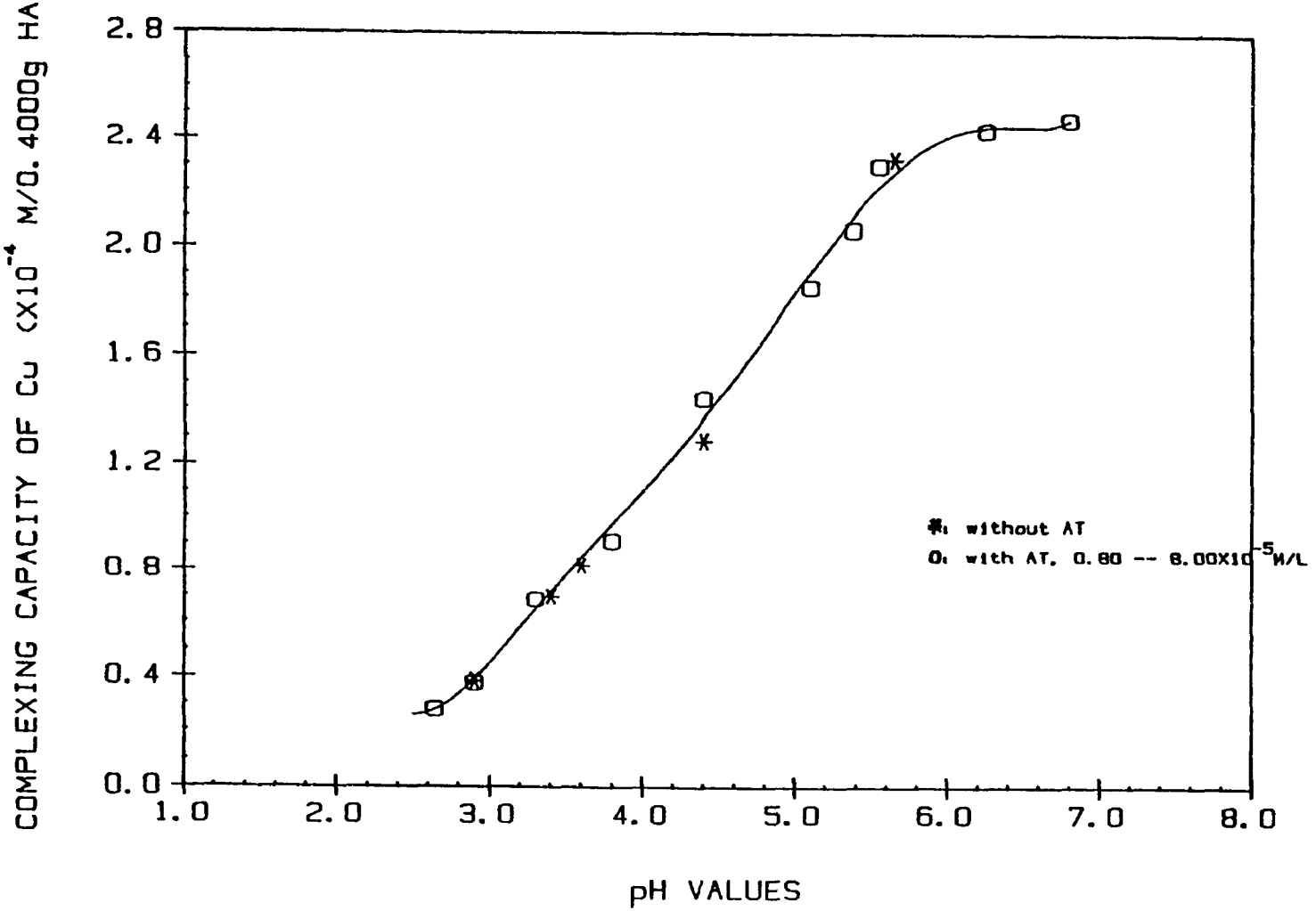

(2) Effect of Excess Cu on AT binding

The experiments were designed in such a way that AT was varied from 0.80×10^{-5} M to 8.0×10^{-5} M in the presence of excess of Cu ions (1.00×10^{-3} M) at each pH value tested. The plots of AT bound vs the total AT added are shown in Fig 4.13.

Comparing Fig 4.13 with Fig 4.2 (Plot of bound AT vs AT total at various pH in low ionic strength), one can immediately find the effect of Cu ions on AT binding. There are two pronounced features in Fig 4.13. (1) unlike Fig. 4.2., no AT binding limit was reached at each pH. (2) the amount of AT bound is the function of total AT added, that is, AT bound increases with the increase of total AT added.

If the bound AT at the highest AT added (8.00×10^{-5} M) is plotted against pH, Fig 4.14 is obtained. The corresponding plot of AT binding capacity vs pH in the absence of Cu ion is also presented in Fig 4.14 as to compare the differences between them.

The most noticeable feature in Fig 4.14 is that the AT bound in the presence of 1.00×10^{-3} M Cu are smaller but not so much smaller than that in low ionic strength in the whole pH range studied. Another feature worth pointing out is the shape and profile of the curve is quite similar with the curve of AT binding capacity vs pH.

A reasonable explanation for this phenomenon (reduction of AT bound, and no binding limit is reached) might be that Cu blocked some specific carboxyl groups available to AT binding (Fig. 4.15).

Another possible explanation for this is that the sorption of Cu could result in the coagulation and conformational changes of HA (similar effects can be found in AT-Cu-FA systems). This

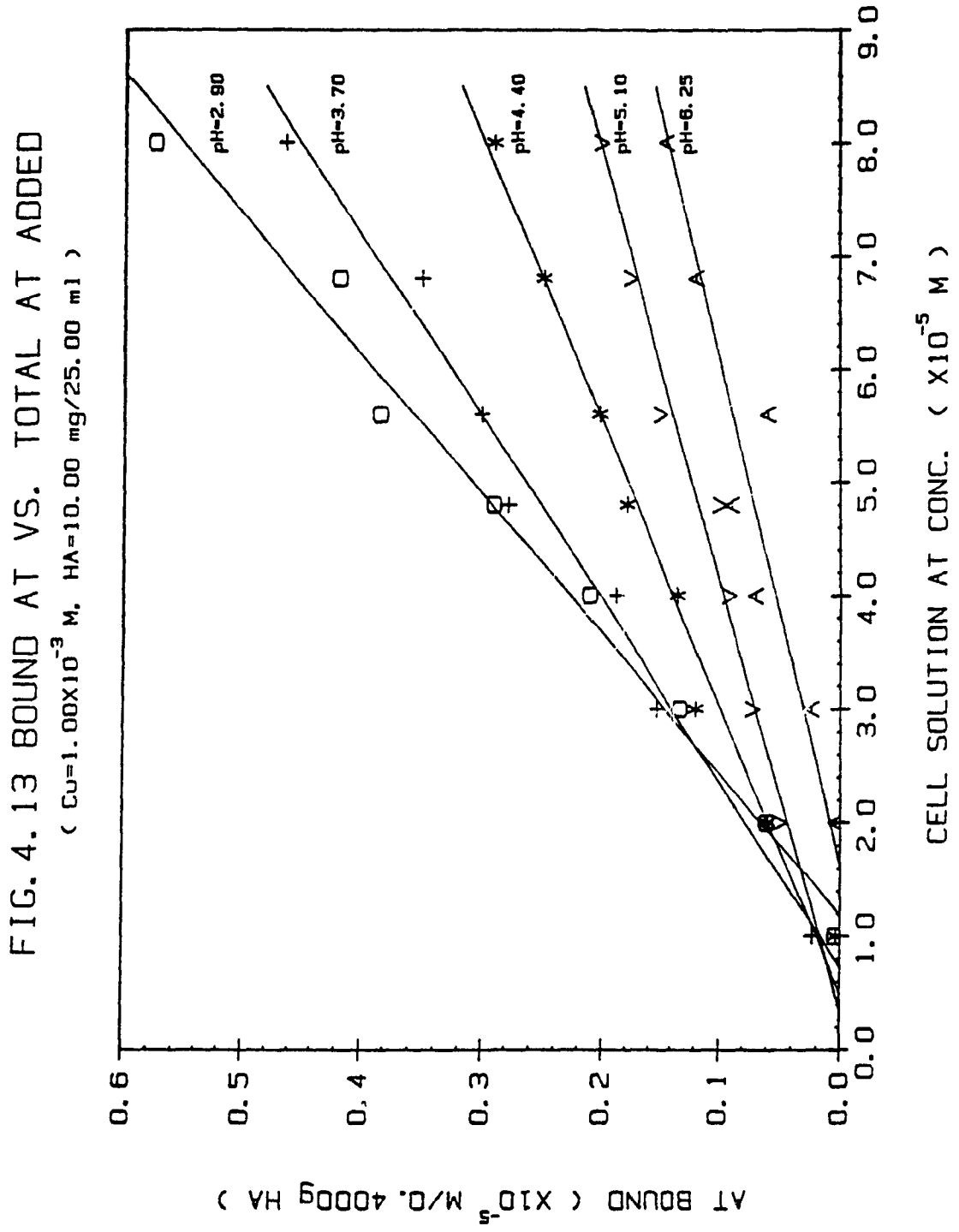
FIG. 4.13 BOUND AT VS. TOTAL AT ADDED
(Cu=1.00X10-3 M, HA=10.00 mg/25.00 ml)
pH=2.90
pH=3.70
pH=4.40
pH=5.10
pH=6.25
AT BOUND (X10-5 M/0.4000g HA)
CELL SOLUTION AT CONC. (X10-5 M)
0.0
0.1
0.2
0.3
0.4
0.5
0.6
1.0
2.0
3.0
4.0
5.0
6.0
7.0
8.0
9.0

FIG. 4.14 AT BINDING CAPACITY VS. pH

(O: no KCl; *: with 1.0×10^{-3} M; +: with 0.1 M KCl)

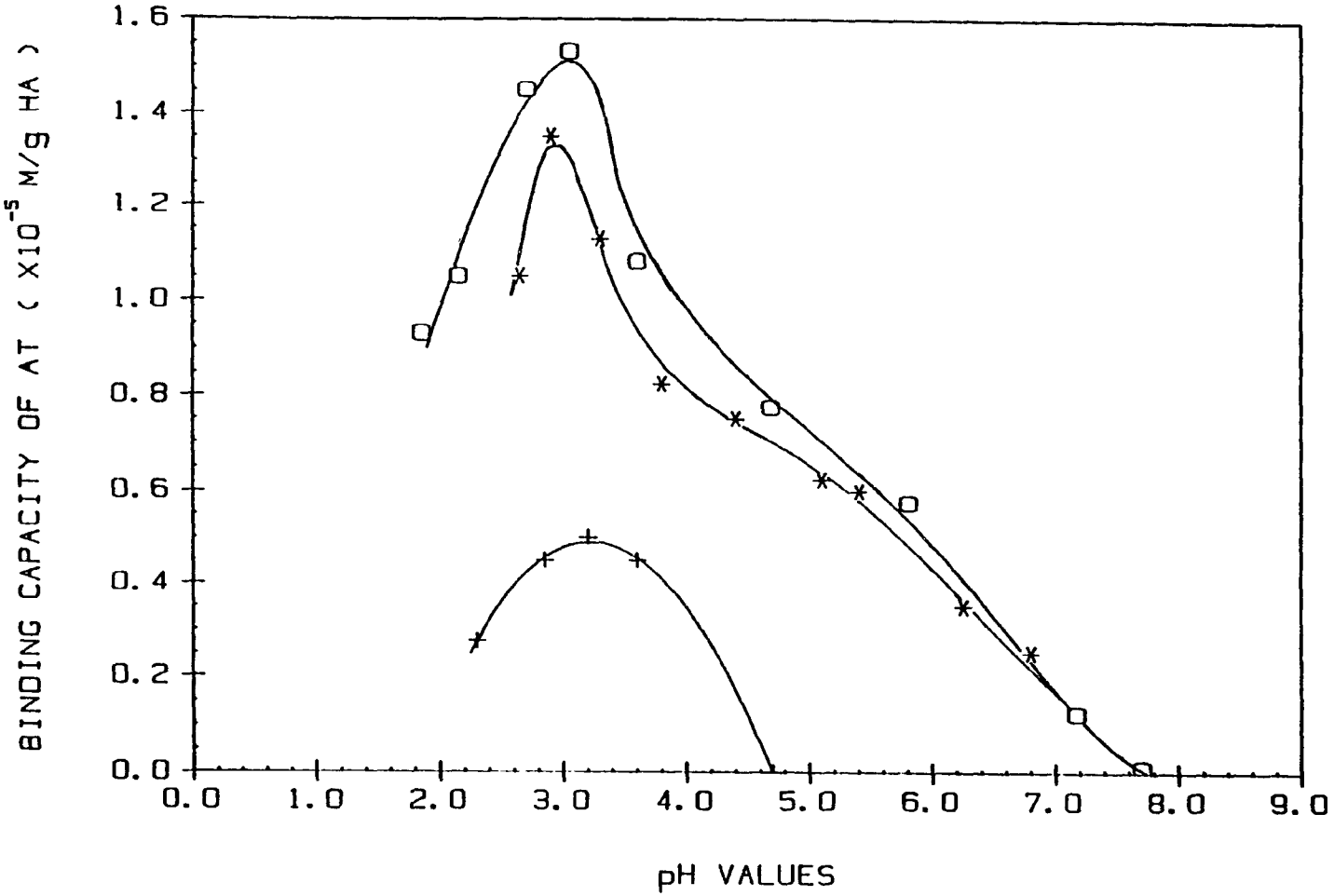

physical and chemical change of HA structure will certainly lead to some loss of those specific sites available to AT binding.

Three main conclusions can be drawn from the present results. First, the presence of low concentration of AT does not affect the Cu sorption by HA. Second, the saturation of carboxyl groups in HA with Cu does not exclude AT from binding to HA but it decreases the amount of AT bound more or less. Third, the reduction of AT bound in the presence of excess Cu could be attributed to the specific sites shown in Fig. 4.15 being blocked by Cu ions, or tc conformational changes of HA.

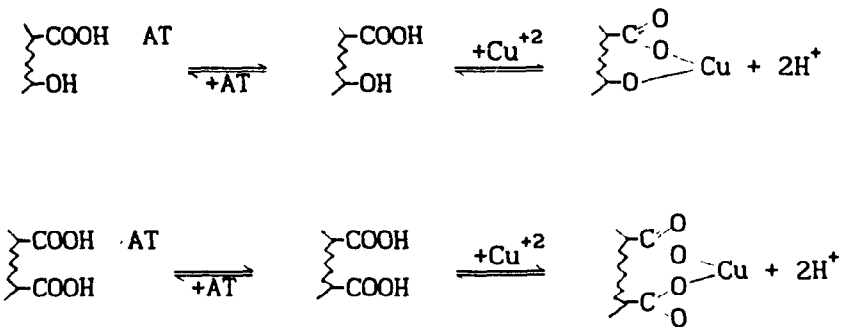

Fig. 4.15 Suggested binding mechanism for Cu(II) in water-swollen HA gel cation exchanger

4.3.7 FTIR Spectra

(1) FTIR spectrum of HA

Fig 4.16 and Fig 4.17 display the FTIR spectra of Laurentian humic acid sample in the 4000 - 500 cm^{-1} and expanded 1800-1000 cm^{-1} region, respectively.

Three observations are immediately obvious from Fig 4.16 and 4.17. (1) protonated carboxyl groups (-COOH) with the typically

FIG. 4.16 FTIR SPECTRUM OF LAURENTIAN HA

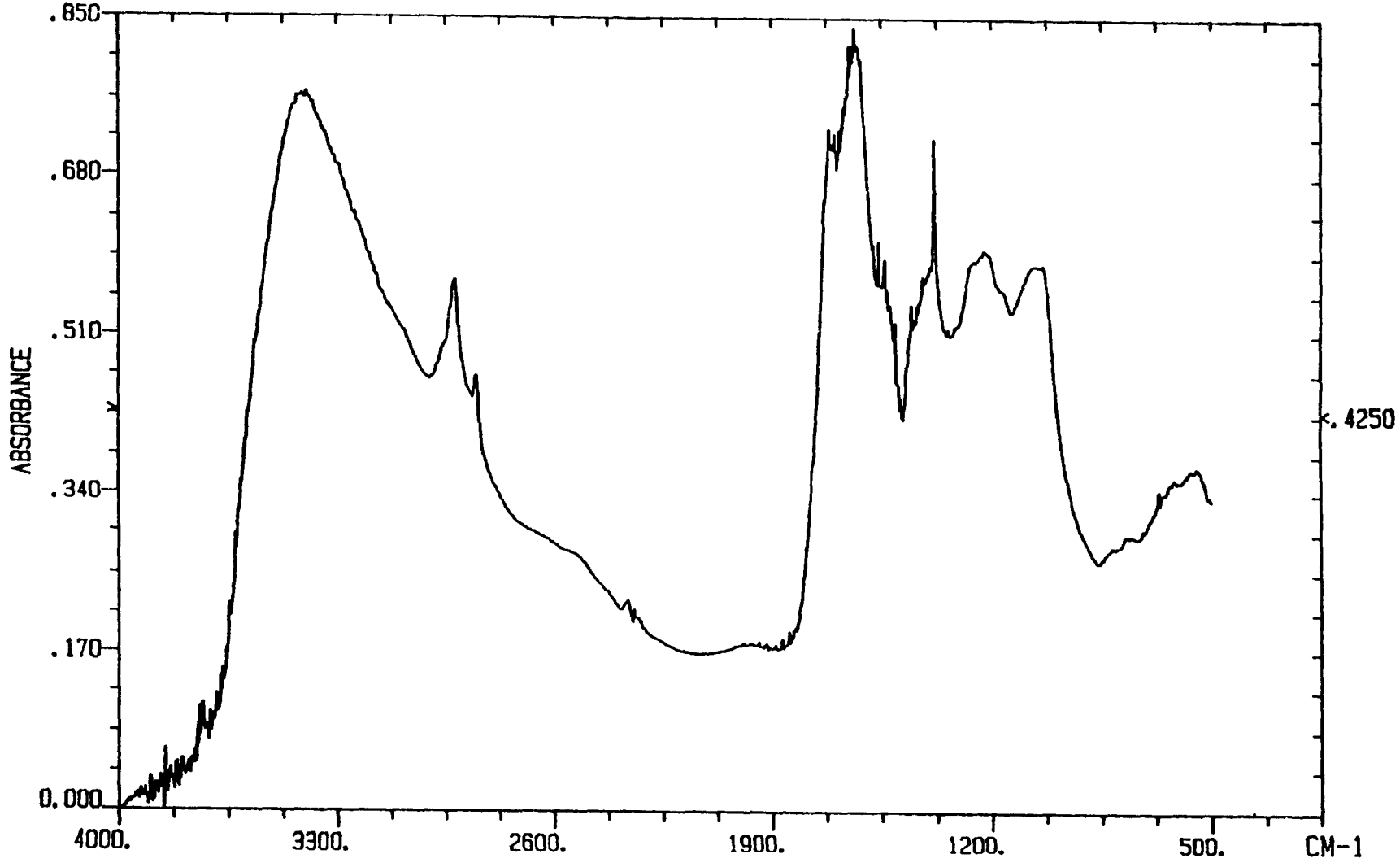

FIG 4.17 FTIR SPECTRUM OF LAURENTIAN HA

IN 1800 -- 1000 cm^{-1} RANGE

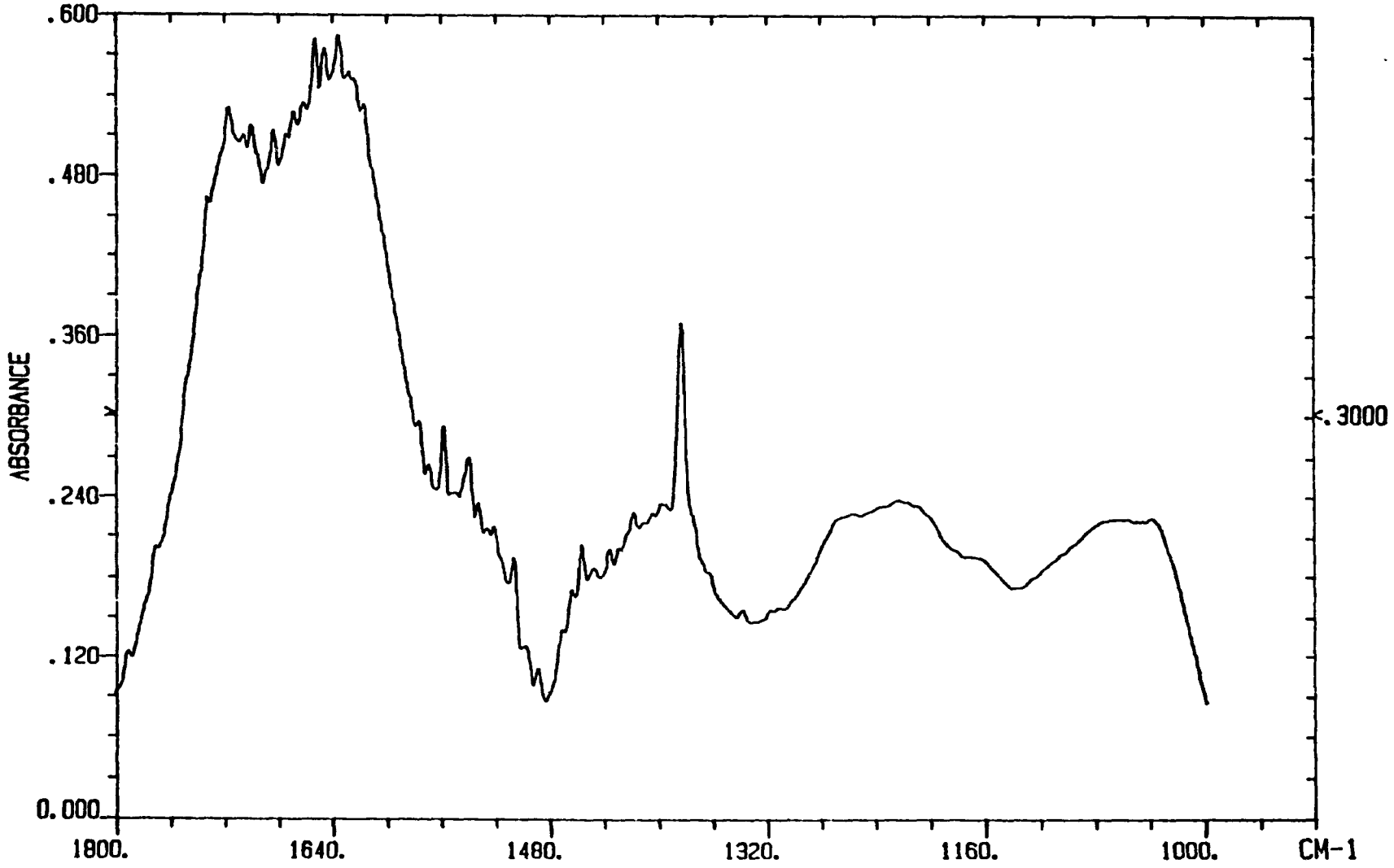

characteristic frequency around 1716 cm^{-1} (this value is also a indicator of existence of some ketones, aldehydes and esters), as well as around 1232 cm^{-1} bands. Carboxylate groups (COO-) have characteristic bands close to 1635 cm^{-1} and 1384 cm^{-1} region. (2) The quite significant bands in the entire spectrum are centered close to 1650 and 1550 cm^{-1}. These are very well-known group frequency values for the amide I and amide II bands of proteins, polypeptides, and other secondary trans-amides [117-120]. The relative intensity of these two bands, and the presence of an amide (III) band in the 1230 cm^{-1} region confirms this assignment. Such amides apparently constitute a certain portion of the sample and may in part be the decomposition products of proteins. (Elemental analysis results in Table 4.1 shows that HA contains 2.3% nitrogen). (3) Carbon-hydrogen bands: The nature of the predominant C-H bands is most clearly indicated in the C-H stretching region below 3000 cm^{-1}. Very sharp bands are observed at 2923 (asymmetric CH_3 and CH_2 stretching) and 2854 cm^{-1} (symmetric CH_3 and CH_2 stretching). Aromatic C-H stretching bands are generally above ~ 3000 cm^{-1}. The absence of much clear and pronounced bands (only a poorly resolved shoulder can be seen) may be caused by extensive substitution of the aromatic ring or masking from the broad OH stretching band. (4) C-O-H bending and C-O stretching (1300 - 1000 cm^{-1}): Two very broad bands, centered at 1230 and 1061 cm^{-1}, respectively, are exhibited in this region. This region is difficult to interpret in detail because the C-O stretching mode of esters, ethers and alcohols, and C-O-H bending modes of alcohols, as well as the amide III modes of secondary amides. absorb in the same frequency range. The band near 1230

cm^{-1} is most probably attributed to the composition of CO stretching and OH deformation of COOH, and to the amide III mode. The band centered at 1061 cm^{-1} could be associated with primary, secondary and tertiary alcohols and some esters. The proposed detailed assignment for the major absorption bands in FTIR spectra of HA is presented in Table 4.12

(2) Comparison of FTIR Spectra of HA with FA

Fig.4.18 and Fig.4.19 put the FTIR spectra of HA ad FA in the 4000-500 cm^{-1} and 1800-1000 cm^{-1} region together so that their structural characteristics can be compared.

The major differences one can immediately see from Fig. 4.18 and 4.19 are that: (1) the FTIR spectra of HA are more complex than of FA. (2) HA shows much sharper and stronger aliphatic C-H stretching bands (2923 and 2854 cm^{-1}) than FA does (this confirmed by stronger aliphatic C-H bending of HA in 1472-1400 cm^{-1} region), which implies HA molecules contain relatively more aliphatic groups. (3) the most characteristic difference can be found in the most important 1800-1300cm^{-1}region. First, HA shows very pronounced amide bands (centered at 1650 and 1550 cm^{-1}), but FA does not. Second,FA shows very strong absorption bands of protonated COOH groups (~1724 cm^{-1}) and medium bands of ionized COO^{-}groups (~1630 cm^{-1}), in contrast to FA, the bands of COOH groups of HA are weaker.

The major similarities of FTIR spectra of HA and FA are that: (1) The whole profile of both spectra are similar. (2) Both show very pronounced OH stretching centered at 3420 cm^{-1}. (3) Both show carboxylic groups absorption bands.

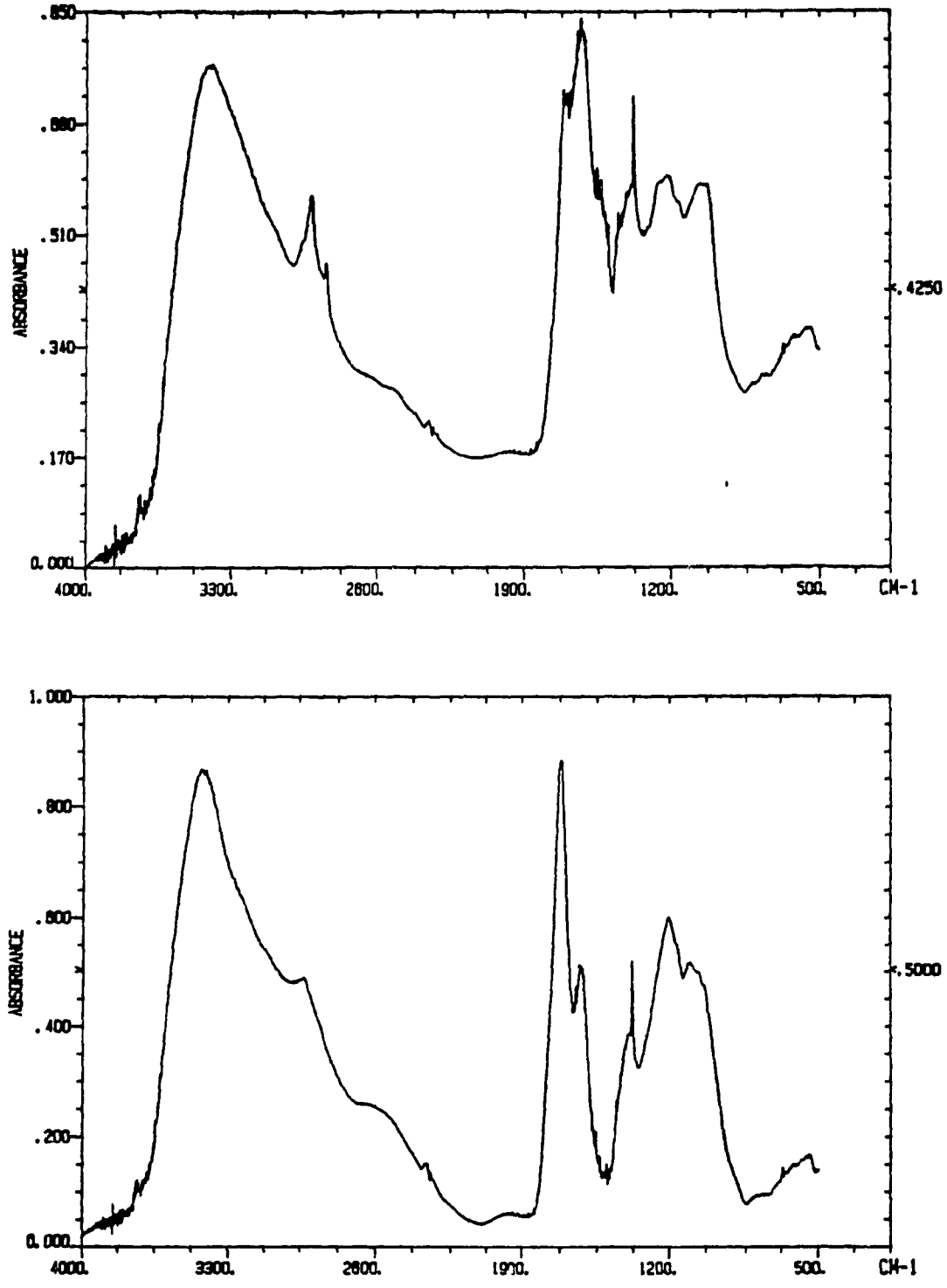

FIG. 4.18 COMPARISON OF FTIR SPECTRA OF HA AND FA

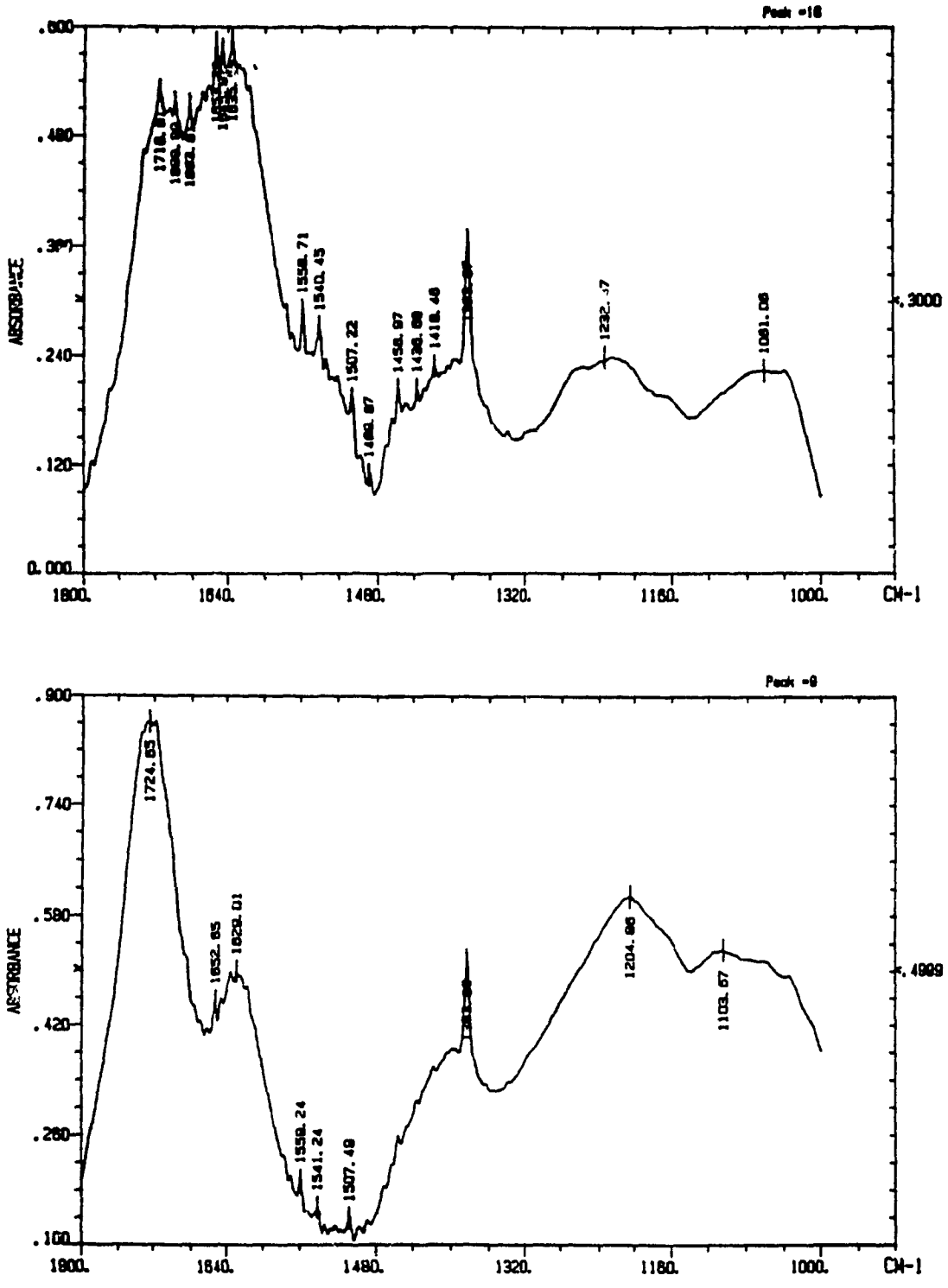

FIG. 4.19 COMPARISON OF FTIR SPECTRA OF HA AND FA IN 1800 -- 1000 cm^{-1} REGION

The detailed comparison of FTIR spectra of FA and HA is shown in Table 4.13.

The greater number of complex bands and peaks of FTIR spectrum of HA indicate more complex structures. This is expected because the molecule is much larger and the molecular weight is much higher for HA.

It has been long understood that the humic substances of soil are the results of decomposition of plant, animal, microbe and other organic residues. So it is reasonable that the macromolecular humic acid exhibit strong amide bands of protein, polypeptides and other secondary trans-amides, which is in good agreement with the element analysis result that HA contain about 2.3% of nitrogen.

It is not surprising that HA contain fewer carboxyl groups per unit weight because the functional groups analysis has indicated that the content of carboxylic groups of HA is much smaller than that of FA. FTIR results are also qualitatively in agreement with the results of functional group analysis.

Table 4.12 Observed FTIR Bands of Laurentian HA and HA-Cu

No	Assignment	HA	HA-Cu
1	OH and NH stretching	3402 cm^{-1}	3402 cm^{-1}
2	hydrocarbon bands		
	aliphatic CH stretching (symmetric and asymmetric stret. of CH_3 and CH_2)	2923 cm^{-1} (very sharp) 2854 cm^{-1}	2923 and 2854 cm^{-1} (sharp)
	aliphatic CH_2 and CH_3 bending	1472-1418 cm^{-1} (many weak peaks)	1472-1418 cm^{-1}
	aromatic CH stretching	~3000 cm^{-1} (weak shoulder)	
3	H-bonded OH stret. of COOH	~2580 cm^{-1}	very weak at ~2580 cm^{-1}
4	carboxylic bands		
	C=O stretching of COOH	1716 cm^{-1}	strong reduction
	C-O stret. and OH deformation of COOH	1230 cm^{-1} region	in absorption at 1716 and 1230 cm^{-1} region
	COO^- symmetric stretching (and C=O of H-bonded conjugated ketone and quinone)	1635 cm^{-1}	1635 cm^{-1}
	COO^- asymmetric stretching (and OH deformation and C-O stret. of phenolic CH)	1384 cm^{-1}	1384 cm^{-1}
5	protein and amide bands		
	amide I (C=O stretching) (and stret. of aromatic C=C)	1700-1630 cm^{-1} (centered at 1645 cm^{-1})	1700-1630 cm^{-1}
	amide II (NH bending, CN stret.) (and aromatic ring stret.)	1560-1490 cm^{-1}	1560-1490 cm^{-1}
	amide III (CN stretching and NH bending)	1230 cm^{-1} band	1230 cm^{-1} band
6	C-OH bending, C-O stretching of alcohols and ethers	1063 cm^{-1} band	1063 cm^{-1} band

Table 4.13 Comparison of FTIR Spectra of FA and HA

Assignment	FA (cm^{-1})	HA (cm^{-1})
OH and NH (trace) stretching	3420	3402
Hydrocarbon bands:		
aliphatic C-H stretching	2940 region (not strong)	2920 and 2854 (sharp peaks)
aliphatic CH_2 and $C-CH_3$ bending	1472, 1464, 1456, 1435, 1417 (weak)	(stronger than peaks of FA)
H-bonded OH stret. of COOH	2600 region	2580 region
NH_4^+ combination band	~2000	/
Carboxylic bands:		
C=O stretching of COOH	1724 (sharp and strong)	1716, 1700
C-O stret. and OH deformation of COOH	1205 region	1230 region
COO^- symmetric stretching (and stret. of aromayic C=C)	1629 region	1635 region
COO^- asymmetric stretching (and OH deformation and C-O stret. of phenolic OH)	1384 region	1384 region
Amide bands:		
C=O stret. of amide, and of H-binded conjugated ketone and quinone	(not significant)	1700-1630 (1700, 1684, 1667, 1660, 1653, 1636)
N-H bending, C-N stretching and aromatic ring stret.	1560-1490 (not significant)	1560-1490 (1560, 1541, 1532, 1522, 1507, 1497)
C-OH bending, C-O stretching of alcohols and ethers	1110 rergion	1063 region

(3) Comparison of FTIR spectra of HA, and Cu-HA

Fig.4.20 shows the FTIR spectrum of the interaction product of Cu(II) with HA in the region of 4000-500 cm^{-1}. Conversion of COOH by the formation of Cu-HA complex led to the reduction in absorption intensity at 1716 cm^{-1} and in the broad band around 1230 cm^{-1} region which are due to the COOH groups vibrations. Another significant band intensity reduction occurs at 3402 cm^{-1} region. This region is characteristic absorption of OH stretching. Clearly, the formation of Cu-HA complex leads to the deprotonation of COOH and phenolic OH groups, subsequently, less OH stretching. The detailed comparison is also presented in Table 4.12.

4.4 DISCUSSION

4.4.1 Binding Capacity and Molecular Structure of HA

Fig. 4.21 shows the plots of the binding capacity of AT vs. pH values for both HA and FA, using the same unit, μM AT/g.

One important conclusion immediately extracted from the interesting comparison of values in Table 4.4 and the curves in Fig.4.21 is that the binding capacity is not directly proportional to the content of carboxyl groups. What must be done next is how to explain such phenomena.

The study brings out four facts which are important to the binding of AT to HA and FA.

(1) The pH-dependence of AT binding suggests that the hydrogen-bonding mechanism is appropriate for both AT-HA and AT-FA interactions.

(2) The binding takes place through the formation of hydrogen-bonding between the electron-donor (nitrogen atoms in

FIG. 4.20 FTIR SPECTRUM OF PRODUCT OF Cu WITH HA

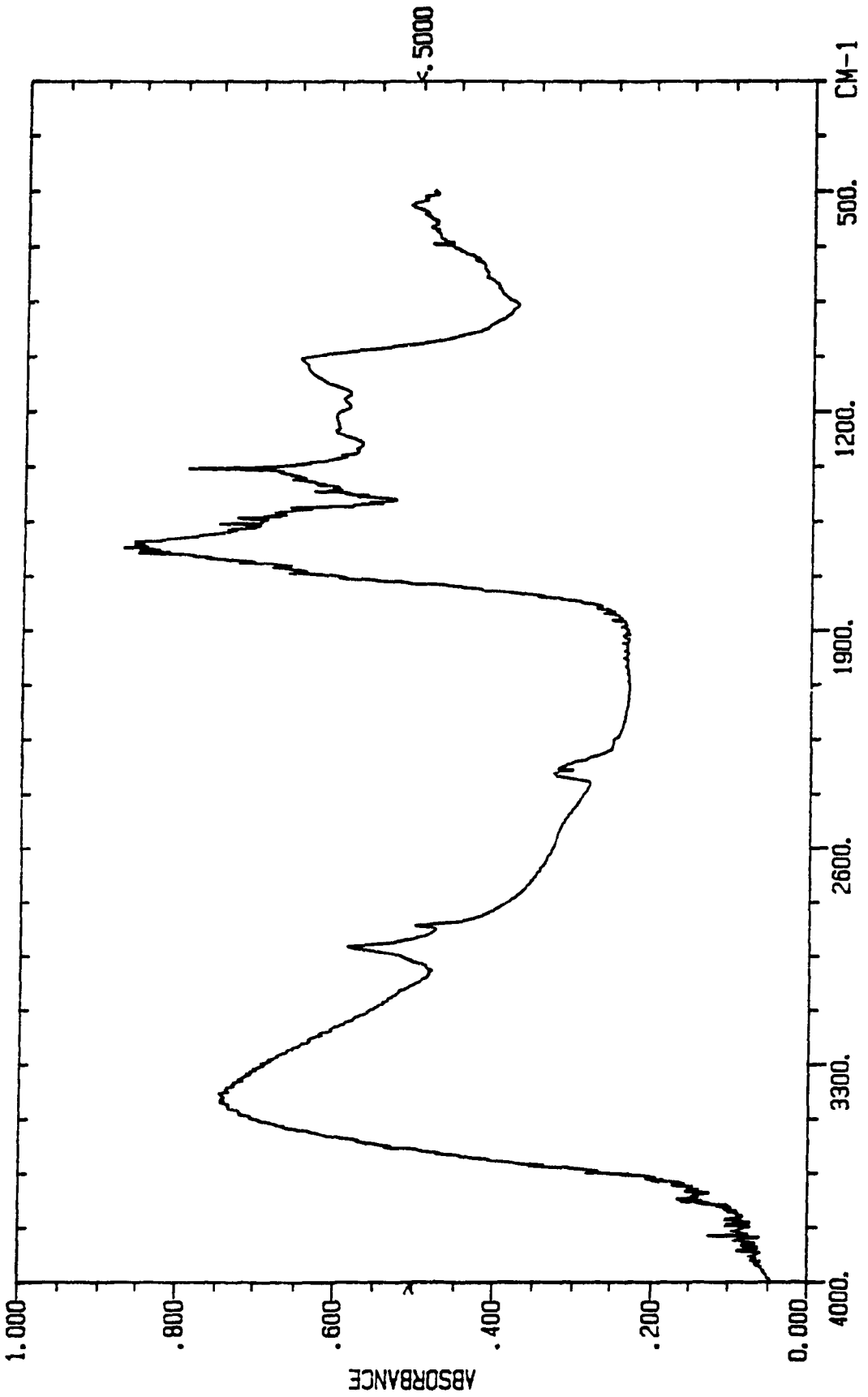

FIG. 4.21 COMPARISON OF BINDING CAPACITYOF AT BY HA OR FA

(KCl=0)

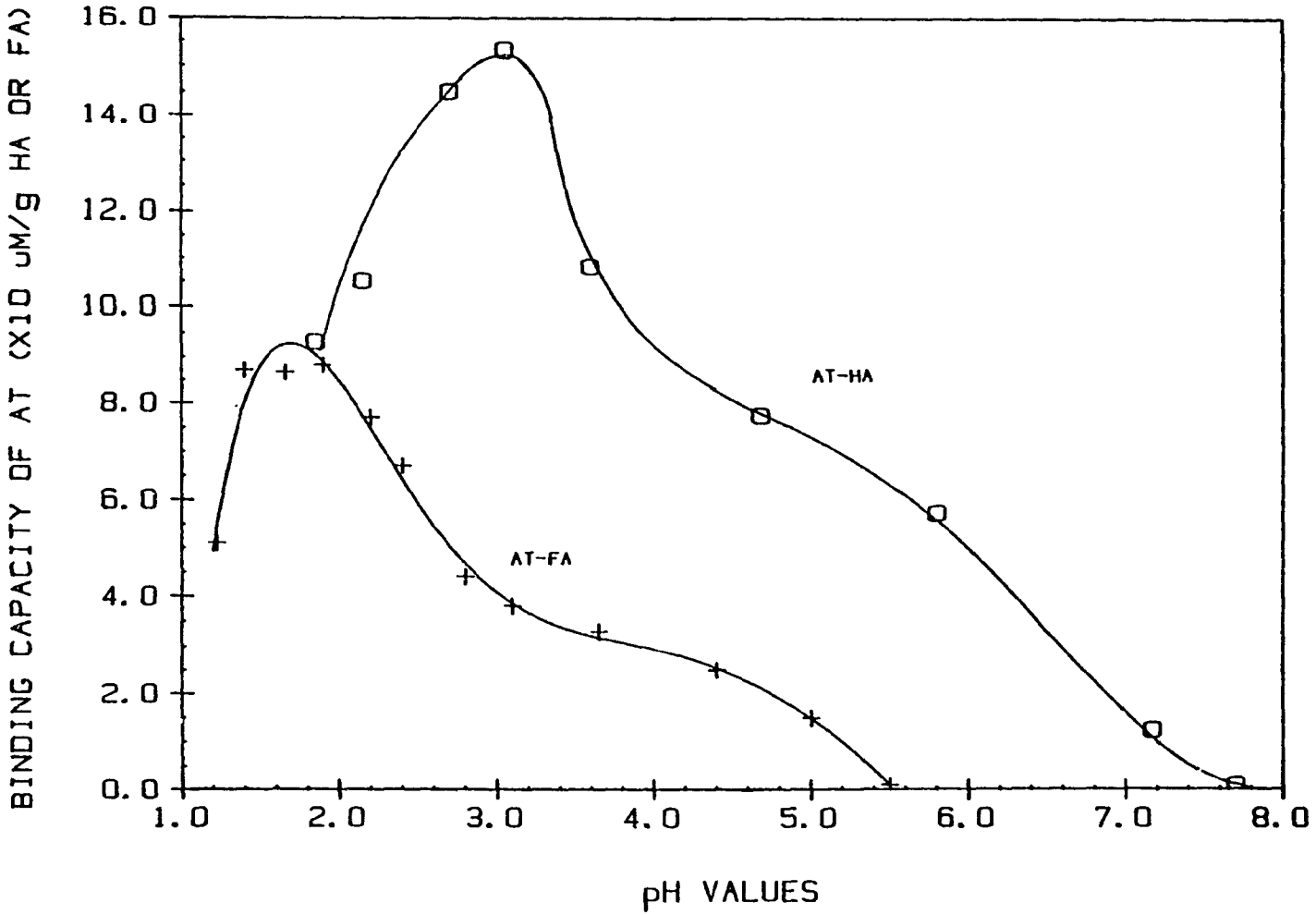

atrazine) and electron-acceptor (protonated carboxyl groups in HA). However, each carboxyl group has its own chemical environment different from others, especially if carboxyl groups are compared with those in FA.

(3) The binding sites of both HA and FA only account for less than 1% of total carboxyl groups. These sites are very specific sites for AT binding.

(4) Binding is preferentially associated with the large fraction of the sample, as has been demonstrated in Chapter 2. The molecular size of HA is definitely much larger than of FA.

According to equation (4), the very concentrated HA in gel solution greatly favors the sorption reaction in the direction to complex formation. The fact (4) suggests the much larger HA molecules could supply much more specific sites suitable for AT sorption than FA molecules do, even though the carboxyl groups contents per gram HA is lower than per gram FA.

Another reasonable interpretation is that not only carboxyl groups, but amide groups can act as electron-acceptor to react with AT forming complex. As the conclusion, HA is shown to be more effective in sorption of atrazine than FA.

4.4.2 FTIR Study

The resolution-enhanced FTIR technique demonstrated that it is a powerful tool for the investigation of the composition and structural characteristics identification of humic substances. The FTIR measurement results have supplied much more detailed information than has been done before. The most prominent spectral features indicates the presence of a considerable amount

of protein decomposition products in the form of amides, in addition to carboxyl groups. The presence of more and longer aliphatic chains is evident. The fact that the aromatics are highly substituted is also evident. The fine and complex structure of bands in the 100 - 1000 cm^{-1} region reveals the structural complexity of HA complex.

4.4.3 New Approach to Determine The Total Bidentate Sites of HA and FA

The study of copper ions on AT binding creates a new approach to determine the total bidentate sites of HA and FA. Table 4.14 shows the number of carboxyl groups and phenolic groups of HA and FA determined by acid-base titration method and by Cu titration method.

It can be seen clearly from Table 4.14 that the results of bidentate complexing capacity by Cu titration method is very similar to the values obtained by the acid-base titration method. There are two different cases. For FA, the number of carboxyl groups is larger than the number of phenolic groups, and Cu ions can form bidentate complexes with FA using salicylic and dicarboxylic groups. In this way the bidentate capacity of 5.7 mmol Cu/g FA was obtained. For HA, however, the number of carboxyl groups is smaller than that of phenolic groups. The most likely chelate to be formed is the salicylic one when all binding sites are saturated by excess of copper ions. A bidentate complexing capacity of 2.5 mmol/g HA found might reflect this assumption.

Table 4.14 Determination of Carboxylic and Phenolic Functional Groups in Humic Acid and Fulvic Acid

	FA (mmol/g)	HA (mmol/g)
Carboxyl group	Type A: 5.11 Type B: 3.49	2.50
Total acidity	11.63	7.60
Phenolic groups	3.03	5.11
Bidentate complexing capacity	5.8	2.5
Bidentate complexing capacity by Cu titration	5.7	2.5

CHAPTER 5

INTERACTION OF ATRAZINE WITH LAURENTIAN SOIL

5.1 BRIEF REVIEW OF SOIL CHARACTERISTICS

The fate of pesticides and their behaviour in soil is influenced by several factors including adsorption, movement and decomposition. Adsorption directly or indirectly influences the magnitude of the effect of other factors. It is generally considered that three major factors determine the extent to which pesticides are adsorbed by soil including (1) physical-chemical characteristics of the adsorbents, (2) nature of the pesticides, and (3) properties of the soil system, such as clay mineral composition, particle size distribution, pH, types and amounts of exchangeable cations, moisture and temperature [4].

The main constituents representing the solid phase in soil are clay minerals, organic matter, and hydrous oxides of aluminum, iron and silicon. The clay and organic matter are believed to be the two major components of significance to adsorption [29].

5.1.1 Clay

The clay includes crystalline minerals (size < 2μ), and crystalline, and amorphous oxides and hydroxides. Some important features of clay most commonly found in soil are the following. (1) The 1:1 type clay (Fig 5.1a), the kaolinite group is an example of a 1:1 structure as it is made up of one sheet of tetrahedrally coordinated cations with one sheet of octahedrally coordinated cations. In general, the 1:1 type layer silicates are electrically neutral or possess a very low negative charge. The

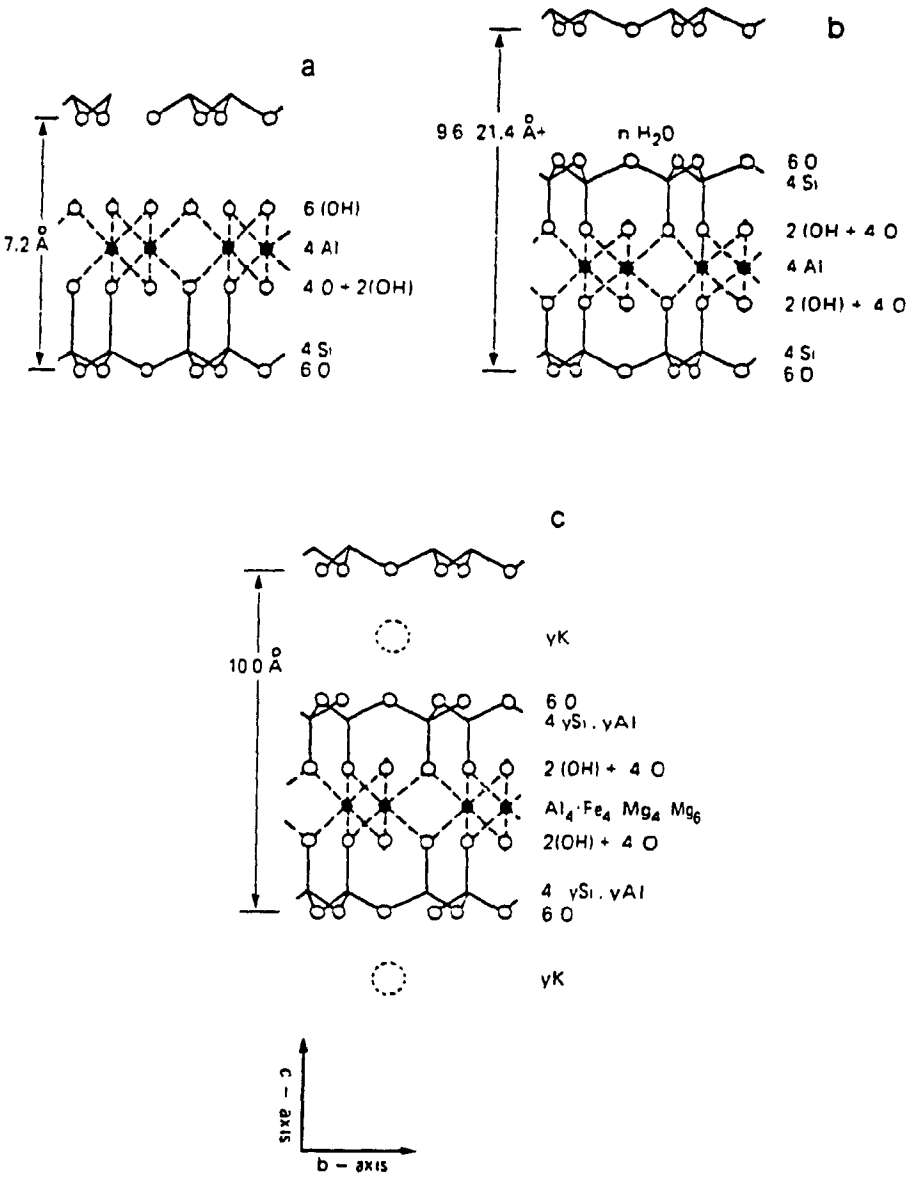

Fig. 5.1 Schematic diagram of the crystal structure of (a) kaolinite, (b) montmorillonite and (c) illite

surface area and the cation exchange capacity of the kaolinite minerals have relatively low value. (2) The 2:1 type clay. The 2:1 clay minerals, such as monmorillomite and vermiculite are made up by combination of two tetrahedrally coordinated sheets of cations, one on either side of an octahedrally coordinated sheets (Fig 5.1b). In the illite, K^+ ions usually balance the charge on the 2:1 layers. The 2:1 type minerals have a high cation exchange capacity and high surface area. (3) Hydrous oxides. Almost all soils contain at least a small proportion of colloidal hydrous oxides of Al, Fe and Mg.

5.1.2 Organic Matter

Soil organic matter always plays an important role in adsorption of pesticides to soil. It contains compounds that may conveniently be grouped into nonhumic and humic substances. A thorough discussion has been given in the introduction and earlier chapters.

Comparative studies between known clay minerals and organic adsorbants suggested that the adsorption capacity of clay for some herbicides followed the order of montmorillonite > illite > kaolinite; and that most pesticides have greater affinity for organic surfaces than for mineral surfaces [126-128].

The cooperative effects of organic matter and clay are often implicated in pesticides adsorption, since in most soils, organic matter is intimately bound to the clay to give a clay-metal-organic complex. Accordingly, clay and organic matter function more as a unit than as separate entities and the relative contribution of organic and inorganic surfaces to adsorption will

depend upon the extent to which the clay is coated with organic substances.

The thorough investigation of atrazine interaction with Laurentian soil becomes possible because the following necessary conditions have been met:

(1) The Laurentian soil together with its FA and HA components are all available and well characterized.

(2) The stoichiometric interaction between AT and homogeneous FA, and AT and heterogeneous HA has been thoroughly studied.

(3) Factors which are important to the binding of AT and ATOH to fulvic acid and humic acid as well to the hydrolysis of AT by fulvic acid and humic acid have been determined.

(4) A model of the special unionized carboxyl sites which bind AT or ATOH through hydrogen-bond has been proposed.

(5) UF-HPLC method has been demonstrated to be sufficiently powerful for the study of binding processes in some detail.

5.2 EXPERIMENTAL

5.2.1 Materials

All materials except Laurentian Soil used in chapter 5 are exactly same as described in chapter 2.

The Laurentian Soil sample was collected from Laurentian Forest Preserve of Laval University, generously supplied by Dr. Visser. The detailed properties and analysis data of Laurentian Soil are presented in Table 5.1, which are taken from "Compilation of Data for CSSC (Canada Soil Survey Committee) Soil Samples"[100].

Table 5.1 Compilation of Data for CSSC Reference Soil Sample

---- Laurentian Soil

1	Particle-size	total sand (2–0.05 mm) 50-69%	total silt (50--2 μm) 18-33%	total clay (2–0 μm) 6-25%
2	pH	3.8-4.3 (4.1) in H_2O (1:1) 3.4-3.8 (3.5) in 0.01M $CaCl_2$		
3	Organic carbon	0.3-13.2% (12%)		
4	Nitrogen	0.28-0.9% (0.54%)		
5	Exchangeable cations and CEC (me/100g)	Ca: 0.0-4.1 (0.3) Al: 1.0-10.7 (6) K: 0.03-0.21 (0.13)	Mg: 0.04-0.2 (0.1) Na: 0.0-0.1 (0.03)	
	Cation Exchange Cpacity (CEC, me/100g)	44.2-75.8 (72)		
6	Dithionite-extractable Fe and Al (%)	Fe: 3.1-4.3 (3.3)	Al: 1.4-2.0 (1.5)	
7	Oxalate-extractable Fe and Al (%)	Fe: 2.4-3.4 (2.7)	Al: 1.34-2.13(1.5)	
8	Pyrophosphate extractable Fe, Al(%)	Fe: 2.2-3.4 (2.6)	Al: 0.56-2.0 (1.6)	
9	Total elemental analysis	(%): Al 6.6, Fe 6.1, Ti 1.8, Ca 1.5 Mg 0.42, K 1.8, Na 0.65 ppm: Mn 518±28, Zn 89±3.9, Cu 7±2.2 Pb 26±2.4, Co 18±2.2, Ni 4±1.0 Cr 16±1.4 Sr 300±32 ppb: Hg 166 Se 710		
10	EDTA extractable elements (ppm)	Al 640, Fe 2120, Mg 68, K 19, Mn 1.3 Zn 2.2, Cu 0.4, Co<0.2, Ni 0.3, Sr 0.2		
11	Hygroscopic water in air dry sample	8.1%		

* The data indicated in parenthesis are tentative best values.

5.2.2 Apparatus

All apparatus used in this chapter are same as described in chapter 2.

5.2.3 Procedure

Aliquots of AT ($1.00x10^{-4}$M) stock solutions were added to exact 500.00 mg soil, and varying volume of deionized water was added to each of samples to about 20 ml. The pH of the resulting suspension was adjusted to the desired values by the addition of dilute HCl or NaOH then each sample was diluted to a final volume of 25.00 ml (preliminary tests should be done to determine the exact amount of HCl or NaOH needed for a particular pH because of the great buffer capacity and slow equilibration of soil solution). The solutions are sealed securely with parafilm. Controls were prepared in the same way but without soil. A series of paired controls and AT-soil samples were put into a box and shaken together for 3 days at room temperature ($21\pm2^{o}C$). After the equilibration period, the pH of suspensions was measured. This was followed by ultrafiltration on a YM-2 1000 MW cut-off membrane by pouring the supernatant solution to ultrafiltration cell, leaving the undissolved soil residue in flasks. The first 10 drops of filtrate were discarded then an aliquot of about 1.0 ml was collected for analysis of free AT and ATOH hydrolyzed from AT during 3 days.

The conditions of the HPLC for determination of AT and ATOH are exactly same as used for AT-FA samples.

5.2.4 Experimental Design

The experiments designed in this chapter are the following:

(1) AT variation at constant pH and low ionic strength. At each pH, AT concentration varied from $0.80x10^{-5}$M to $8.00x10^{-5}$M and soil weight was kept constant, 0.5000g/25.00ml. The tested pH ranged from 2.0 to 10.0 including pH2.50, 3.00, 3.45, 3.90, 4.45, 5.00, 5.55, 6.00, 7.15, 7.85, 8.75 and 9.45. The binding capacity values of AT obtained at each pH were plotted against pH so as to see the pH effect on AT sorption.

(2) AT variation at constant pH and in the presence of 0.1M KCl. This series of experiments was the same as (1) except for the addition of KCl to the solutions. The aim was to see the effect of electrolyte on AT sorption by soil.

(3) Variation of soil weight at constant pH (pH 5.00) and constant AT ($4.00x10^{-5}$M) in the absence of KCl.

(4) pH variation at constant AT ($3.85x10^{-5}$M) and soil weight.

(5) Competition between AT and ATOH for sorption sites

(6) AT sorption in the presence of $1.00x10^{-3}$ M copper ions at different pH values.

(7) AT binding studies on AT-(FA+Soil), AT-(FA+HA) and AT-(HA+Soil) at varying pH values. The AT concentration used was $6.00x10^{-5}$M. The FA concentration used was 1.000g/L, and the HA and soil weight used were 10.00mg and 0.5000g per 25.00 ml, respectively.

In consideration of the complexity and unevenness of soil samples, duplicate experiments were run, and all experimental data were the average of duplicate results

5.3 RESULTS

5.3.1 AT Variation at Constant pH and Low Ionic Strength -- pH Effect

The conclusion drawn from over 500 data points is that: (1) Binding can be observed in the whole range of pH tested (pH 2-10). Compared to AT-FA (no binding occurs above pH 5.5) and AT-HA (no binding occurs above pH7.70) cases, this feature is quite prominent. (2) No ATOH is detected within 3 days at any pH higher than 3.90. (3) Clear evidence of a role for protonated carboxyl groups of some organic components in soil is seen. That is, the measurable amount of ATOH hydrolyzed from AT in AT-soil samples is always larger than in the corresponding AT controls having the same pH values. Representative binding curves for AT-soil at pH 2.50 is shown in Fig 5.2.

Same as in AT-FA and AT-HA case, the AT in controls could be fitted to a straight line whereas the AT in soil solutions could be fitted to two separated lines.

Using the data calculated from the linear regression curves established for soil-free controls in conjunction with signals obtained in AT-soil suspension, the bound AT, and the ATOH hydrolyzed from AT by carboxyl groups of soil organic matter could be evaluated. Table 5.2 and 5.3 present the data necessary for plotting of bound AT vs. the total AT added at pH 2.50 and pH 5.00.

FIG. 5.2 AT BINDING CURVES BY LAURENTIAN SOIL

(SOIL=0.5000 g/25.00 ml, pH=2.50)

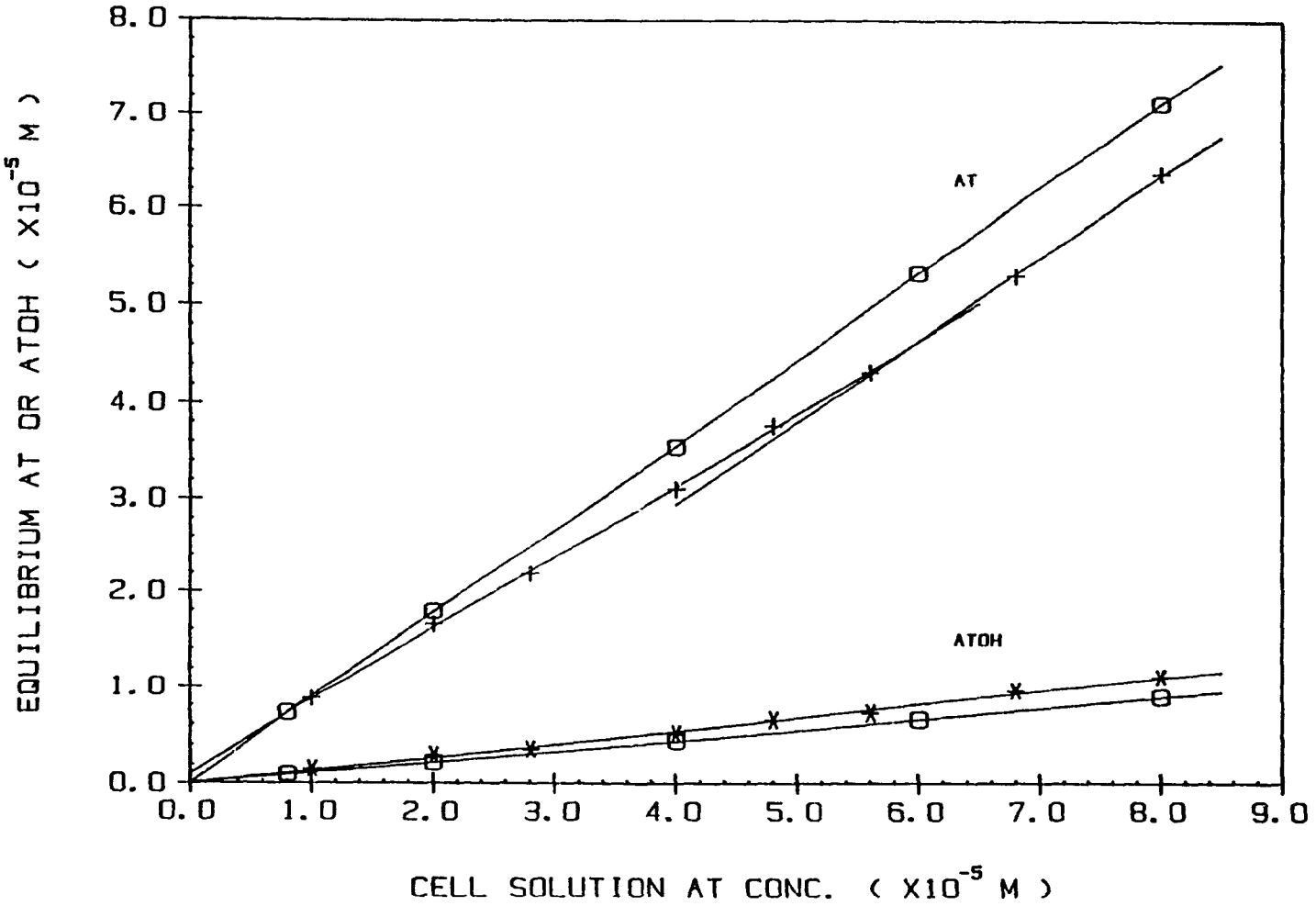

Table 5.2 Determination of Bound AT and Hydrolyzed ATOH by Soil

(pH=2.50, soil=0.5000g/25.00ml, stock AT=1.00x10^{-4}M)

Added AT (ml)	in cont. (x10^{-5}M)		in AT-Soil (x10^{-5}M)		Bound AT (x10^{-5}mol/20g soil)	Hydrolyzed ATOH (x10^{-5}mol/20g soil)
	AT	ATOH	AT	ATOH		
2.50	0.891	0.118	0.865	0.158	0.026	0.040
5.00	1.779	0.228	1.650	0.301	0.129	0.073
7.00	2.490	0.316	2.191	0.366	0.299	0.050
10.00	3.555	0.448	3.111	0.526	0.444	0.078
12.00	4.266	0.535	3.765	0.660	0.501	0.125
14.00	4.977	0.623	4.328	0.733	0.649	0.110
17.00	6.043	0.755	5.302	0.956	0.741	0.201
20.00	7.109	0.887	6.362	1.106	0.747	0.219

Table 5.3 Determination of Bound AT by Soil

(pH=5.00, soil=0.5000g/25.00ml, stock AT=1.00x10^{-4}M)

Added AT (ml)	Free AT in cont. (x10^{-5}M/L)	Free AT in AT-soil (x10^{-5}M/L)	Bound AT (μmol/20g soil)
2.50	1.007	0.957	0.50
5.00	2.006	1.847	1.59
7.00	2.805	2.621	1.84
10.00	4.003	3.650	3.53
12.00	4.801	4.368	4.33
14.00	5.599	5.116	4.83
17.00	6.797	6.289	5.08
20.00	7.995	7.512	4.83

Fig 5.3 shows plots of AT bound against AT total at various pH values including the plots at pH 2.50 and 5.00. From Fig 5.3 it can be seen that a limit can be reached for most of pH values tested. Therefore, an empirical binding capacity could be defined at each pH. A very significant feature in Fig 5.3 is that the concentration at which AT bound reachs saturation becomes smaller and smaller with the pH increases. For example, at pH 2.50, bound AT reaches to binding limit at about 6.8×10^{-5} M, and at pH 8.75 bound AT reaches to the limit at only 4.00×10^{-5} M.

Fig.5.4 shows plots of ATOH, hydrolysis product of AT, vs. total added AT at pH 2.50 and pH 3.00. It is evident in Fig.5.4 that the lower the pH, more AT was hydrolyzed to ATOH.

The plot of binding capacity of AT vs. pH for the data in Fig.5.3 is shown in Fig.5.5. One can immediately see that the shape of the curve is significantly different from that of AT-FA and AT-HA: (1) There is not a significant maximum of binding capacity vs. pH. (2) The binding of AT occurs in the whole range of pH studied (pH 2 - pH 10). However, for AT-FA, no binding is observed at pH 5.5 and higher; and for AT-HA, no AT binding is observed at pH7.7 and higher. (3) The binding capacity decreases with the increase of pH, but the changing of the binding capacity with pH is slow.

5.3.2 Electrolyte Effect

The experiments were conducted in the same way as in section 5.3.1. The tested pH in this section included pH 2.05, 2.70, 3.40, 4.60, 5.60, 6.40, 7.25, 7.70 and 8.20. AT variation is from 0.80×10^{-5}M to 8.00×10^{-5}M at each pH. The plots of equilibrated AT

FIG. 5.3 BOUND AT VS. TOTAL AT ADDED

(SOIL=0.5000 g/25.00 ml. KCl=0)

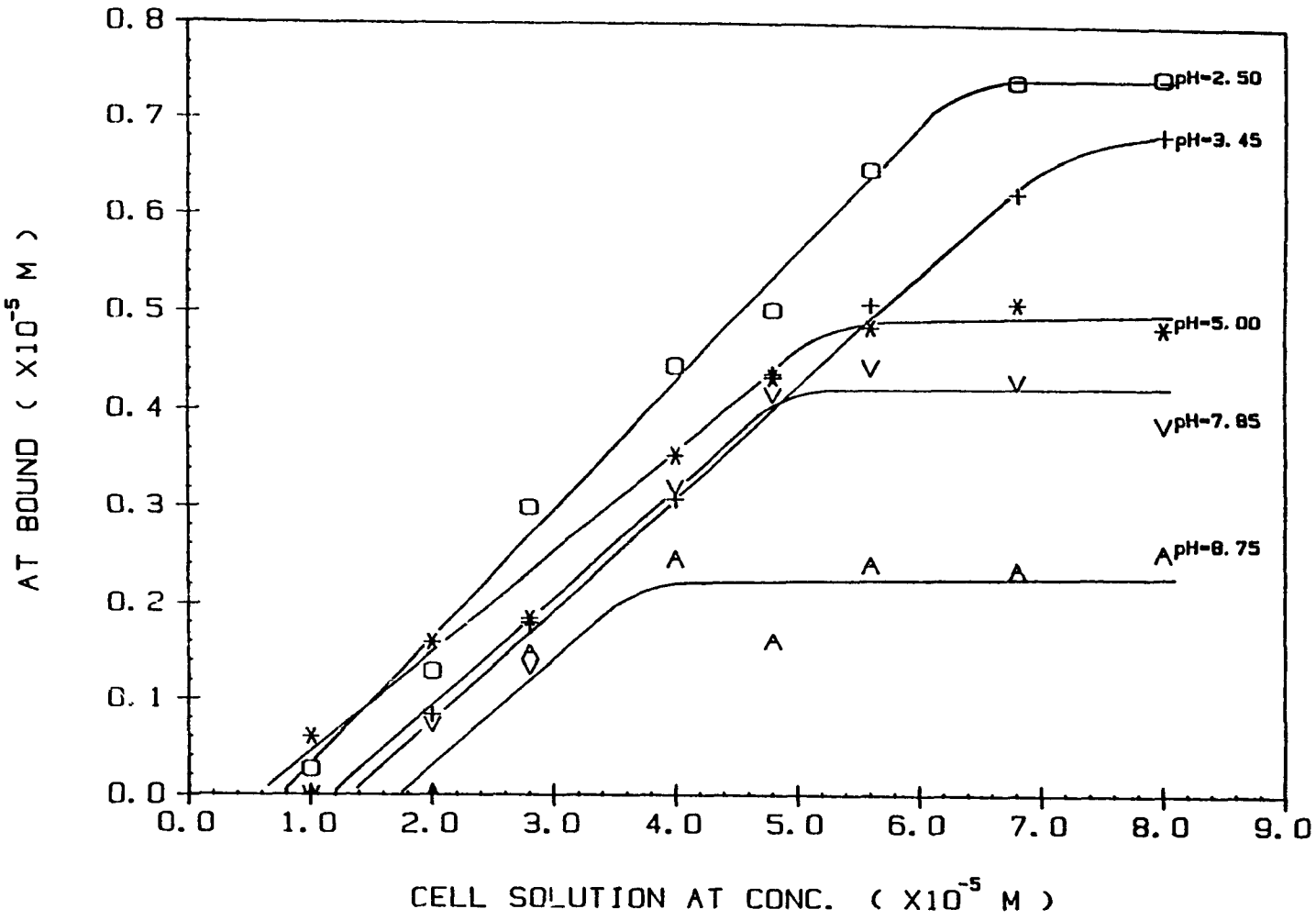

FIG. 5.4 HYDROLYZED ATOH BY SOIL VS. TOTAL AT ADDED

(SOIL=0.5000 g/25.00 ml, KCl=0)

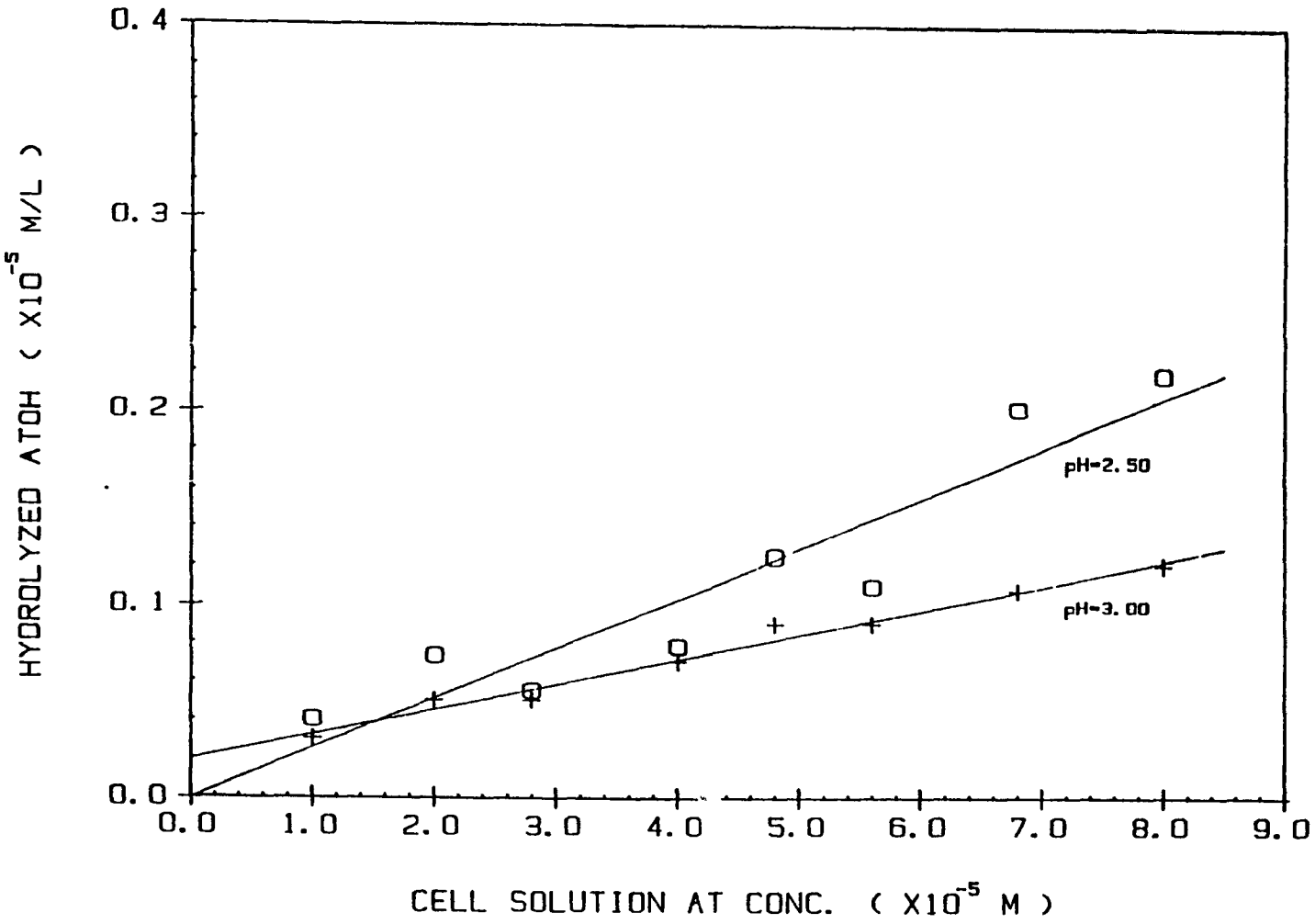

FIG. 5.5 BINDING CAPACITY OF AT BY SOIL VS. pH

(SOIL=0.5000 g/25.00 ml, KCl=0)

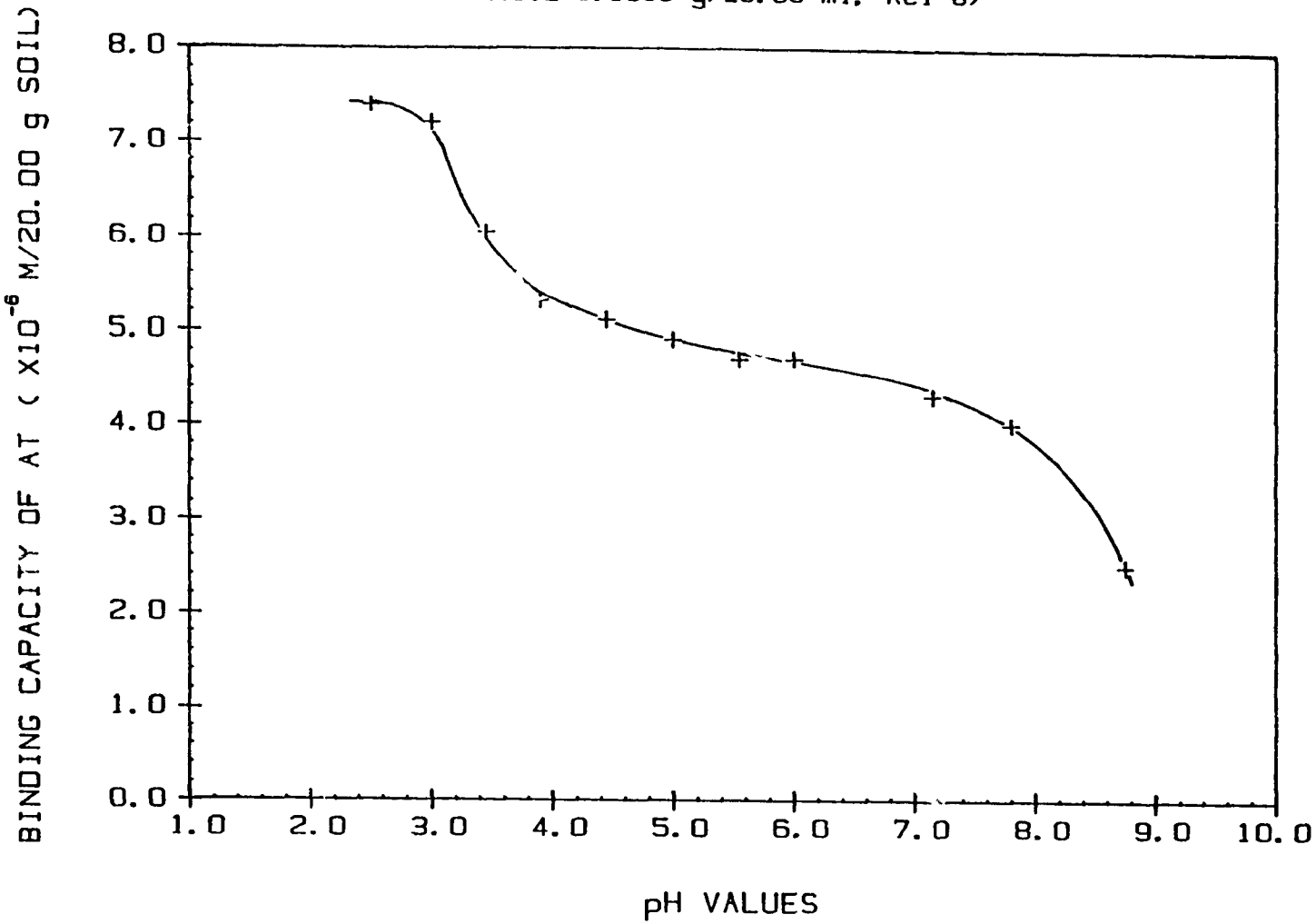

and ATOH versus the total AT added are similar to that in the absence of KCl: (1) For those solutions which pH were lower than 3.5, ATOH were formed from hydrolysis of AT by proton and carboxyl groups. (2) The amount of ATOH in AT-soil sample was constantly higher than that of the corresponding AT control having same pH. (3) No AT hydrolysis was observed during 3 days for those solutions which pH were higher than 3.5. (4) Bound AT was a function of total AT added before the equivalent point.

Table 5.4 presents the bound AT and ATOH at pH 2.05.

Table 5.4 Determination of Bound AT and Hydrolyzed ATOH by Soil (pH=2.05, soil=0.5000g/25.00ml, KCl=0.1M, stock AT=1.00×10^{-4}M)

Added AT (ml)	in cont. ($\times10^{-5}$M)		in AT-Soil ($\times10^{-5}$M)		Bound AT	Hydrolyzed ATOH
	AT	ATOH	AT	ATOH	(μmol/20g soil)	
2.50	0.900	0.109	0.876	0.117	0.24	0.08
5.00	1.801	0.203	1.668	0.211	1.32	0.08
7.00	2.521	0.278	2.313	0.285	2.10	0.08
10.00	3.602	0.392	3.198	0.410	4.04	0.18
12.00	4.322	0.467	3.877	0.494	4.45	0.27
14.00	5.043	0.542	4.552	0.571	4.91	0.40
17.00	6.123	0.654	5.535	0.787	5.88	1.34
20.00	7.204	0.767	6.560	0.889	6.44	1.22

Fig.5.6 shows the plots of AT bound vs. AT total at pH2.05, 3.40, 5.60 and 7.70 in the presence of 0.1M KCl.

From Fig.5.6, the binding capacity of AT in the presence of 0.1M KCl can be defined at each pH, which is presented in Table 5.5. (the plot is shown in Fig.5.5, too) For comparison, the

FIG. 5.6 BOUND AT VS. TOTAL AT ADDED

(SOIL=0.5000 g/25.00 ml, KCl=0.1M)

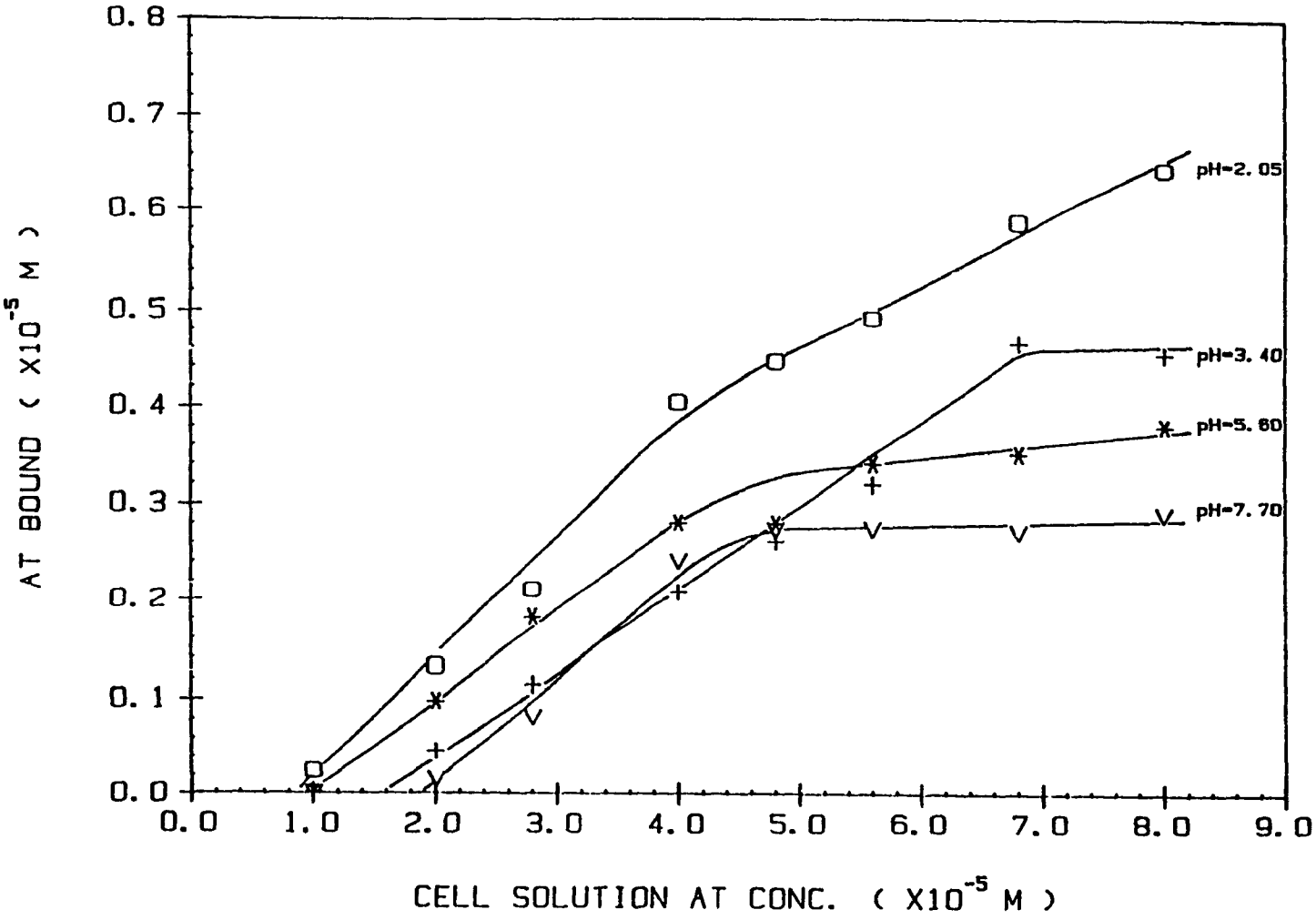

corresponding binding capacity for solutions without KCl is also shown in Table 5.5.

Table 5.5 Binding Capacity of AT at Various pH in The Absence and Presence of 0.1M KCl

pH	Binding capacity(no KCl) (μmol AT/20.00g soil)	pH	Binding capacity(0.1M KCl) (μmol AT/20.00g soil)
2.50	7.4	2.05	6.1
3.00	7.2	2.70	6.1
3.45	6.1	3.40	4.6
3.90	5.3	4.60	3.7
4.45	5.1	5.60	3.6
5.00	4.9	6.40	3.4
5.55	4.7	7.25	3.5
6.00	4.7	7.70	2.8
7.15	4.3	8.20	2.4
7.80	4.0		
8.75	2.5		

Two pronounced features seen from Fig.5.5 are that (1) the trend of the curve with an ionic strength of 0.1M KCl is approximately the same as the corresponding one but without KCl. (2) unlike AT-FA and AT-HA case, the effect of electrolyte on AT binding by soil is not so great--only approximately 1 μmol bound AT reduction at almost all pH values tested is observed.

5.3.3 Effect of Soil Weight on AT Binding

The effect of soil weight on AT binding was investigated quantitatively at pH 5.00 in low ionic strength. Soil weights were

varied from 0.1000g to 1.0000g per 25.00 ml. The equilibrium AT concentration and the amount of AT bound are presented in Table 5.6. The bound AT is expressed by μM/L and μM/g soil in order to compare the effect of soil weight on AT binding.

Table 5.6 Determination of Equilibrium and Bound AT at Various Quantities of Soil Examined

(initial AT=4.00x10^{-5}M, pH=5.00, total volume=25.00 ml)

soil weight (mg)	equilibrium AT (x10^{-5}M/L)	bound AT (μmol/L)	bound AT (μmol/g soil)
100	3.96	0.35	0.088
200	3.93	0.70	0.088
300	3.87	1.3	0.108
400	3.84	1.6	0.100
500	3.82	1.8	0.090
600	3.79	2.1	0.088
750	3.74	2.6	0.087
1000	3.64	3.6	0.090
average			0.092±0.008

The plotting of bound AT (μM/L) vs. soil weight is shown in Fig.5.7. The straight line of bound AT vs. soil weight clearly indicates that the bound AT is directly proportional to soil weight in a quite wide range of soil weight.

5.3.4 Competition between AT and ATOH

Competition experiments between AT and ATOH on soil (in which the ratio of added AT to Added ATOH was kept constant 2:1) were

FIG. 5.7 EFFECT OF SOIL WEIGHT ON AT BINDING

(pH=5.00, KCl=0)

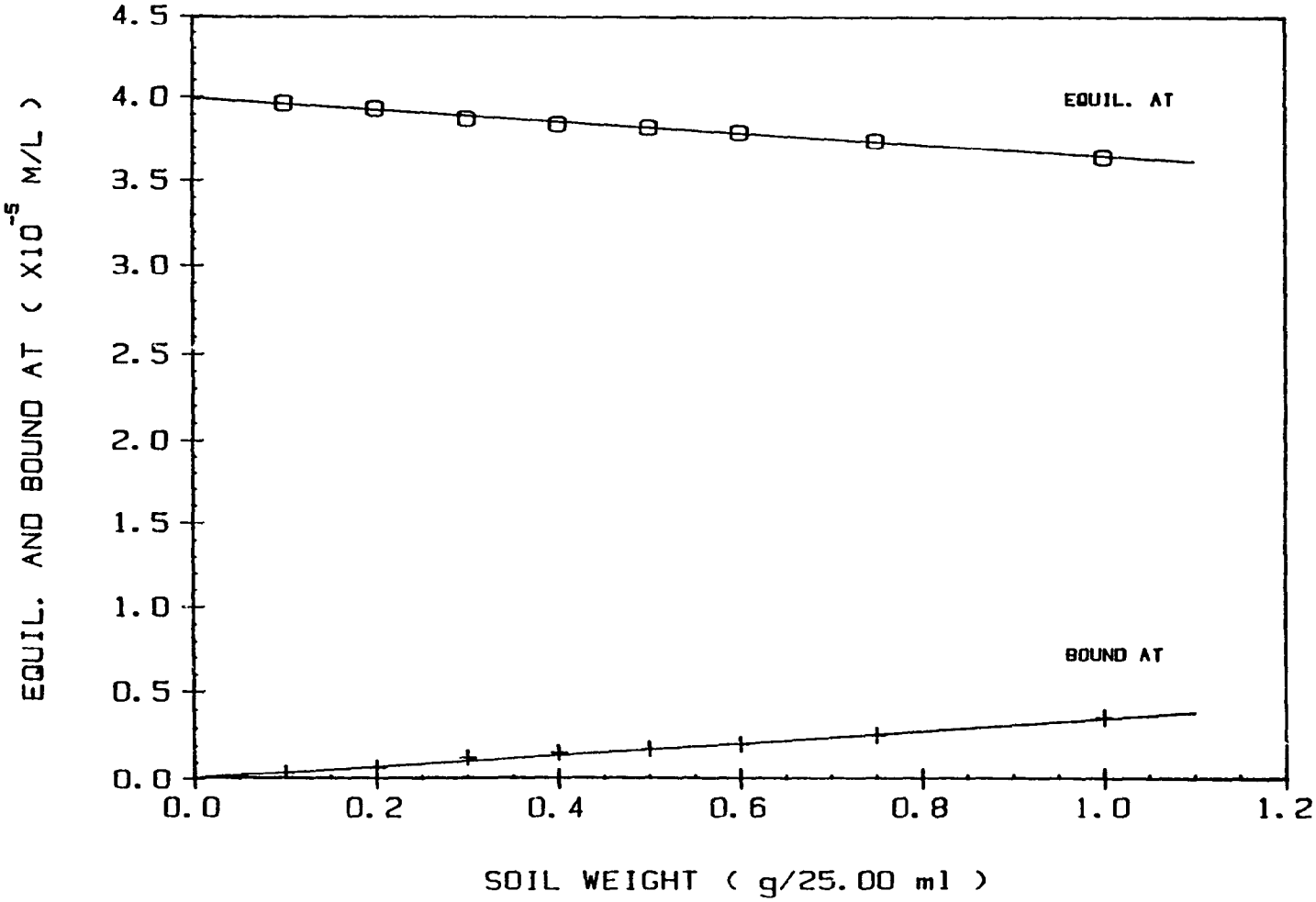

conducted at pH 3.05, 3.75 and 4.40. Representative binding curves at pH3.05 are shown in Fig. 5.3.

Using the linear analytical curves established in (AT+ATOH) controls with the equilibrium data obtained for AT and ATOH in the filtrate of (AT+ATOH)-soil samples, bound AT and ATOH were evaluated. Table 5.7 shows the data for the added AT and ATOH, and bound AT and ATOH at 3 tested pH. Plots of AT bound vs. AT total, and plots of ATOH bound vs. ATOH are shown in Fig.5.9A and 5.9B, respectively.

Table 5.7 Binding Competition between AT and ATOH to Soil

(soil=0.5000g/25.00ml)

AT added ($x10^{-5}$M/L)	ATOH added	Bound AT(μM/20g soil)			Bound ATOH(μM/20gsoil)		
		pH3.05	pH3.75	pH4.40	pH3.05	pH3.75	pH4.40
0.80	0.40	0.986	0.805	0.317	0.310	0.648	0.350
1.20	0.60	2.03	1.33	0.772	0.344	0.972	0.710
1.60	0.80	2.40	1.41	1.23	0.458	1.30	1.16
2.00	1.00	3.00	2.49	1.39	0.782	1.96	1.79
2.40	1.20	3.34	2.42	1.55	0.889	2.36	1.97
3.20	1.60	5.63	4.42	2.69	1.54	3.43	2.50
4.00	2.00	6.00	4.63	3.36	2.49	4.08	3.13

It can be seen from Fig.5.8 and 5.9 that (1) The plots of bound AT vs. added AT are analytically linear, which suggests the bound AT is still not reaching the binding limit. This fact is in agreement with that in Fig.5.3. (2) No binding limit is reached for ATOH at any pH. (3) Compared with the results in section

FIG5.8 BINDING CURVES OF AT IN PRESENCE OF ATOH

(pH=3.05, SOIL=0.5000 g/25.00 ml, ATOH=0.4--2.4X10^{-5} M)

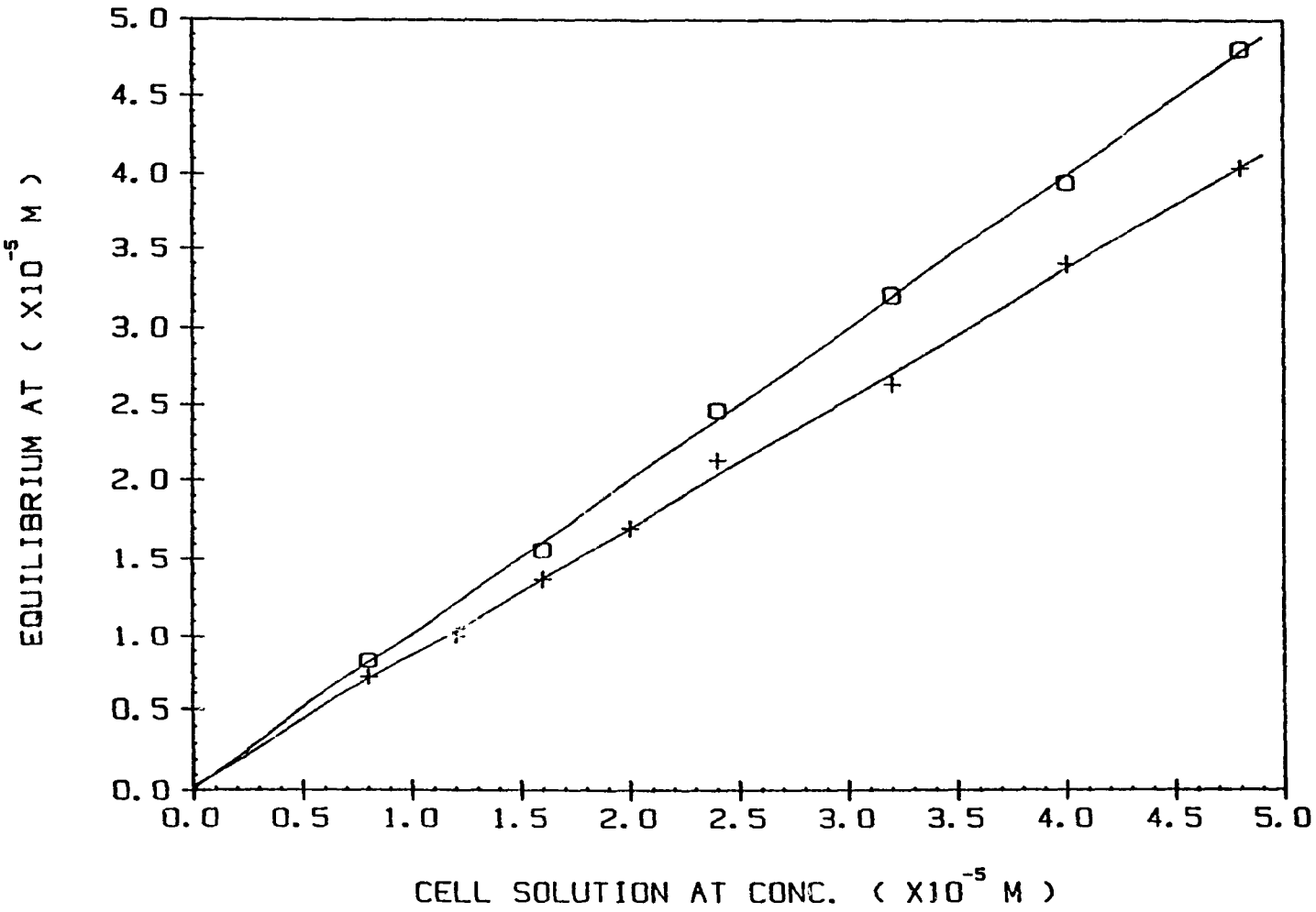

FIG. 5.9A BINDING COMPETITION OF AT AND ATOH

(SOIL=0.5000 g/25.00 ml, ATOH=0.4--2.4X10^{-5} M)

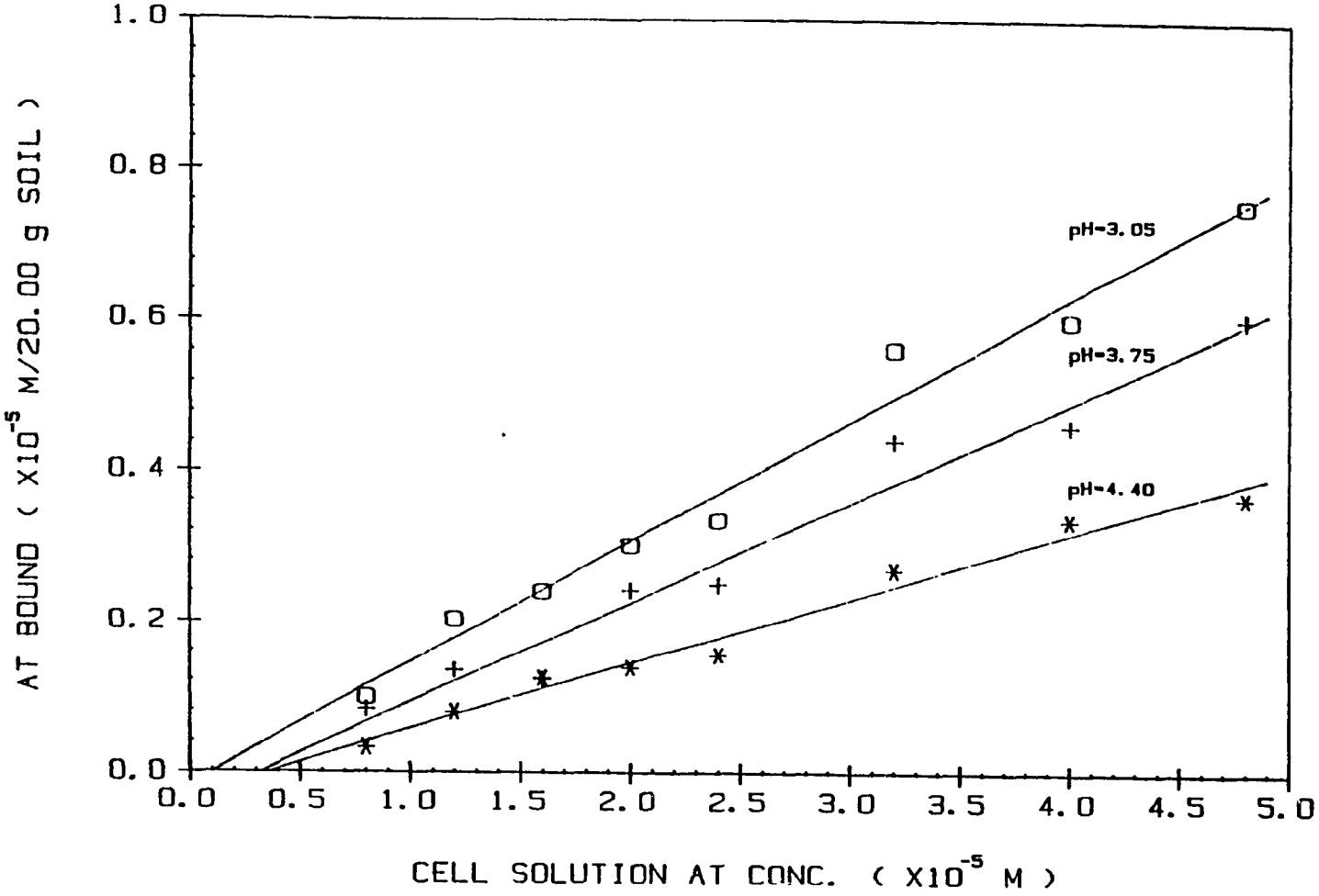

FIG. 5.9B BINDING COMPETITION OF AT AND ATOH

(SOIL=0.5000 g/25.00 ml, AT=0.8--4.8X10 M)

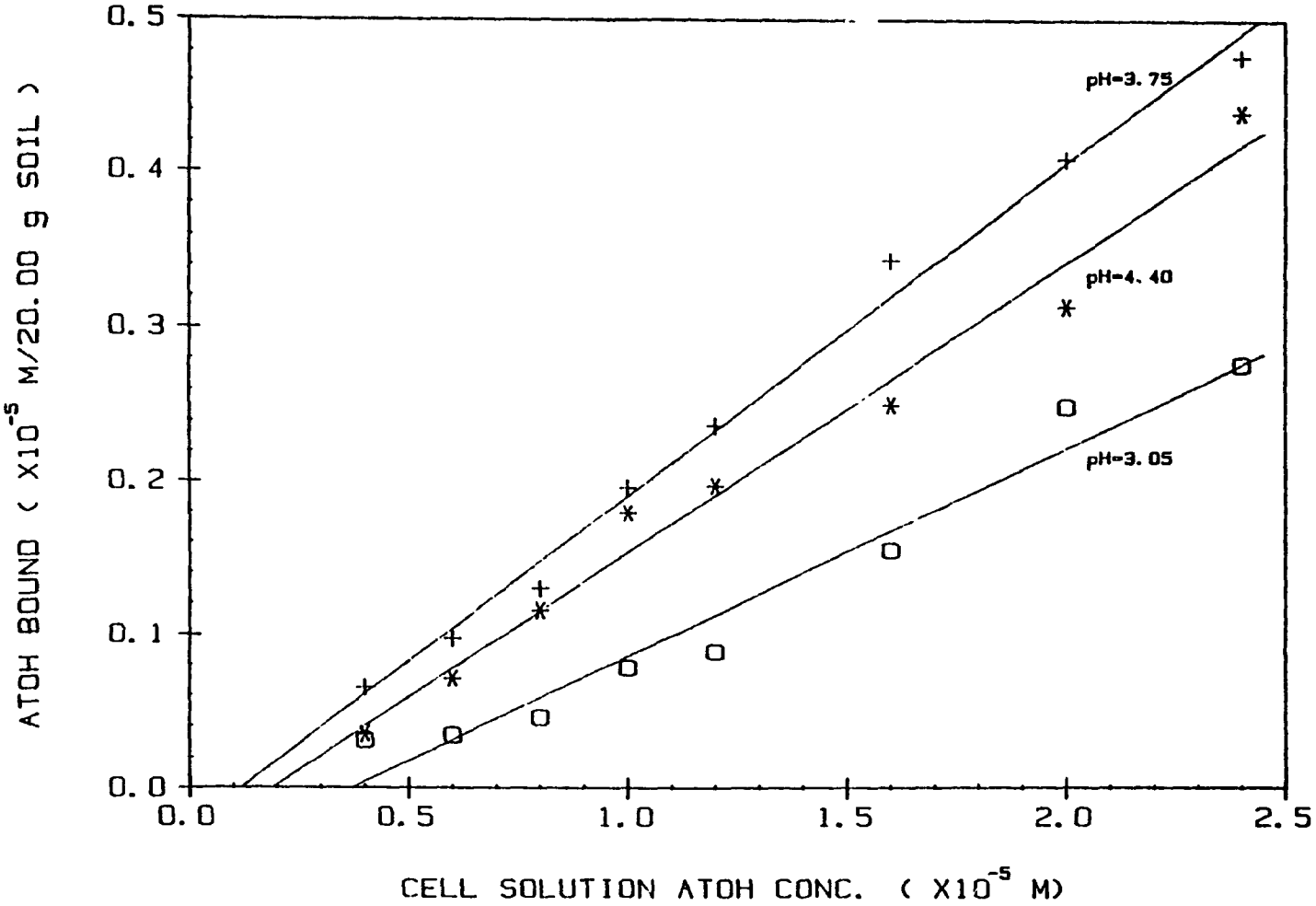

5.3.1, it could be concluded that there is no significant competition between AT and ATOH for the available binding sites.

5.3.5 AT Binding in The Presence of Copper Ions

(1) AT binding in the presence of various concentration of Cu(II)

The experiments designed are in such a way that the AT concentration added was kept constant, and Cu varied from 0.40×10^{-4} to 10.0×10^{-4} M so that the effect of Cu in a wide range of concentration on AT binding could be thoroughly studied. Table 5.8 shows the measurement results at pH 4.00, and titration curves are presented in Fig. 5.10.

Table 5.8 Determination of bound AT in the presence of various Cu (added AT=4.00×10^{-5}M, pH=4.00, soil=0.5000g/25.00ml)

Added Cu	in Cu-AT control		in Cu-AT-soil		Bound AT
($\times 10^{-4}$M)	Cu($\times 10^{-4}$M)	AT($\times 10^{-5}$M)	Cu($\times 10^{-4}$M)	AT($\times 10^{-5}$M)	(μmoles)
0.40	0.429	3.94	0.188	3.50	5.0
0.70			0.236	3.58	4.2
1.00	1.067	3.94	0.432	3.58	4.2
2.00	2.057	3.94	0.762	3.51	4.9
4.00	4.051	4.05	1.570	3.61	3.9
6.00			2.356	3.61	3.9
8.00	7.952	3.97	3.581	3.61	3.9
10.0	9.933	4.10	4.79	3.61	3.9
Average					4.2 (S=0.5)

The average value of bound AT was found to be 4.2 μmol/20.00g soil in the presence of Cu.

FIG. 5. 10 AT BINDING BY SOIL IN PRESENCE OF Cu

(pH=4.00, SOIL=0.5000 g/25.00 ml, ADDED AT=4.00X10^{-5} M)

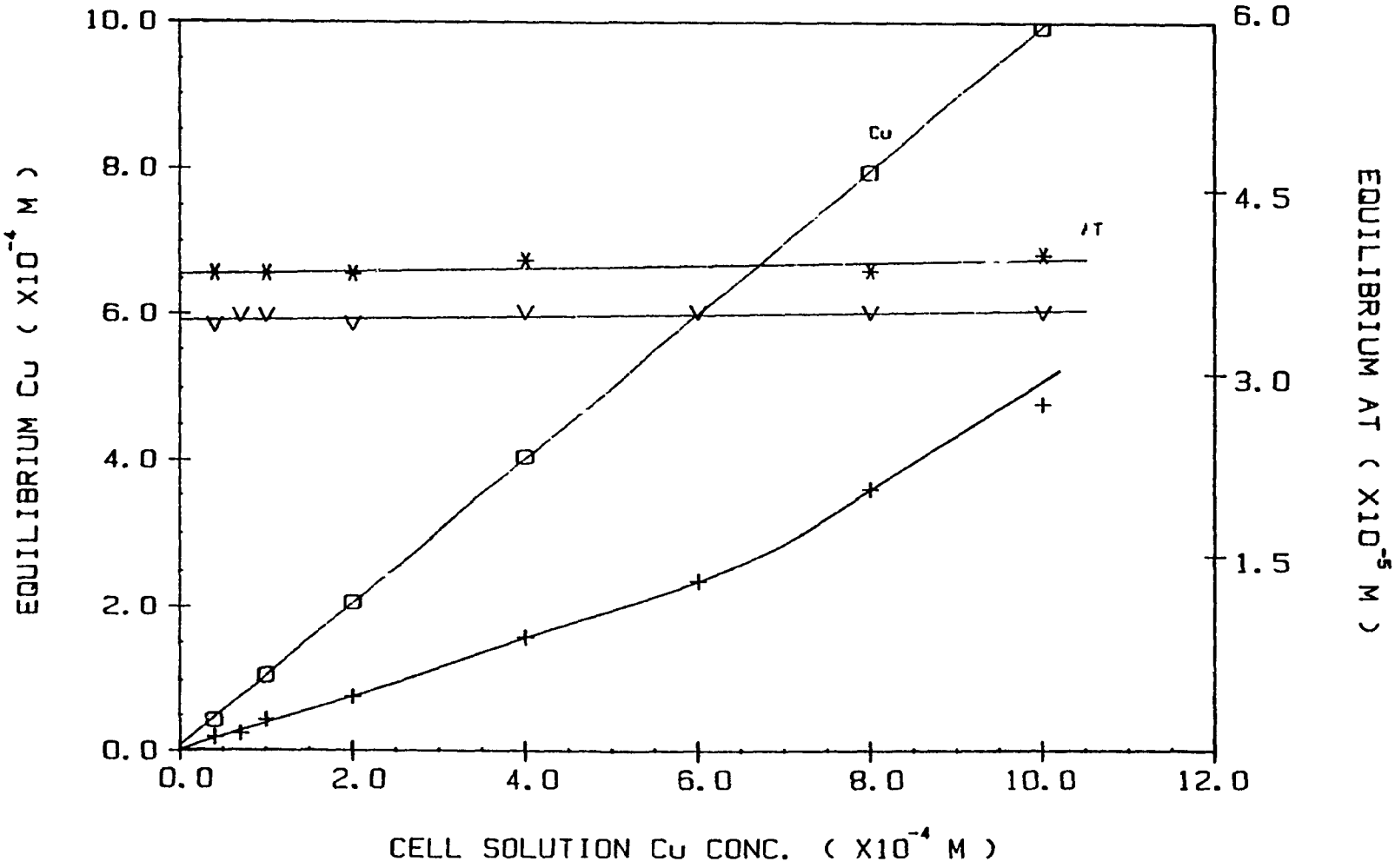

(2) AT variation at constant pH in the presence of excess Cu(II)

the titration curves at pH3.90 in the presence of excess Cu ($1.00x10^{-3}$ M) are shown in Fig.5.11. The experimental data for Fig.5.11 is listed in Table 5.9.

Table 5.9 Determination of bound AT in the presence of excess Cu (added Cu=$1.00x10^{-3}$M, pH=3.90, soil=0.5000g/25.00ml)

Added AT	in Cu-AT cont.	in Cu-AT-soil		Bound AT	Bound Cu
($x10^{-5}$M)	AT($x10^{-5}$M)	Cu($x10^{-4}$M)	AT($x10^{-5}$M)	(μM/20g)	($x10^{-3}$M/20g)
1.00	0.9987	0.516	1.000	0.00	0.484
2.00	1.999	0.492	1.748	2.52	0.508
2.80	2.799	0.492	2.425	3.75	0.508
4.00	4.000	0.488	3.497	5.03	0.512
4.80	4.800	0.492	4.286	5.14	0.508
5.60	5.601	0.513	5.133	4.67	0.487
6.80	6.801	0.496	6.262	5.38	0.504
8.00	8.002	0.506	7.501	4.99	0.494
average		0.502			0.498

The binding capacity of AT at pH 3.90 in the presence of Cu was found from Fig.5.11 to be 5.1 μmol per 20.00 grams soil. Exactly the same experiments were conducted at various pH values including pH 2.85, 3.40 4.40 4.60, 5.35 and 6.10. Table 5.10 lists out the copper complexing capacity and AT binding capacity at each pH.

FIG. 5. 11 AT BINDING IN VARIOUS CONC. OF Cu

(pH=3. 90, SOIL=0. 5000 g/25. 00 ml, ADDED Cu=1. 00X10^{-3} M)

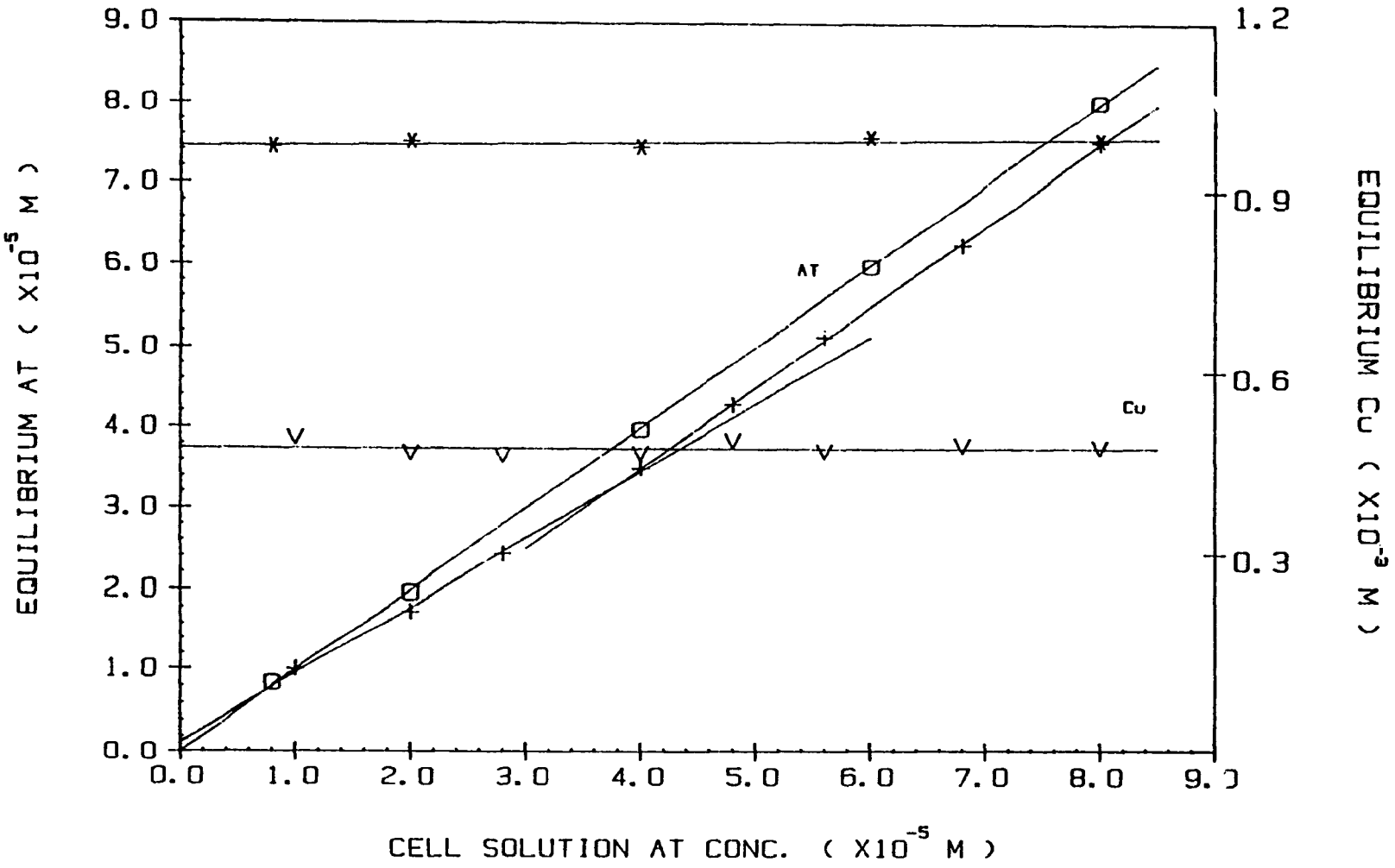

Table 5.10 Complexing capacity of Cu and binding capacity of AT (added Cu=1.00^{-3}M, added AT=0.80-8.00x10^{-5}M, soil=0.5000g/25.00ml)

pH	complexing capacity of Cu (x10^{-4}mol/20.00g soil)	binding capacity of AT (μmol/20.00g soil)
2.85	0.64	6.1
3.40	2.37	5.3
3.90	4.98	5.1
4.40	9.10	4.8
4.60	9.59	4.8
5.35	9.91	4.5
6.10	9.86	4.25

The plot of AT binding capacity vs. pH in the presence of excess of Cu is shown in Fig.5.12, the corresponding curves in the low and high ionic strength are also shown in Fig.5.12 for comparison. It can be seen from Fig.5.12 that the shape and the changing trend of binding capacity against pH of these three curves are qualitatively similar. The effect of the addition of $1.0x10^{-3}$M Cu on AT binding seems not so great, especially at high pH. The general trend is that the effect of Cu addition on AT binding gradually increases as pH decreases. The comparison of binding capacity differences due to the addition of Cu and KCl are presented in Table 5.11.

FIG. 5. 12 COMPARISON OF CURVES OF AT BINDING CAPACITY VS pH

IN THE ABSENCE AND PRESENCE OF KCl OR Cu

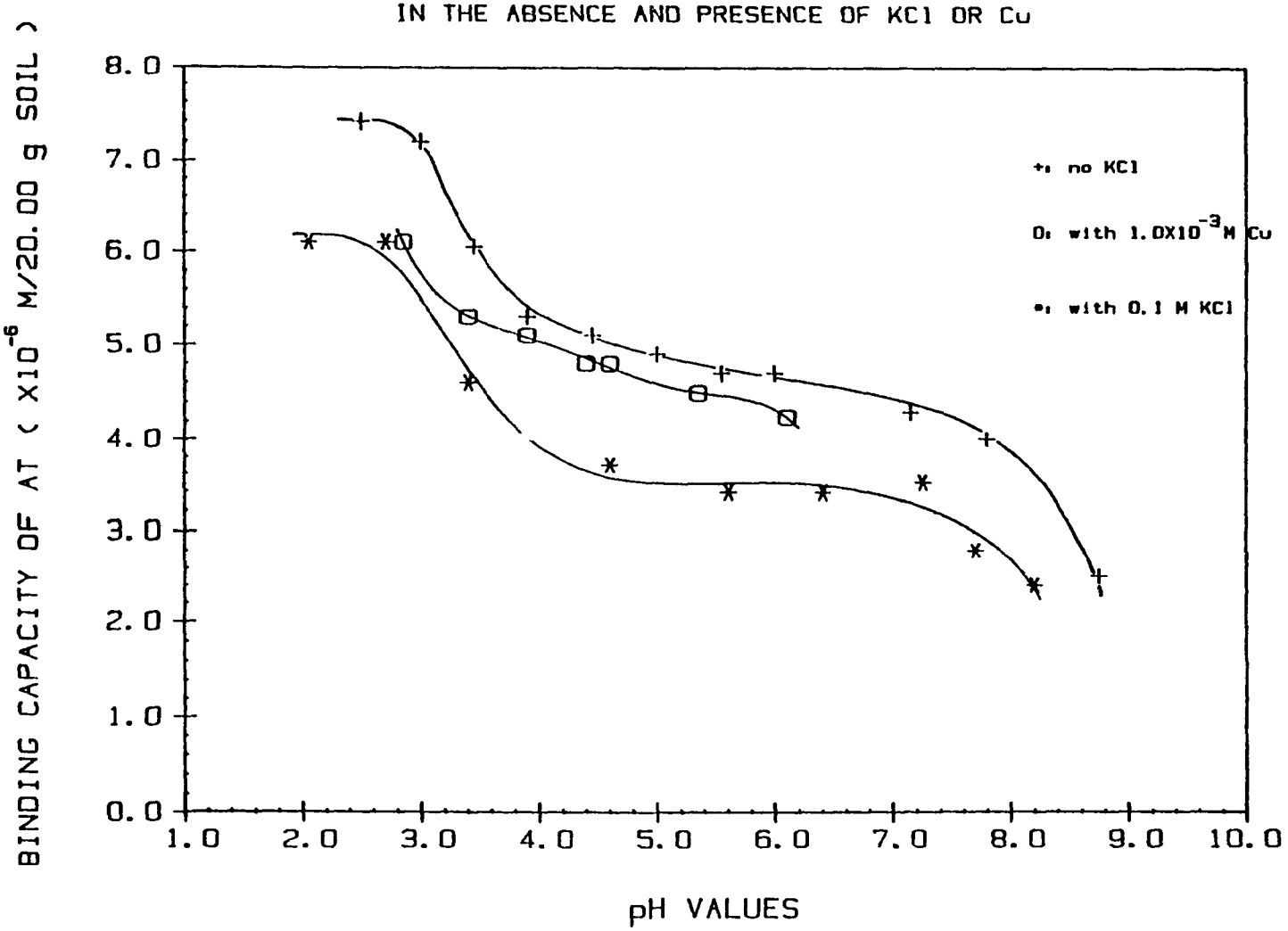

Table 5.11 Comparison of binding capacity differences of AT due to the addition of Cu(II) and KCl

pH	Differences between curve 1 and curve 2 (μmol AT/20.00g soil)	Differences between curve 1 and curve 3 (μmol AT/20.00g soil)
3.0	1.5	1.3
3.5	1.4	0.6
4.0	1.2	0.25
4.5	1.25	0.25
5.0	1.2	0.2
5.5	1.1	0.2
6.0	1.1	0.3
6.5	1.0	
7.0	1.0	
7.5	1.0	
8.0	1.0	

* curve 1 is for AT-soil in low ionic strength.
curve 2 is for AT-soil in the presence of 0.1M KCl.
curve 3 is for AT-soil in the presence of 1.0×10^{-3}M Cu.

5.3.6 AT Binding by (FA+HA), (FA+Soil) and (HA+Soil)

Since FA, HA and soil can bind with AT, it is important to determine the amount of AT bound when excess FA or HA is mixed with soil. These quite interesting experiments were conducted in the following way: Aliquots of FA stock solution (1.000g/L) or 10.00 mg HA were added to 0.5000g soil for sample preparation. The initial concentration of AT, 6.00×10^{-5} M, was used because the bound AT at this concentration can be considered to have reached saturation. pH was adjusted to the desired value by the

addition of HCl or NaOH. The final volume was 25.00ml. The data of AT bound by (FA+HA), (FA+soil) and (HA+soil) are shown in Table 5.12, together with the corresponding theoretical values of AT binding capacities, according to Fig. 2.12, 4.4 and 5.5.

Table 5.12 Comparison of experimental AT bound by (FA+HA), (FA+soil) and (HA+soil) with the corresponding AT binding capacity

Theoretical values (μmol/L)			
pH	(AT-FA)+(AT-HA)	(AT-FA)+(AT-SOIL)	(AT-HA)+(AT-SOIL)
2.50	11.5	13.1	12.6
3.00	9.85	10.7	12.7
3.50	8.1	9.0	10.5
4.00	6.8	8.1	9.1
4.50	5.6	6.1	7.5
5.00	4.4	4.6	6.6
5.50	2.9	4.0	6.0

Experimental values (μmol/L)					
pH	AT-(FA+HA)	pH	AT-(FA+SOIL)	pH	AT-(HA+SOIL)
2.40	8.8	2.95	7.5	2.60	9.6
2.65	8.0	3.50	6.8	3.25	8.6
3.10	7.4	3.90	6.2	4.00	5.9
4.10	5.1	4.85	5.4	4.60	5.4
5.50	2.8	5.80	4.3	5.80	4.5

Fig. 5.13, 5.14 and 5.15 show the plots of experimental and theoretical AT bound by (FA+HA), (FA+soil) and (HA+soil) vs. pH for the data in Table 5.12, respectively. The curves of AT bound by FA, HA and soil are also presented in the respective figures so as to compare the differences between them.

FIG. 5. 13 COMPARISON OF CALCUL. AND EXPERI. AT BOUND

(AT=6.00X10^{-5} M, FA=1.000 g/L, HA=10.00 mg/25.00 ml)

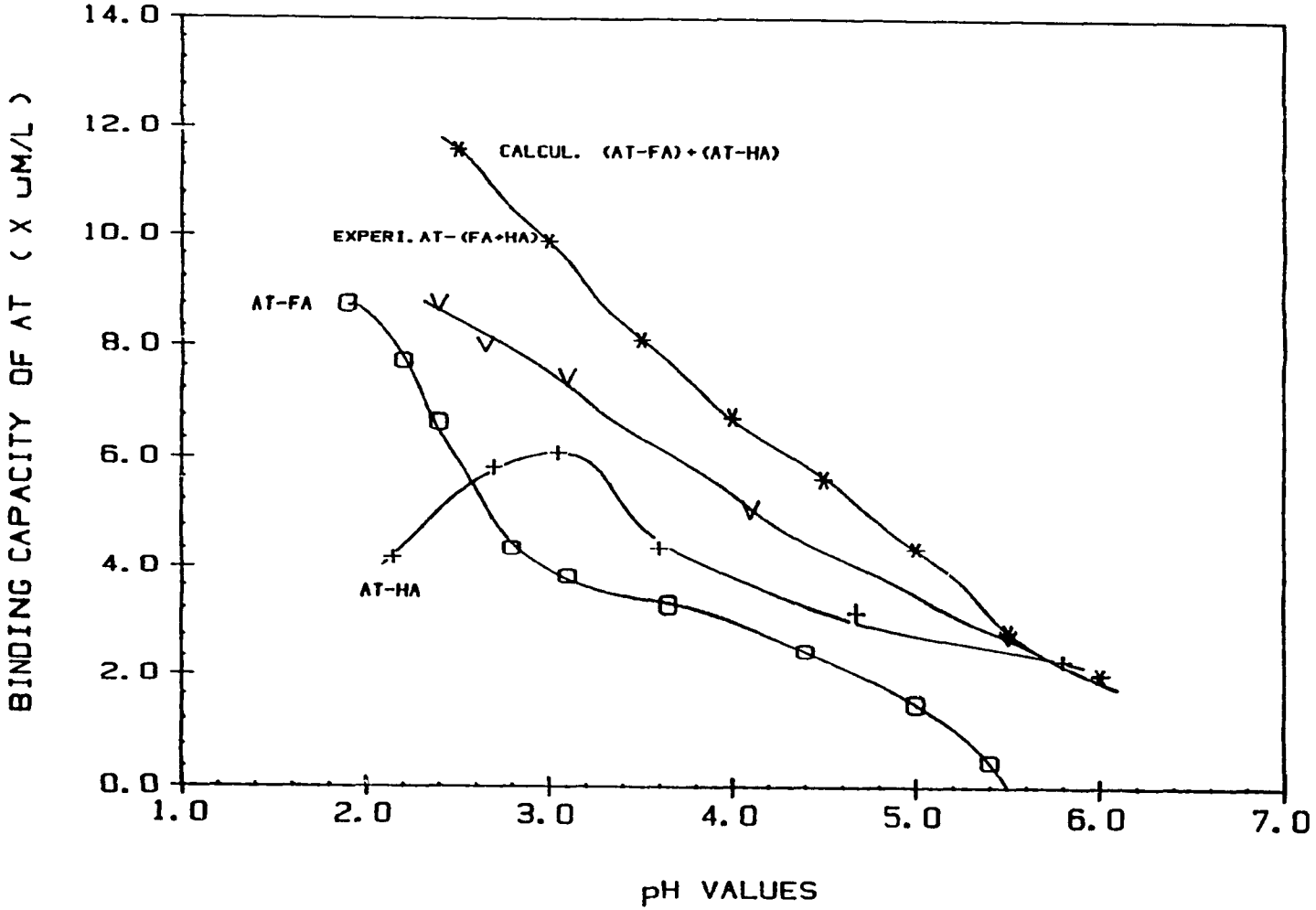

FIG. 5.14 COMPARISON OF CALCUL. AND EXPERI. AT BOUND

(AT=6.00X10^{-5} M, FA=1.000 g/L, SOIL=0.5000 g/25.00 ml)

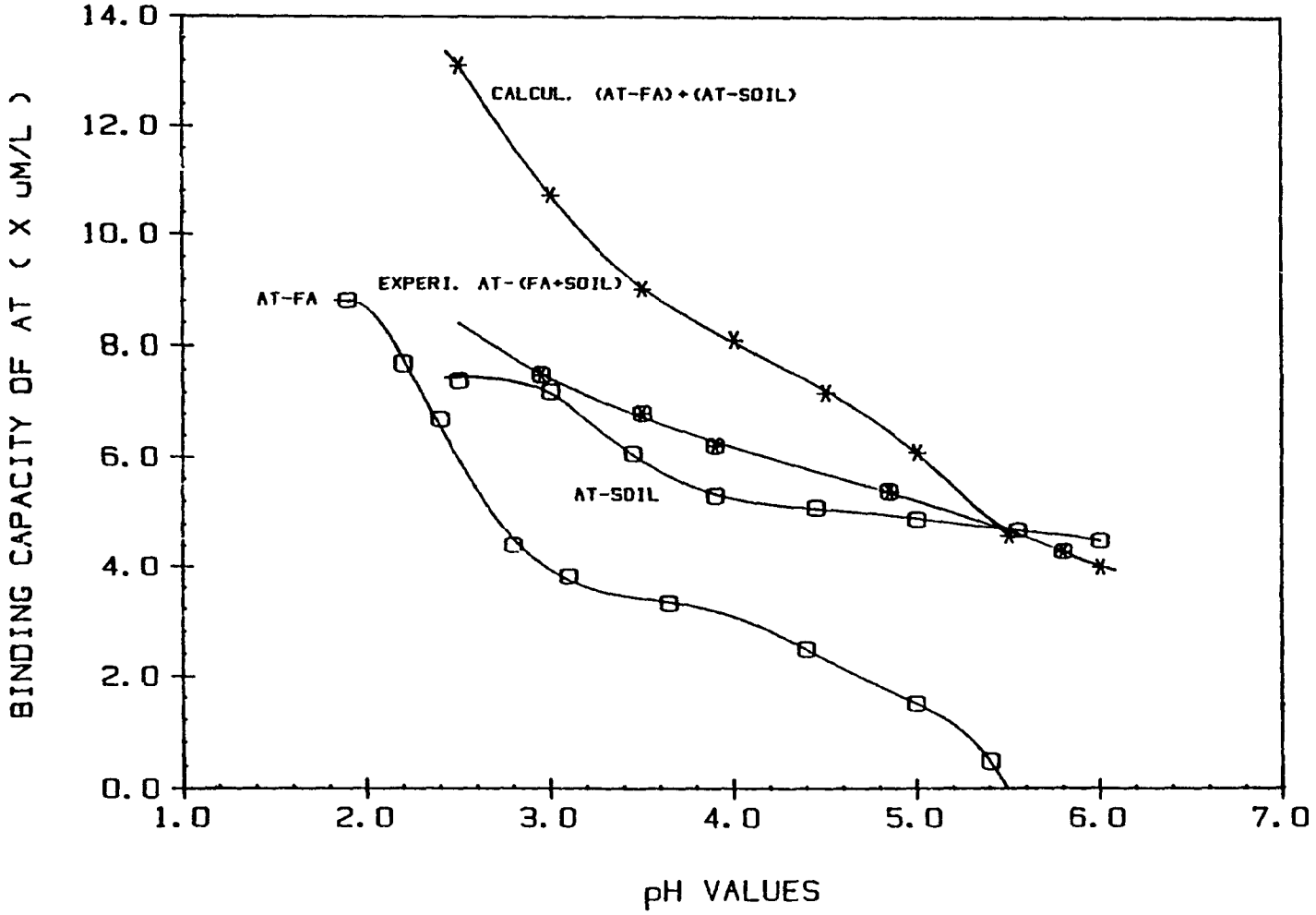

FIG. 5. 15 COMPARISON OF CALCUL. AND EXPERI. AT BOUND

(AT=6.00X10^{-5} M, HA=10.00 mg/25.00 ml, SOIL=0.5000 g/25.00 ml)

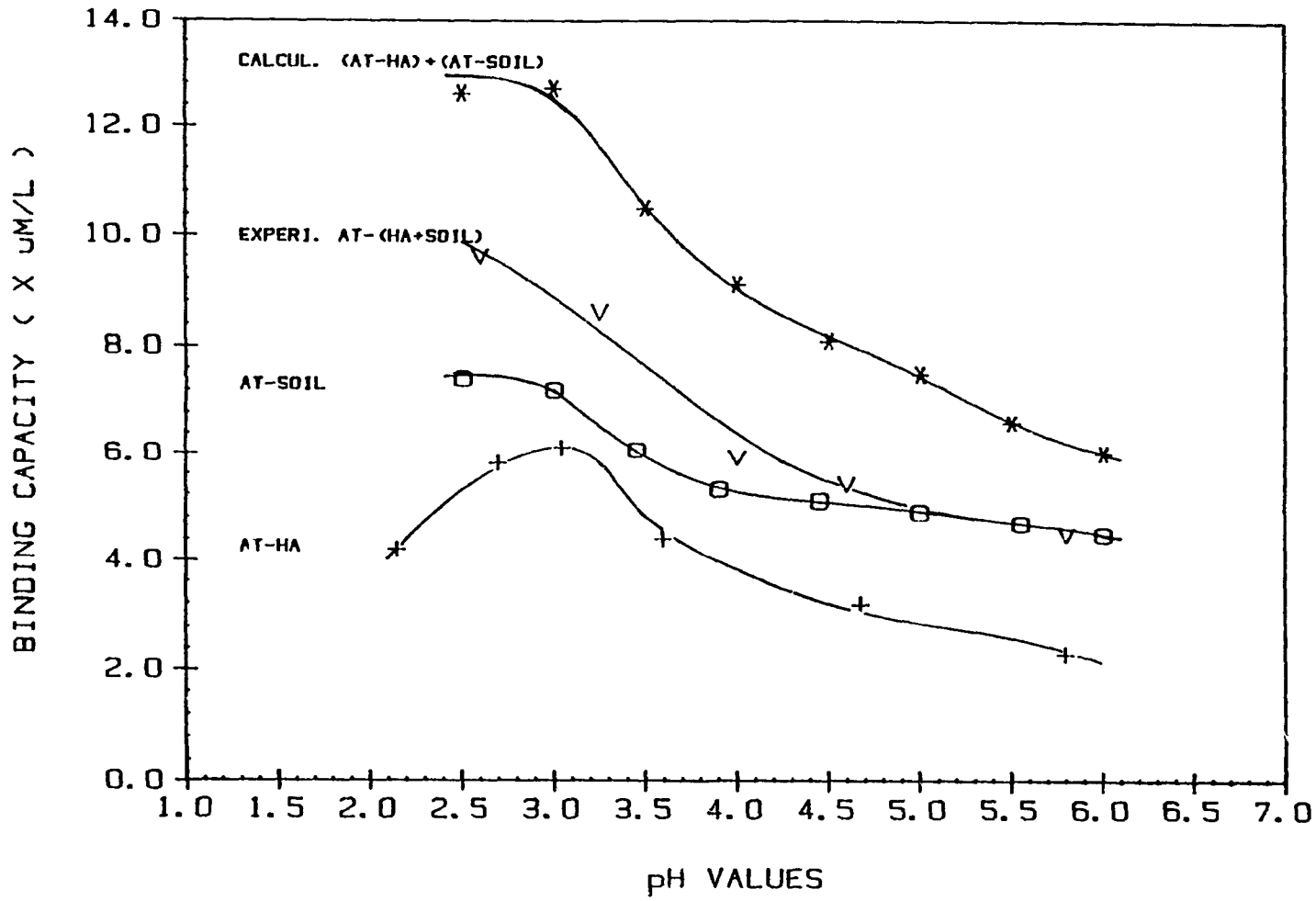

Several distinguishing features can be seen in Fig. 5.13, 5.14 and 5.15: (1) Experimental values of AT bound are smaller than theoretical ones in the whole range of pH studied. (2) The difference between the theoretical and experimental curve reduces as pH increases. (3) For Fig. 5.13 and 5.14, the theoretical and experimental curves finally converge to AT-HA or AT-soil curve as pH increases to a certain value.

The differences of AT binding capacity at each pH between the theoretical and experimental curve were shown in Fig. 5.16. It can be seen from the curves in Fig. 5.16 that the differences of AT binding capacity obvioursly decrease with pH increase.

5.4 DISCUSSION

5.4.1 AT Binding Mechanism by Soil

Soils vary greatly in organic matter content [4]. Typical soils such as Laurentian Forest Soil may contain 5-6% organic matter (humus) in the top 15-20 cm. A study was made of the distribution of ^{14}C in fractions of the soil organic matter [130] as follows:

Fraction	Recovery of residual ^{14}C
fulvic acid	11.8-18.9%
humic acid	19.5-26.4%
humin	49.4-54.7%
unaccounted for	5.0-12.9%

According to the above distribution of soil organic matter, very reasonable contents of FA and HA in 0.5g of Laurentian Soil should be between 2.0 to 5.0 mg. If the ratio of Laurentian FA and HA is assumed to be 1:1 (5.0mg FA and 5.0mg HA in 0.5g soil), or

FIG. 5. 16 DIFFERENCES OF BINDING CAPACITY OF AT

BETWEEN CALCULATED AND EXPERIMENTAL VALUES

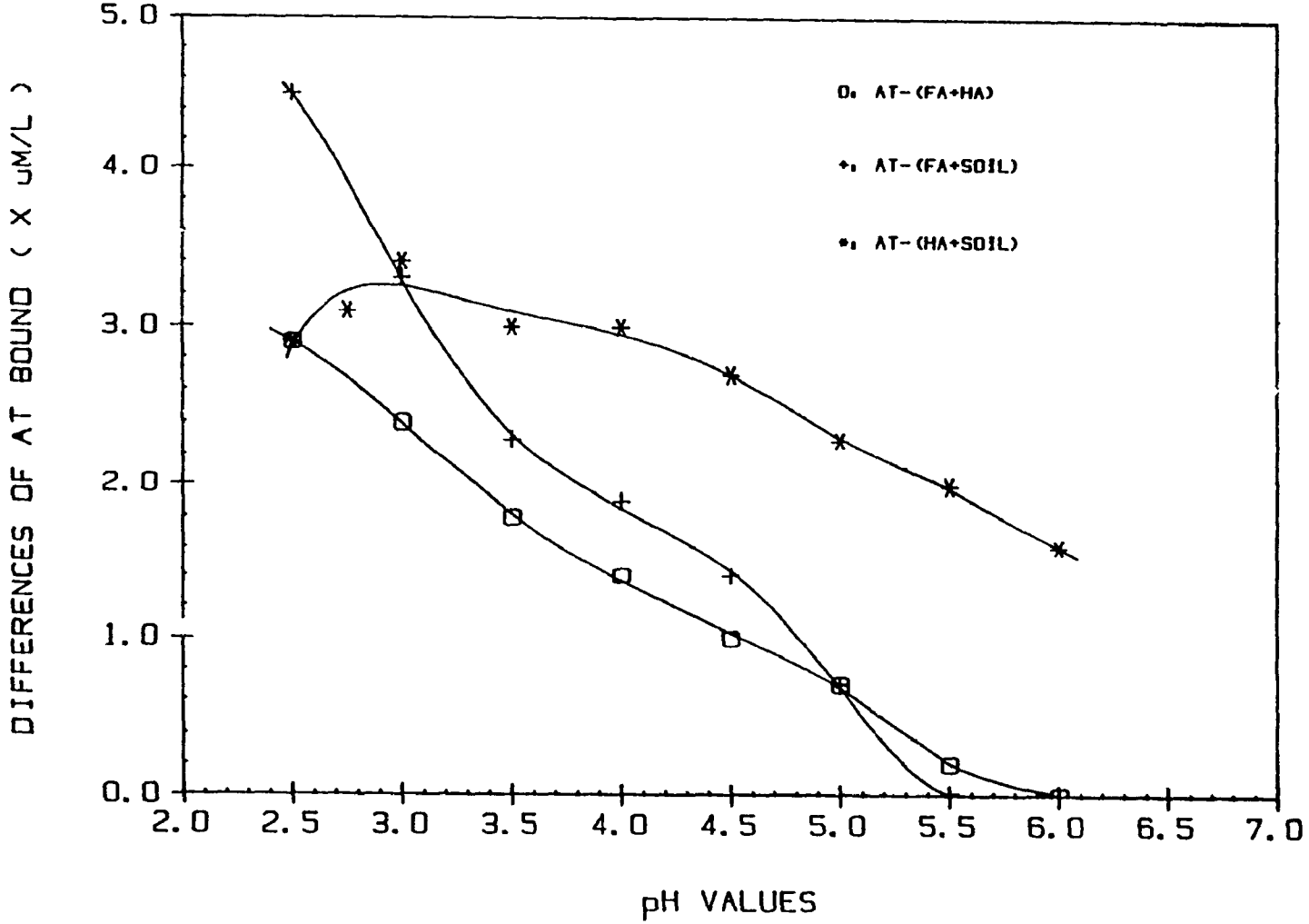

1.5:1 (3.75 mg FA and 2.5 mg HA in 0.5g soil), or 1:1.5 (2.5 mg FA and 3.75 mg HA in 0.5g soil), AT binding capacity by soil, composed from AT binding capacity of AT-FA and AT-HA, at various pH values can be obtained (it is shown in Table 5.13). The values of AT binding capacity by soil minus 4.0 μmol is also presented in Table 5.13 for comparison. The 4.0 μmol is here assumed to be the amount of AT bound attributable to clay, and the remaining AT bound after 4.0 μmol is subtracted from the total AT binding capacity by soil is assumed to be mainly attributable to FA and HA. It will be discussed later in details

Table 5.13 AT binding capacities composed from AT-FA and AT-HA binding capacities

pH	(5.0mg FA+5.0mg HA) (μmol AT/L)	(3.75mg FA+2.5mg HA) (μmol AT/L)	(2.5mg FA+3.75mgHA) (μmol AT/L)
2.0	3.90	2.37	2.50
2.5	3.92	2.27	2.63
3.0	3.78	2.49	2.64
3.5	3.14	1.73	2.20
4.0	2.48	1.38	1.72
4.5	2.12	1.18	1.48
5.0	1.76	0.96	1.25
5.5	1.26	0.63	0.95
6.0	1.00	0.50	0.75
6.5	0.74	0.37	0.56
7.0	0.26	0.13	0.20

(AT binding capacity by soil)-4.0μmol (μmol AT/20.00g soil/L)

pH	value	pH	value	pH	value
2.50	3.40	4.45	1.10	6.00	0.70
3.00	3.2[illegible]	5.00	0.90	7.15	0.30
3.45	2.05	5.55	0.70	7.80	0.00
3.90	1.30				

Using the data listed in Table 5.13, four curves of composed binding capacities of AT vs. pH were obtained, as shown in Fig.5.17.

Fig.5.17 clearly shows the binding curve of AT by soil (experimental data - 4.0μmol) is located between curves B, C and D, and the shape of pH dependence indicates organic behaves very like clay free organics. This phenomenon has its important significance for understanding the mechanism of AT binding by soil, for it reveals the fraction of AT bound attributable to the humic substances, mainly FA and HA, in soil, and another fraction of AT bound attributable to the clay. That is, the total AT bound by soil could be accounted to a good sum of FA, HA and clay. Also, the fact that 4.0 μmol is the pH independent part in the total binding capacity might indicate AT binding by clay is less pH dependent if compared with AT binding by FA and HA. A very interesting feature in Fig.5.17 is that unlike the curves of binding capacity vs. pH for AT-FA and AT-HA, no significant maximum of binding capacity appears in the range of tested pH, pH 2.0-8.0. The maximum for AT-FA and AT-HA is located around pH 1.4-1.9 and pH 3.0, respectively. When both FA and HA coexist in a solution, the summation of the binding capacity by FA and HA just makes the binding maximum disappear.

It has been recognized that clay is another soil component which is responsible for pesticide adsorption, in addition of soil organic matter. Bailey et al [44] have studied adsorption of organic herbicides by Montmorillonite, and found that the adsorption of basic organic compounds appears to be dependent upon surface acidity of clay, not upon the pH of the suspension.

FIG. 5. 17 COMPARISON OF BINDING CAPACITY OF AT

BY SOIL AND BY ASSUMED (FA+HA) MIXTURES

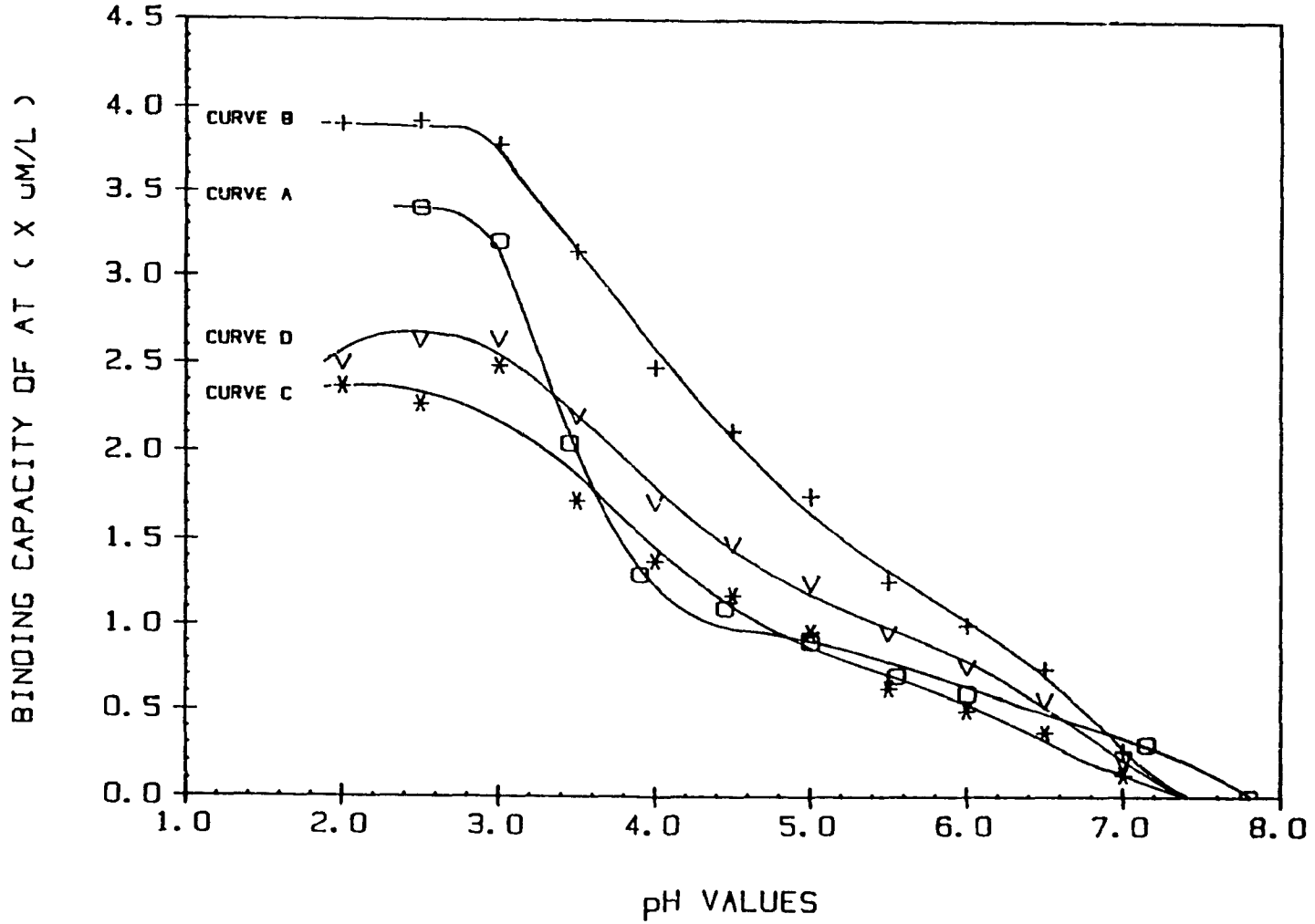

Recently, the work on AT binding by organic soil has been done in our lab [131]. As we know, organic soil are mainly composed by humic substances and clay minrals. Unlike soil, it only contains a small fraction of inorganic matters such as sand and silt (less than 10%). So its interaction behaviour with AT could be reasonablly considered as a sum of FA, HA and clay. The experimental results indicate that (1) the binding of AT occurs in the whole range of pH tested (pH 1.0-9.0). (2) the binding capacity decreases with the increase of pH in the range of pH 2.0-9.0, but the changing of the binding capacity with pH is slow. (3) more important, the trend and profile of the curve of AT binding capacity vs. pH (pH 2.0-9.0) is quite similar to that by the whole soil. These results may confirm the conclusion drawn from work with the whole soil that the AT binding by whole soil could be accounted to a sum of FA, HA and clay.

The possible mechanism postulated for AT adsorption by alumino-silicate clay in Laurentian Soil could be the following:

(1) Physical adsorption. AT adsorption by clay due to Van der Waal's forces.

(2) Chemical adsorption. This kind of AT adsorption by clay could occur in two different ways. First, protonation at the silicate surface and reaction of AT with the hydronium ion on the exchange sites. This is important because the surface acidity of clay can be 3-4 pH unit lower than the suspension pH [44]. second, protonation of AT in the solution phase with subsequent adsorption of the protonated AT via ion exchange. This occurs at low pH because AT (pK_a=1.65) can exist as ATH^+ form only at low pH. It is worth pointing out that Laurentian Soil has a quite high cation

exchange capacity for many cations (see Table 5.1).

(3) Hydrogen bonding. This mechanism would be a prime mechanism for the AT adsorption by clay. The clay is oxygen-rich contents on its surface. The N-H groups of AT on the ring and chains can easily form hydrogen-bond with the oxygen and -OH of the clay surface. Here the H atom of N-H group is electron-acceptor, and the O atom of the clay surface is electron-donor. (it is different from AT-FA and AT-HA cases in which the N atom of AT N-H group is electron-donor, and the H atom of COOH groups is electron-acceptor) So it should be expected that this kind of hydrogen bonding would be less pH-dependent.

Other important groups which are rich on clay surfaces and can also form hydrogen bonds with AT are -OH groups. This kind of hydrogen bonding is also expected to be less pH-dependent.

The following equations express the AT adsorption mechanisms described above:

$$\text{AT-NH} + \text{O-Clay} \rightleftharpoons \text{AT-NH} \quad \text{O-Clay}$$

$$\text{AT} + [\text{H}^+\text{-Clay}] \rightleftharpoons [\text{ATH}^+\text{-Clay}]$$

$$\text{ATH}^+ + [\text{H}^+\text{-Clay}] \rightleftharpoons [\text{ATH}^+\text{-Clay}] + \text{H}^+$$

$$\text{ATH}^+ + \text{Clay} \rightleftharpoons [\text{ATH}^+\text{-Clay}]$$

$$\text{AT} + \text{HO-Clay} \rightleftharpoons [\text{AT} \quad \text{HO-Clay}]$$

Even though we have separately discussed the adsorption of AT by organic matter and clay above, one must understand that the individual effects are not as easily distinguished as might be supposed. The reason is that, in soil, organic matter is often intimately attached to the clay, probably as a clay-metal-organic complex [4]. The relative contribution of organic and inorganic surfaces to adsorption of AT depends upon the extent to which the

clay is coated with organic humic substances.

One definite conclusion which can be drawn from the experiments of AT binding by soil and the analysis of the experimental data is that humic substances, mainly FA and HA, are the main components in soil responsible for AT adsorption, in addition to clays.

5.4.2 Self-Binding of Humic Substances and Clay-Humic Interaction

(1) Self-binding of humic substances

In chapter 2 it has been pointed out that one of the important factors which affect AT binding is that self-binding can occur between small and large MW fraction of fulvic acid, and AT binding is preferentially associated with the large fraction of the samples. When FA is mixed with HA, it behaves in same way. Fig.5.13 supports this conclusion.

It has been clearly understood that the MW of humic acid is much larger than fulvic acid. So it can be expected that: (1) the protonated carboxyl groups will bind with protonated or unprotonated carboxyl groups mainly via the hydrogen bond when FA is added to HA (Fig.5.18 shows some of the possible interaction between FA and HA). (2) the lower the pH, the more and the stronger the binding between FA and HA. (3) theoretically, the smaller molecules of FA prefer to first bind larger HA molecules for the reason that there is less steric hinderance.

Evidently, the self-binding must result in the reduction of those specific sites available for AT binding. Consequently, the AT binding capacity decreases. As pH increases, the self-binding reduces, followed by the decrease of the differences between the

theoretical and experimental binding capacity. When pH increases to 6.0, almost all carboxyl groups of FA exist in the form of ionized molecules, it has little effect on AT binding with HA or soil, resulting in both the theoretical and experimental curves converging to the AT-HA binding curve.

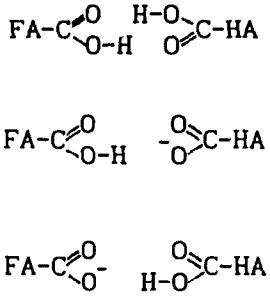

FIG.5.18 POSSIBLE SELF-BINDING OF HUMIC SUBSTANCES

(2) Clay-humic interaction

The clay-humic interaction, however, could be predominant over the self-binding of humic substances if FA or HA is added to soil. As we described in section 5.1, clay is a major component with significant importance in soil. The negative charges of clay crystals on the internal and external surfaces are satisfied by exchange cations. The layers or sheets of clay allow other molecules (e.g., water) to penetrate between them thereby causing swelling and shrinking. It has been pointed out [4] that one way in which organic substances are retained in soil is that they are held on clay mineral surfaces. Organic matter may be bound through cation and anion exchange, bridging by polyvalent cations

(clay-metal-humus), H-bonding and Van der Waal forces. Fig. 5.19 shows a schematic diagram of a possible clay-humate complex in soil.

The importance of polyvalent cations in adsorbing humic and fulvic acids has been emphasized [4]. The main polyvalent cations responsible for the humic and fulvic acids interactions with soil clay are Ca^{+2}, Fe^{+3}, and Al^{+3}. The polyvalent cations can act as a bridge between two charged sites. Other bonding forces may also operate between organic anions and the clay surface, including H-bonding between polar groups of the organic molecule and adsorbed water molecules or oxygens of the silicate surface.

This clay-humic interactions must also result in the reduction of the sites available for AT binding, which is clearly demonstrated in Fig. 5.14 and 5.15.

The fact that the experimental AT-(FA+HA) curve, and the experimental AT-(FA+soil) and AT-(HA+soil) curves finally converge to AT-HA and AT-soil binding curve, respectively, as pH increases to pH 6.0 implies that AT binding behaviour may mainly depend on the larger and more complex one when two kinds of humic substances coexist in a system, or when FA or HA is added to soil.

5.4.3 KCl effect and clay-humic complex

It has been shown in the previous sections that KCl has quite a large effect on AT binding. The order of KCl effect on AT binding is: by HA > by FA > by soil. Table 5.14 lists some difference values of binding capacities in the presence and absence of 0.1M KCl for these three cases.

What must be explained here is why KCl only has a small

effect on AT binding by soil , compared with AT binding by HA and FA. Two points should be emphasized again are that: (1) Agrregation of humic and fulvic acids themselves will occur at low pH especially when HA and FA are exposed to high concentration of KCl. (2) Most of humic and fulvic acids in soil has been already held and evenly distributed on clay mineral surfaces, and the amount of humic substances is usually quite low relative to clay.

Table 5.14 The differences of binding capacities in the absence and presence of 0.1M KCl

AT-FA		AT-HA		AT-SOIL	
pH	Δ(μmol/g FA)	pH	Δ(μmol/g HA)	pH	Δ(μmol/20g soil)
1.5	5.8	2.5	10	2.5	1.3
2.0	4.7	3.0	10.5	3.0	1.5
2.5	2.8	4.0	6.3	4.0	1.2

In aqueous solution acidic functional groups of the humic colloid are more or less dissociated and the polymer assumes a stretched configuration because of mutual repulsion of negatively charged functional groups, COO^-. When KCl is added, the cation K^+ is attracted to negative groups, thus causing a reduction in intermolecular coulombic repulsion in the polymer chain. This in turn favours coiling of the chain, consequently causing the reduction of the binding sites available for AT.

But, for soil, the situation is quite different. As shown in Fig 5.19, adsorption of humic and fulvic acids by clay minerals via the formation of coordination complex with polyvalent cations. Unlike Na^+ and K^+, polyvalent cations present in soil are able to

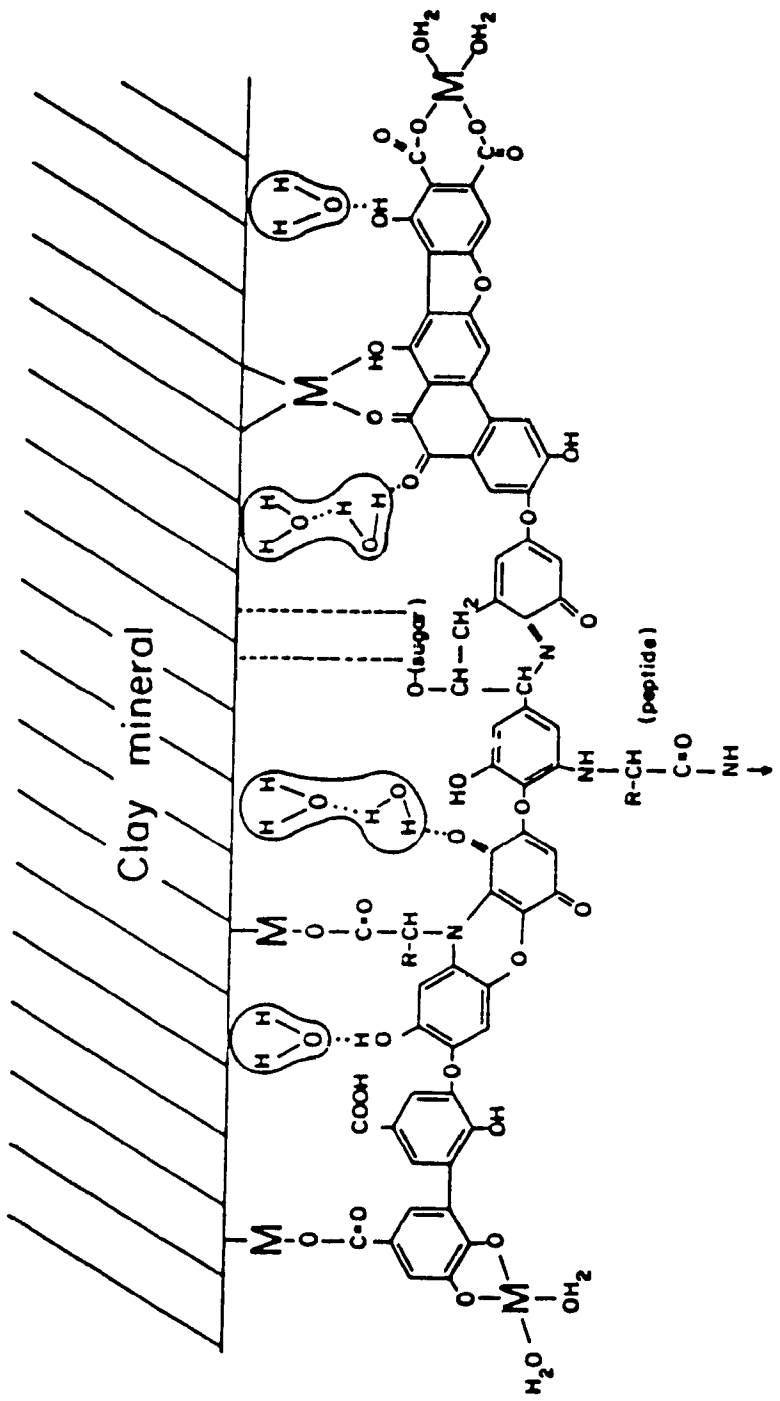

Fig. 5.19 Schematic diagram of a clay-humate complex in soil[4]

maintain neutrality at the surface by neutralizing both the charge on the clay and acidic functional group, here mainly COO^- of the organic matter. The main polyvalent cations responsible for the binding of humic and fulvic acids to soil clays are Ca^{+2}, Fe^{+3}, and Al^{+3}. These coordination complexes formed through Al^{+3} and Fe^{+3} are quite stable and strong. The divalent Ca^{+2} ion does not form such a coordination complex and would be effective only to the extent that a bridge linkage could be formed [129]. Even so, it is impossible to displace these bound metals by monovalent K^+. Therefore, it can be expected that the addition of KCl to soil has little effect on the configurational and conformational changes of organic matter bound to clay, except to a very small fraction of FA and HA not bound to clay mineral. This interaction mechanism results in that KCl has only small effect on AT binding by soil, compared to AT binding by FA and HA.

For similar reasons, the weight of the soil has almost no effect on AT binding (see Table 5.6).

5.4.4 AT hydrolysis

The hydrolysis of AT has been discussed in the previous chapter. Protons and protonated carboxyl groups are two kinds of components responsible for AT hydrolysis. In soil, the hydrolysis mechanism is exactly the same as in FA and HA. But it must be remembered that the protonation of AT also can occur at the silicate surface by reaction with the hydronium ion on the exchange sites, in addition to protonation in solution phase by proton and unionized carboxyl groups.

It should be noted that the AT-soil work is a exploratory

work. It can be regarded as a useful beginning which could lead to deeper understanding of pesticides-soil interactions. The reasons are that this work reveals some important phenomena such as some sorption capacities, some sorption equilibrium parameters, and some effect of pH, ionic sthength, and metal ion site blocking trends on atrazine sorption, as well as the roles and behaviours of organics and clay in AT binding process. However, direct experimental evidences for some explaination might be not enough. More experiments such as the interaction of clay with AT, and sorption equilibrium in longer periods, therefore, should be set up and carried out. Also the wider concentration of AT should be used in AT-soil binding interaction as to obtain more experimental data points and to confirm the binding limit is reached with confidence.

CHAPTER 6

CONCLUSION AND SUGGESTION FOR FUTURE RESEARCH

6.1 CONCLUSION

The work presented in this thesis has systematically studied the interaction (binding and catalysis) of the polar herbicide atrazine, first with the soluble fraction soil organic matter known as fulvic acid, second by the insoluble fraction known as humic acid, and finally by the whole soil. All three components FA, HA and soil which were derived from a sample of a podzol collected in the Laurentian Forest Preserve of Laval University have been well chemically characterized. The aim of this study, that the interaction mechanisms could be elucidated by proceding from the case of dissolved polyelectrolyte binding (FA), through the case of three dimensional colloidal gel particles where Donnan equilibria are present (HA), to the whole Laurentian soil, has been achieved.

The method used for binding and catalysis studies is the ultrafiltration-HPLC method newly developed in our laboratory. This method has been demonstrated to be sufficiently powerful, accurate and precise, rapid, and conservative of materials. The two major pitfalls of separation technique stressed by Saar and Weber [82] have been overcome: first, the experimental error caused by adsorption is minimized by using the advanced hydrophilic membranes with minimal adsorption and by using the point to point batch dilution curve method in which controls and samples are simultaneously run and measured; second, the

possibility of shifting equilibrium is eliminated by ultrafiltration of less than 5% of the cell solution.

(1) Atrazine is a polar basic compound. It exist in two forms, protonated and unprotonated, depending on the pH value of the system. It can be hydrolyzed to hydroxyatrazine. The only two acid catalysts so far identified in humic materials for atrazine hydrolysis are hydrogen ion and unionized carboxyl groups. It has not yet been determined whether base catalysts can also exist in mineral soils.

(2) Laurentian FA contains 5.11 mmole Type A and 3.49 mmole Type B carboxyl groups per gram FA, and 3.03 mmole phenolic groups per gram FA. Laurentian HA contains 2.50 mmole carboxyl groups and 5.10 mmole phenolic groups per gram HA. Structurally, they are polymer mixtures.

(3) FA can be dissolved in both acid and alkali, forming a pseudo-homogeneous solution. HA forms a heterogeneous solution having an aqueous solution phase and a gel structure phase. The solubility of HA is pH dependent, and HA in the gel phase behaves like a carboxylic type cation exchanger. The differences in AT binding behaviors by FA and HA arise from the structural differences between FA and HA, which lead to the latter form 3-dimentional particles.

(4) AT binding by FA is accompanied by conformational and configurational changes of FA molecules, an idea supported by UV

and Fluorescence studies of FA fractions.

(5) The AT-humic substance interaction model proposed in this study has its significant importance and generality in the stoichiometrical understanding of the nature and features of pesticide binding with humic substances. Two approaches have been applied to calculate the average weighted function and the differential equilibrium function of AT-FA and AT-HA. The second treatment based on the well defined binding capacity, however, is preferably recommended for the interpretation and treatment of experimental results for it more truly reflect the real situation of AT binding. The other method remains of interest only because it corresponds to the treatment used in the literature where binding capacity have not been identified.

(6) Atrazine-FA solution phase work and the atrazine -HA heterogeneous solution work, as well atrazine-soil colloid work have all indicated that unionized carboxyl groups are involved in AT binding sites. In soil, another important component which is responsible for AT binding is probably clay mineral. It must be realized that only a very small fraction of total carboxylate (less than 1% of total carboxylate) act in AT binding sites--these are special binding sites. These special sites are created by dynamic rearrangement in FA. The maximal binding of AT by FA, HA and soil are 8.8 μmoles/g FA (at pH 1.4-1.9), 15.3 μmoles/g HA (at pH 3.05), and 7.4 μmoles/20.00g soil (at pH 2.50), respectively.

(7) Two main factors which largely affect FA and HA aggregation

are hydrogen ion and electrolyte concentration. In the presence of 0.1M KCl and at high H^+ concentration the aggregation of fulvic acid and humic acid becomes significant and important. The order of KCl effect on AT binding is HA > FA > soil. The appearance of maximum of AT binding capacity is probably the result of competition between aggregation and increase of protonated carboxyl groups.

(8) Binding of atrazine by FA or HA is not competitive with binding of hydroxyatrazine. The similar molecules AT and ATOH have their own specific binding sites, respectively. An important practical implication is there is no catalyst poisoning by the reaction product hydroxyatrazine.

(9) Binding is preferentially associated with larger molecules of sample. It is true not only for FA fractions, but also for the mixture of FA and HA, FA and soil, and HA and soil. When FA (or HA) is mixed with HA (or soil), some self-binding between FA and HA (or soil) molecules occurs. It results in the reduction of AT binding.

(10) The predominant mechanism for AT-FA and AT-HA interaction is probably the formation of hydrogen bonding between the protonated carboxyl groups and ring or chain nitrogen of AT. The nitrogen atom is electron-donor and the hydrogen atom of protonated carboxyl groups is electron-acceptor. The calculated free energies of AT binding are of the order of hydrogen bond energies, and correspond to the formation of one or two hydrogen bonds.

6.2 SUGGESTION FOR FUTURE RESEARCH

(1) The present work proposed an AT-humic substance interaction model. The experiments have demonstrated that this model may be the best model for interpreting the interaction between AT and humic substances. Two questions must still answered. (1) What is the generality of this model? (2) Can it be applied to interpret the experimental phenomena of other pesticides by humic substances (especially those pesticides with smaller water solubility than AT)? The nonpolar and less hydrophilic pesticide, lindane, could be chosen to evaluate the generality of the model, and to expand the application of this model. Great attention should be paid to the FA (or HA) concentration effect on lindane binding because the appropriate concentration of FA or HA may be extremely important to study the binding behaviour of lindane. If the concentration of FA or HA is too high, the binding limit may not be reached, which would create a false impression leading to incorrect assignment of interaction mechanism.

(2) It has been demonstrated that only those special site carboxylic groups bind AT. AT hydrolysis to ATOH by carboxyl groups could occur only after AT are bound by carboxyl groups. The previous kinetic model often related the hydrolysis of AT to total carboxylic groups. Further kinetics study should be done, and the more reliable and accurate mathematical treatment should be developed on the basis of the observed binding capacity, followed by the proposal of a more precise model. Especially, account must be taken of the fact that AT and ATOH bind at

different sites so that no catalyst poisoning is expected.

(3) Structural characterization of Laurentian Fulvic Acid has been done by UV-VIS spectrophotometry, Fluorescence and NMR. Similar structural characterization work on Laurentian Humic Acid should be done in order to deepen understanding of the relation between binding by HA and the structure of HA.

(4) It has been demonstrated that the ultrafiltration-HPLC method is a powerful tool to determine the free and bound pesticide, as well as Cu^{+2} ion. It should be further developed and improved to analyze other pesticides and other possibly metals such as Hg^{+2} with some environmental importance, and to yield more quantitatively definitive information, with less dependence on empirical correlation. The method is promising for those metals for which ion selective electrodes are not available.

REFERENCES

1. M. Schnitzer, S. U. Khan, "Humic Substances in Environment", Marcel Dekker, Inc., New York, 1972.
2. E. M. Thurman, R. L. Malcolm, in "Aquatic and Terrestrial Humic Substances", R. F. Christman and E. T. Gjessing, Eds., Ann Arbor Science. Ann Arbor, MI, 1983, 4.
3. M. Schnitzer, in "Soil Organic Matter", M. Schnitzer and S. U. Khan, Eds., Elsevier/North Holland, Armsterdam, 1978, 1.
4. F. J. Stevenson, Humus Chemistry, John Wiley & Sons, New York, 1982, 36.
5. D. S. Gamble, Can. J. Chem., 48,2662(1970).
6. P. G. Hatcher, M. Schnitzer, L. W. Dennis, and G. E. Maciel, Soil Sci. Soc. Am. J., 45, 1089(1981).
7. P. G. Hatcher, G. E. Maciel, and L. W. Dennis, Org. Geochem., 3, 43(1980).
8. R. H. Newman, K. B. Tate, P. F. Barron, and M. A. Wilson, J. Soil. Sci., 31, 623(1980).
9. C. M. Preston, B. A. Blackwell, Soil Sci., 139, 88(1985).
10. C. M. Preston, M. Schnitzer, Soil Sci. Soc. Am. J., 48, 305(1984).
11. M. Schnitzer, C. M. Preston, Soil Sci. Soc. Am. J., 50, 326(1986).
12. D. N. Norwood, R. F. Christman, and P. G. Hatcher, Environ. Sci. Techno., 21, 791(1987).
13. M. Schnitzer, C. A. Hindle, and M. Meglic, Soil Sci. Soc. Am. J., 50, 913(1986).
14. H. R. Schalten, G. Abbt-Braun and F. H. Frimmel, Environ. Sci. Technol., 21, 349(1987).

15. K.Ghosh, M.Schnitzer, Soil Sci., 129,266(1980).

16. E.M.Thimman, R.L.Wershaw, R.L.Malcolm, D.J.Pinckney, Org. Geochem., 4,27(1982).

17. C.H.Langford, D.S.Gamble, A.W.Underdown, S.Lee, in "Aquatic and Terrestrial Humic Substances", R.F.Christman and E.T.Gjessing, Eds., Ann Arbor Science. Ann Arbor, Mich., 1983, Chapter 11.

18. A.W.Underdown, C.H.Langford, D.S.Gamble, Environ. Sci. Technol., 19,132(1985).

19. A.J.Lapen, W.R.Seits, Anal.Chim.Acta.,134, 31(1982).

20. C.H.Lochrnuller, S.S.Saavedra, Anal.Chem., 58,1978(1986).

21. J.Buffle, in "Metal Ions in Biological System", Vol.18., H.Sigel, Ed., Marcel Dekker, New York, 1984, Chapter 4.

22. A.E.Smith, D.C.G.Muir and R.Grover, in "Analysis of Pesticides in Water (Vol 3)", A.S.Y.Chau and B.K.Afghan, Eds., CRC Press , Boca Raton, Florida, 1982. Chapter 3.

23. S.J.Plust, J.R.Loche, F.J.Fehor, J.H.Benedict and H.F.Herbrandson, J.Org.Chem., 46,3661(1981).

24. S.Horrobin, J.Chem.Soc., 4130(1963).

25. S.U.Khan, Pestic.Sci., 9,39(1978).

26. D.S.Gamble, S.U.Khan, Can.J.Soil Sci., 65,435(1985).

27. J.R.Plimmer, P.C.Kearney, and U.I.Klingebiel, J.Agric.Food Chem., 19, 572(1971).

28. N.Burkhardt, J.A.Guth, Pesti.Sci., 7, 65(1976).

29. S.U.Khan, "Pesticides in The Soil Environment", Elsevier, New York, 1980.

30. P.C.Kearney, Residue Review, Vol. 32 (1970),

31. G.J.Sirons, R.Frank and T.Sawyer, J. Agric.Food Chem., 21, 1016(1973).

32. J.J.Richard, G.A.Junk, M.J.Avery, N.L.Nehring, J.S.Fritz and H.J.Svec, Pestic.Monit.J., 9, 117(1975).

33. D.C.G.Muir, J.Y.Yoo, and B.E.Baker, Arch.Environ.Contam. Toxical., 7, 221(1978).

34. R.Frank, G.J.Sirons, Sci.Total Environ., 12, 223(1979).

35. S.U.Khan, P.B.Marriage, J. Agric.Food Chem., 25(6), 1408(1977).

36. S.U.Khan, M.H.Akhtar, J. Agric.Food Chem., 31, 641(1983).

37. S.U.Khan, S.Kacew, S.J.Molnar, J. Agric.Food Chem., 33, 712(1985)

38. S.U.Khan, P.B.Marriage, A.S.Hamill, J. Agric.Food Chem., 29, 216(1981).

39. S.U.Khan, T.S.Foster, J. Agric.Food Chem., 24(4),768(1976).

40. P.Capriel, A.Haisch, S.U.Khan, J. Agric.Food Chem., 33, 567(1985).

41. J.D.Weete, P.Pillai, D.D.Davis, J. Agric.Food Chem.,28, 636(1980).

42. H.E.Christensen, Ed., Toxic Substances List, Published by the U.S. Dept. of Health, Education and Welfare, National Institute for Occupational Safety and Health, pp519 (1972).

43. F.A.Gunther, Ed., Residue Review, Vol. 32, New York, 1970.

44. G.W.Bailey, J.L.White, S.Oblak, J.Chem.Soc., A.905(1968).

46. M.H.Hayes, Residue Review, Vol. 32, 1970, pp131-174.

47. Jr.J.D.Sullivan, Jr.G.T.Felbeck, Soil Sci., 106, 42(1968).

48. M.I.Haniff, Ph. D Thesis, Concordia University, 1984.

49. J.T.Gilmour, N.T.Coleman, Soil Sci.Soc.Am.Proc., 35,

256(1971).

50. J.D. Rusell, M.Cruz, J.L. White, J.Agric. Food Chem., 16, 21(1968).

51. D.S.Gamble, Can J.Chem., 48, 2662(1970).

52. D.S.Gamble, Can J.Chem., 50, 2680(1972).

53. D.S.Gamble, S.U.Khan, Can.J.Chem., 66, 2605(1988).

54. D.S.Gamble, S.U.Khan, Can.J.Soil Sci., 65, 435(1985).

55. G.Zweig, Ed., Analytical Methods for Pesticides, Plant Growth Regulators, and Food Additives, Vol.4, Academic Press, New York. 1964.

56. H.G.Henkel and W.Ebing, J.Chromatogr., 19, 283(1963).

57. E.D.Chilwell and D.Hughes, J.Sci.Food Agric., 13, 425(1962).

58. C.A.Benfield and E.D.Chilwill, Analyst, 89, 475(1964).

59. R.Deleu and A.Copin, J.High Resolut.Chromatogr. & Chromatogr. Comm., 3,299(1980).

60. J.A.Burke and W.holswade, J.Assoc.Off.Anal.Chem., 49, 324(1966).

61. A.M.Mattson, R.A.Kahrs and J.Schneller, J.Agric. & Food Chem., 13, 120(1965).

62. R.C.Tindle, C.W.Gehrke and W.A.Aue, J.Assoc.Off.Anal.Chem., 51, 682(1968).

63. S.U.Khan, and R.Purkayastha, J.Agric. & Food Chem., 23, 311(1975).

64. K.Ramsteiner, W.D.Hormann and D.O.Eberle, J.Assoc.Off.Anal. Chem., 57, 192(1974).

65. D.C.Muir and B.E.Baker, J.Agric. & Food Chem., 24, 122(1976).

66. H.Roseboom and H.H.Herbold, J.Chromatogr., 202, 431(1980).

67. T.R.Steinheimer and M.G.Brooks, Intern. J.Environ.Anal.Chem.,

17, 97(1984).

68. M.I.Haniff, R.H.Zienius, C.H.Langford, and D.S.Gamble, J.Environ.Anal.Chem., B20(2), 215(1985).

69. D.S.Gamble, M.I.Haniff, and R.H.Zienius, Anal.Chem., 54, 732(1986).

70. D.S.Gamble, M.I.Haniff, and R.H.Zienius, Anal.Chem., 54, 727(1986).

71. D.C.Muir, B.E.Baker, J.Agric. & Food Chem., 26, 420(1978).

72. D.G.Stoks, and A.W.schwartz, J.Chromatogr., 168,455(1979).

73. K.A.Ransteiner, W.D.Hormann, J.Agric. & Food Chem., 27, 934(1979)

74. V.Solinas, P.Melis, C.Gessa, Agrochimica, 26, 138(1982).

75. T.H.Byast, J.Chromatogr., 134, 216(1977).

76. Y.Xu, W.Lorenz, G.Pfister, M.Bahador, F.Korte, Freseniu'z Anal.Chem., 325(4), 377(1986).

77. G.Sposito, CRC Critical Review in Environmental Control, 13, March 1982.

78. D.S.Gamble, Can.J.Chem., 51, 3217(1973).

79. A.W.Underdown, C.H.Langford and D.S.Gamble, Environ.Sci. Technol., 19, 132(1985).

80. S.E.Cabaniss and M.S.Shuman, Geochimica et Cosmochimica Acta, 52,195(1988).

81. S.E.Cabaniss and M.S.Shuman, Geochimica et Cosmochimica Acta, 52, 185(1988).

82. R.A.Saar, J.H.Weber, Environ.Sci.Technol., 16(9), 510A(1982).

83. C.Staub, J.Buffle, W.Haerdi, Anal Chem., 56, 2843(1984).

84. J.Buffle, and C.Staub, Anal. Chem., 56, 2837(1984).

85. J.Buffle, F.L.Greter, W.Haerdi, Anal Chem., 49, 216(1977).

86. R.F.C.Mantoura, J.P.Riley, Anal.Chim.Acta., 78, 193(1975).

87. W.T.Bresnahan, C.L.Grant, J.H.Weber, Anal.Chem., 50, 1675(1978).

88. G.Sposito, K.M.Holtzclaw, C.S.Levesque-Madore, Soil Sci.Soc. Am.J., 43,1148(1979).

89. D.L.hunston, Anal. Biochem., 63, 99(1975).

90. A.K.Thakur, P.J.Munson, D.L.Hunston, D.Rodbard, Anal. Biochem., 103, 240(1980).

91. M.S.Shaman, B.J.Collins, P.J.Fitzgerald, D.L.Olson, in "Aquatic and Terrestrial Humic Substances", R.F.Christman, and E.T.Gjessing, Eds., Ann Arbor Science, Ann Arbor, MI, 349(1983).

92. E.M.Perdue, C.R.Lytle, Environ. Sci. Technol., 17, 654(1983).

93. E.M.Perdue, C.R.Lytle, in "Aquatic and Terrestrial Humic Substances", R.F.Christman, E.T.Gjessing, Eds., Ann Arbor Science, Ann Arbor, MI, 295(1983).

94. D.S.Gamble, M.Schnitzer, I.Hoffman, Can.J.Chem., 48, 3197(1970).

95. D.S.Gamble, A.W.Underdown, C.H.Langford, Anal.Chem., 48,3197(1980).

96. D.S.Gamble, M.Schnitzer, H.Kerndorff, C.H.Langford, Geochim. Cosmochim. Acta, 47, 1311(1983).

97. D.R.Burch, C.H.Langford, D.S.Gamble, Can.J.Chem., 56, 1196(1978).

98. V.Tramonti, M.Sc. Thesis, 1988, Concordia University, Montreal.

99. L.E.Sojo, Ph.D. Thesis, 1988, Concordia University, Montreal.

100. J.A.McKeague, B.H.Sheldrick, J.G.Desjardin, "Compilation of

Data for CSSC Reference Soil Samples", Land Resource Research Center, Ottawa, Ont., K1A 0C6, 1978.

101. D.Burch, C.H.Langford, D.S.Gamble, Can. J. Chem., 56, 1196 (1978).

102. D.S Gamble, J.A.Marinsky, C.H.Langford, in "Ion Exchange and Solvent Extraction", Vol.9, J.A.Marinsky and Y.Marcus, Eds., Marcel Dekker, New York, 1985, Chapter 9.

103. D.S.Amstrong, G.Chesters, and R.F.Harris, Soil Sci. Soc. Amer. Proc., 31, 61(1967).

104. M.Schnitzer, S.I.Skinner, Soil Sci., 105, 392(1968).

105. S.M.Griffith, M.Schnitzer, Soil Sci. Soc. Amer. Proc., 39, 861(1975).

106. F.J.Stevenson, Humus Chemistry, John Wiley & Sons, New York, 1982, p223.

107. R.J.Hamilton and P.A.Sewell, "Introduction to High Performance Liquid Chromatograph", John Wiley & Sons, New York, 1978.

108. S.U.Khan, R.Greenhalph, W.P.Cochrane, J. Agric. Food Chem., 23(3), 430(1975).

109. R.S.Schroeder, N.R.Patel, L.W.Hedrick, W.C.Doyle, J.R.Riden, and L.V.Phillips, J. Agric. Food Chem., 20, 1286(1972).

110. J.D.Rusell, M.Cruz, J.L.White, Science, 160, 1340(1968).

111. C.B.Brown, S.F.Rahman, Soil Sci. Soc. Amer. Proc., 41, 141(1977).

112. H.D.Shipper, V.V.Volk, M.M.Mortland and K.V.Rainan, Weed Sci., 26,461(1978).

113. A.Albert, E.P.Serjeant, "Ionization Constants of Acids and Bases", John Wiley & Sons, New York, 1962.

114. T.M.Ward, and J.B.Weber, Spectrochimica Act., 25A, 1167 (1969).

115. D.S Gamble, S.U.Khan, O.S.Tee, Pestic. Sci., 14, 537(1983).

116. J.B.Weber, S.B.Weed, T.M.Ward, Weed Sci., 17, 417(1969).

117. A.Piccolo, F.J.Stevenson, Geoderma, 27, 195(1982).

118. N.Senesi, C.testini. Geoderma, 28, 129(1982).

119. W.V.Gerasimovicz, D.M.Byler, and H.Susi, Appl. Spectrosc., 40(4), 504(1986).

120. D.M.Ryley, W.V.Gerasimovicz, H.Susi, and M.Schnitzer, Appl. Spectrosc., 41(8), 1428(1987).

121. W.Kemp, Organic Spectroscopy, The Macmillan Press Ltd., London, 1981.

122. F.Helfferich, Ion Exchange, McGraw-Hill, New York, 1962.

123. D.S.Gamble, S.U.Khan, and O.S.Tee, Pestic.Sci., 14,537(1983).

124. K.Ghosh and M.Schnitzer, J. Soil Sci., 30, 735(1979).

125. K.Ghosh and M.Schnitzer, Can. J. chem., 60, 373(1980).

126. G.W.Bailey, J.L.White, Residue Review, vol.32, 29(1970).

127. J.B.Weber, P.W.Perry, K.Ibaraki, Weed Sci., 16, 134(1968).

129. D.J.Greenland, Soil Sci., 111, 34(1971).

130. H.Sørensen, Soil Sci., 95,45(1963).

131. D S.Gamble, and S.U.Khan, J.Agric. & Food Chem., in press.